The role of flavonoids in the interaction between the plant, *Medicago truncatula* and the nematode, *Meloidogyne javanica*

A thesis submitted for the degree of

Doctor of Philosophy

of

The Australian National University

Declaration

This thesis is my own work and does not contain any results that have been generated by persons other than me, except where reference and acknowledgement have been made. Results presented in this thesis have not been used for the award of another degree at any other university.

Sabrina Li San Chin
signed 21/8/18

Acknowledgements

Thank you to my supervisors, Prof. Ulrike Mathesius and my associate supervisor Assoc. Prof. Carol Behm for the help and guidance throughout my PhD. Thank you for supporting my crazy ideas and coming up with the finances fund those. I also would like to extend my thanks to other associate supervisors, Assoc. Prof Peter Solomon and Dr. Stephen Trowell for helps and suggestions on my experiments.

I would also like to acknowledge the Australian Government, ANU, Tim Healey Memorial Scholarship and the Australian Society for Parasitology for their financial contributions to this PhD.

Massive credits to Dr Thy Truong who spent a lot of time and effort in helping with my mass spec work. To Dr Terry Neeman, thank you so much for making me sound smart in stats.

I'd like to my plant heroes in the RSB Plant Services, Steve, Darren, Gavin, Christine who helped kept my plants happy, healthy and most importantly, alive. Thanks Tom and RSB IT team who helped me with tech setups and keeping my computer running 24/7 for the past 4 years.

To my dear colleagues in the lab, both past and current, it was great having you around. Thank you Samira and Chooi for teaching me the ropes in the lab (sometimes the hard way) and for the great times. Jason, you get to win the best colleague award because frankly, you're the only who's still around after all these years. Thanks Giel for stimulating discussions about science. To Chris, I know you've stolen my pipettes, so I hope they give you some good luck.

I'd like to give special thanks to all my friends and family who came onto this journey with me. Jacinta, great job for keeping me emotionally and mentally fit. Veronica, thanks for the fun shenanigans after work. Also to my lovely friends, Estee, Meenu Alice and Sophie, thank you for your companionship and fellow PhD cohorts, Diep and John who finished way earlier to ~~pressure~~ inspire me to finish my PhD.

I'd like to dedicate this thesis to my grandparents, both who passed away during the course of my PhD. Thank you for nurturing this little sprout with all your kindness and love. Whilst this is no darling buds of May,

> So long as men can breathe, or eyes can see,
> So long lives this, and this gives life to thee.

Last but not least, my knight in shining armour, JJ. Love you to the moon and back.

My sincerest thanks to everyone who helped me make this thesis look good and my apologies to people whom I've accidentally forgotten (I blame it on my Permanent Head Damage).

Abstract

Flavonoids are plant secondary metabolites which are common in all vascular plants. They play numerous functions in plants, ranging from UV protection, pigments, signalling molecules, defence to auxin transport inhibition for plant development. Flavonoids are potentially manipulated by the root-knot nematodes, *Meloidogyne* spp. to hijack multiple plant functions. This is especially of interest in the study of *Meloidogyne* parasitism because these nematodes have an extraordinarily broad host range (>2000 plant species), thus indicating their mastery of basal and essential plant machineries.

Flavonoids may mediate the plant-nematode interactions by acting as defence compounds, signalling molecules in the rhizosphere and as auxin transport modulators in nematode feeding site (gall) development. To test these hypotheses, flavonoids in wild-type *Medicago truncatula* cv. 2HA were systematically profiled using tandem mass spectrometry across seven time points which represented different stages of nematode parasitism. The results revealed that flavonoid induction began at 24 hours, with upstream flavonoids pathways such as the chalcones and flavanones and specific flavonols eg. kaempferol glycosides and the flavone, 7,4'-DHF were dramatically increased. In contrast, a different pattern of flavonoid accumulation occurred at 4 weeks, where in addition to the chalcones and flavanones, isoflavonoids and pterocarpans accumulated at high levels, suggesting their role in nematode defence.

Subsequently, involvement of isoflavonoids and pterocarpans in defence were tested by observing nematode infection in 7 different genotypes of *M. truncatula* with flavonoid variations. The genotypes included naturally occurring accessions, F83005 and DZA045, bred cultivars, 2HA and A17 and transgenics with silenced *isoflavone synthase (IFS)* genes and over-expressing *IFS* gene. Plants that accumulated high levels of the pterocarpan, medicarpin either early in infection, eg. *IFS* over-expression line, or extremely high levels of medicarpin eg. F83005 exhibited reduced nematode egg numbers. In addition, plants over-expressing *IFS* also showed better infection outcome, with minimal biomass loss due to infection, less galls and smaller galls. These results were complemented with *in vitro* chemotaxis and motility assays, which revealed that the medicarpin and afromosin were effective nematode repellent and motility inhibitor respectively.

Lastly, the roles of isoflavonoids in auxin transport inhibition in the gall were elucidated using *M. truncatula IFS* transgenics and wild-type 2HA. Isoflavonoids were found to be unlikely involved in auxin transport inhibition in the gall as the over-production of isoflavonoids resulted in delayed auxin transport inhibition, whereas the under-production of isoflavonoids resulted in strong and early auxin transport inhibition.

Conclusively, medicarpin and afromosin played specific roles in protecting the plant against the nematodes, and isoflavonoid pathway modification showed that isoflavonoids were unlikely auxin transport inhibitors in gall development.

Table of Contents

Abbreviations

2HID	2-hydroxyisoflavanone dehydratase
4-Cl-IAA	4-chloro-indole-3-acetic acid
7,4'-DHF	7,4'- dihydroxyflavone
AMFG	S-adenosylmethionine-flavonoid 7-O-glucosyltransferase
Api-neo	apigenin-7-*O*-neohesperidoside
CIM	callus inducing medium
CHI	chalcone isomerase
CHS	chalcone synthase
CHR	chalcone reductase
Daid-7-gluc	daidzein-7-*O*-glucoside
Daid-8-gluc	daidzein-8-*C*-glucoside
DHF glyc-like	dihydroxyflavone glycoside-like
DMID	7,2'-dihydroxy-4'-methoxy-isoflavonol dehydratase
DMSO	dimethyl sulfoxide
DFR	dihydroflavonol 4-reductase
EDM	embryo development medium
EIM	embryo inducing medium
ESI	electrospray ionisation
F3'H	flavonoid-3'-hydroxylase
F3'M	flavonoid 3'-monooxygenase
F6H	flavanone-6-hydroxylase
FLS	flavonol synthase
FNS	flavone synthase

FSII	flavone synthase II
Form-7-gluc	formononetin-7-*O*-glucoside
Gen-7-gluc	genistein-7-*O*-glucoside
I2'H	isoflavone-2'-hydroxylase
I7GT	isoflavone-7-O glucosyl transferase
IAA	indole-3-acetic acid
IAA-Ala	indole-3-acetic acid-alanine
IAA-Asp	indole-3-acetic acid-aspartate
IAA-Ile	indole-3-acetic acid-isoleucine
IAA-Leu	indole-3-acetic acid-leucine
IAA-Phe	indole-3-acetic acid-phenylalanine
IAA-Trp	indole-3-acetic acid-tryptophan
IAA-Val	indole-3-acetic acid-valine
IBA	indole-3-butyric acid
IFD	2-hydroxyisoflavanone dehydratase
IFS	isoflavone synthase
IFSi	*isoflavone synthase* gene silenced
IFSOE	*isoflavone synthase* gene over-expression
IOMT	isoflavanone-O-methyltransferase
IFR	isoflavone reductase
J2s	second stage juveniles
K-gluc	kaempferol glucoside
K-3-gluc	kaempferol-3-*O*-glucoside
K-7-gluc	kaempferol-7-*O*-glucoside
K-3-glucu	kaempferol-3-*O*-glucuronide

K-3-rutinoside	kaempferol-3-*O*-rutinoside
K-glyc-like	kaempferol glycoside-like
K-gluc-rham	kaempferol 3-*O*-glucosyl-rhamnosyl-galactoside or kaempferol 3-*O*-glucosyl-rhamnosyl-glucoside
LC-ESI- Q-TOF-MS/MS	liquid chromatography –electrospray ionization-quadrupole-time of flight-mass tandem spectrometry
LOD	limit of detection
LOQ	limit of quantification
MeOH	methanol
Methoxyisoflav 1	methoxyisoflavone glycoside-like 1
Methoxyisoflav 2	methoxyisoflavone glycoside-like 2
N7OG	naringenin 7-O-glucosyltransferase
Nar-7-gluc	naringenin-7-*O*-glucoside
NPA	*N*-1-naphthylphthalamic acid
OE	over-expression
OPLS-DA	orthogonal partial least squares discriminant analysis
PAA	phenylacetic acid
ppm	parts per million
RKN(s)	root knot nematode(s)
RNAi	RNA interference
tt	*transparent testa*
VR	vestitone reductase

List of Figures

	experiments involving *M. truncatula* accessions/ cultivars (2HA, A17, DZA045 and F83005) and transgenics (wild-type 2HA, IFSi 101-2, IFSi 42-7 and IFSOE 10-3).	
S4.1	PCR- based DNA genotyping of transgenic *M. truncatula* via *nptII* transgene.	192
S4.2	Liquiritigenin concentrations based on fresh weight in root segments of uninfected and *Meloidogyne javanica* infected roots (galls) of *Medicago truncatula* cultivars, 2HA, A17, DZA045 and F83005.	195
S4.3	Naringenin concentrations based on fresh weight in root segments of uninfected and *Meloidogyne javanica* infected roots (galls) of *Medicago truncatula* cultivars, 2HA, A17, DZA045 and F83005.	196
S4.4	Compound 784 concentrations based on fresh weight in root segments of uninfected and *Meloidogyne javanica* infected roots (galls) of *Medicago truncatula* cultivars, 2HA, A17, DZA045 and F83005.	197
S4.5	Methoxyisoflav 1 concentrations based on fresh weight in root segments of uninfected and *Meloidogyne javanica* infected roots (galls) of *Medicago truncatula* wild type cv. 2HA and isoflavone synthase transgenics, silenced lines, IFSi 101-2 and IFSi 42-7 and over-expression line, IFSOE 10-3.	198
S4.6	Methoxyisoflav 2 concentrations based on fresh weight in root segments of uninfected and *Meloidogyne javanica* infected roots (galls) of *Medicago truncatula* wild type cv. 2HA and isoflavone synthase transgenics, silenced lines, IFSi 101-2 and IFSi 42-7 and over-expression line, IFSOE 10-3.	199
S4.7	DHF glyc-like concentrations based on fresh weight in root segments of uninfected and *Meloidogyne javanica* infected roots (galls) of *Medicago truncatula* wild type cv. 2HA and isoflavone synthase transgenics, silenced lines, IFSi 101-2 and IFSi 42-7 and over-expression line, IFSOE 10-3.	200
S4.8	Isoliquiritigenin concentrations based on fresh weight in root segments of uninfected and *Meloidogyne javanica* infected roots (galls) of *Medicago truncatula* wild type cv. 2HA and isoflavone synthase transgenics, silenced lines, IFSi 101-2 and IFSi 42-7 and over-expression line, IFSOE 10-3.	201
S4.9	Liquiritigenin concentrations based on fresh weight in root segments of uninfected and *Meloidogyne javanica* infected roots (galls) of *Medicago truncatula* wild type cv. 2HA and isoflavone synthase transgenics, silenced lines, IFSi 101-2 and IFSi 42-7 and over-expression line, IFSOE 10-3.	202
S4.10	Naringenin concentrations based on fresh weight in root segments of uninfected and *Meloidogyne javanica* infected roots (galls) of *Medicago truncatula* wild type cv. 2HA and isoflavone synthase transgenics, silenced lines, IFSi 101-2 and IFSi 42-7 and over-expression line, IFSOE 10-3.	203
S4.11	Compound 578 concentrations based on fresh weight in root segments of uninfected and *Meloidogyne javanica* infected roots (galls) of *Medicago truncatula* wild type cv. 2HA and isoflavone	204

	synthase transgenics, silenced lines, IFSi 101-2 and IFSi 42-7 and over-expression line, IFSOE 10-3.	
S4.12	Compound 462 concentrations based on fresh weight in root segments of uninfected and *Meloidogyne javanica* infected roots (galls) of *Medicago truncatula* wild type cv. 2HA and isoflavone synthase transgenics, silenced lines, IFSi 101-2 and IFSi 42-7 and over-expression line, IFSOE 10-3.	205
S4.13	Compound 784 concentrations based on fresh weight in root segments of uninfected and *Meloidogyne javanica* infected roots (galls) of *Medicago truncatula* wild type cv. 2HA and isoflavone synthase transgenics, silenced lines, IFSi 101-2 and IFSi 42-7 and over-expression line, IFSOE 10-3.	206
S4.14	Number of eggs per galls in *Medicago truncatula* wild-type cv. 2HA and isoflavone synthase transgenics, silenced lines, IFSi 101-2 and IFSi 42-7 and over-expression line, IFSOE 10-3 at 6 weeks post inoculation with *Meloidogyne javanica*.	207
S4.15	Examples of *Meloidogyne javanica* J2 chemotaxis responses.	208
S4.16	Average motility of *Meloidogyne javanica* J2s based on mean motility movement against ten purified flavonoids.	209
S4.17	Average motility of *Meloidogyne javanica* J2s based mean motility movement against root exudates of *Medicago truncatula* wild type cv. 2HA and transgenics IFSi 101, IFSi 42 and IFSOE 10	210
S4.18	Afromosin concentrations based on fresh weight in root segments of uninfected and *Meloidogyne javanica* infected roots (galls) of *Medicago truncatula* cultivars, 2HA, A17, DZA045 and F83005.	211
S4.19	Afromosin concentrations based on fresh weight in root segments of uninfected and *Meloidogyne javanica* infected roots (galls) of *Medicago truncatula* wild type cv. 2HA and isoflavone synthase transgenics, silenced lines, IFSi 101-2 and IFSi 42-7 and over-expression line, IFSOE 10-3.	212
S4.20	Medicarpin concentrations based on fresh weight in root segments of uninfected and *Meloidogyne javanica* infected roots (galls) of *Medicago truncatula* cultivars, 2HA, A17, DZA045 and F83005.	213
S4.21	Medicarpin concentrations based on fresh weight in root segments of uninfected and *Meloidogyne javanica* infected roots (galls) of *Medicago truncatula* wild type cv. 2HA and isoflavone synthase transgenics, silenced lines, IFSi 101-2 and IFSi 42-7 and over-expression line, IFSOE 10-3.	214
5.1	Acropetal auxin transport in uninfected roots of wild-type *Medicago truncatula* cv. 2HA and transgenics, isoflavone synthase silenced lines, IFSi 42-7 and IFSi 101-2 and isoflavone synthase over-expression line, IFSOE 10-3 at 24 hours, 4 days and 4 weeks.	231
5.2	Acropetal auxin transport in infected roots of wild-type *Medicago truncatula* cv. 2HA and transgenics, isoflavone synthase silenced lines, IFSi 42-7 and IFSi 101-2 and isoflavone synthase over-	232

List of tables

S4.5	Pairwise comparisons of lower 10th and upper 90th quantiles for the multivariate distributions of percentage nematode motility inhibitions for ten purified flavonoids.	222
5.1	Percentage change in auxin transport between uninfected and infected roots of wild-type *Medicago truncatula* cv. 2HA and transgenics of isoflavone synthase silenced lines, IFSi 42-7, IFSi 101-2, and isoflavone synthase overexpression line, IFSOE 10-3 at 4 days and 4 weeks post inoculation with *Meloidogyne javanica*.	239
5.2	Percentage change in auxin transport between nematode inoculated segments and corresponding downstream segments in *Medicago truncatula* cv. 2HA and transgenics of isoflavone synthase silenced lines, IFSi 42-7, IFSi 101-2, and isoflavone synthase overexpression line, IFSOE 10-3 at 4 days and 4 weeks post inoculation with *Meloidogyne javanica*.	239
5.3	Summary of the types of galls formed at nematode inoculation in wild-type *Medicago truncatula* cv. 2HA and transgenics, isoflavone synthase silenced lines, IFSi 42-7 and IFSi 101-2 and isoflavone synthase over-expression line, IFSOE 10-3 at 4 weeks post inoculation with *Meloidogyne javanica*.	240
5.4	A summary of three auxin assays on nematode-infected roots of *M. truncatula* 2HA at 24 hours, 4 days and 4 weeks.	253
6.1	P-values of simple linear regressions of the relationship between flavonoid and auxin concentrations (log 10) in *Medicago truncatula* cv. 2HA in uninfected and infected roots at 6 hours, 24 hours, 4 days, 2 weeks and 4 weeks post inoculation with *Meloidogyne javanica*.	270

Chapter 1: General introduction

1.1. Introduction to plant-parasitic nematodes
1.2. Introduction to root-knot nematodes
1.3. Plant-nematode interactions
1.4. Flavonoids in plants
1.5. Flavonoids as defence compounds against nematodes
1.6. Flavonoids in the development of nematode feeding sites
1.7. Aims

Note: An adapted version of this chapter will be published as a review in Plants.

1.1 Introduction to plant-parasitic nematodes

Nematodes are small roundworms with bilaterally symmetrical and unsegmented body (Abad and Williamson, 2010). Whilst most nematodes are free-living, ~7% (> 4,100 species) of the characterized nematodes belong to the plant-parasitic nematode (PPN) group (Bird, 1987, Nicol et al., 2011, Decraemer and Hunt, 2006). PPNs are agricultural pests that cause significant crop damage and crop loss, estimated at up to $US 125 billion globally per annum (Chitwood, 2003, Nicol et al., 2011, Sasser and Freckman, 1987). This is due to the diversion of host nutrients to PPNs and interference to transport processes, as well as physical damage caused during feeding or migration, which can also result in secondary infections (Jones et al., 2013, Perry and Moens, 2011).

PPNs are classified into three orders, the Triplonchida, Dorylaimida and Tylenchida, with the majority of agriculturally damaging nematodes belonging to the last order, which includes root-knot nematodes (*Meloidogyne* spp.) and cyst nematodes (*Globodera* and *Heterodera* spp.) (Abad and Williamson, 2010, Tytgat et al., 2000). These PPNs have evolved a highly specialized feeding structure, termed the stylet, to feed on plant tissues, and often display complex life-stages to suit their environment (Grandison, 1977, Kikuchi et al., 2017, Quitst et al., 2015). The tylenchids are classified based on their trophic niche, either as aerial nematodes or root parasitic nematodes (Tytgat et al., 2000).

1.2 Introduction to root-knot nematodes

Root-knot nematodes are one of the most damaging PPNs, due to (1) the difficulty in diagnosing above ground symptoms, which resembles general nutrient deficiency symptoms, (2) high reproduction capacity, (3) global distribution and adaptations to different climates, (4) broad host range, which includes most commercial crops, (5) other secondary infections arising from nematode entry into the root and (6) inadequate control strategies, with effective nematicidies being banned due to toxicity (Moens et al., 2009, Nicol et al., 2011, Stirling and Stanton, 1997, Stirling and Pattison, 2008, Taylor et al., 1982). The most agriculturally problematic root-knot nematodes are *M. incognita, M. hapla, M. arenaria* and *M. javanica* (Moens et al., 2009), with *M. javanica* being the most prevalent root-knot nematode in Australian crops (Stirling et al., 1992, Walker and Stirling, 2008). As such, *M. javanica* has been selected as the root-knot nematode for this thesis.

These nematodes begin their life cycle at the egg stage, and post embryogenesis, reaches the first-stage juvenile (J1) (Moens et al., 2009). Whilst still in the egg, the nematode undergoes its first moulting and becomes the second-stage juvenile (J2). Next, the pre-parasitic J2 hatches from the egg and migrates around the rhizosphere to locate a suitable host (Curtis et al., 2009). Once a host has been selected, the J2 penetrates behind the root tip and enters the root. Thereafter, within 24 hours, the J2 migrates intercellularly to reach the vascular bundle and begins to secrete effectors into selected procambium cells to induce these into its feeding cells (giant cells) (Figure 1.1) (Bird, 1962). Inadvertently, the cells neighbouring the giant cells, the cortical and pericycle cells undergo cell divisions to accommodate the growing nematode and giant cells. By around two weeks, the J2 then continues to sequentially moult into J3, J4 and finally the adult stage, either as a sedentary pear-shaped female or a vermiform male (Figure 1.1) (Bird, 1959b). The adult female recommences feeding and starts to produce eggs.

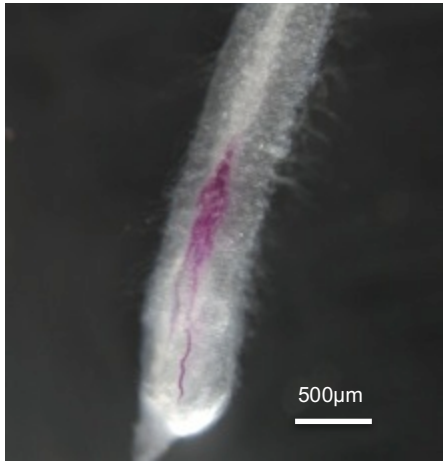

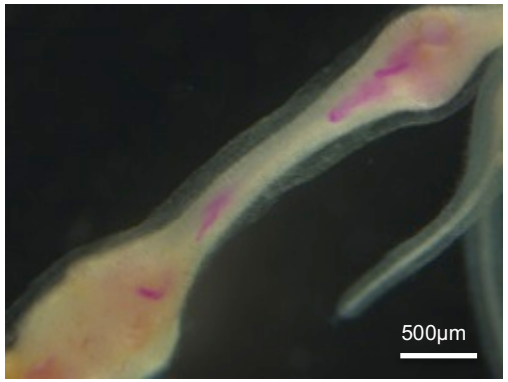

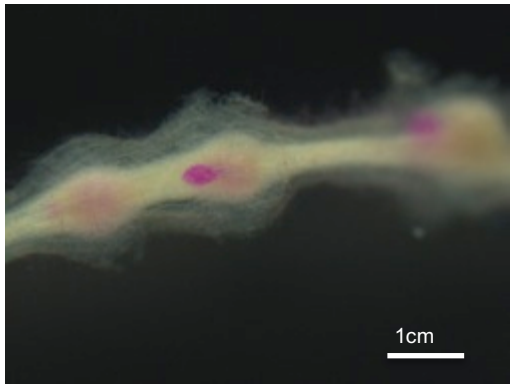

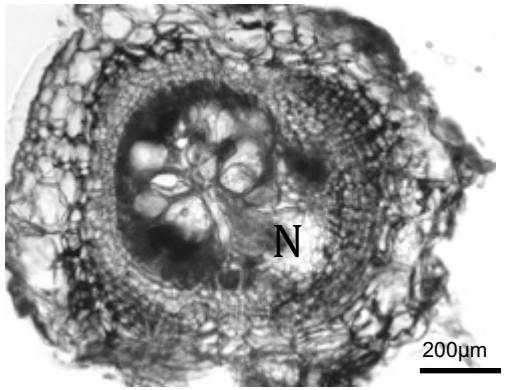

~24 hours | ~2 weeks | ~4 weeks

No gall
J2s invade the root and migrate intercellularly to establish a feeding site

Young gall
J2s had established a feeding site and are moulting

Mature gall
Adult females remain in the root and continues to feed and reproduce

Figure 1.1: Life cycle of the root-knot nematode, *Meloidogyne javanica*. Nematodes were stained pink using acid fuschin staining or indicated as N. Parasitism begins when second-stage juveniles (J2s) infect the root and migrate intercellularly to select procambium cells for feeding. By around 2 weeks, J2s, which had established their feeding sites, stopped feeding to moult several times, until finally becoming an adult. Adult female nematodes remained sedentary and continued to feed and reproduce eggs.

1.3 Plant-nematode interactions

Plant-nematode interactions often begin in the soil (Figure 1.2), where the PPNs perceive various host cues using chemosensing, mechanosensing, thermosensing, redox potential sensing, humidity sensing, osmotic sensing and electrosensing (Curtis, 2008, Gang and Hallem, 2016, Perry, 1996). It is thought that PPNs possess similar neuroanatomy and neurobiology as the free-living nematode model, *Caenorhabditis elegans*, and that taxis towards a source of plant cues relies mainly on chemosensation, although these processes are poorly understood in PPNs (Perry, 1996, Rengarajan and Hallem, 2016).

Chemosensation in PPNs is strongly linked to their host range, with PPNs with narrow host ranges thought to have sensitive chemosensation, such as the potato cyst nematode, *Globodera pallida* and *G. rostochiensis,* and the soybean cyst nematode, *Heterodera glycines,* as they respond very strongly to specific chemicals in the root exudates by hatching and moving towards the chemical (Tefft and Bone, 1985, Rasmann et al., 2012). In contrast, PPNs with a broad host range, such as the root-knot nematodes, *Meloidogyne* spp. also rely on non-specific abiotic cues, namely low pH and CO_2 gradient (Pline and Dusenbery, 1986, Wang et al., 2009a). These signals are concurrently analyzed by the chemoreceptors in the anterior receptors, the amphids, and in some PPNs, the posterior receptors, the phasmids, to determine the orientation of the PPN (Curtis, 2008, Rasmann et al., 2012). In the event of a positive response, the PPN orients itself towards the cue and begins its migration towards the source (Figure 1.2). If the PPN does not find a compatible cue within its pre-parasitic life cycle (*i.e.* egg and juvenile stages), it will reduce its metabolism, either by undergoing a quiescence process, e.g. the pre-parasitic juvenile nematode ceases movement until stimulated, or it will enter a diapause process such as delaying egg hatching (Evans and Perry, 2009, Sommerville and Davey, 2002).

The next interaction occurs at the root interface, whereby root nematodes penetrate the root tissue or remain external to the root, whereas aerial nematodes

continue to migrate upwards to the stem (Figure 1.2). Next, the PPNs commence feeding and mature, and finally start to reproduce inside or outside the host. Aerial nematodes can feed on the bulb, stem and foliage, whereas root nematodes feed exclusively on the root (Tytgat et al., 2000, Lambert and Bekal, 2002). Root PPNs deploy different parasitic strategies, being (1) either migratory or sedentary during feeding, and (2) being either endoparasitic or ectoparasitic during feeding and reproduction (Sijmons et al., 1994, Tytgat et al., 2000, Wyss and Grundler, 1992). The most damaging PPNs belong to the sedentary endoparasitic group, the root knot nematodes (*Meloidogyne* species) and cyst nematodes (*Globodera* and *Heterodera* species), followed by the migratory endoparasites, the root lesion nematodes (*Pratylenchus* species) and the burrowing nematodes (*Radopholus* species) (Bird and Kaloshian, 2003, Jones et al., 2013). The success of root sedentary endoparasities can be attributed to the sophisticated exploitation of many different plant response pathways to alter plant defence responses and to induce long-term feeding sites, and to the difficulty in diagnosing infections due to below ground symptoms (Bird and Kaloshian, 2003, Lambert and Bekal, 2002). Overall, there has been limited success in controlling PPNs via chemicals, biological control or creating effective plant resistance (Davies and Spiegel, 2011, Fuller et al., 2008, Stirling and Pattison, 2008).

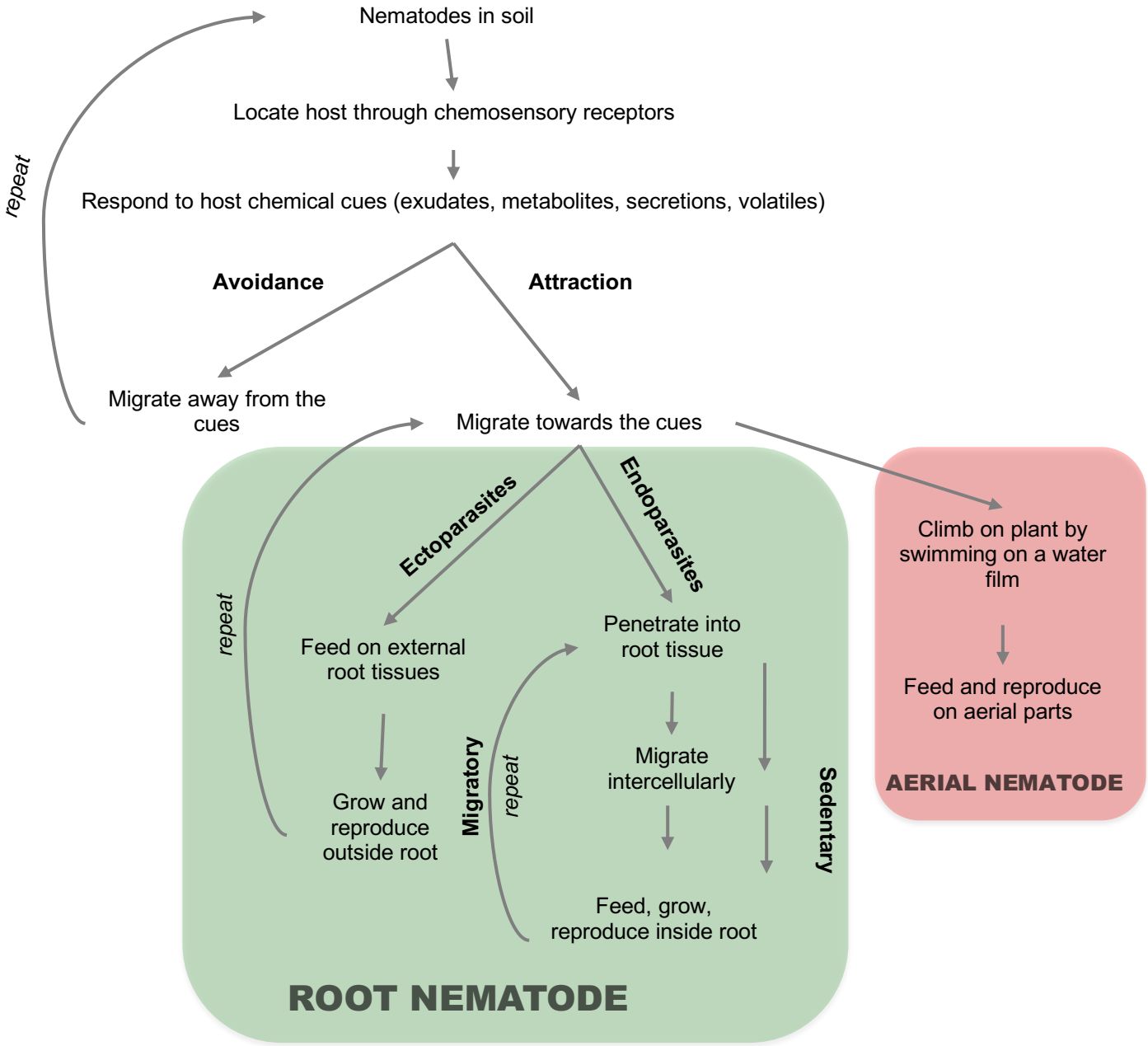

Figure 1.2: Summary of interactions between plant hosts and plant-parasitic nematodes. Plant hosts are infected by both root and aerial nematodes. Their interaction starts in the soil with the perception of host cues by the nematode, followed by attraction or repulsion towards the host. Root nematodes include ecto- and endoparasites, with endoparasites causing the greatest damage due to their induction of a complex feeding site, in which they reproduce.

1.4 Flavonoids in plants

Flavonoids constitute a large class of secondary carbon-based metabolites present in all land plants. More than 10,000 different types of flavonoids have been described from a variety of plant species. Flavonoids are derived from the phenylpropanoid pathway by the activity of a cytosolic multienzyme complex in the endoplasmic reticulum and typically contain a backbone C3-C6-C3 ring, which forms the basis of flavonoid subgroup classification (Petrussa et al., 2013). There are several flavonoid subgroups based on their structural properties, including the chalcones, flavones, flavonols, flavandiols, anthocyanins, condensed tannins, aurones (not ubiquitous), isoflavonoids and pterocarpans (Hassan and Mathesius, 2012, Winkel-Shirley, 2001, Winkel-Shirley, 2002) (Figure 1.3). Flavonoids within the subgroups are extensively modified through secondary modifications of the backbone, for example by hydroxylation, glycosylation, methylation, malonylation, prenylation, acylation, dehydration and polymerization (Falcone Ferreyra et al., 2012). The functions of individual flavonoids are strongly affected by their structure and include roles in plant development via the control of auxin transport, flower pigmentation, as antioxidants (ROS scavengers), as defence compounds, chemoattractants, signals for plant-microbe interactions (notably nodulation), male fertility in some species and help in nutrient mining (Hassan and Mathesius, 2012). Flavonoids are actively exuded into the rhizosphere, likely using ABC transporters and multidrug and toxic compound extrusion (MATE) transporters in both aglycones and glycosidic forms (Badri et al., 2008, Cesco et al., 2010, Sugiyama et al., 2007). Small amounts of flavonoids also diffuse into the soil during root cap sloughing (Hawes et al., 2008). Most studies on flavonoid exudation have measured flavonoid concentrations from the nano- to micromolar ranges in growth medium under (semi)sterile laboratory conditions (Cesco et al., 2010). Hence, their functions, bioavailability, mobility, concentrations and gradients in real soil situations with rhizosphere microorganisms are still poorly understood.

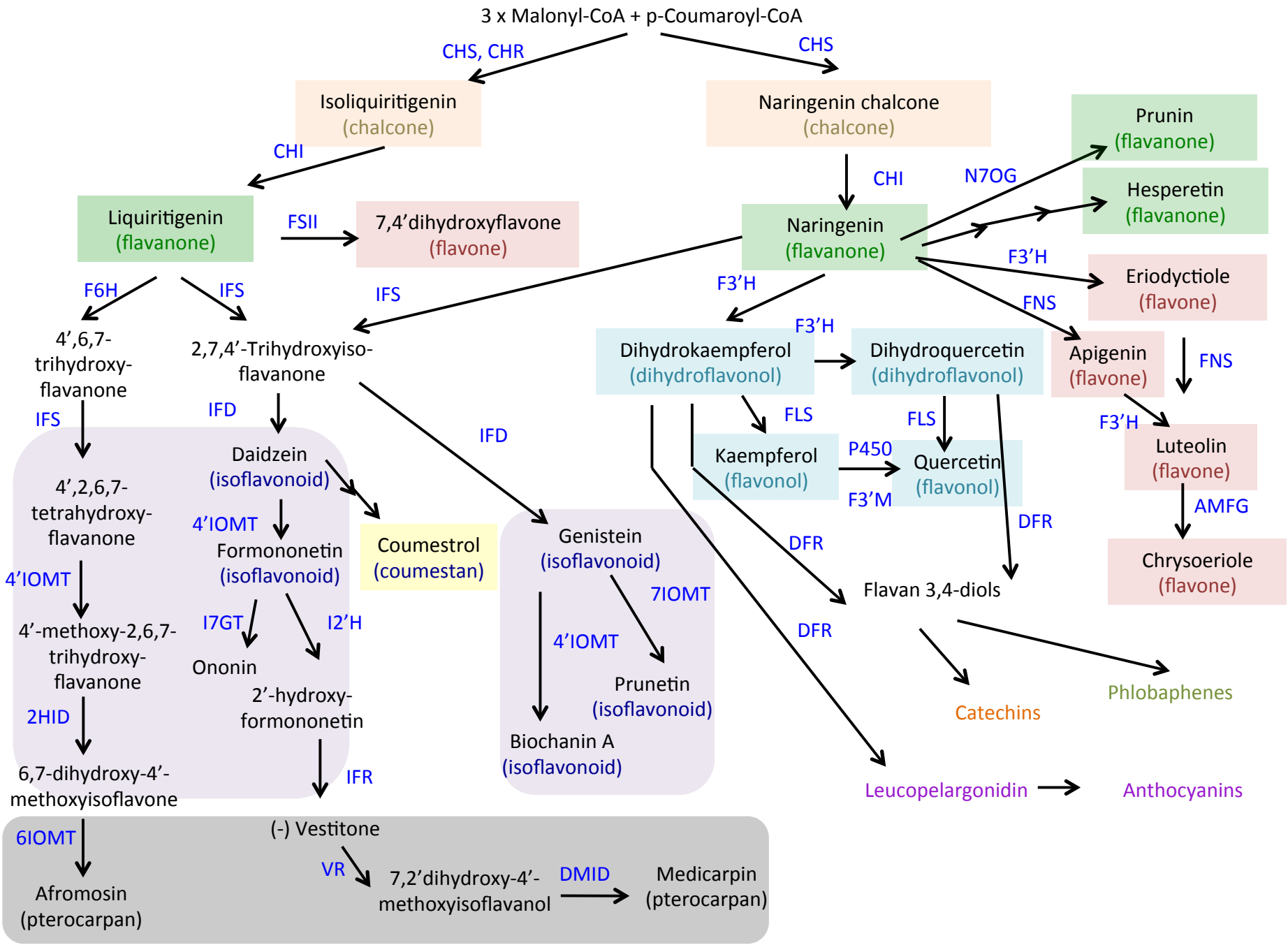
3 x Malonyl-CoA + p-Coumaroyl-CoA
CHS, CHR
CHS
Isoliquiritigenin (chalcone)
Naringenin chalcone (chalcone)
CHI
CHI
Liquiritigenin (flavanone)
FSII
7,4'dihydroxyflavone (flavone)
Naringenin (flavanone)
N7OG
Prunin (flavanone)
Hesperetin (flavanone)
F3'H
Eriodyctiole (flavone)
FNS
F6H
IFS
IFS
F3'H
4',6,7-trihydroxy-flavanone
2,7,4'-Trihydroxyiso-flavanone
Dihydrokaempferol (dihydroflavonol)
F3'H
Dihydroquercetin (dihydroflavonol)
Apigenin (flavone)
FNS
IFS
IFD
IFD
FLS
FLS
F3'H
4',2,6,7-tetrahydroxy-flavanone
Daidzein (isoflavonoid)
Kaempferol (flavonol)
P450
F3'M
Quercetin (flavonol)
Luteolin (flavone)
4'IOMT
Coumestrol (coumestan)
Genistein (isoflavonoid)
DFR
DFR
AMFG
4'IOMT
Formononetin (isoflavonoid)
7IOMT
Chrysoeriole (flavone)
4'-methoxy-2,6,7-trihydroxy-flavanone
I7GT
I2'H
Flavan 3,4-diols
DFR
2HID
Ononin
2'-hydroxy-formononetin
4'IOMT
Prunetin (isoflavonoid)
Phlobaphenes
Catechins
6,7-dihydroxy-4'-methoxyisoflavone
IFR
Biochanin A (isoflavonoid)
Leucopelargonidin
Anthocyanins
6IOMT
(-) Vestitone
VR
7,2'dihydroxy-4'-methoxyisoflavanol
DMID
Medicarpin (pterocarpan)
Afromosin (pterocarpan)

Figure 1.3: Flavonoid biosynthesis in the plant, *Medicago truncatula*. Enzymes are shown in blue and are abbreviated as follows: AMFG= S-adenosylmethionine-flavonoid 7-O-glucosyltransferase; CHI= chalcone isomerase; CHR= chalcone reductase; CHS= chalcone synthase; DFR= dihydroflavonol 4-reductase; DMID= 7,2'-dihydroxy-4'-methoxy-isoflavonol dehydratase; 2HID= 2-hydroxyisoflavanone dehydratase; F3'H= flavonoid-3'-hydroxylase; F6H= flavanone-6-hydroxylase; F3'M= flavonoid 3'-monooxygenase; FLS= flavonol synthase; FNS= flavone synthase; FSII= flavone synthase II; I2'H= isoflavone-2'-hydroxylase; IFD= 2-hydroxyisoflavanone dehydratase; IFR= isoflavone reductase; IFS= isoflavanone synthase; I7GT= isoflavone-7-O glucosyl transferase; IOMT= isoflavanone-O-methyltransferase; N7OG= naringenin 7-O-glucosyltransferase; P450= cytochrome P450; VR= vestitone reductase. Figure summarized from Kegg Pathway database (available at https://www.genome.jp/kegg/pathway.html)[assessed on 13th August 2018].

1.5. Flavonoids as defence compounds against nematodes

A PPN will first encounter flavonoids in the soil when it is locating its host (Figure 1.2). This can occur whilst the PPN is in the egg or juvenile stage. For PPNs in the egg stages, flavonoids can inhibit egg hatching (Figure 1.4), as shown in a study by Wuyts et al. (2006b), in which kaempferol inhibited *Radopholus similis* egg hatching. As for juvenile PPNs, flavonoids can (1) induce quiescence by slowing down their movement, resulting in periods of reversible inactivity, (2) modify their migration towards the roots by repelling them and (3) kill them (Figure 1.4). For example, the flavonols kaempferol, quercetin and myricetin repelled and slowed *M. incognita* juveniles at micromolar concentrations (Wuyts et al., 2006b). Patuletin, patulitrin, quercetin and rutin were shown to kill the juveniles of *H. zeae* at various concentrations and durations of exposure (Faizi et al., 2011). Flavonoid effects on PPNs are also species-specific. Using similar concentrations of flavonols, kaempferol, quercetin and myricetin repelled *M. incognita* and *R. similis* juveniles, but not *Pratylenchus penetrans,* whereas the flavonols inhibited the motility of *M. incognita* juveniles but not *R. similis* and *P. pratylenchus* juveniles (Wuyts et al., 2006b). Interestingly, in *C. elegans* exposure of young adults (L4 stage) to 100μM flavonols, particularly kaempferol in liquid and plate media, prolonged their lifespan through effects on an ageing-associated gene, the transcription factor DAF-16 and by reducing mitochondrial reactive oxygen species (ROS) (Grünz et al., 2012, Kampkötter et al., 2007, Kampkötter et al., 2008). The differences in flavonoid effects in different nematode species is likely due to the differences in chemosensory receptors, flavonoid receptor binding affinities, cell signaling cascade and solute permeability across cuticle in different species, although this has not been studied yet. Furthermore, not much is known about the existence or functions of putative flavonoid receptors in any PPN.

Once the PPN has reached the plant, it inflicts mechanical damage to the plant tissue to penetrate and/or to feed on the tissue. This is followed by the production and release of defence compounds (i.e. phytoalexins and phytoanticipins) to respond to PPN attack (Figure 1.4). Although some flavonoids such as *(E)*- chalcone, patuletin and rutin killed pre-parasitic stages of cyst nematodes (González and Estévez-Braun, 1998, Faizi et al., 2011), its accumulation, concentrations and activity *in planta* is

unclarified. In addition, numerous studies have found increased flavonoid gene expression and flavonoid accumulation at infections sites of both endo- and ectoparasitic PPNs, and induction of flavonoids has repeatedly been found to be higher in resistant compared with susceptible host cultivars (summarized in Table 1.1). Flavonoids that have most commonly been implicated as defence compounds against PPNs mostly belong to the isoflavonoids and pterocarpan classes, (e.g. coumsterol, glyceollin (soybean-specific), formononetin and medicarpin) as well as the flavonols (e.g. kaempferol and quercetin) (Table 1.1). Some studies have also shown that flavonoid glycosides are likely involved in defence, such as medicarpin glucoside malonate and formononetin glucoside malonate (Cook et al., 1995).

The plant host and the PPN itself can manipulate the flavonoid pathway during PPN pathogenesis directly or indirectly. One study suggested that yellow-coloured cyst nematodes, *G. pallida* and *G. rostochiensis*, modified quercetin and kaempferol into a nematode-unique flavonoid, quercentagetin (Vlachopoulos and Smith, 1993). Flavonoids are likely taken up by the PPN's digestive system as the PPN feeds on the cytoplasmic content. In endoparasitic PPNs, flavonoids may also diffuse through the cuticle from nearby plant cells that surround the parasite within the root tissue. Nonetheless, it is not well understood to what extent flavonoids accumulate inside nematodes, how they are processed or whether they play a role in the infection process.

The flavonoid pathway in the plant can be induced by a broad pathogenesis response through jasmonic acid, salicylic acid, ethylene, auxin and ROS cross-talks, likely triggered when the PPNs cause mechanical damage and wounding during feeding and penetration (Goverse and Smant, 2014, Holbein et al., 2016). Flavonoids are also likely to be released from storage in the cytosol, vacuole, endoplasmic reticulum, chloroplast, nucleus and small vesicles during tissue damage or cell rupture (Zhao and Dixon, 2009). Flavonoids have been found to be induced in roots in plants only infected by nematodes in the shoot, suggesting that systemic signals may induce flavonoid synthesis in infected plants, but so far it is unknown what these systemic signals are (Edwards et al., 1995). Some of the flavonoid biosynthesis pathways can be manipulated by the PPN via the secreted enzyme chorismate mutase, which regulates the shikimate pathway and thereby the downstream flavonoid, salicylic acid, auxin and amino acid pathways in the plant (Dewick, 1998). Chorismate mutase

gene(s) or enzymes have been found in juveniles of endoparasitic PPNs such as *M. javanica, M. incognita, M. arenaria, H. glycines, H. schachtii* and *G. pallida,* in the esophageal glands, and are potentially involved in the induction of their feeding sites, after being secreted into giant cells (Bekal et al., 2003, Doyle and Lambert, 2003, Huang et al., 2004, Jones et al., 2002, Lambert et al., 1999, Lambert et al., 2005, Vanholme et al., 2009).

The flavonoids that accumulate at PPN feeding sites may affect nematode fertility and fecundity (Figure 1.4) by limiting egg production or skewing the ratio of males to females as more females are formed in high nutrition and *vice versa* (e.g. *Meloidogyne* spp. and *Heterodera* spp.) (Grundler et al., 1991). A study by Jones et al. (2007) found that infection of *transparent testa* (*tt*) mutants of *Arabidopsis,* which are defective in parts of the flavonoid pathway, i.e. *tt4/tt6, tt4/tt5 and tt6,* resulted in an increased number of female cyst nematodes (Jones et al., 2007). In contrast, a similar study by Wuyts et al. (2006a) using different *Arabidopsis* flavonoid mutants, i.e. *tt3, tt4, tt5* and *tt7,* infected with *M. incognita,* found that the defects in the flavonoid pathway did not affect the number of adult females, egg masses, eggs or juveniles. A systematic dissection of the effects of specific flavonoid metabolites on fertility in different types of nematodes still remains to be done.

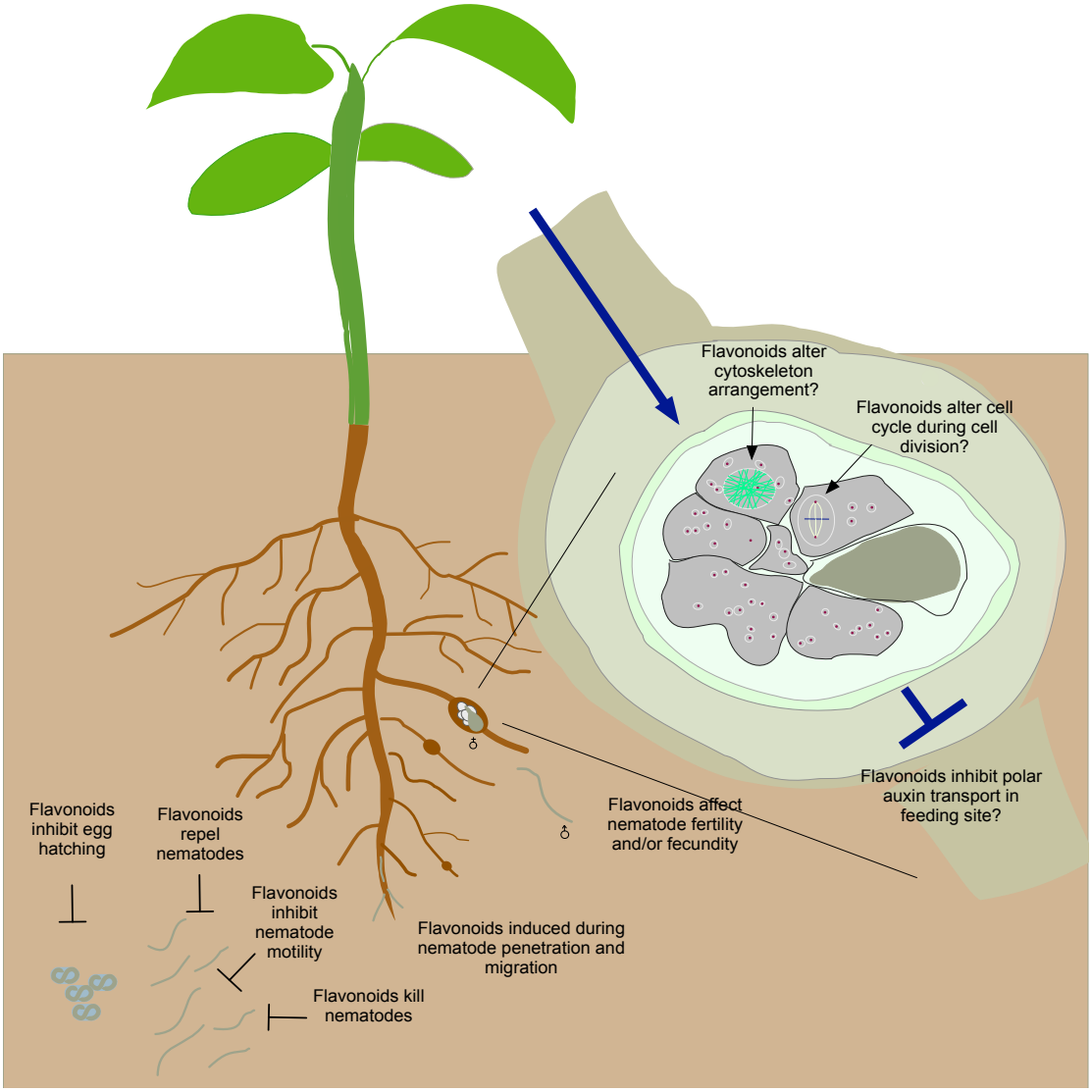

Figure 1.4: Summary diagram of multiple roles of flavonoids during a plant-nematode interaction. The example shown here is for root-knot nematodes. Flavonoids in the rhizosphere can have effects on the pre-parasitic stages by inhibiting egg hatching, repelling hatched nematodes, inhibiting their movement and by killing them. Expression of flavonoids is induced when the nematodes penetrate and migrate inside the root; they can act as defence compounds or signals for defence via cross talk with other defence/stress pathways. Flavonoids can affect adult stages of nematodes by altering their fertility and/or fecundity. The role(s) of flavonoids in feeding site development is less understood. They are postulated to be involved in the inhibition of auxin transport, cell cycle regulation and cell cytoskeleton rearrangement.

Name of enzyme/gene/metabolite	Flavonoid accumulation site	Suggested flavonoid function	Host studied	Nematode studied	Methods used	Reference
Sakuranetin	Leaf	Present only in resistant cultivars- suggested to be involved in defence	Rice	Stem nematode, *Ditylenchus angustus*	Chemical profiling of flavonoids using HPLC in resistant and susceptible cultivars	Plowright et al. (1996)
i. Formononetin-7-O-glucoside-6"-O-malonate ii. Formononetin iii. Medicarpin-3-O-glucoside-6"-O-malonate iv. Medicarpin	Roots, meristems, leaves	Suggested that resistance to nematodes is associated with a rapid activation of plant defences and suppression of secondary opportunistic infection	White clover, *Trifolium repens*	Stem nematode, *Ditylenchus dipsaci*	Chemical profiling of flavonoids using HPLC in resistant and susceptible cultivars	Cook et al. (1995)
i. Medicarpin glucoside malonate ii. Formononetin-7-O-glucoside-6"-O-malonate iii. Formononetin glucoside iv. Coumesterol glucosides	Roots	Suggested that isoflavonoid conjugate accumulation correlated with resistance. Interestingly, these flavonoids accumulated in roots, although infection sites were in the shoots, thereby indicating the presence of a systemic signal/defence.	Lucerne, *Medicago sativa*	Stem nematode, *Ditylenchus dipsaci*	Chemical profiling of flavonoids using HPLC and enzymatic assays in resistant and susceptible cultivars	Edwards et al. (1995)

i. O-methyl-apigenin-C- hexoside-O-deoxyhexoside ii. Apigenin-C-hexoside-O-pentoside iii. Luteolin-C-hexoside-O-pentoside	Roots and shoots during *P. neglectus* and *H. avenae* infection	Flavonoids possibly acted as broad defence compounds- induced in methyl jasmonate and nematode treated plants. Plants treated with root extracts from methyl-jasmonate induced plants had reduced infection.	Oats, *Avena sativa*	Root lesion nematode, *Pratylenchus neglectus,* Cereal cyst nematode, *Heterodera avenae,* Stem nematode, *Ditylenchus dipsaci*	Chemical analysis of methyl jasmonate and nematode-induced compounds using HPLC, followed by LC-MS for structural identification. Biological activities of these compounds were tested in *H. avenae* and *P. neglectus* infected plants.	Soriano et al. (2004)
i. Coumesterol ii. Psoralidin	Roots	Coumestrol and psoralidin accumulated in roots and were localised at lesion sites caused by nematodes only in lima bean. Coumestrol significantly inhibited nematode motility at 10-15μg/ml concentrations.	Lima bean, *Phaseolus lunatus* and snap bean, *P. vulgaris*	Root-lesion nematode, *Pratylenchus scribneri*	Root extracts of nematode infected *P. lunatus* and *P. vulgaris* were separated on TLC plates and these compounds were purified, characterised and tested for effects on nematode motility.	Rich et al. (1977)
i. Phenylalanine ammonia lyase ii. Chalcone synthase iii. Isoflavone reductase iv. Caffeic acid *O*-methyltransferase v. Medicarpin	Roots	Medicarpin is implied to play a role in nematode resistance- flavonoid enzyme gene expressions were constitutively higher in resistant plants; medicarpin levels were higher in two resistant cultivars compared with susceptible plants and medicarpin inhibited *P. penetrans* in a concentration dependent manner.	Alfalfa, *Medicago sativa*	Root-lesion nematode, *Pratylenchus penetrans*	Gene expression analysis of flavonoid enzymes via Northern blot and root extract analysis via HPLC in resistant and susceptible cultivars. *In vitro* motility assay to test the effect of medicarpin on *P. penetrans* motility.	Baldridge et al. (1998)
Glyceollin	Stele in roots	Suggested that glyceollin was associated with the incompatible interaction between the resistant	Soybean, *Glycine max*	Root-knot nematodes, *Meloidogyne incognita* and *M. javanica*	Gyceollin was quantified from root extracts, stele and cortex of two soybean	Kaplan et al. (1980a)

		cultivar and *M. incognita*: accumulation was localised in the stele of resistant roots, high concentrations of glyceollin in resistant cultivar and glyceollin only inhibited the motility of *M. incognita*.			cultivars infected with either *M. incognita* or *M. javanica* using TLC. In addition, an *in vitro* motility test of the effect of gyceollin was tested on *M. incognita* and *M. javanica*.	
i. Phenylalanine ammonia lyase ii. Chalcone synthase iii. Chalcone isomerase iv. 4-coumarate-CoA ligase v. Glyceollin	Roots	Suggested that nematode resistance is associated with the induction of the expression of enzymes in the phenylpropanoid pathway, *ie*. phenylalanine lyase, chalcone synthase, chalcone isomerase and 4-coumarate-CoA ligase to produce the defence compound, glyceollin.	Soybean, *Glycine max*	Soybean cyst nematode, *Heterodera glycines* and root-knot nematode, *Meloidogyne incognita*	Quantified gene expression of enzymes in the phenylpropanoid pathway in resistant and susceptible cultivars during *H. glycines* and *M. incognita* infection. This was followed by an enzyme activity assay and glyceollin quantification.	Edens et al. (1995)
Phenylalanine ammonia lyase	Roots	Proposed that plants grown at 27°C had optimal phenylalanine ammonia lyase activity, which enabled the plants to synthesise phenylpropanoids used in nematode defence, as opposed to 32°C, which inhibited enzyme activity.	Tomato, *Lycopersicum esculentum*	Root-knot nematode, *Meloidogyne incognita*	Tested phenylalanine ammonia lyase activity from plants grown at 27°C and 32°C.	Brueske (1980)
Glyceollin	Roots	Glyceollin I and III accumulated faster, at higher levels in tissues immediately adjacent to the nematode head in the resistant cultivar compared with the susceptible cultivar. The authors concluded that glyceollin was the predominant flavonoid produced in incompatible interactions for nematode defence.	Soybean, *Glycine max*	Soybean cyst nematode, *Heterodera glycines*	Quantified glyceollin content (µg/g) using HPLC in resistant and susceptible cultivars. This was complemented by radioimmunoassay of syncytium sections to quantify and localise trace amounts of glyceollin (nmole/ml)	Huang and Barker (1991)

Glyceollin	Leaves	The authors suggested that glyceollin accumulates at sufficiently high concentrations at infection sites to result in a localised hypersensitive response by inhibiting nematode motility and respiration as well as plant tissue death via inhibition of mitochondrial electron transport system.	*In vitro* system	Root-knot nematodes, *Meloidogyne incognita* and *M. javanica*	Soybean leaf glyceollin was tested on *M. incognita* and *M. javanica* J2s for motility inhibition. The authors also tested the effect of glyceollin on *M. incognita* J2 and soybean mitochondria respirations.	Kaplan et al. (1980b)
Phaseollin	Hypocotyl and root	Phaseollin was extracted only from *P. penetrans* infected tissue. Phaseollin was absent in uninfected controls. The survival of *P. penetrans* juveniles incubated for 16 hours in 47μg/ml of phaseollin solution were unaffected.	Common bean, *Phaseolus vulgaris*	Root-lesion nematode, *Pratylenchus penetrans*	Solvent extraction of phaseollin with thin layer chromatography from infected tissues.	Abawi et al. (1971)
i. Quercetagetin (hydroxyflavone) ii. Aurone iii. Chalcone	Adult female extracts	The yellow colouration in *G. rostochiensis and G. pallida* is attributed to flavonoid quercetagetin which was present in pathotypes with yellow colour and absent in paler pathotype. The authors also suggested that these nematodes can modify host flavonoids as shown by the accumulation of quercentagetin which is absent in the potato host but derived	N/A	Potato cyst nematodes, *Globodera rostochiensis* and *G. pallida*	Adult female extracts of *G. rostochiensis* and *G. pallida* pathotypes were separated using TLC and spots were identified with UV light, with spectra recorded using a spectrophotometer.	Vlachopoulos and Smith (1993)

		from plant quercetin and kaempferol.				
i. Flavan-3,4-diols ii. Condensed tannins	Roots	Flavan-3,4-diols and condensed tannins are postulated to be involved in defence as they accumulated after nematode infection.	Banana, *Musa*	Burrowing nematode, *Radopholus similis*	Chemical profiling of different banana cultivars using TLC and HPLC.	Collingborn et al. (2000)
Quercetin 7-glucoside and other phenols	Root extracts	Root extracts inhibited nematode motility, reduced nematode egg hatching and reduced galls numbers.	*Lantana camara* L.	Root-knot nematode, *Meloidogyne javanica*	Root extracts were tested on nematodes were identified using TLC and paper chromatography.	Shaukat et al. (2003)
Flavonoid pathways: chalcone synthase, chalcone isomerase and flavonoid 3' hydroxylase	N/A	*tt* mutant lines of single and double *tt4*, *tt5* and *tt6* did not reduce the number of adult females, with several lines reporting more female nematodes. The authors suggested that flavonoids are not essential for the formation/develop-ment of nematode feeding sites.	*Arabidopsis thaliana*	Sugar beet nematode, *Heterodera schachtii*	*Arabidopsis tt* mutants were infected with *H. schachtii* and the number of adult females that developed was counted.	Jones et al. (2007)
Chalcone isomerase	Roots	Chalcone isomerase was upregulated in the partially resistant cultivar, CE109, but not in the highly resistant cultivar, CE31. *In silico* analyses predicted that chalcone isomerase, chalcone synthase, dihydroflavonol 4-reductase and flavonoid 3' hydroxylase interacted in CE109. Authors suggested different cultivars utilised different metabolic pathways for defence against nematodes.	Cowpea. *Vigna unguiculata* L. Walp	Root-knot nematode, *Meloidogyne incognita*	Proteins were extracted from a highly and a partially resistant cowpea cultivars were infected with *M. incognita*. These were separated and identified using protein databases. A selected few identified proteins were checked for transcript expression using qRT-PCR and protein-protein interactions were predicted *in silico*.	Villeth et al. (2015)
Chalcone isomerase Auxin-induced protein	Roots	Chalcone isomerase transcripts and proteins were upregulated at 4, 5 and 6 days post inoculation. This upregulation was proposed to increase	Cowpea. *Vigna unguiculata* L. Walp	Root-knot nematode, *Meloidogyne incognita*	Proteins were extracted from inoculated and non-inoculated cowpea resistant cultivar, CE31	Oliveira et al. (2014)

		phenylpropanoid production in defence response and perhaps the use of flavonoids to regulate auxins in nematode feeding sites.			and were separated. More abundant proteins were selected for identification and qRT-PCR analysis.	
Flavonoid pathways: i. *Arabidopsis:* chalcone synthase, chalcone isomerase and flavonoid 3' hydroxylase, dihydroflavonol 4- reductase ii. Tobacco: phenylalanine lyase enzyme, anthocyanidins	Roots	*M. incognita* reproduction was significantly higher in tobacco mutant with higher anthocyanidin content. *M. incognita* reproduction in *Arabidopsis tt* mutants and wild-type plants were similar.	Tobacco, *Nicotiana tabacum* & *Arabidopsis thaliana*	Root-knot nematode, *Meloidogyne incognita*	Tobacco and *Arabidopsis* mutants were initially characterised for changed phenylpropanoid metabolism with HPLC or by staining methods. Next, these plants were infected with *M. incognita* and the infection phenotypes were scored.	Wuyts et al. (2006a)
i. Daidzein ii. Genistein iii. Other isoflavonoids	Roots	Daidzein and genistein increased in susceptible Sussex cultivar at two and four days post inoculation. Isoflavonoid production was enhanced in nematode infected plants in susceptible Sussex and resistant Hartwig cultivar at two and three days post inoculation. The authors speculated that isoflavonoids do not play a protective role against nematodes.	Soybean, *Glycine max*	Soybean cyst nematode, *Heterodera glycines*	Root extracts from susceptible Sussex cultivar were analysed using HPLC for flavonoid changes. Overall isoflavonoid production in root extracts was indirectly measured via the activation of a *nod* gene fused to β-galacoside reporter.	Kennedy et al. (1999)
Several compounds from the chalcone, flavone, flavanone, isoflavonoid and flavonol pathways.	Purified compounds and plant extracts.	The flavonols, kaempferol, quercetin and myricetin repelled *R. similis* and *M. incognita* juveniles at concentrations ranging 60-84 µg/ml. In addition, the flavone, luteolin and	N/A	Burrowing nematode, *Radopholus similis*, root-lesion nematode, *Pratylenchus penetrans* and root-knot nematode,	Multiple phenolic compounds at four concentrations, 200, 100, 50 and 20 µg/ml were tested on nematode	Wuyts et al. (2006b)

		isoflavonoids, daidzein and genistein repelled *R. similis* at higher concentrations, 100-142 µg/ml. Flavonols such as kaempferol, quercetin, myricetin, rutin and quercitrin inhibited 13- 41% of *M. incognita* juveniles after 48 hours of incubation. The flavonones, naringenin and hesperetin, the flavone, apigenin, the isoflavonoid, daidzein and the flavonol, kaempferol reduced egg hatching in *R. similis* up to 21%. This study showed that purified flavonoids have different effects of nematode juveniles at a range of concentrations.		*Meloidogyne incognita*	juveniles using *in vitro* approaches to test for effects on chemotaxis, motility and hatching inhibition.	
(*E*)-chalcone	Purified compound	(*E*)-chalcone killed nematodes at 33µM within 24 hours and completely inhibited egg hatching at <10µM within 15 days. The authors proposed that (*E*)-chalcone is an effective alternative to hazardous chemicals to control potato cyst nematodes.	N/A	Potato cyst nematodes, *Globedera rostochiensis* and *G. pallida*	Juveniles and eggs of *G. rostochiensis* and *G. pallida* were soaked in (*E*)-chalcone solution to test the nematicide and hatch inhibition activity of (*E*)-chalcone.	González and Estévez-Braun (1998)
i. Patuletin ii. Patulitrin iii. Quercetin iv. Rutin	Purified compounds and marigold, *Tagetes patula* L. flower extracts	Patuletin killed 100% of nematodes at various dilutions after 72 hours, whereas patulitrin killed 10-50% and quercetin killed 70-80% of nematodes. On the other hand, higher concentration of rutin, 0.5-1% killed all nematodes within 24 hours. The authors suggested that flower extracts containing the active nematicidal compounds could be used to control nematodes.	N/A	Corn cyst nematode, *Heterodera zeae*	Juveniles of *H. zeae* were soaked in the flower extracts or purified compounds to determine their nematicide activity.	Faizi et al. (2011)
i. Chalcone synthase gene	Root tissue	Most genes from the chalcone synthase, chalcone flavanone	Soybean, *Glycine max*	Soybean cyst nematode, *Heterodera glycines*	RNA was extracted from uninoculated and	Ithal et al. (2007)

ii. Chalcone flavanone isomerase gene iii. Isoflavone reductase gene (putative) iv. Dihydroflavonol 4-reductase gene v. Quercetin 3-O-methyltransferase 1 gene vi. 4-coumarate-CoA ligase vii. *PIN 2* gene		isomerase, isoflavone reductase, dihydroflavonol 4- reductase, 4-coumarate-CoA ligase and quercetin 3-O-methyltransferase 1 and *PIN 2* genes were upregulated in nematode infected roots.	L. Merr. cv. Williams 82	Ichinohe	inoculated plants at 2, 5 and 10 days post inoculation. These samples were used on Affymetrix Gene Chip with the soybean genome array to quantify gene expression changes. This was followed by validation of gene expression changes using qPCR.	
i. Chalcone isomerase ii. Chalcone synthase iii. Isoflavone reductase iv. Flavonoid 3'-monooxygenase v. Isoflavone-7-o-methyltransferase vi. Phenylalanine ammonia lyase vii. Dihydroflavonol 4- reductase viii. Caffeoyl-CoA 3-O-methyltransferases ix. 4-coumarate CoA-ligase x. Cinnamoyl CoA	i. Syncytium cells ii. Uninoculated neighbouring pericycle cells	At 3 and 6 dpi, syncytium cells suppressed flavonoid genes compared to uninoculated pericycle cells. In contrast, these genes were induced at 9dpi syncitium. In addition, these flavonoid gene expressions were found to increase from 3dpi to 6dpi and 6dpi to 9dpi syncytia. The authors suggested that flavonoids were synthesised as phytoalexins during a later resistance response which starts at 6dpi.	Soybean, *Glycine max* genotype PI 88788	Soybean cyst nematode, *Heterodera glycines* population NL1-RHg/ HG-type 7	Syncytium cells and uninoculated pericycle and neighbouring cells were collected using laser capture microdissection. RNA was extracted from these samples and was used on Affymetrix Gene Chip with the soybean genome array to quantify gene expression changes.	Klink et al. (2010)

reductase						
i. Chalcone synthase genes, *CHS1, CHS2, CHS3* ii. Auxin responsive gene, *GH3*	Root tissue	*CHS1::gusA, CHS2::gusA* and *CHS3::gusA* expressions overlapped with *GH3::gusA* expression at 48 hours, 72 hours and 120 hours post inoculation.	White clover, *Trifolium repens* cv. Haifa	Root-knot nematode, *Meloidogyne javanica*	*CHS::gusA* and *GH3::gusA* reporter constructs were transformed into the roots of white clovers. These roots were inoculated with *M. javanica* and were subsequently stained for GUS staining to compare gene expression localisations.	Hutangura et al. (1999)
iii. Chalcone synthase	Root tissue	Flavonoid deficiency did not affect gall numbers. Flavonoid deficient roots had shorter galls and less pericycle cell division compared to roots with flavonoids.	Barrel medic, *Medicago truncatula*	Root-knot nematode, *Meloidogyne javanica*	*M. truncatula* roots were transformed with a RNAi construct that targeted chalcone synthase genes to silence flavonoid production in the root. Roots were then screened for flavonoid deficiency based on lack of autofluorescent flavonoids. These roots were infected with *M. javanica* and gall sizes and cell sizes were measured	Wasson et al. (2009)

Table 1.1: Summary of the involvement of plant flavonoids in plant-nematode interactions. Rows in red indicate studies demonstrating the role of flavonoids in nematode defence responses, whereas rows in blue indicate studies demonstrating the role of flavonoids in nematode feeding sites and rows in purple indicate studies intersecting across both roles.

1.6 Flavonoids in the development of nematode feeding sites

Feeding sites are essential to the survival and the establishment of PPN parasitism. The PPNs feed on the cytoplasm of the cells, and sometimes mitochondria and plastids using their stylet (Wyss, 2002). Feeding sites are usually established by the second-stage juvenile (pre-parasitic stage), with some exceptions in *Naccobus aberrans, Tylenchus semipenetrans, Rotylenchulus* spp., whereby the adult females induce the feeding sites (Smant et al., 2018). PPNs form a variety of feeding sites, which are influenced by their life-style (e.g. migratory vs sedentary), with different degrees of plant cell manipulation. Migratory PPNs such as *Bursaphelenchus, Aphelenchoides* spp. and *Pratylenchus* spp. typically do not induce feeding sites, but rather feed off plant material directly, causing physical wounding. Sedentary PPNs with extended feeding duration induce specific and complex feeding sites inside their hosts. These include galls induced by root knot nematodes, which are characterized by multinucleate giant cells, and syncytia induced by the cyst nematodes. Inside the cells of the feeding site, PPNs cause multiple host cell responses to increase the starch, sugar and amino acid content, and turning the feeding cell into a metabolic sink by increasing transporter and plasmodesmatal networks, increasing cell surface area by cell wall invagination, and altering cell metabolism (Kyndt et al., 2013).

Feeding site formation also involves control of the plant cell cycle. Giant cells originate from approximately 3-10 procambium cells within the root endodermis. These cells undergo multiple endoreduplication and acytokinetic mitosis, resulting in enlarged, multi-nucleated cells with dense cytoplasm and elaborate ingrowths (Bird, 1961, Palomares-Rius et al., 2017). The hypertrophy of giant cells and nematode enlargement causes secondary cell divisions in the surrounding pericycle and cortical cells to accommodate these growths (Cabrera et al., 2015a). As a result, galls, or 'root knots', are formed on the root. Similarly to giant cells, syncytia are also multinucleate but are formed from the protoplast fusion and cell wall dissolution of several adjacent pericycle or procambium cells (Davies et al., 2012). As there are no secondary cell divisions, no gall is formed.

Flavonoids may be involved in the regulation of polar auxin transport to enhance auxin accumulation in nematode feeding sites (Figure 1.4). Some flavonoids inhibit cell-to-cell polar auxin transport and/or the inhibiting auxin efflux transporters, PIN and PGP (Peer

et al., 2004, Peer and Murphy, 2007). In addition, some flavonoids can control auxin content by regulating IAA oxidase (Stenlid, 1963). The initiation and development of both feeding sites requires local auxin accumulation and redistribution for cell division, cell differentiation, cell wall loosening and the growth of new vascular tissue (Balasubramanian and Rangaswami, 1962, Karczmarek et al., 2004, Ng et al., 2015a). Studies by Kyndt et al. (2016) and Grunewald et al. (2009) showed that root knot and cyst nematodes modulate PIN proteins to increase auxin levels and redistribute auxin in feeding sites and neighboring cells. For example, the expression of *PIN2* and *PIN7* was suppressed in giant cells and syncytia, presumably to increase auxin transport into those cells. Furthermore, transcriptomic and proteomic analysis in root knot and cyst nematode-infected roots demonstrated a correlation between flavonoid gene/protein expressions with auxin inducible gene/protein expression. For instance, Oliviera et al. (2014) found the chalcone flavone isomerase protein and auxin-induced protein were upregulated in cowpea at 4-6 days post inoculation with *M. incognita,* whereas Ithal et al. (2007) found upregulation of several flavonoids in soybean (eg. chalcone synthase, chalcone isomerase, isoflavone reductase) and *PIN2* transcripts in cyst nematode infected roots. A study by Hutangura et al. (1999) observed that the induction of *CHS1* and *CHS2* (chalcone synthase enzyme is the first enzyme in flavonoid synthesis) in root-knot nematode galls, coincided spatially and temporally with increased auxin response, within 120 hours of inoculation. These studies suggest that flavonoids could be employed by nematodes early during feeding site development to facilitate auxin accumulation. Nevertheless, there are gaps in the link between flavonoids and auxins in nematode feeding sites, as there has neither been any research demonstrating *in vitro* or *in planta* manipulation of flavonoids resulted in the inhibition of PIN proteins. We also don't know which specific flavonoid metabolite is used in this process. We postulate that flavonols such as kaempferol, quercetin and their glycosides would be likely used by these nematodes for auxin regulation as they have been shown to inhibit polar auxin transport (Jacobs and Rubery, 1988, Yin et al., 2014, Ng et al., 2015a).

Even though flavonoids may be involved in feeding site development, they appeared unessential and are unlikely involved in feeding site initiation as (Wasson et al., 2009) demonstrated that root knot nematodes can still initiate galls in flavonoid-deficient roots of *Medicago truncatula*. However, as these galls were reported to be smaller, with reduced numbers of dividing pericycle cells, perhaps due to reduced local auxin accumulation in the gall. This suggests that flavonoids may be required to maintain local auxin maxima in feeding

sites for long-term maintenance and development. As mentioned above,Wuyts et al. (2006a) also showed that flavonoid deficiency in *Arabidopsis* did not alter the infection and reproduction capacity of *M. incognita*.

Flavonoids may also be involved in the cell cycle regulation of PPN feeding sites (Figure 1.4). PPN feeding sites commonly contain enlarged nuclei with higher DNA content compared to other cells (de Almeida Engler et al., 1999), a process achieved through endoreduplication in the S-phase of mitosis during cell proliferation (de Almeida Engler and Gheysen, 2012). It is presumed that endoreduplication is a strategy used to increase DNA content and gene dosage, thereby increasing cell metabolism and growth in feeding sites (Siddique and Grundler, 2015). These processes are mostly studied in giant cells and syncytia, in which endoreduplicating cells bypass the transition from G2 to mitosis phase and remain in repeated loops of G2-, G1-, S- and back to G2 via the activity of cyclin-dependent kinases and other regulators e.g. *CCS52* classes (de Almeida Engler et al., 2015, de Almeida Engler et al., 2012). Flavonoids such as quercetin, genistein, persicogenin, artemetin, luteolin, penduletin and vitexicarpin inhibit cell cycle progression from G2 to mitosis and induce cell apoptosis in mammalian models (Li et al., 2014). It is plausible that flavonoids could be used to regulate endoreduplication by PPNs with an additional regulation to prevent cell apoptosis but this has not been substantiated in plant models. Furthermore, the cell cycle regulation in giant cells is complicated by the switch between endoreduplication and acytokinetic mitosis, indicating the ability of root-knot nematodes to up and down-regulate different sets of cyclin-dependent kinases and potentially specific types of flavonoids.

Giant cells and syncytia undergo extensive cytoskeleton rearrangement for their initiation and development. Root knot nematodes induce partial depolymerisation of actin filaments, particularly in phragmoplasts (resulting in incomplete cytokinesis) in giant cells, whereas cyst nematodes induce complete depolymerisation of actin filaments in syncytia, although it unknown how this occur (de Almeida Engler et al., 2010). In addition, root knot and cyst nematodes can modify actin transcription. For instance, the actin genes ACT2 and ACT7 were upregulated in giant cells and syncytia during early infection (de Almeida Engler et al., 2004). These PPNs may partly achieve this via flavonoids (Figure 1.4) as Böhl et al (2007) discovered that kaempferol, quercetin, fisetin and genistein could depolymerize actin and inhibit actin transcription in a dose dependent manner at micromolar concentrations. In contrast, epigallocatechin stimulated actin polymerization and transcription (Böhl et al.,

2007). So far, flavonoid deficient mutants have not been utilized to study the effects of flavonoids on the cytoskeleton inside feeding sites *in planta*.

1.7 Aims and hypotheses

This thesis aims to dissect the roles of flavonoids in plant defence mediation during *M. javanica* infection in the host, *Medicago truncatula* and as auxin transport regulators during gall development. Whilst the former role has been extensively explored as aforementioned, most studies had focused on a single pathway or a handful of flavonoids at late infection, whereas the latter role is still contentious.

The first aim of this thesis is to screen for flavonoids elicited in *M. javanica* infection in the selected plant model, *M. truncatula*. *M. truncatula* was selected for this study because it has a well described flavonoid pathway, particularly the isoflavonoid pathways which are unique to legumes (Chu et al., 2014, Deavours et al., 2006, Farag et al., 2007, Farag et al., 2008, Kowalska et al., 2007) (Figure 1.3) and has been shown to be infected by *M. javanica* and other *Meloidogyne* spp. (Dhandaydham et al., 2008, Isabelle et al., 2012). This chapter started with the optimisation of tandem mass spectrometry techniques for best flavonoid detection and a detailed flavonoid profile in infected roots across seven time points, *i.e.* pre-infection, 30 minutes, 6 hours, 24 hours, 2 weeks and 4 weeks. Moreover, the results of this preliminary study were used to narrow down the critical time points and specific flavonoid pathways.

The second aim was to determine the function of flavonoids in defending the plant against nematodes. The experimental strategy involved the generation of full transgenic *M. truncatula* with silenced or over-expressed isoflavonoids and different accessions and cultivars with varying susceptibilities to root-knot nematodes. Flavonoids that were significantly upregulated in transgenics, accessions, and cultivars were selected for *in vitro* motility and chemotaxis assays to test their bioactivities in inhibiting nematode movement and in repelling nematodes. Furthermore, the effects of *in planta* modulation of isoflavonoids on nematode infection were tested using transgenic lines. Based on literature review, isoflavonoids are prime candidates as they are broad defence compounds, and as such, the over-production of isoflavonoids may result in poorer outcomes for the nematodes.

Lastly, the third aim investigated auxin homeostasis in galls and subsequently, if isoflavonoids were used as auxin transport regulators, as part of the homeostasis. As

current literature in auxin homeostasis in galls were lacking, auxin transport, auxin response and auxin concentrations were measured at 24 hours, 4 days and 4 weeks post inoculation, prior to testing the effects of altering *in planta* isoflavonoids on auxin transport in galls. Although flavonoids appeared to be non-essential as auxin transport inhibitors for gall initiation (Wasson et al., 2009), changes in flavonoids may influence gall development, and subsequently, gall size.

Chapter 2: Materials and Methods

2.1 Plant preparations
- 2.1.1. Plant materials
- 2.1.2. Plant growth media
- 2.1.3. Seed germination
- 2.1.4. Plant growth conditions

2.2 Nematode preparations
- 2.2.1. Nematode culture
- 2.2.2. Isolation and sterilization of pre-parasitic (J2) nematodes

2.3. Nematode inoculation on roots
- 2.3.1. Nematode handling practices
- 2.3.2. Infected plant growth conditions
- 2.3.3. Phenotyping nematode infection
  - 2.3.3.1.Gall numbers
  - 2.3.3.2.Gall size
  - 2.3.3.3.Egg numbers

2.4 Liquid chromatographs tandem mass spectrometry techniques for flavonoid and auxin quantification
- 2.4.1. Flavonoid quantification
  - 2.4.1.1. Flavonoid standards
  - 2.4.1.2. Flavonoid extraction protocols
    - 2.4.1.2.1. Flavonoid extraction of roots
    - 2.4.1.2.2. Flavonoid extraction of root exudates
  - 2.4.1.3. Liquid chromatography –electrospray ionization-quadrupole time of flight-mass tandem spectrometry (LC-ESI- Q-TOF-MS/MS) methods
  - 2.4.1.4. Data analysis
- 2.4.2. Auxin quantification
  - 2.4.2.1. Auxin standards
  - 2.4.2.2. Auxin extraction protocols
  - 2.4.2.3. LC-ESI- Q-TOF-MS/MS methods
  - 2.4.2.4. Data analysis

2.5 Generation of *Medicago truncatula* transgenics with modified flavonoid pathways
- 2.5.1 Cloning inserts for transformation
- 2.5.2 Transformation and regeneration methods
- 2.5.3 Transgenic plant growth conditions
- 2.5.4 DNA genotyping of transgenics
- 2.5.5 Phenotyping transgenics

2.1 Plant preparations

2.2.1. Plant materials

Medicago truncatula cv. 2HA, A17, DZA045 and F83005 seeds were purchased from The South Australian Research and Development Institute (SARDI), Adelaide, Australia.

M. truncatula GH3::GUS transgenics were generated by Tursun Kerim and Flavia Pellerone. *GH3::GUS* promoter fusion construct was cloned by Pellerone (van Noorden *et al*., 2007). Kerim transformed the construct into *Agrobacterium tumafaciens* AGL1 into highly somatic embryogenic *M. truncatula* cv. 2HA (Chabaud et al., 2007). Positive homozygotes were selected and maintained for 10 generations.

2.1.2. Plant growth media

Plants were grown on enriched Fåhraeus media. Stock solutions were prepared as below and were autoclaved before use;

Chemical	**Stock concentration**	**ml/ L water**
$CaCl_2 \cdot_2 H_20$	13.2g/100mL water	1
$MgSO_4 \cdot_7 H_20$	12g/ 100mL water	1
KH_2PO_4	10g/ 100mL water	1
$Na_2HPO_4 \cdot_{12} H_20$	15g/ 100mL water	1
$C_6H_5FeO_7$	0.5g/ 100mL water	1
Gibson's trace elements: **H_3BO_3** **$MnSO_4 \cdot_4 H_2O$** **$ZnSO_4 \cdot_7 H_2O$** **$CuSO_4 \cdot_5 H_2O$** **$H_2MoO_4 . H_2O$** **$Na_2MoO_4 \cdot_2 H_2O$**	 2.96g/ 1L water 2.03g/ 1L water 220mg/ 1L water 80mg/ 1L water 90mg/ 1L water 121mg/ 1L water	1
KNO_3	25.28g/ 100mL water	1
Agar (J3 grade)	N/A	10g

2.1.3. Seed germination

M. truncatula seeds were lightly scarified with sand paper and surface- sterilized in 6% (w/v) sodium hypochlorite for 10 minutes with 15 rpm vertical rotation. Next, the seeds were washed with sterile MiliQ water five times. The seeds were further sterilized and imbibed in 0.25mg ml^{-1} augmentin for 6 hours with 15 rpm vertical rotation. Thereafter, the seeds were rinsed with sterile MiliQ water five times and were plated on a plate of enriched Fåhraeus medium. The seeds were stratified for two days in the dark at 4°C. Germination was initiated by incubating the seeds inverted in 25°C for 16-18 hours. Seedlings with radicles were transferred to enriched Fåhraeus medium, with 5 seedlings per 15cm diameter round plate (Figure 2.1). Each plate was sealed ¾ from each side, leaving the top bare for plant respiration. The plates were arranged vertically in a container, with the roots covered with a black cardboard.

2.1.4. Plant growth conditions

The plants were grown in a controlled temperature room at 25°C with 16 hour light photoperiod, at 200 μE light intensity.

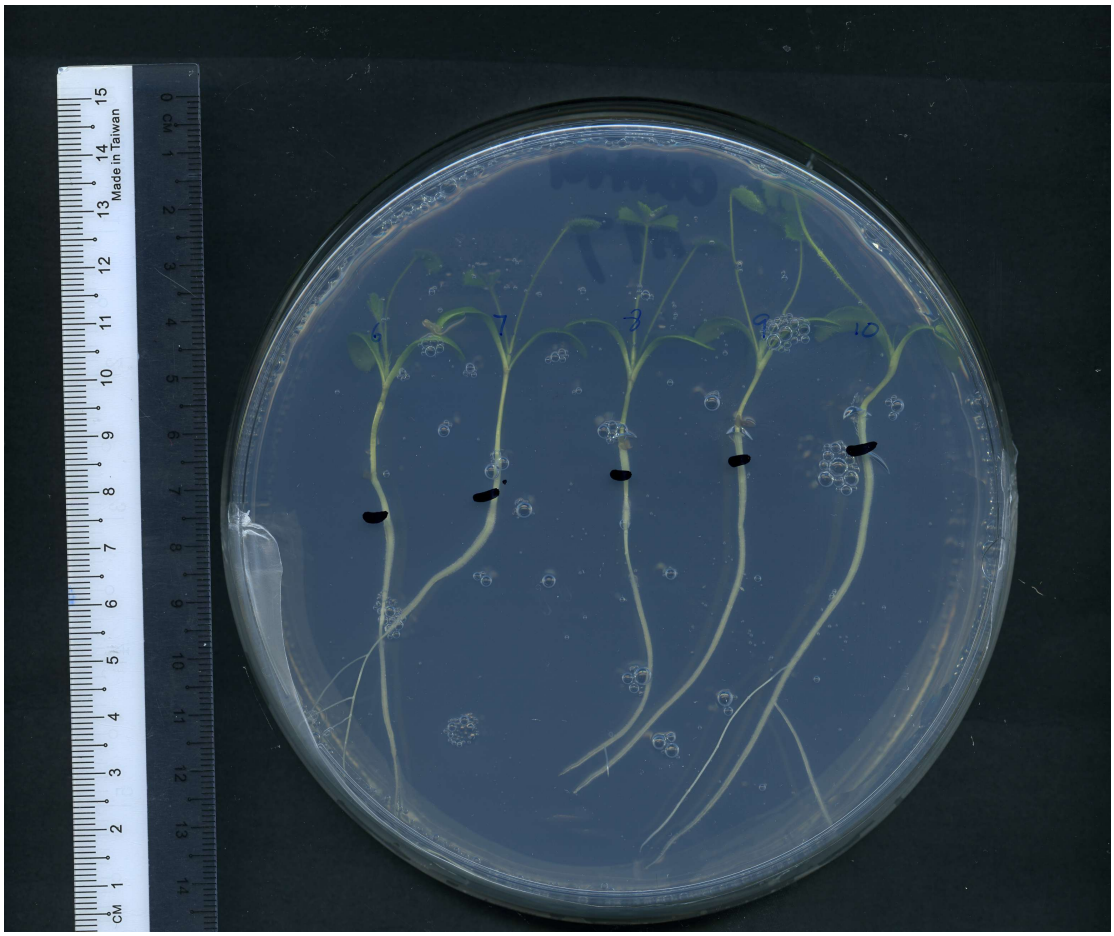

Figure 2.1: Five seedlings of *Medicago truncatula* were arranged in a 15cm diameter plate containing enriched Fåhraeus media. Seedlings shown here were 10 days old.

2.2 Nematode preparations

2.2.1. Nematode culture

The nematodes used in infection assays were *Meloidogyne javanica* isolated from Kiola, Australia. They were morphologically identified by Sofia Costa and PCR-identified using *M. javanica* specific primers (Zijlstra et al., 2000). Nematodes were cultured on *M. truncatula* cv. A17.

2.2.2. Isolation and sterilization of pre-parasitic (J2) nematodes

About 15 J2s were initially inoculated on the root tip of a week old *M. truncatula* cv. A17 grown in enriched Fåhraeus media. At five to six weeks post-inoculation, egg sacs were manually picked with a sharp forcep into 460 μl water in a 1.5ml Eppendorf tube. 40 μl of 12.5% sodium hypochlorite was added to the 460 μl suspension to make up 1% (w/v) sodium hypochlorite. The egg sacs were dissolved in the 1% (w/v) sodium hypochlorite for 4 minutes with intermittent shaking at room temperature. Post-incubation, the sodium hypochlorite was diluted with 1 ml sterile water. The eggs were centrifuged at 4000 rpm for 5 minutes. The supernatant was aspirated and eggs were rinsed with 500 μl sterile water. This washing step was repeated three times. After the final wash, the eggs were suspended in 500 μl sterile water. The eggs were then transferred onto a sterile 25 μm nylon mesh nematode sieve under 3 ml water immersion in a sterile 50 ml Falcon tube. The nematode sieve was made by cutting the conical end of a 15 ml Falcon tube with a searing hot scalpel to create a slightly melted blunt end with adheres to a 25 μm nylon mesh. The 50 ml Falcon tube was capped to maintain content sterility. The tube was placed on a tube rack and placed in a 25°C incubator in the dark. The eggs were incubated for 5-7 days to hatch fresh J2s. Based on the 25 μm size exclusion, only J2s will pass through the sieve. These J2s were pipetted into two 1.5 ml Eppendorf tubes and were centrifuged at 1467 x g for 10 minutes. Aspirated the supernatant. The J2s were surface-sterilized with 1 ml of a mixture of 0.002% (w/v) Triton X-100, 0.004% (w/v) sodium azide and 0.004% (w/v) mercury chloride for 10 minutes with 10 rpm vertical rotation.

Subsequently, the J2s were pelleted at 1467 x g for 5 minutes. The supernatant was removed and J2s washed with 1 ml sterile water three times, then re-suspended in 200 μl sterile water and counted in three aliquots of 5 μl on a glass slide under an upright microscope.

2.3 Nematode inoculation on roots

2.3.1. Nematode handling practices

A week old *M. truncatula* seedlings were inoculated by pipetting ~15-20 nematodes. Inoculation sites were marked with a black dot.

2.3.2. Infected plant growth conditions

Infected plants were grown as Section 2.1.4.

2.3.3. Phenotyping nematode infection

2.3.3.1. Gall numbers

Galls were counted at either 4 weeks or 6 weeks post inoculation, with the latter time chosen when egg numbers were concurrently counted. The galls were magnified for counting under the dissecting microscope, Nikon SMZ745 (Nikon, Japan) or Leica M205FA (Leica, Germany). The number of galls per plant was counted.

2.3.3.2. Gall size

Photos of galls were taken using the dissecting microscope, Leica M205FA (Leica, Germany) and gall size was measured using the area measurement function on Leica Application Suite v4.12 (Leica, Germany).

2.3.3.3. Egg numbers

Egg sacs were picked as described in Section 2.2.b from multiple root systems and were pooled into one or two 1.5 ml Eppendorf tube. The egg sacs were dissolved in sodium hypochlorite and rinsed in water as previously described (Section 2.2.2) to release the eggs from the egg sacs. Eggs were counted from three aliquots of 5 μl egg suspension from 500 μl final volume of egg suspension. The numbers of eggs were averaged across the three aliquots and multiplied by 100 to account for the final volume.

2.4 Liquid chromatography tandem mass spectrometry techniques for flavonoid and auxin quantification

2.4.1. Flavonoid quantification

2.4.1.1. Flavonoid standards

Afromosin and medicarpin standards were purchased from Apin Chemicals (UK). Apigenin, apigenin-7-O-neohesperidoside, coumesterol, kaempferol, naringenin, naringenin-7-O-rhamnoglucoside (naringin) and umbelliferone standards were purchased from Sigma (USA). 5,7- dihydroxyflavone (chrysin), 7,4'-dihydroxyflavone, biochanin A, daidzein, daidzein-7-O-glucoside (daidzin), daidzein 8-*C*-glucoside (puerarin), formononetin, formononetin-7-O-glucoside (ononin), genistein, glycitein, isoliquiritigenin, luteolin, quercetin, quercetin-3-O-rutinoside (rutin), standards were purchased from Indofine (USA). Genistein-7-O-glucoside (genistin), kaempferol-3-O-*D* glucoside, kaempferol-7-O- ß-glucoside, liquiritigenin, and naringenin-7-O-glucoside standards were purchased from Extrasynthese (France).

2.4.1.2. Flavonoid extraction protocols

2.4.1.2.1. Flavonoid extraction of roots

A 1 cm root segment was harvested from each infected root around the infection or gall formation site, placed into a clean mortar and pestle, and flash-frozen in liquid nitrogen. For earlier time-points in which galls were not visible, such as pre-infection, 30 minutes, 6 hours and 24 hours post-infection, root segments were taken from the marked nematode inoculation point. The frozen roots were macerated in the mortar and pestle that had been pre-cleaned with 100% (v/v) ethanol and 100% (v/v) methanol. These samples were split into flavonoid and auxin extraction protocols. Approximately 100 mg frozen tissue was weighed into each 1.5 ml Eppendorf tube. Next, the roots were lyophilized in a VirTis Benchtop Freeze Dryer (SP Scientific, USA) overnight. The roots were spiked with 25 μl of 1 ppm internal standard, umbelliferone (Sigma, USA), vortexed, and the internal standard was allowed to soak into the root material for 20 minutes. This was followed by the addition of 500 μl extraction solvent (methanol:water, 80:20, v/v) and vortexed to mix. The roots were

sonicated in a sonicator bath for one hour at 4°C and the samples centrifuged at 16100 x g for 15 minutes at 4°C. The supernatant was pipetted into a clean 1.5 ml Eppendorf tube. The extraction step was repeated by adding another 500 μl extraction solvent to the roots. After the flavonoid extraction, the solvent was dried down in a Speedvac centrifuge (Eppendord Concentrator 5301, Germany) at 30°C for 3.5 hours. The dried extracts were resuspended in 50 μl 80% methanol and vortexed. The solutions were filtered through a 0.2 µm regenerated cellulose micro-spin filter (CIRO, USA) by centrifuging at 16100 x g for 2 minutes at room temperature, and the resuspension step was repeated once. Finally, the filtrates were transferred into 1.5mL amber glass vials with insert (Agilent, USA) and vacuum-dried for storage at -80°C. Prior to analysis, the samples were thawed at room temperature for 10 minutes and resuspended in 50 μl 80% methanol.

2.4.1.2.2. Flavonoid extraction of root exudates

The whole root systems of five to six plants grown on 245 x 245mm rounded square plates (Corning™, USA) and the corresponding growth media were weighed. The growth media, consisting of the enriched Fåhraeus medium and agar, were freeze dried overnight in 50 mL Falcon tubes, with each tube being filled with 13-14 g of media in a VirTis Benchtop Freeze Dryer (SP Scientific, USA). An additional extraction control consisting of Fåhraeus medium without roots was used. The extraction solvent was prepared as 80% methanol, with the addition of 0.4 ppm umbelliferone as internal standard. To each Falcon tube, 20 ml of extraction solvent was added and flavonoids were extracted in the dark at 4°C with 40 rpm shaking on the orbital mixer (Ratek Instruments, Australia) for 2 hours. The flavonoid extracts were divided into 8-10 10 ml glass tubes and dried down in a Centrivap Benchtop Centrifugal Vacuum Concentrator with acrylic lid and Heat Boost (Labconco, USA). Dried extracts were resuspended in 100 μl 80% methanol (without umbelliferone) and the corresponding samples were pooled into one 10mL glass tube. The samples were vacuum centrifuged again. This was followed by addition of another 200 μl 80% methanol. The resuspended extracts were filtered through Amicon Ultra- 0.5 ml Centrifugal Filter Units with Ultracel-10 membrane to remove salts originating from the enriched Fåhraeus media. Finally, the filtrates were transferred into 1.5 ml amber

vials with insert and vacuum-dried for storage at -80°C until analysis. Prior to analysis, the samples were thawed at room temperature for 10 minutes and were resuspended in 50 μl 80% methanol.

2.4.1.3. Liquid chromatography –electrospray ionization-quadrupole-time of flight-mass tandem spectrometry (LC-ESI- Q-TOF-MS/MS) methods

An Agilent 6530 Accurate Mass LC-MS Q-TOF (Santa Clara, CA, USA) or Agilent LC-1290 Infinity coupled to 6550 iFunnel Q-TOF (Santa Clara, CA, USA) was used for mass spectrometry. Agilent 6530 Accurate Mass KC-MS Q-TOF was decommissioned in 2015 and was replaced with Agilent LC-1290 Infinity system. Flavonoid methods described in Chapter 3 were performed on the former system, whereas methods used in other chapters were performed on the latter. Both instruments were comparable, albeit with some minor retention time shifts. Seven µl of samples were injected into an Agilent Zorbax Eclipse reverse phase, C18, 1.8 µm, 2.1 x 50 mm column (Agilent, USA) for separation. Positive- and negative-ion mass spectra were acquired for method development and thereafter; only positive-ion mass spectra were acquired as most flavonoids were better detected in positive ionization (Chapter 3). Positive and negative ESI was performed in Jetstream interface with the settings as following: gas temperature 250°C, drying gas 5 l/min, nebulizer 30 psig, sheath gas temperature 350°C and flow rate of 11 l/min, capillary voltage 2500 V, nozzle voltage 500 V and fragmentor voltage 138 V. Solvent A consisted of 0.1% (v/v) formic acid/water, whereas solvent B consisted of 90% acetonitrile/water (v/v) with 0.1% (v/v) formic acid. Linear gradient of solvent B starts from 0-10% for 2 minutes, 10-25% for 7 minutes, 25-50% for 10 minutes, 50-70% minutes for 15 minutes, 70-90% for 20 minutes, and held at 90% until 24 minutes. The flow rate was 200 µl/min, with 400 bar pressure and the column temperature was kept at 35°C. Mass spectra were recorded over the range 100-1000 *m/z* at 3 spectra/s using collision induced dissociation with 18 psi N_2 collision gas and 1.3 *m/z* isolation window.

2.4.1.4. Data analysis

Agilent Technologies MassHunter (version B.5.0) software was used to analyze mass spectrometry data. Commercial flavonoid standards were used to determine elution times and collision energies. Additionally, to detect endogenous flavonoids in which commercial standards were absent, 600 mg of root bulk extract was run on tandem mass spectrometry. Limit of detection (LOD) and quantification (LOQ) was calculated for the internal standard, umbelliferone.

$$LOD = 3 \times \frac{signal}{noise}$$

$$LOQ = 5 \times \frac{signal}{noise}$$

Relative concentration of each analyte against the internal standard was calculated as shown (for root):

$$Relative\ concentration\ of\ analyte\ \left(\frac{ng}{g}\right) = \frac{Analyte\ area}{Internal\ standard\ area} \times \frac{Internal\ standard\ weight\ (ng)}{Root\ fresh\ weight\ (g)}$$

Relative concentration of each analyte against the internal standard was calculated as shown (for root exudate):

$$Relative\ concentration\ of\ analyte\ \left(\frac{ng}{g}\right) = \frac{Analyte\ area}{Internal\ standard\ area} \times \frac{Internal\ standard\ weight\ (ng)}{Root\ fresh\ weight + growth\ media\ weight\ (g)}$$

2.4.2. Auxin quantification

2.4.2.1. Auxin standards

Indole-3-acetic acid (IAA), IAA- aspartate, IAA-alanine, IAA-isoleucine, indole-3-butyric acid (IBA), and phenylacetic acid were purchased from Sigma (USA). IAA-phenylalanine, IAA-leucine, IAA-valine, IAA-tryptophan, and 4-chloroindole-3-acetic acid (4-Cl-IAA) were purchased from OlChemim (Czech Republic). The internal standard, deuterated IAA, indole-2,4,5,6,7-d5-3-acetic acid was purchased from Cambridge Isotope Laboratories (USA).

2.4.2.2. Auxin extraction protocols

Root segments were harvested as per flavonoid extraction protocol. The samples included the 6 hours, 4 days, 2 weeks and 6 weeks post inoculation root segments. The time points pre-infection, 30 minutes and 24 hours were excluded due to the lack of samples. Auxin extraction was done as (Ng et al., 2015b). Approximately 100 mg of macerated root tissue was weighed into a 1.5 ml Eppendorf tube and spiked with 20 µl of the internal standard (1 ug/ml 3-[$^{2}H_{5}$] indolylacetic acid). The samples were vortexed and the internal standard was allowed to soak into the tissue for 10 minutes. A volume of 500 µl of extraction solvent was added (methanol: propan-2-ol: glacial acetic acid, 20: 79:1, v/v/v) and the samples vortexed. The samples were then sonicated in a sonicator bath for 30 minutes at 4°C. Next, the samples were centrifuged at 16100 x g for 15 minutes at 4°C. The supernatant was transferred into a fresh 1.5 ml Eppendorf tube and this auxin extraction step repeated. The supernatants from both extraction steps were pooled in the same Eppendorf tube and vacuum-centrifuged in the dark at room temperature until the solvent had dried off. The supernatant was resuspended in 50 µl 100% methanol by vortexing. The suspension was passed through a 0.2 µm regenerated cellulose micro-spin filter (CIRO, USA) by centrifuging at 16100 x g for 2 minutes at room temperature. The resuspension step was repeated once. The filtrate was transferred into a fresh amber glass vial with an insert. Solvent was evaporated via vacuum centrifugation and capped for subsequent storage at -80°C. Prior to analysis, the samples were thawed at room temperature for 10 minutes and were resuspended in 50 μl of 100% methanol.

2.4.2.3. LC-ESI- Q-TOF-MS/MS methods

An Agilent LC-1290 Infinity coupled to 6550 iFunnel Q-TOF (Santa Clara, CA, USA) was used for auxin mass spectrometry. Seven µl of each sample was injected into an Agilent Zorbax Eclipse reverse phase, C18, 1.8 µm, 2.1 x 50 mm column (Agilent, USA) for separation. Based on Ng *et al*. (2016), the auxins IAA, IBA and IAA-Ala were ran on the positive mode, other species were ran on the negative mode. Positive and negative ESI was performed in Jetstream interface. Positive ionization was done with these settings: gas temperature 250°C, drying gas 5 l/min, nebulizer 30

psig, sheath gas temperature 250°C and flow rate of 11 l/min, capillary voltage 2500 V, nozzle voltage 500 V and fragmentor voltage 138 V. Solvent A consisted of 0.1% (v/v) formic acid, whereas solvent B consisted of 90% methanol/water (v/v) with 0.1% (v/v) formic acid. Solvent B gradient starts at 10-50% for 8 minutes, 50-70% at 12 minutes, held at 70% until 20 minutes. The flow rate was 200 µl/min, with pressure maintained at 400 bar and the column temperature was kept at 35°C. Mass spectra were recorded over the range 100- 950 *m/z* at 3 spectra/s using collision induced dissociation with 18 psi N_2 collision gas and 1.3 *m/z* isolation window. Negative ionization was done as follows: gas temperature 290°C, drying gas 5 l/min, nebulizer 25 psig, sheath gas temperature 350 °C and flow rate of 11 l/min, capillary voltage 3000 V, nozzle voltage 500 V and fragmentor voltage 140 V. The same solvents and elution settings were used as per positive ionization. Mass spectra were recorded over the range 100-1000 *m/z* at 3 spectra/s using collision-induced dissociation with 18 psi N_2 collision gas and 1.3 *m/z* isolation window.

2.4.2.4. Data analysis

Agilent Technologies MassHunter (version B.5.0) software was used to analyze mass spectrometry data. Commercial auxin standards were used to determine elution times and collision energies. Limit of detection (LOD) and quantification (LOQ) was calculated for the internal standard, d5-IAA.

$$LOD = 3 \times \frac{signal}{noise}$$

$$LOQ = 5 \times \frac{signal}{noise}$$

Absolute concentration of each analyte against the internal standard was calculated as shown:

$$Absolute\ concentration\ of\ analyte\ \left(\frac{ng}{g}\right) = \frac{Analyte\ area}{Internal\ standard\ area} \times \frac{Internal\ standard\ weight\ (ng)}{Root\ fresh\ weight\ (g)} \times Response\ factor$$

$$Response\ factor = \frac{Internal\ standard\ concentration\ (ppm)}{Analyte\ concentration\ (ppm)} \times \frac{Analyte\ area}{Internal\ standard\ area}$$

2.5. Generation of *Medicago truncatula* transgenics with modified flavonoid pathways

2.5.1. Cloning inserts for transformation

The vector used for silencing the flavonoid pathways was pk7WIWG2D(II), whereas the vector used for the overexpression of the flavonoid pathways was pK7WG2D. Samira Hassan has previously generated these vectors in *Escherichia coli* DH5α. These constructs were subsequently cloned into *Agrobacterium tumafaciens* AGL1 for *A. tumafaciens* mediated transformation. The sequences used for cloning are listed in Table 2.1.

Gene	Primer sequences	Gene sequence
Flavonol synthase (*FLS)* RNAi: derived from *FLS* XM_003614733, BT146097.1, XM_003614732.3	5'AGGAACAACAACGGTCCAAG3' 5'CCATCCTCTTTTCCCACTCA3'	1 GGAACAACAA CGGTCCAAGG TGTGAAACTT GGGGTACCAA TAATAGATTT CAGCAACCCA 61 GATGAGGTAA AGGTGCAAAA TGAGATAATA GAAGCAAGTA AAGAGTGGGG AATGTTTCAA 121 ATTGTGAACC ATGAAATTCC AAATGAAGTT ATAAGAAAGT TGCAAAGTGT TGGTAAAGAG 181 TTTTTTGAGT TACCACAAGA TGAAAAAGAG GTTTATGCTA AACCTGTTAT TGGATCTGAT 241 GTTTCTTCTG AAGGGTATGG TACAAAGCAT CAGAAAGAGT TGAGTGGGAA AAGAGGATGG
Isoflavone synthase (IFS) RNAi: derived from *IFS1,* XM_013601477.2, XM_0.13601742.2 and a putative *IFS* sequence	5'TCTTGCAGGAACAGACTCCA3' 5'CCCGTCGATCTCACATTCTT3'	1 CTTGCAGGAA CAGACTCCAC CGCCGTGTCT ACAGAATGGA CTTTATCAGA GCTCATCAAT 61 AATCCTAGAG TGTTGAAGAA AGCTCGAGAG GAGATTGACT CTGTTGTGGG AAAAGATAGA 121 CTGGTTGATG AATCAGATGT TCAGAATCTT CCTTACATTA AAGCCATCGT AAAAGAAGCA 181 TTTCGCTTGC ACCCACCACT ACCTGTAGTC AAAAGAAAAT GTACACAAGA ATGTGAGATC 241 GACGG
FLS over-expression (OE) derived from MTR_5g059140	5'ATGGAGGTAGAAAGGGTACA3' 5'TTATTGAGGGATCTTATTAA3'	1 ATGGAGGTAG AAAGGGTACA AACAATAGCT CATAAATCCA AAAACACTAC AATACCATCC 61 ATGTTCGTTA GGTCAGAAAC TGAGTCACCA GGAACAACAA CGGTCCAAGG TGTGAAACTT 121 GGGGTACCAA TAATAGATTT CAGCAACCCA GATGAGGTAA AGGTGCAAAA TGAGATAATA 181 GAAGCAAGTA AAGAGTGGGG AATGTTTCAA ATTGTGAACC ATGAAATTCC AAATGAAGTT 241 ATAAGAAAGT TGCAAAGTGT TGGTAAAGAG TTTTTTGAGT

		TACCACAAGA TGAAAAAGAG 301 GTTTATGCTA AACCTGTTAT TGGATCTGAT GTTTCTTCTG AAGGGTATGG TACAAAGCAT 361 CAGAAAGAGT TGAGTGGGAA AAGAGGATGG GTGGACCATT TTTTTCATAT CATATGGCCA 421 CCTTCATCTG TTAATTACAG TTGTTGGCCA AATAACCCTA CTTCCTATAG GGAGGTGAAT 481 GAGGAATATG GCAAGTACCT CCGTAGAGTG TCAAACAAAT TGTTCAATAT CATGTTAGTA 541 GGACTTGGGT TTGAAGAAAA TGAACTCAAG TCAGTTGCAG ATGAAAATGA GTTGATTCAC 601 CTATTGAAAA TCAATTACTA CCCACCATGT CCATGTCCTG ATCTGGTACT AGGTGTGCCA 661 CCACACACAG ATATGTGTTA TATTACCCTT CTCATACCCA ATGAAGTGGA GGGTCTTCAA 721 GCCTCTAGAG ATGGTCAATG GTATGATGTT AAGTATGTCC CCAATGCCCT CATTATTCAC 781 GTTGGTGACC AAATGCAGAT ACTAAGCAAT GGGAAATATA AGGCTGTATT GCACAGAACA 841 ACTGTAAACA AAGATGAGAC AAGAATGTCG TGGCCAGTGT TCATAGAACC CAAGCCAGAA 901 AACGAAGTTG GTCCTCACCC AAAGTTTGTT AACCAAGAGA ATCCTCCAAA GTACAAAACC 961 AAGAAATATA AGGATTATGC TTACTGTAAG CTTAATAAGA TCCCTCAATA A
IFS OE derived from *IFS1* (AY939826.1)	5'ATGTTGGTGGAACTTGCAGT3' 5'TTAGGAGGAAAGAAGTTTAT3'	1 ATGTTGGTGG AACTTGCAGT TACTCTATTG CTCATTGCTC TCTTCTTACA CTTGCGTCCA 61 ACACCTACTG CAAAATCAAA GGCTCTTCGC CACCTTCCAA ATCCACCAAG CCCTAAACCA 121 CGTCTTCCAT TCATAGGTCA TCTTCACCTT TTGGATAACC CACTTCTTCA CCACACTCTT 181 ATCAAGTTAG GAAAGCGTTA TGGCCCTTTG TACACTCTTT ACTTTGGTTC CATGCCTACC 241 GTTGTTGCAT CCACTCCTGA CTTGTTTAAA CTTTTCCTTC AAACCCATGA AGCTACTTCC 301 TTTAACACAA GATTCCAAAC CTCTGCTATT AGTCGTCTTA CCTATGACAA CTCTGTTGCT 361 ATGGTTCCAT TTGCACCTTA TTGGAAGTTT ATTAGAAAGC TTATCATGAA CGACTTGCTC 421 AACGCCACCA CTGTTAACAA ATTGAGGCCA TTGAGGAGCC GAGAAATCCT TAAGGTTCTT 481 AAGGTCATGG CTAATAGTGC TGAAACTCAA CAGCCACTTG ATGTCACTGA GGAGCTTCTC 541 AAGTGGACAA ACAGCACAAT CTCTACCATG ATGTTGGGTG AGGCCGAAGA GGTTAGAGAT 45 601 ATTGCTCGTG ATGTTCTTAA

		GATCTTTGGA GAATATAGTG TTACAAACTT TATTTGGCCT 661 TTGAACAAGT TTAAGTTTGG AAACTATGAT AAGAGAACTG AGGAGATTTT CAATAAGTAT 721 GATCCTATCA TTGAAAAGGT TATCAAGAAA CGACAAGAGA TTGTGAACAA AAGAAAAAAT 781 GGAGAAATCG TAGAAGGCGA GCAGAATGTT GTTTTTCTTG ACACTTTGCT TGAATTTGCA 841 CAAGATGAGA CCATGGAGAT CAAAATTACA AAGGAACAAA TCAAGGGTCT TGTTGTGGAT 901 TTTTTCTCTG CAGGAACAGA CTCCACCGCC GTGTCTACAG AATGGACTTT ATCAGAGCTC 961 ATCAATAATC CTAGAGTGTT GAAGAAAGCT CGAGAGGAGA TTGACTCTGT TGTGGGAAAA 1021 GATAGACTGG TTGATGAATC AGATGTTCAG AATCTTCCTT ACATTAAAGC CATCGTAAAA 1081 GAAGCATTTC GCTTGCACCC ACCACTACCT GTAGTCAAAA GAAAATGTAC ACAAGAATGT 1141 GAGATCGACG GGTATGTGGT TCCAGAAGGA GCACTAATAC TTTTCAATGT CTGGGCAGTG 1201 GGAAGAGACC CAAAATATTG GGTAAAGCCA TTGGAATTTC GTCCAGAGAG GTTCATAGAA 1261 AATGTTGGTG AAGGTGAAGC AGCTTCAATT GATCTTAGGG GTCAACATTT CACACTTCTA 1321 CCATTTGGGT CTGGAAGAAG GATGTGTCCT GGAGTCAATT TGGCTACTGC AGGAATGGCC 1381 ACAATGATTG CATCTATTAT CCAATGCTTC GATCTCCAAG TACCTGGTCA ACATGGAGAA 1441 ATATTGAATG GTGATTATGC TAAGGTTAGC ATGGAAGAGA GACCTGGTCT CACAGTTCCA 1501 AGGGCACATA ATCTCATGTG TGTTCCTCTT GCAAGAGCTG GTGTCGCAGA TAAACTTCTT 1561 TCCTCCTAA

Table 2.1: Sequences for cloning inserts in RNAi and OE vectors for *A. tumafaciens* mediated transformation.

2.5.2. Transformation and regeneration methods

The highly somatic embryogenic *M. truncatula* cultivar, Jemalong 2HA (SARDI, Australia) was used in this protocol. The transformation and regeneration of *M. truncatula* 2HA was adapted from Chabaud et al. (2007). Young leaflets from 2-3 week old axenic 2HA plants were selected. These were wounded using a scalpel in a moist environment to avoid desiccation. Next, the leaflets were inoculated with *A. tumafaciens* AGL1 by submerging them in bacterial liquid culture for a minute. Post-

incubation, about the leaflets were transferred to a petri dish containing solid callus inducing medium (CIM), added with 50 mg/l kanamycin with their abaxial side up. Then, the dishes were sealed and leaflets were co-incubated with *A. tumafaciens* for 3 days in 25ºC at 16 hours light and 8 hours dark photoperiod. The leaflets were decontaminated in 20 ml of fresh liquid CIM, which contained 50 mg/l kanamycin and 400 mg/l augmentin in a sterile 50 ml Falcon tube. The solution and leaflets were continually agitated for 3 days in 25ºC at 16 hours light and 8 hours dark photoperiod. After the decontamination step, the leaflets were induced to make calli by culturing them on solid CIM, with the addition of 50 mg/l kanamycin and 400 mg/l augmentin. The leaflets were subcultured into fresh solid CIM with the same antibiotics every 3 weeks. Each callus sized around 1 cm diameter was picked off the leaflets and was transferred to embryo-inducing medium (Mukhtar et al., 2015), supplemented with 50 mg/l kanamycin and 200 mg/l augmentin. The callus was subcultured in fresh solid EIM with the same antibiotics every 3 weeks. Embryos that developed on calli were removed and cultured on embryo-development medium (Kakar et al., 2008) which included 50 mg/l kanamycin and 200 mg/l augmentin. The embryos were refreshed in new EDM with the same antibiotics every 3 weeks. Leaves that developed from the embryos were rooted in plant development medium. Plantlets with developed leaves and roots were transferred into a GA-7 Magenta™ box (Sigma Aldrich, USA). Additional clones of the transformed plantlets were made by taking cuttings at the apical node every 2 months. Large plantlets were slowly acclimatized to green house conditions by gradually opening the box's lid weekly. Once the plant has acclimatized to green house conditions, it was transferred to Coco Mix (recipe in Section 2.5.3.).

2.5.3. Transgenic plant growth conditions

Transgenics were grown in Coco Mix (SARDI, Australia).
Recipe is as below (makes ~1000 L)
540 L Coco peat (Galaku, Australia) with 220 L water
100 L Waikerie sand
Steamed for an hour.
Added fertilizers, 180 g doimite lime, 600 g agricultural lime, 240 g hydrated lime, 180 g gypsum, 180 g superphosphate, 450 g iron sulphate, 30 g iron chelate, 180 g

micromax, 450 g calcium nitrate. This was allowed to cool. Finally, added 1800 g Osmocote Exact Mini 3-4M (Everris, USA) and mixed.
Plants were grown in glasshouses at day temperatures of 24-26°C, and night temperatures of 19-23°C. Flowering adult plants were supplemented with 0.17% (w/v) Thrive Soluble All Purpose Plant Food (Yates, Australia) once a week. Seed pods were collected 2-3 times per week and were dried for a minimum of 2 days in 30°C.

2.5.4. DNA genotyping of transgenics

Rapid mass genomic DNA extraction of transgenics was adapted from (Edwards et al., 1995). Samples for PCR were collected by pinching the leaf with the lid of a clean 2 ml safe lock microcentrifuge tube (Qiagen, USA). The leaf disc was frozen in liquid nitrogen. A 5 mm stainless steel bead was added to the tube for tissue maceration in the TissueLyser LT (Qiagen, USA) at 45 Hz for 1 minute, with a 30 second interval to re-freeze the sample in liquid nitrogen. A volume of 200 µl of the extraction buffer (200 mM Tris HCl pH 7.5, 250 mM NaCl, 25 mM EDTA, 0.5% SDS) was added to the ground tissue and vortexed for 5 seconds. Subsequently, the sample was centrifuged at 16100 x g for 5 minutes. A volume of 170 µl of supernatant was pipetted into a clean 1.5 ml Eppendorf tube and 170 µl isopropanol was added to the supernatant and inverted three times. Tubes were centrifuged at 16100 x g for 5 minutes and the supernatant discarded. The DNA pellet was washed with 200 µl 100% ethanol and centrifuged at 16100 x g for 5 minutes. The supernatant was removed and the DNA dried in a fume hood. Finally, the DNA was re-suspended in 600 µl MilliQ water, of which 5 µl of the solution was used for PCR.

The *NptII* (kanamycin resistance) gene was used as the transformation marker to identify transgenics. The primers nptII (Table 2.1) were designed to amplify a 533 base pair fragment. PCR was done on a C1000 Touch™ Thermal Cycler (BioRad, USA) using EconoTaq DNA polymerase (Lucigen, USA) as per manufacturer's instructions, with the exception of the annealing step, which was set at 55°C for 30 seconds and the extension step, which was set at 72°C for one minute. PCR products

were visualized on 0.8% TAE agarose gel dyed with 1x SYBR® Safe DNA gel stain (Thermo Fisher). As the DNA ladder, 5 µl HyperLadder™ 1kb (Bioline, USA) was used and 20 µl PCR product was pipetted into each well. The gel was run at 100 V for 35 minutes and bands visualized on a transilluminator Gel Doc XR+ (BioRad, USA).

2.5.5. Phenotyping transgenics

2.5.5.1 Flavonoid synthase gene expression phenotyping using quantitative real-time PCR

Medicago truncatula wild-type cv. 2HA and isoflavone synthase transgenics were germinated as Section 2.1.3. with the exception that IFSi 101-2 and IFSi 42-7 were germinated for 40 hours. 5-6 plants per genotype were grown in 200ml enriched Fahreus medium in 245x 245mm rounded square plates (Corning™, USA) for six weeks. At the end of the sixth week, the whole root system was harvested individually in liquid nitrogen. The root tissue was macerated with mortar and pestle in liquid nitrogen. ~100mg root tissue was used RNA extraction using Spectrum™ Plant Total RNA Kit (Sigma Aldrich, USA). The extraction was done as per manufacturer's protocol A with on-column DNase digestion. RNA concentration and quality was determined with NanoDropND-1000 (LabTech International). The 100ng of RNAs were used to synthesize cDNAs using First Strand cDNA Synthesis Kit (Thermo Fisher Scientific, USA) as per manufacturer's instructions. Primers used are listed in Table 2.2. qRT-PCR mixes were prepared with Fast SYBR®Green Master Mix (Thermo Fisher Scientific, USA) in 384-well plates (Thermo Fisher Scientific, USA). The reactions were run in ViiA 7 Real-Time PCR System (Thermo Fisher Scientific, USA). Results were analysed using LinReg (Ruijter et al., 2009).

Gene	Function	Primer sequence	Primer product (bp)
nptII	Determine expression of kanamycin resistance transgene in transformed plants	5'-TTCAGTGACAACGTCGAGCA-3' 5'-GGTGCCCTGAATGAACTCCA-3'	96
CHS	Determine the expression levels of 11 *CHS* gene members, including *CHS* RNAi target	5'-CACCGCTGTCACATTTCGTG-3' 5'-CGGGGTCAGAGCCAACAATA-3'	107
IFS	Determine the expression level of *IFS* RNAi target	5'-ACACTTGCGTCCAACACCTA-3' 5'-TGGAAGACGTGGTTTAGGGC-3'	82
GAPDH	Housekeeping gene	5'-TGCCTACCGTCGATGTTTCAGT-3' 5'-TTGCCCTCTGATTCCTCCTTG-3'	100

Table 2.2: Primer sequences used to DNA genotyping and RNA phenotyping of *Medicago truncatula* transgenics.

2.5.5.2 Flavonoid metabolite phenotyping of transgenic roots and root exudates via LC-ESI- Q-TOF-MS/MS

Flavonoids were extracted from ~100 mg root tissue (an aliquot of the whole root system). Root exudates were collected from the plant growth media. The flavonoid extraction of roots and root exudates protocols and mass spectrometry was done as Sections 2.4.1.2.1. and 2.4.1.2.2.

2.6 Auxin response analysis via GUS histochemical assay for *Medicago truncatula* GH3::GUSa infected with nematodes

M. truncatula GH3:: GUSa transgenics were inoculated with *M. javanica* J2s as described in Section 2.3.1.. Roots were harvested for GUS staining at 6 hours, 4 days, 2 weeks and 6 weeks post inoculation. Roots were fixed in 0.5% *p*-formaldehyde in 100 mM potassium phosphate buffer, pH 7.2, on ice under 500 mbar vacuum for 10 minutes, followed by rinsing the roots with potassium phosphate buffer three times. Roots were then submerged in X-gluc buffer [100 mM potassium phosphate buffer, 1 mM EDTA, 5 mM potassium ferri- and ferrocyanide, 50 mg/ml 5-bromo-4-chloro-3-inodolyl-beta-D-GlcUA (X-Gluc Direct)] at room temperature under 500 mbar vaccum for 10 minutes. Next, the roots were incubated in the buffer at 37°C for 4 hours. To stop the staining process, roots were removed from the buffer and rinsed with potassium phosphate buffer three times and were stored in the potassium phosphate buffer.

Whole root photos were taken with Leica dissecting microscope M205FA (Leica, Germany). Two roots with galls that were selected for sectioning were embedded in 3% DNA grade agarose (Amresco, USA) and were sectioned on a Vibratome (1000 Plus; Vibratome Company) at 100 µm thickness. Sections were mounted on glass slides in water and viewed with Leica DM5500 (Leica, Germany).

2.7 Acropetal auxin transport capacity measurement on uninfected and nematode-infected roots of *Medicago truncatula*

M. truncatula 2HA, IFSOE 10-3, IFSi 101A and IFSi 42-7 seeds were germinated as described in Section 2.1.3. with some modifications, whereby seeds of IFSOE 10-3, IFSi 101A and IFSi 42-7 were germinated in 21ºC for 16 hours, followed by 28ºC for 6 hours due to low germination rate. As such, seedlings in this experiment shared similar developmental age, instead of chronological age. The seedlings were infected as described in Section 2.3.1. Auxin transport capacity measurement was performed at 24 hours, 4 days and 4 weeks post inoculation and uninoculated controls as described by (Ng and Mathesius, 2016), with some adaptations. Sample preparations described below are illustrated in Figure 2.1.

For acropetal auxin transport capacity measurement at 24 hours and 4 days, the roots were excised 12 mm from the root tip. Thereafter, ^{3}H-IAA block was placed on the incision site for 6 hours in the dark at root temperature, with the roots placed vertically. After 6 hours, the roots were cut at every 4 mm segments. The first 4 mm segment, which was directly in contact with the ^{3}H-IAA block, was discarded, whereas the remaining two 4 mm segments (first or second segment consisted of inoculation spot, depending on root growth rate, whereas the second segment consisted of the root tip) were placed in 6 ml polyethylene scintillation vials (Perkin Elmer, USA) containing 2 ml scintillation fluid, Emulsifier safe (Perkin Elmer, USA). The radioactivity emitted from these segments was measured in the TriCarb 2800TR scintillation counter (Perkin Elmer, USA).

By 4 weeks, mature galls of variable morphologies were present, with up to 5 mm in length and 3-4 mm in diameter. Gall morphologies were divided into terminal or non-terminal galls (example diagram in Chapter 5, Table 5.3.). Galls were classified as terminal galls when primary root terminated at the gall, resulting in the loss of root tip and vice versa for non-terminal galls. Auxin transports in these galls were quantified by excising 16 mm of root segments, which included the galls. 16 mm segments were divided into 4 smaller segments of 4mm roots. The first 4 mm segment was discarded as described above, leaving the remaining 12 mm segments, which were used for quantification.

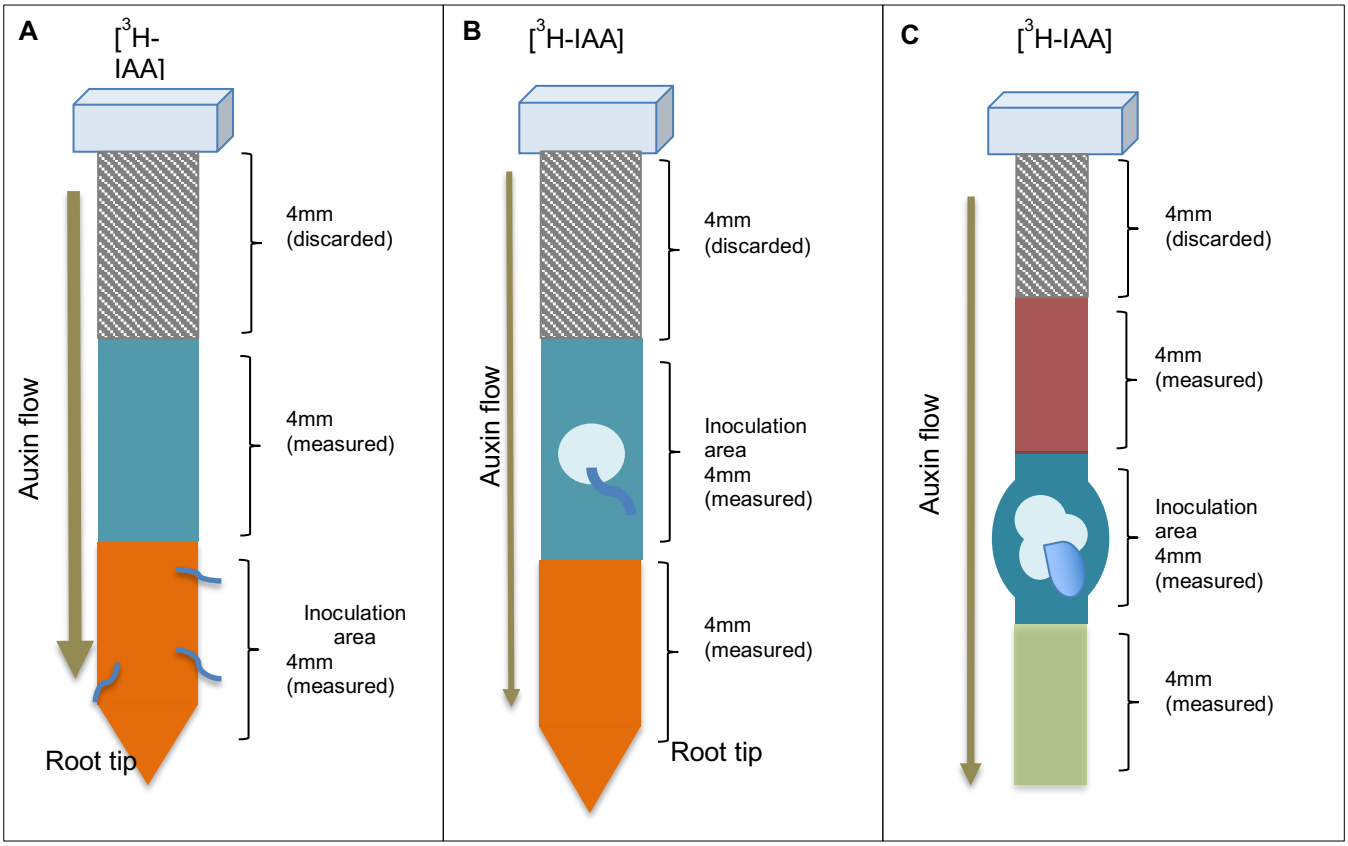

Figure 2.2: An illustration of acropetal auxin transport measurements in *M. truncatula* wild-type 2HA and IFS transgenics at 24 hours, 4 days and 4 weeks post inoculation. Auxin blocks were placed on excised root segment and the first 4mm segment was discarded. (A) Auxin transport measurement at 24 hours time with 12mm root segment which included the root tip. J2s were inoculated at the root tip. (B) Auxin transport measurement at 4 days time with 12 mm root segment which included the root tip. As the root had grown, the inoculation area had shifted away from the root tip. (C) Auxin transport measurement at 4 weeks with 16mm root segment.

2.8. *In vitro* studies of the effect of flavonoids and root exudates on the pre-parasitic stage of *Meloidogyne javanica*

Nematodes were hatched from eggs as described in Section 2.2.2. Freshly hatched, 3-4 days old nematodes were collected. The triple sterilization steps used for nematode juveniles were omitted, as the presence of sodium azide and mercury chloride can affect nematode behaviors.

2.8.1. *In vitro* nematode motility test

Flavonoid stocks at the concentration of 10 μM were prepared in 80% HPLC grade methanol. Working concentrations of 0.1 μM, 0.01 μM, 1 nM, 0.1 nM, 0.01 nM, 10 pM and 1 pM were prepared via serial dilutions in MilliQ water. A solvent control of each methanol dilution was also included. To each well of a 96 well black microplate with transparent bottom (Merck, USA), 80 μl of MilliQ water was added, followed by 30 nematodes suspended in 10 μl of water and 10 μl of tested compound, in a final volume of 100 μl. Each compound was tested in triplicate. The plate was covered with a lid to reduce evaporation and wrapped in aluminum foil to minimize light stress. The nematodes were incubated for 2 hours at room temperature with gentle shaking at 20 rpm on an Innova™ 2100 platform shaker (Eppendorf, Germany). Prior to visualization, the plate was briefly centrifuged at 1000 rpm for 10 seconds on an Allegra® X-15R centrifuge (Beckman Coulter, USA) to pellet the nematodes to the bottom of the well. Each well was visualized under an inverted microscope, Olympus IX71 (Olympus, Japan) attached to a video camera, Leica MC120 HD (Leica, Germany) at 20 x magnification. Nematode movement was captured for 10-15 seconds and analyzed with the "WormAssay" application (Marcellino et al., 2012) using "Open for Testing" function. The average J2 motility, denoted as the arbitrary motility movement unit (mmu) was calculated across the triplicates. In addition, % motility inhibition was calculated as follows:

$$\%\ motility\ inhibition = (control\ mmu - test\ mmu) \div control\ mmu\ \times\ 100\%$$

2.8.2. *In vitro* nematode chemotaxis test

Three working concentrations were selected for chemotaxis test based on the results of nematode motility test. Twenty three percent pluronic gel was adapted from Wang et al. (2009b). Briefly, 46g of Pluronic® F-127 was dissolved in 160ml cold sterile MiliQ water with a magnetic stirrer in an ice bath for several hours to make 200ml gel. The gel was stored in 4°C. 5ml of cold gel was pipetted gently onto a 50 x 12mm round plastic petri dish with minimal bubbling. Excess bubbles were removed by gently tapping the dish or pipetting the bubbles. ~120 J2s were pipetted into the gel and the dish was swirled well to distribute the J2s across the dish. The gel was let to set in room temperature for 10-20 minutes. 5μl of the test compound was pipetted to the center of the well. The plate was incubated in 25°C incubator, Mini Oven (Watson Victor, Australia) for 5 hours. Post-incubation, the plate was observed under the steromicroscope, Olympus SZ61, adapted with transmitted light base, SZX-ILLB2-200. Location of each J2 was noted using a felt tip pen on the lid. The numbers of J2s in each concentric ring of 1cm, 2cm, 3cm, 4cm and 5cm diameters were counted (Figure 2.1). J2 density of each area and its relative density were calculated. The relative densities of triplicate plates were averaged and plotted.

$$Density = number\ of\ J2s \div ring\ area$$
$$Relative\ density = density\ of\ an\ area \div total\ density$$

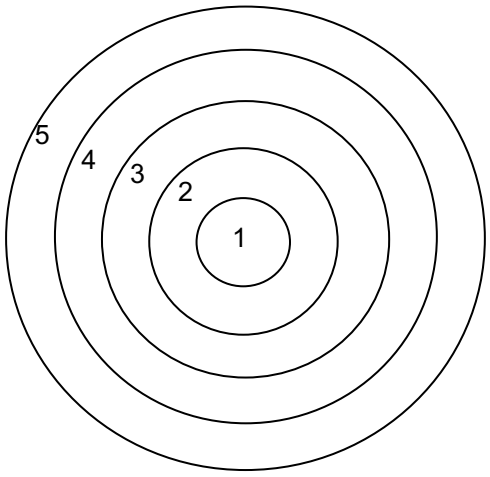

Figure 2.3: Chemotaxis grid with corresponding positions labeled.

2.9. Statistical analysis

The following statistical analyses were performed on R Studio version 1.0.143. : a) correlation matrix calculation using cor function, b) linear mixed model analysis using lme4, lmerTest and emmeans packages, c) OPLS-DA using ropls package, d) linear regression using lme4 package and e) partial least squares using caret package.

Chapter 3: Screening for flavonoids elicited during *Meloidogyne javanica* nematode infection in *Medicago truncatula* cv. 2HA

3.1 Abstract

Flavonoids are ubiquitous secondary metabolites in vascular plants that play multiple roles in the plant. This chapter investigates a time-course of changes in flavonoid abundance during the course of infection of *Medicago truncatula* with the root-knot nematode, *Meloidogyne javanica*. To achieve this, a liquid chromatography-electrospray ionization-quadrupole-time of flight- tandem mass spectrometry (LC-ESI-QTOF-MS/MS) method was optimised for 28 flavonoids from the chalcone, flavanone, flavonol, flavone, isoflavonoid and pterocarpan groups. These flavonoids were chosen because they had been detected in *M. truncatula* in previous studies. The LC-ESI-QTOF-MS/MS protocol was then used to quantify and detect flavonoids in infected roots sampled at seven time points, pre-infection, 30 minutes, 6 hours, 24 hours, 2 weeks and 4 weeks post nematode inoculation. The most prominent differnces in flavonoid accumulation occurred between the 24 hours and 4 weeks post inoculation time points of infected roots, and chalcone, flavanones and isoflavonoids were differentially regulated at these times. Several kaempferol glycosides and 7,4'-DHF were elicited at 24 hours. The chalcone and flavonones were likely upregulated to increase flavonoid biosynthesis flux, followed by induction of specific isoflavonoids that may be involved in defence against nematodes.

3.2 Introduction

The study of flavonoids typically employs the use of liquid chromatography (LC) with soft electrospray ionisation (ESI) coupled to mass spectrometry (MS) with sophisticated MS/MS capabilities (eg. QTOF, QQQ, orbitraps). The advantages of this technique are greater sensitivity, which allows better detection of less abundant molecules, structural characterisation based on molecular mass and fragmentation patterns, so that both aglycones and conjugates can be analysed, and high-throughput analysis, particularly with newer instruments (Cuyckens and Claeys, 2004, de Rijke et al., 2006). Moreover, as flavonoids are non-volatile molecules, they are unsuitable for the derivatisation steps required in gas chromatography techniques (Cuyckens and Claeys, 2004). Numerous aglycone and glycosylated flavones, isoflavonoids, flavanones, chalcones, pterocarpans and flavonols were successfully detected, identified and quantified on LC-MS/MS (Farag et al., 2007, Farag et al., 2008, Staszków et al., 2011, Urbanczyk-Wochniak and Sumner, 2007). As such, we had chosen the LC-ESI-QTOF-MS/MS technique and had established a protocol using this technique.

Flavonoids play diverse functions, ranging from UV protection, development regulation, pigmentation, defence against pathogens, nutrient mining, allelopathy and signalling molecules in plant-microbe interactions (Winkel-Shirley, 2001; Weston and Mathesius, 2013). During plant-nematode interactions, flavonoids have been implicated in the defence against nematodes by acting as nematode repellents, nematode motility inhibitors, by delaying egg hatching, killing nematodes and regulating gall development. Flavonoids particularly from the isoflavonoid and pterocarpan group (although not limited to those), such as formononetin glycosides, medicarpin, medicarpin glycosides and glyceollin accumulated more strongly in PPN resistant cultivars, as opposed to susceptible cultivars (Cook et al., 1995, Baldridge et al., 1998, Edwards et al., 1995, Kaplan et al., 1980a, Edens et al., 1995). These flavonoids were suggested to be instrumental in the protecting these resistant cultivars from PPNs, although the precise mechanism(s) underlying their apparent protection of plants against nematodes *in planta* is currently unclear. *In vitro* studies revealed that some some flavonols, eg. kaempferol, quercetin and myricetin and isoflavonoids, eg. daidzein and genistein inhibited nematode motility, delayed egg hatching and repelled nematodes at different concentrations in the J2 stages of other PPNs (Wuyts et al., 2006b). Moreover,

in some cases, quercetin and quercetin-3-*O*-rutinoside killed the J2s of *Heterodera zeae* (Faizi et al., 2011). Nevertheless, the information pertaining the temporal production of these flavonoids is lacking, as the flavonoids were quantified at one time point, in the later stages of infection and most studies concentrated their flavonoid quantification to one subgroup of flavonoids. Therefore, the experiments in this chapter aim to examine flavonoid production at various time points relating to *M. javanica* root infection and targeted five flavonoid subgroups in *M. truncatula*, the chalcones, flavaonones, flavonols, flavones and isoflavonoids (including pterocarpans). The time points chosen were pre-infection, 30 minutes, 6 hours, 24 hours, 4 days, 2 weeks and 4 weeks post inoculation. A pre-infection environment was simulated by separating *M. truncatula* roots from *M. javanica* J2s using a 12 kDa permeable membrane for 30 minutes (Viskase, USA) to determine if nematode signals that may alter flavonoid induction are perceived by the plant before physical contact is made. Early time points such as 30 minutes, 6 hours and 24 hours represented the stages at which J2s move towards the roots, penetrate the root tip, migrate intercellularly and establish early feeding sites (Bird, 1959b). At 4 days, 2 weeks and 4 weeks, the nematodes were feeding, with interim moulting and feeding arrest at 2 weeks. At these stages, galls were visible and were at different stages of development, and full gall maturation was reached at 4 weeks.

It was hypothesised that flavonoid groups such as flavonols and isoflavonoids are elicited during nematode infection at late time-points, particularly at 4 weeks post inoculation based on aforementioned studies. To investigate this, the following chapter aims to:

1) Establish a time course of infection that represents major stages in the infection of *M. javanica* on *M. truncatula* under the conditions used in this thesis.
2) Establish a LC-ESI-QTOF-MS/MS protocol for flavonoid quantification from root extracts
3) Identify flavonoid pathways up or down regulated significantly in response to nematode infection.
4) Determine the temporal regulation of flavonoid pathways during nematode infection.

3.3 Results

3.3.1 LC-ESI-Q-TOF-MS/MS protocol optimisation for flavonoid quantification

3.3.1.1 Flavonoid standard preparation optimisation

The method for LC-ESI-Q-TOF-MS/MS on flavonoids was adapted from (Ng et al., 2015b) with modifications. Similar to Ng et al. (2015), the same mobile phases, liquid chromatography column, mobile phases and flavonoid extraction solvents were used. The method modifications were, 25 ng (final concentration 4 μg/g) umbelliferone was used as the internal standard and the flavonoids were extracted by ultrasonication in the dark at 4ºC for an hour. The flavonoid deglycosylation step was omitted, as glycosylated flavonoids were also targeted in this analysis. Additionally, the in-house flavonoid standard library was expanded from 12 to 28 commercial flavonoid standards.

Commercial flavonoids were solubilised in solvents to prepare concentrated stock solutions to calculate calibration curves. Most of these flavonoids solubilised well in 80%-100% methanol, with the exception of coumesterol, chrysin, medicarpin, afromosin, genistein-7-*O*-glucoside, formononetin-7-*O*-glucoside (form-7-gluc), glycetein and genistein. The flavonoids with low solubility in methanol were dissolved in 100% HPLC-grade dimethyl sulfoxide (DMSO). Thus, the solvent composition of the flavonoids was altered to a mixture of methanol and DMSO, which resulted in ion suppression or enhancement for different flavonoids in both ionisation modes (Figure 3.1).

Three types of solvents were prepared to determine the solvent that yielded the highest peak area count: 1) mixed (78% methanol, 22% DMSO), 2) 80% methanol and 3) 80% DMSO. For both 80% methanol and 80% DMSO solvents, the initial solvent was evaporated off using a vacuum centrifuge. Next, the dried flavonoids were dissolved in the respective solvents. The peak area counts were calculated for a sample of six flavonoids, umbelliferone, isoliquiritigenin, liquiritigenin, biochanin A, glycitein and 7,4'-dihydroxyflavone (DHF) (Figure 3.1). Due to time constraints, this optimisation was not extended to the remaining 22 flavonoids. 80% methanol was selected as the

running solvent as it resulted in higher peak area counts in four out of six flavonoids when compared to methanol and DMSO mixture and 80% DMSO solvents (Figure 3.1).

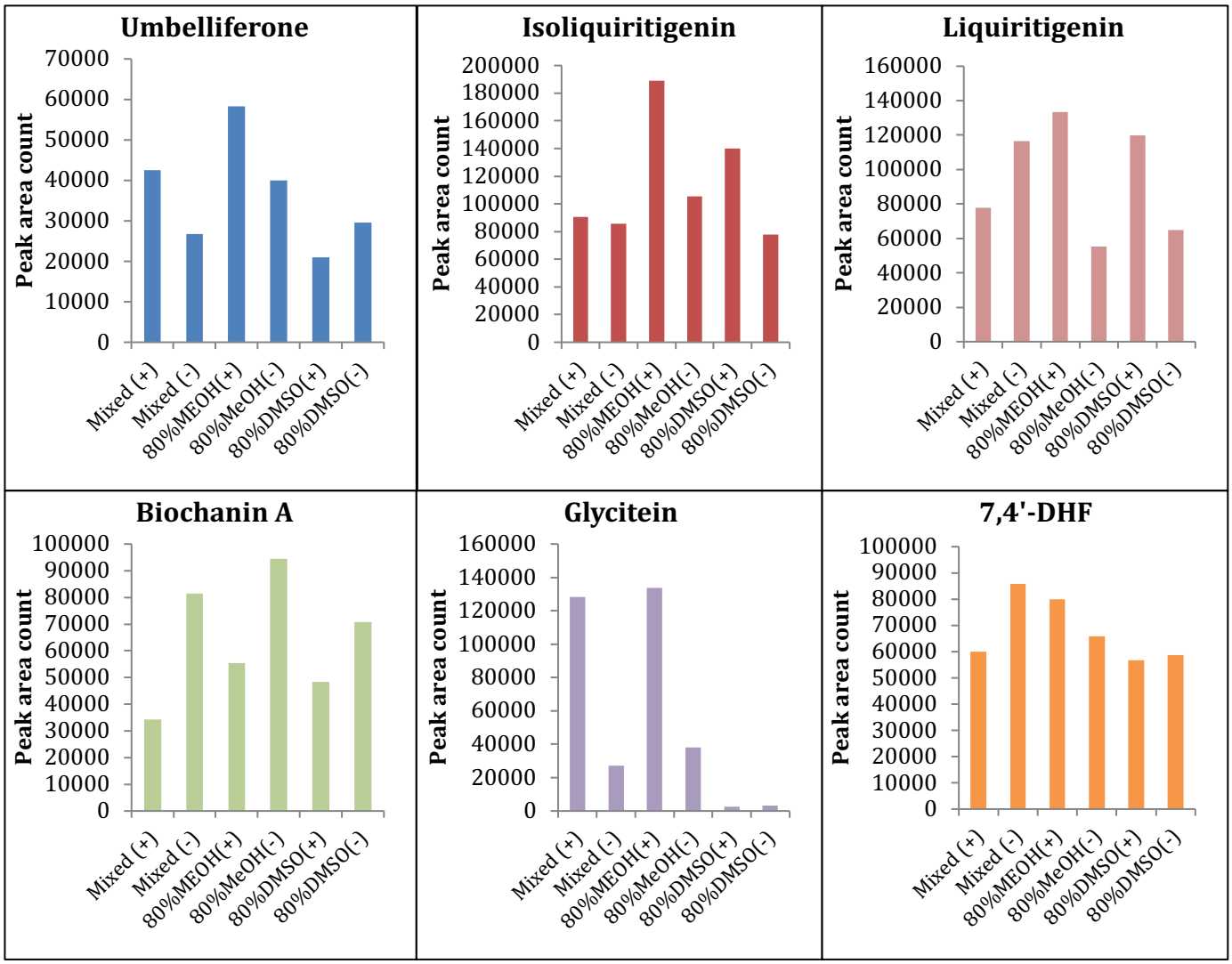

Figure 3.1: Effects of varying analyte solvent composition and ionisation on the detection of six flavonoids based on peak area counts acquired from LC-ESI-QTOF-MS/MS. The solvents tested were a mixture of 78% methanol and 22% DMSO, 80% methanol (MeOH), and 80% DMSO. (+) refers to positive ionisation, whereas (-) refers to negative ionisation.

3.3.1.2 Ion polarity modes and collision energy optimisation using commercial flavonoid standards

The standards were run in both positive and negative ionisation modes with eight collision energies ranging from 10 eV to 45 eV, in 5 eV increments. Optimal collision energy was obtained by comparing the near-complete fragmentation of precursor ions to produce the most abundant product ions at eight different collision energies (Figure 3.2)

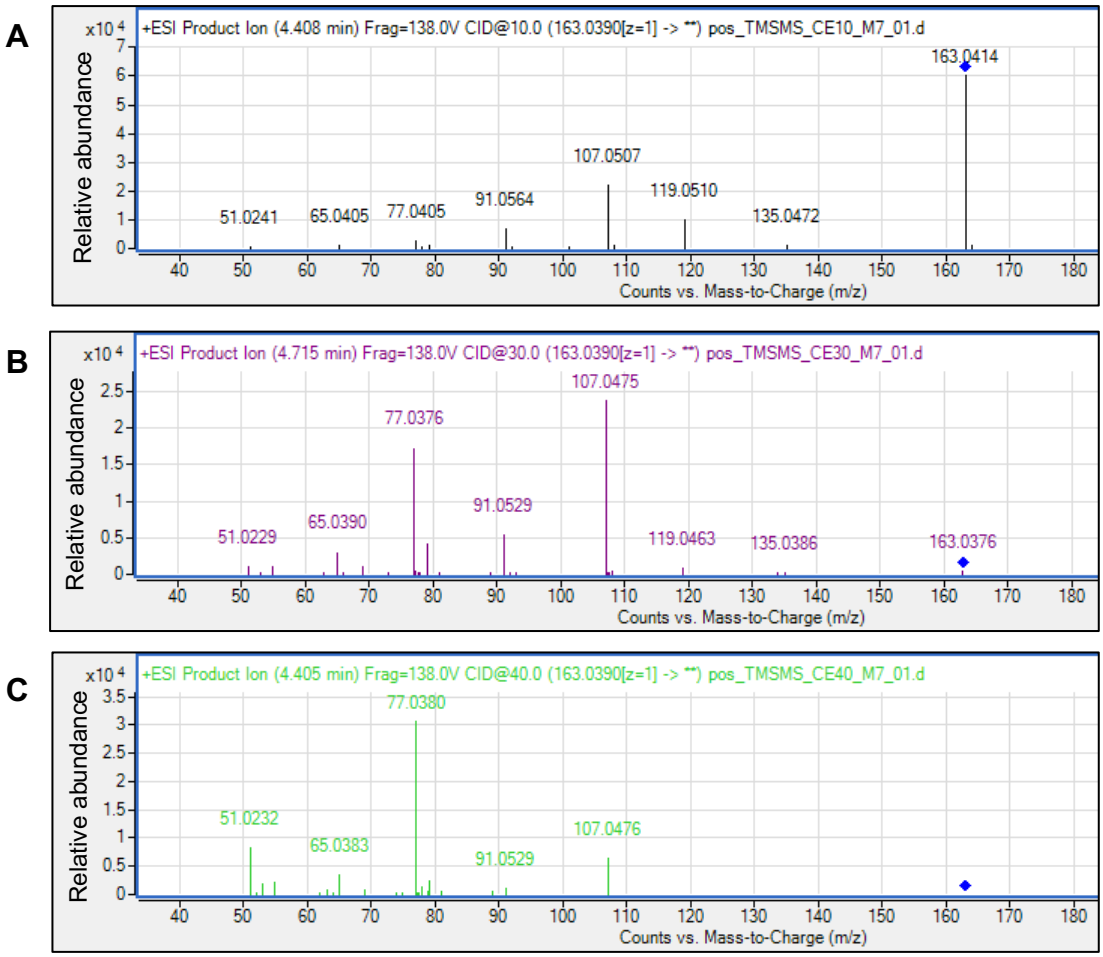

Figure 3.2: Example for optimisation of the collision energy using umbelliferone. Blue diamonds represent precursor ions. (A) Product ion spectrum for umbelliferone under 10 eV collision energy. This collision energy was too low, resulting in incomplete fragmentation of precursor ion, as shown by the high abundance of precursor ions. (B) Product ion spectrum for umbelliferone under 30 eV. Optimum collision energy resulted in dissociation of ~90% of the precursor ion. Product ions showed higher abundance to enable easy identification of compound based on MS/MS fragmentation signature. (C) Product ion spectrum for umbelliferone under 40 eV. This collision energy was too high, resulting in complete dissociation of the precursor ion and changed MS/MS fragmentation signature, as well as promoting additional "noise" fragments.

Chromatographic peak shapes, and MS/MS product ion spectra of flavonoids were good in both ionisation modes. Positive ionisation was selected based on enhanced peak area counts in a sample of six flavonoids, in which positive ionisation yielded the higher peak area counts in three types of running solvents for all tested flavonoids, with the exception of biochanin A (Figure 3.1).

The isomers kaempferol-3-glucoside (k-3-gluc) and kaempferol-7-glucoside (k-7-gluc) were resolved using an Agilent 6530 mass spectrometer, but were not resolved using an Agilent 6550 mass spectrometer, although the same reverse phase C18 column was used. We used an Agilent 6530 mass spectrometer in this chapter, whereas in Chapter 4, an Agilent 6550 mass spectrometer replaced the former instrument. A summary of MS/MS product ions, retention times, collision energies, limit of detections (LODs) and limit of quantifications (LOQs) (equations in Table 3.1) in positive ionisation based on the newer instrument, Agilent 6550 is shown in Table 3.1.

Flavonoid group	Compound name	CAS No.	Chemical formula	MW (g/mol)	$[M+H]^+$ Precursor ion (*m/z*)	MS/MS fragmentation				
						Product ions (*m/z*, most to least intense)	Retention time (min)	Optimised Collision energy (eV)	LOD[a] (ng/g)	LOQ[a] (ng/g)
Internal standard	Umbelliferone	93-35-6	$C_9H_6O_3$	162.14	163.039	107.0504, 77.0395	11.177± 0.0958	30	0.0249	0.04156
Chalcone	Isoliquiritigenin	961-29-5	$C_{15}H_{12}O_4$	256.25	257.0808	137.0187, 147.0388, 119.0453, 81.0309	11.009± 11.0106	25	0.00078	0.0023
Flavanone	Liquiritigenin	578-86-9	$C_{15}H_{12}O_4$	256.26	257.0808	137.0187, 147.0388, 119.0453, 81.0309	9.297± 0.0876	25	0.00167	0.005
	Naringenin	480-41-1	$C_{15}H_{12}O_5$	272.26	273.0757	153.0175, 147.0435, 119.0481	10.293± 0.00265	30	0.00014	0.00024
	Naringenin-7-*O*-glucoside	529-55-5	$C_{21}H_{22}O_{10}$	434.40	435.1286	273.0717, 85.0271, 147.0429, 195.0266	7.892± 0.00256	10	0.00137	0.00229
	Naringenin-7-*O*-rhamnoglucoside (N.D.)	10236-47-2	$C_{27}H_{32}O_{14}$	580.54	581.1865	273.0635, 85.0283, 271.0579, 129.0534	7.641± 0.0135	20	0.01890	0.03151
Flavonol	Kaempferol (N.D.)	520-18-3	$C_{15}H_{10}O_6$	286.24	287.055	153.0158, 68.9967, 121.0261, 93.032	10.439± 0.0037	45	1.5	2.5
	Kaempferol 3-*O*-*D* glucoside/ Kaempferol 7-*O*-ß-*D*-glucoside	480-10-4 / 16290-07-6	$C_{21}H_{20}O_{11}$	448.38	449.1078	287.0514, 288.0599, 85.0278	7.821± 0.0022	10	0.00623	0.01038

	Quercetin	117-39-5	$C_{15}H_{10}O_7$	302.24	303.0499	153.0169, 137.0154, 229.0411	9.622± 000039	40	2.5	4.167
	Quercetin 3-*O*-rutinoside (Rutin)	153-18-4	$C_{27}H_{30}O_{16}$	610.52	611.1607	303.0481, 465.0998	6.769± 0.00256	10	0.00023	0.00039
Flavones	Luteolin	491-70-3	$C_{15}H_{10}O_6$	286.24	287.055	153.02, 68.9983, 89.0396	9.564± 0.00374	45	5	8.33
	Apigenin	520-36-5	$C_{15}H_{10}O_6$	270.24	271.0601	153.0175, 91.0534, 119.0477	10.384± 0.00242	45	0.5172	0.862
	Apigenin 7-*O*-neohesperoside	17306-46-6	$C_{27}H_{30}O_{14}$	578.52	579.1708	271.0618, 433.108, 85.0276, 129.0538	7.996± 0.00256	15	0.01255	0.02092
	7,4'-dihydroxyflavone	2196-14-7	$C_{15}H_{10}O_4$	254.24	255.0652	81.0348,137.0224, 68.9984	9.0593± 0.00427	47	0.42857	0.7143
	Chrysin	480-40-0	$C_{15}H_{10}O_4$	254.24	255.0652	68.9967, 103.0525, 153.0163	12.121± 0.00362	45	0.8333	1.3889
Isoflavonoids	Daidzein	486-66-8	$C_{15}H_{10}O_4$	254.24	255.0652	91.0545, 152.0613, 137.0223	5.56± 0.00082	40	7.5	12.5
	Daidzein 7-*O*-glucoside (Daidzin)	552-66-9	$C_{21}H_{20}O_9$	416.38	417.118	255.061, 199.0741, 227.0691	5.5342± 0.0276	10	0.00273	0.00455
	Daidzein 8-*C*-Glucoside (Puerarin)	3681-99-0	$C_{21}H_{20}O_9$	416.38	417.118	297.0742, 267.0634, 321.073	4.365± 0.058	30	0.09677	0.16129

	Formononetin	485-72-3	$C_{16}H_{12}O_4$	268.26	269.0808	213.0571, 197.0619, 157.0661, 141.0707	10.422± 0.00237	35	0.15789	0.26316
	Formononetin 7-*O*-glucoside (Ononin)	486-62-4	$C_{22}H_{22}O_9$	430.4	431.1337	269.0832, 270.0807, 254.0548, 213.0906	8.963± 0.00659	15	0.00075	0.00125
	Genistein	446-72-0	$C_{15}H_{10}O_5$	270.241	271.0601	153.0175, 91.0534, 119.0477	10.384± 0.00243	45	0.51724	0.8621
	Genistein 7-*O*-Glucoside (Genistin)	529-59-9	$C_{21}H_{20}O_{10}$	432.38	433.1129	271.0542, 387.0357, 351.0352, 153.0167	6.874± 0.0161	15	0.00673	0.01122
	Biochanin A	491-80-5	$C_{16}H_{12}O_5$	284.27	285.0757	213.0531, 242.0559, 124.0143	12.548± 0.00256	40	2.3077	3.8462
	Glycitein	40957-83-3	$C_{16}H_{12}O_5$	284.26	285.0757	242.0553, 118.039, 168.0534	9.486± 0.0041	40	0.00212	0.00353
	Afromosin	550-79-8	$C_{17}H_{16}O_5$	298.29	299.0914	256.0781, 132.0593, 284.0732	11.289± 0.0057	40	0.00779	0.01298
Isoflavonoid: pterocarpan	Medicarpin	32388-76-9	$C_{16}H_{14}O_4$	270.28	271.0965	137.0593, 161.0543, 123.0385, 147.0388	12.023± 0.00242	15	0.01462	0.02438
Coumestan	Coumesterol	479-13-0	$C_{15}H_8O_5$	268.22	269.0444	213.055, 197.0593, 157.065	10.408± 0.00256	35	0.00505	0.00843

Table 3.1: Quality parameters for targeted commercial flavonoid standards on positive polarity on LC-ESI-QTOF MS/MS. The parameters include collision induced product ions, retention times, optimised collision energies, LODs[a] and LOQs[b]. Injection precision (n=6), data shows mean and standard deviation.

[a v]LOD= 3 x signal to noise ratio, [b] LOQ = 5 x signal to noise ratio

3.3.1.3 The discovery of tentative *in planta* flavonoids in the absence of commercial standards

In addition to the detected flavonoids as previously described, several unknown chromatograms of 'non-targeted' metabolites were discovered and were tentatively annotated by using plant metabolite databases available on Phenol Explorer, Metlin, Pubchem and Massbank, and by manual interpretation of fragmentation patterns (Matsuda et al., 2009). A large sample of *M. truncatula* root tissue (600 mg) was processed to extract flavonoids as described in Chapter 2.4.1.2.1. to generate chromatograms for annotations. A list of tentatively identified flavonoids is available in Table 3.2 and their fragmentation patterns are available in Supplementary Figure 3.1. Three kaempferol glycosides, one DHF glycoside-like compound, two methoxyisoflavone glycoside-like compounds and eight tentative compounds were manually annotated based on their fragmentation into their respective aglycone backbone (Table 3.2). For example, the protonated kaempferol aglycone formed a precursor ion with the mass to charge ratio of 287.055. Fragmentation of glycosylated kaempferols, such as k-3-gluc and k-7-gluc, produced the kaempferol aglycone product ion with the mass to charge of 287.055, as well as fragmentation products that represented the masses of each glucose group.

Identified Analyte (no commercial standards)		**Chemical formula**	**MW (g/mol)**	**$[M+H]^+$ (*m/z*)**	**MS/MS fragmentation**			**MS/MS Database Confirmation ID**	**Peer-reviewed publications citing analyte**
Name	**CAS No.**				**Product ions (*m/z*)**	**Retention time (min)**	**Optimised collision energy (eV)**		
Kaempferol-3-*O*-rutinoside (nicotiflorin)	17650-84-9	$C_{27}H_{30}O_{15}$	594.159	595.166	287.0562, 449.1071, 85.0253, 129.0532	7.181± 0.098	10 (25*)	Metlin: 50150 Pubchem: 5318767 Massbank tolerance: ±0.3ppm	(Pardede et al., 2017) (Lee and Chung, 2014) (Kim et al., 2017)
Kaempferol glycoside-like	N/A	$C_{27}H_{30}O_{15}$	594.159	595.166	287.0531, 85.0277, 71.00489, 129.0537	6.46± 0.0739	30	N/A	N/A
Kaempferol 3-*O*-glucosyl-rhamnosyl-galactoside **OR** Kaempferol 3-*O*-glucosyl-rhamnosyl-glucoside	136449-09-7 N/A	$C_{33}H_{40}O_{20}$	756.211	757.219	449.1059, 287.0544, 129.0545, 85.0288	4.483± 0.136	25	FoodB: http://foodb.ca/compounds/FDB000164 http://foodb.ca/compounds/FDB000165 Phenol-Explorer ID: 321, 322	(Dou et al., 2007) (Kelebek, 2016)
Dihydorxyflavone glycoside- like	N/A	$C_{21}H_{19}O_{10}$	431.098	432.1051	256.0613, 257.0712, 255.0584	5.625±0.107	15	N/A	N/A
Methoxyisoflavone glycoside-like 1	N/A	$C_{22}H_{30}O_{17}$	626.148	627.1556	285.074, 571.1553, 609.1343, 313.069	14.54± 0.071	30	N/A	N/A
Methoxyisoflavone glycoside-like 2	N/A	$C_{27}H_{30}O_{17}$	626.148	627.1556	609.1366, 285.0737, 591.1275, 313.0693	14.99±0.0025	35	N/A	N/A

448	N/A	$C_{21}H_{20}O_{11}$	448.101	449.1078	365.1045, 381.0772, 166.957	0.599± 0.0032	20	N/A	N/A
462	N/A	$C_{21}H_{18}O_{12}$	462.08	463.0871	180.9744, 240.9941, 283.005, 210.9851	0.844± 0.0023	30	N/A	N/A
464	N/A	$C_{21}H_{20}O_{12}$	464.096	465.1028	217.0451, 271.0429	8.402± 0.0026	15	N/A	N/A
578	N/A	$C_{27}H_{30}O_{14}$	578.164	579.1708	127.0339, 205.0916, 188.0661	1.611± 0.2304	15	N/A	N/A
594	N/A	$C_{27}H_{30}O_{15}$	594.159	595.1657	457.1152, 599.141, 559.14, 541.13	4.676± 0.1532	20	N/A	N/A
610	N/A	$C_{27}H_{30}O_{16}$	610.153	611.1607	81.0331, 97.0279, 151.0376, 237.058	8.524± 0.179	20	N/A	N/A
740	N/A	$C_{33}H_{40}O_{19}$	740.216	741.2237	205.0972, 188.0671, 291.1428, 535.1352	1.6198± 0.1755	20	N/A	N/A
784	N/A	$C_{34}H_{40}O_{21}$	784.206	785.2135	86.0921, 217.1302, 227.1702, 136.0701	9.947± 0.4538	48	N/A	N/A

Table 3.2: Quality parameters and MS/MS database confirmation of tentative flavonoids detected in *Medicago truncatula* root extracts in the absence of commercial standards on positive polarity on LC-ESI-QTOF MS/MS. The quality parameters include collision-induced product ions, retention times and optimised collision energies. Injection precision (n=6), data shows means and standard deviations. N/A= not available

3.3.2 The flavonoid pathway is altered by *M. javanica* nematode infection in wild-type *M. truncatula* cv. 2HA

3.3.2.1 Flavonoid precursors and specific flavonols and isoflavonoid end products are up-regulated differentially at early and late infection stages

The flavonoid profiles of wild- type *M. truncatula* cv. 2HA plants infected with *M. javanica* J2s were monitored and compared with uninfected plants over seven time points that encompassed different infection stages: 1) pre-infection, 2) 30 minutes, 3) 6 hours, 4) 24 hours, 5) 4 days, 6) 2 weeks and 7) 4 weeks (Figure 3.3). At each time point, the harvested infected root segments were developmental matched with control, i.e. the early stages were harvested from the root tip, whereas the later stages were root segments further away from the root (Figure 3.3).

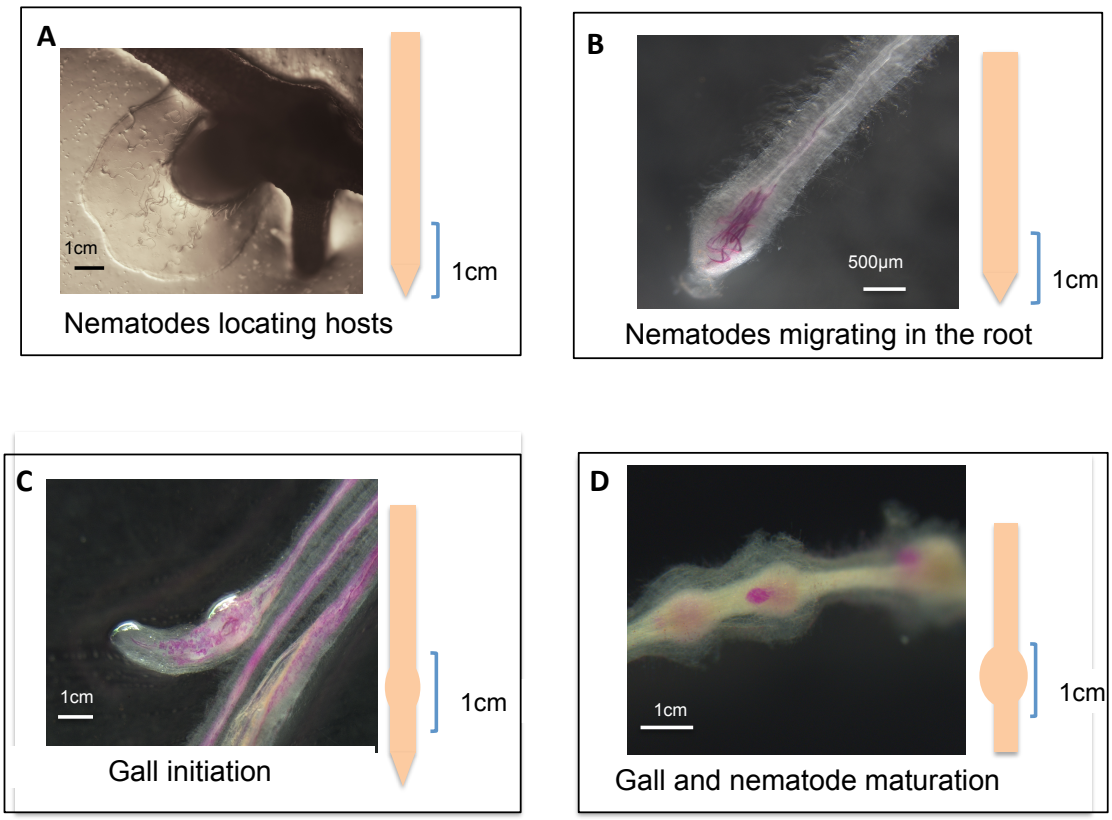

Figure 3.3: The different stages of *M. javanica* nematode infection on *M. truncatula* cv. 2HA roots, with cartoons illustrating the segments harvested for flavonoid quantification (and auxin quantification; Chapter 5). Nematodes were stained in pink with acid fuschin stain. (A) J2s locate hosts within pre-infection, 30 minutes and 6 hours post inoculation. One centimeter of root tips were harvested at these time points, as fastest J2s may have reached the root tip. (B) J2s begin to migrate inside the root at 24 hours post inoculation. One centimeter of root tips were harvested at this time point as most J2s would have begun root penetration at the root tip. (C) J2s have initiated giant cells and gall formations at 4 days post inoculation. One centimeter of galls were harversted. (D) At 2 weeks and 4 weeks post inoculation, nematodes and galls continue to mature. One centimeter of galls were harvested.

Flavonoid precursors located at the beginning of the flavonoid biosynthetic pathway, the chalcone and flavanone pathways, i.e. isoliquiritigenin, liquiritigenin, naringenin and nar-7-gluc, first showed significant concentration increases at 24 hours post inoculation (p.i.) (Figure 3.4). For isoliquiritigenin, naringenin and nar-7-gluc, the maximum concentrations were achieved at 24 hours p.i. at ~40 ng/g (fresh root weight), 4 ng/g and 10 ng/g, respectively (Supplementary Figure 3.2). At 4 days, isoliquiritigenin and liquiritigenin levels were still upregulated in infected roots, although their levels had decreased compared with 24 hours (Supplementary Figure 3.2). Thereafter, isoliquiritigenin levels were maintained around the same levels at 15-20 ng/g at 2 weeks and 4 weeks p.i. (Supplementary Figure 3.2). In contrast, naringenin and nar-7-gluc were downregulated at 4 days, with nar-7-gluc showing a significant decrease. At 2 weeks, liquiritigenin and naringenin levels significantly increased again, with the former reaching its maximum concentration (Supplementary Figure 3.2). By 4 weeks, most chalcones and flavanones did not show significant changes.

The flavones targeted in this experiment were 7,4'-DHF, a DHF-glycoside-like compound, chrysin, apigenin and apigenin-7-*O*-neohesperidoside (api-neo). 7,4'-DHF was observed to be slightly increased as early as pre-infection to 6 hours, whereas DHF glyc-like showed down regulation (Figure 3.4). Both compounds were significantly increased at 24 hours and had reached their maximum concentrations (Figure 3.4 and Supplementary Figure 3.3). At time points after 24 hours, 7,4'-DHF concentration was maintained at about the same level, whereas DHF glyc-like levels tapered off (Supplementary Figure 3.3). Apigenin was undetected, and its glycoside, api-neo did not show significant changes, similar to chrysin (Figure 3.4).

The targeted isoflavonoids and pterocarpans were formononetin, formononetin-7-*O*-glucoside (form-7-gluc), daidzein, coumesterol, genistein and genistein-7-*O*-glucoside (gen-7-gluc), medicarpin and afromosin. Genistein was undetected and its glycoside, gen-7-gluc did not show significant changes in response to infection (Figure 3.4 and Supplementary Figure 3.4). Similarly, formononetin and coumesterol did not fluctuate much due to nematode infection (Figure 3.4 and Supplementary Figure 3.4). However, unlike its aglycone, form-7-gluc was significantly induced at 24 hours, 4 days and 4 weeks p.i. in infected roots (Figure 3.4). Daidzein was only strongly increased at 24

hours p.i. (Figure 3.4). On the other hand, the pterocarpan, medicarpin and isoflavonoid afromosin, significantly increased at 2 weeks and 4 weeks p.i. and were detected at very high concentrations, up to ~150 ng/ng (Figure 3.4 and Supplementary Figure 3.5).

The targeted flavonols were kaempferol, quercetin, kaempferol-3-*O*-glucoside(k-3-gluc), kaempferol-7-*O*-glucoside (k-7-gluc), kaempferol-3-*O*-rutinoside (k-3-rutinoside) and kaemoferol glycoside-like (k glyc-like). The aglycone flavonols, kaempferol and quercetin were undetected. K-3-gluc and k-7-gluc showed significant increases at 24 hours p.i. (Figure 3.4). This was followed by further reduction in concentrations until the minimum concentrations were reached at 4 weeks p.i. (Figure 3.4 and Supplementary Figure 3.6). Although k-3-rutinoside and k-glyc like concentrations did not fluctuate significantly, their trends were similar to k-3-gluc and k-7-gluc, whereby at 24 hours p.i., infected roots were observed to have higher concentration compared with uninfected roots, followed by an eventual decrease to a minimum at 4 weeks p.i. (Figure 3.4 and Supplementary Figure 3.6).

As for the tentatively identified compounds, compounds 462, 578 and 594 were observed to increase significantly at 4 weeks, with compound 578 showing an additional significant increase at 2 weeks, whereas compound 740 experienced significant overall fluctuations (not time-specific) due to nematode treatment (Figure 3.4 and Supplementary Figure 3.7). Whilst compound 448 increased over time, this trend was similar in both uninfected and uninfected plants (Figure 3.4 and Supplementary Figure 3.7).

In summary, the flavonoid pathway was induced by nematode infection, starting with the flavonoids at the beginning of the pathway at 24 hours p.i.. Medicarpin and afromosin showed the strongest induction especially at 2 weeks and 4 weeks p.i.. As for the flavones and other isoflavonoids, only specific flavonoids were affected by nematode infection, as shown by their significant increase in concentrations, mostly at 24 hours p.i.. Most tentatively identified compounds presented late increases in concentrations in infected roots compared to uninfected roots, resembling the patterns seen with the medicarpin and afromosin. Generally, linear mixed model analysis showed that the flavonoids influenced by nematode treatment also showed time dependent changes, with some flavonoids having strong combined treatment and time influences. Interestingly, whilst linear mixed model analysis did not find significant

nematode treatment effects for all flavonols, nonetheless, k-3-gluc and k-7-gluc showed significant concentration increases in infected roots compared with uninfected roots at 24 hours p.i. (Supplementary Figure 3.7). This is due to subtler fold changes between infected and uninfected roots, as opposed to other flavonoids such as daidzein, DHF-glyc-like and 7,4'-DHF, which were also only significantly increased in infected roots at one time point (Figure 3.4). In addition, whilst decreases in concentration were observed in some flavonoids, significant concentration changes were only observed for upregulated flavonoids.

3.3.2.2 Nematode infection alters the host's flavonoid response in a time-dependent manner

As aforementioned, most flavonoids were significantly induced by nematode infection the earliest at 24 hours and at later times, such as 2 weeks and 4 weeks p.i.. To determine whether multivariate datasets of flavonoid responses can be distinguished by a variable, several models were generated using orthogonal partial least squares-discriminate analysis (OPLS-DA), with R^2Y values showing the fraction of variance explained by a component, whereas Q^2Y predicts the fraction of variance explained by a component (a model is considered robust when R^2 and Q^2 values exceeds 0.5) (Blasco et al., 2015, Worley and Powers, 2013).

Flavonoid responses in infected plants were weakly discriminable by time variable using OPLS-DA (Figure 3.5A), with pareto-scaling by OPLS-DA explaning 42% of the infected flavonoid responses (R^2Y= 0.42). However, predictive value of the model is low, at 21% (Q^2Y= 0.21.). The time discrimination was distinct at 24 hours and 4 week time points, as shown by separated data fraction (Figure 3.5A), whereas the remaining time points show overlaps (Figure 3.5A). The flavonoids that showed variations in concentrations modelled by OPLS-DA over the seven time points were nar-7-gluc, k-glyc-like, api-neo, liquiritigenin, isoliquiritigenin and k-3-gluc (Figure 3.5C).

Additional modelling based on nematode treatment variable using data focusing on flavonoids responses at 24 hours and 4 weeks (included both uninfected and infected) revealed that 89.5% of flavonoid responses in uninfected and infected plants could be robustly separated at 24 hours and 4 weeks p.i. time points, without any overlap (Figure 3.5B) (R^2Y= 0.895, Q^2Y= 0.746.) and 74.6% of flavonoid response can be accurately predicted as uninfected or infected at 24 hours and 4 week post inoculation . Flavonoids that showed different responses at 24 hours and 4 weeks between infected and uninfected plants were liquiritigenin, afromosin, medicarpin, isoliquiritigenin, 7,4'-DHF, 594, form-7-gluc and naringenin (Figure 3.5D).

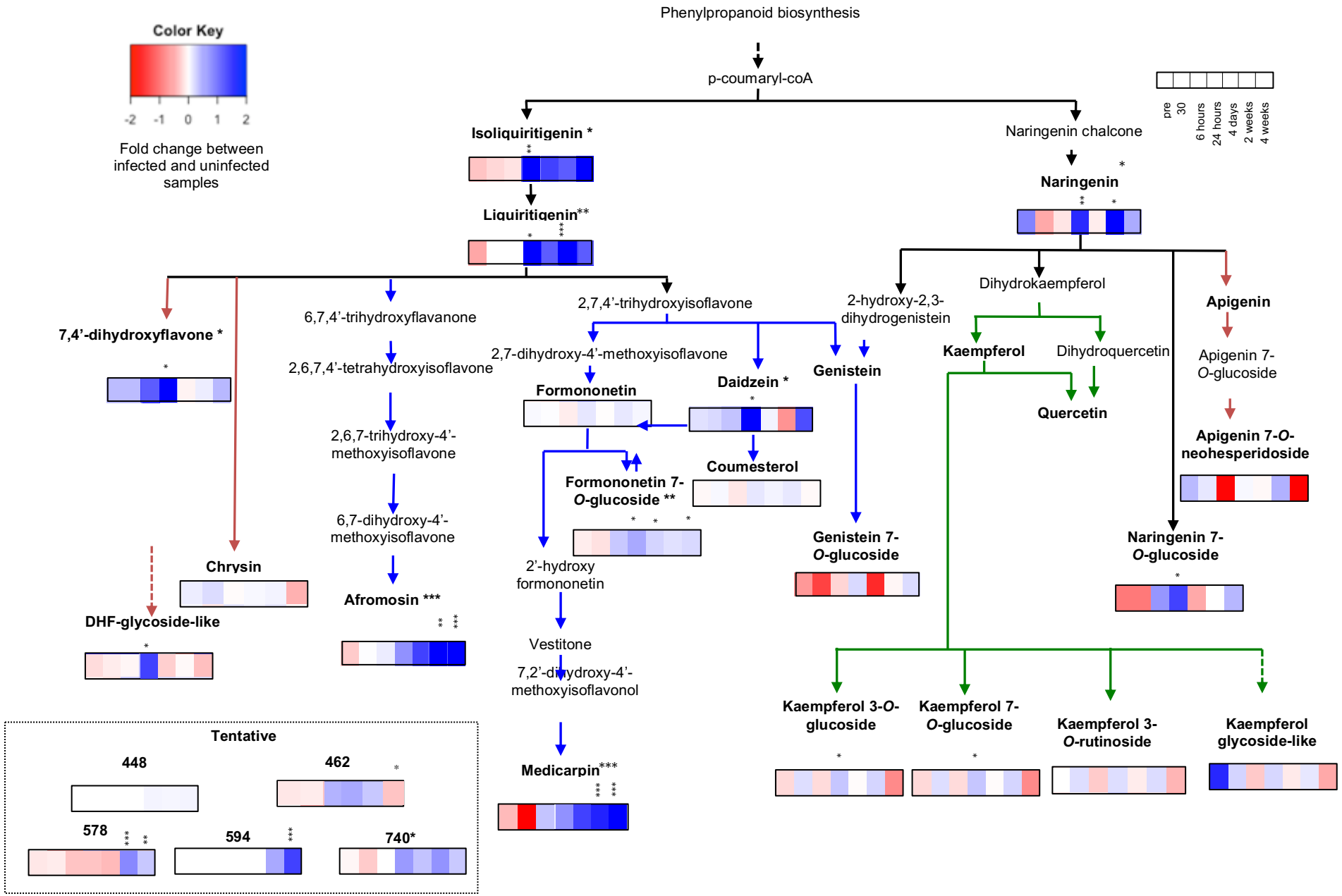
Color Key
-2 -1 0 1 2
Fold change between infected and uninfected samples
Phenylpropanoid biosynthesis
p-coumaryl-coA
pre
30
6 hours
24 hours
4 days
2 weeks
4 weeks
Isoliquiritigenin *
Liquiritigenin**
Naringenin chalcone
Naringenin
7,4'-dihydroxyflavone *
6,7,4'-trihydroxyflavanone
2,6,7,4'-tetrahydroxyisoflavone
2,6,7-trihydroxy-4'-methoxyisoflavone
6,7-dihydroxy-4'-methoxyisoflavone
Afromosin ***
Chrysin
DHF-glycoside-like
2,7,4'-trihydroxyisoflavone
2,7-dihydroxy-4'-methoxyisoflavone
Formononetin
Daidzein *
Coumesterol
Formononetin 7-O-glucoside **
2'-hydroxy formononetin
Vestitone
7,2'-dihydroxy-4'-methoxyisoflavonol
Medicarpin***
Genistein
Genistein 7-O-glucoside
2-hydroxy-2,3-dihydrogenistein
Dihydrokaempferol
Kaempferol
Dihydroquercetin
Quercetin
Apigenin
Apigenin 7-O-glucoside
Apigenin 7-O-neohesperidoside
Naringenin 7-O-glucoside
Kaempferol 3-O-glucoside
Kaempferol 7-O-glucoside
Kaempferol 3-O-rutinoside
Kaempferol glycoside-like
Tentative
448
462
578
594
740*

Figure 3.4: Simplified schematic representation of concentration fold-changes in the flavonoid pathway in *Medicago truncatula* cv. 2HA during *Meloidogyne javanica* infection at seven time points, pre-infection, 30 minutes, 6 hours, 24 hours, 4 days, 2 weeks and 4 weeks post inoculation. Statistical analysis was done with linear mixed model analysis with post hoc test. Compounds in bold indicate those targeted in the LC-ESI-QTOF- MS, with detected compounds showing seven coloured boxes which depict the relative concentration change between uninfected and infected plants. Conversely, undetected compounds do not have coloured boxes. Compounds with asterisks indicate those with statistically significant changes due to treatment ($p<0.05$), whereas asterisks above coloured boxes indicate significant statistical result for the post hoc test of time effect. Compounds in bold indicate those targeted in the LC-QTOF-MS/MS. Arrows in blue indicate flavonoids in the isoflavone synthase pathway, red indicate flavonoids in the flavanone pathway, and green indicate flavonoids in the flavonol pathway. The pterocarpan medicarpin is grouped with isoflavonoids in this diagram for simplicity, as it is derived from the isoflavonoid pathway. Dashed arrows show undetermined flavonoid pathway for putative flavonoids. Unidentified compounds are omitted.

A

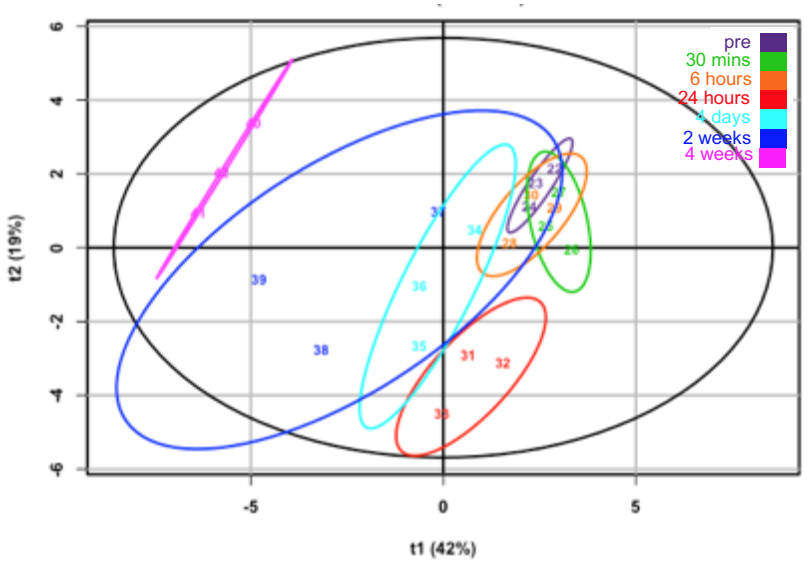
Infected x time
pre
30 mins
6 hours
24 hours
4 days
2 weeks
4 weeks
t1 (42%)
t2 (19%)

B

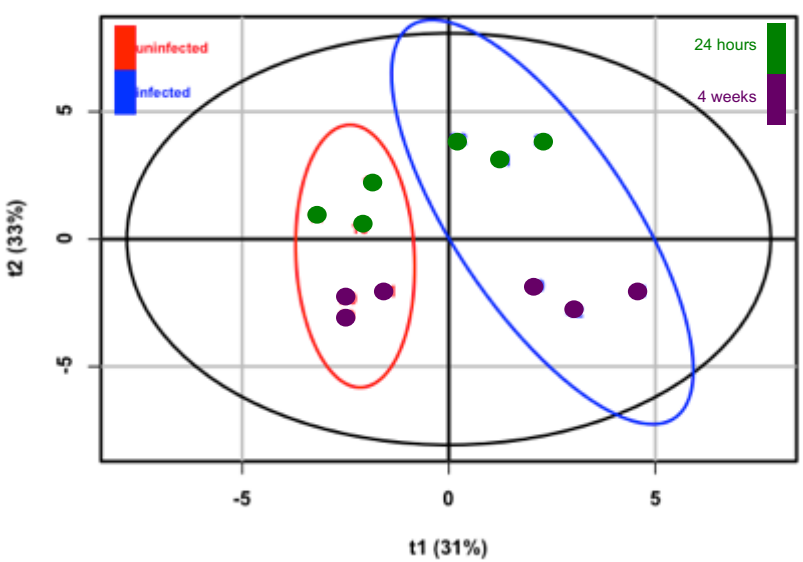
Treatment x (24 hr & 4 weeks)
uninfected
infected
24 hours
4 weeks
t1 (31%)
t2 (33%)

C

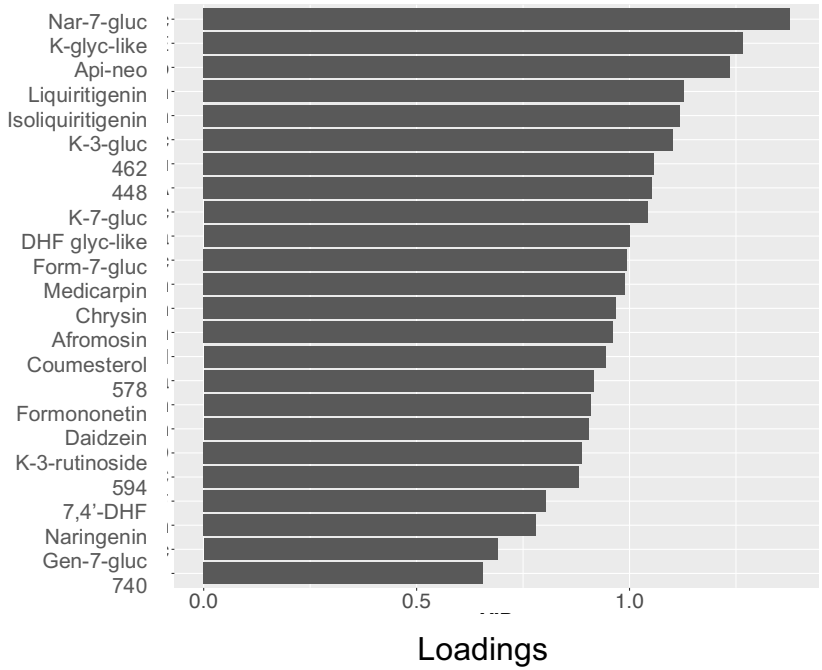
Nar-7-gluc
K-glyc-like
Api-neo
Liquiritigenin
Isoliquiritigenin
K-3-gluc
462
448
K-7-gluc
DHF glyc-like
Form-7-gluc
Medicarpin
Chrysin
Afromosin
Coumesterol
578
Formononetin
Daidzein
K-3-rutinoside
594
7,4'-DHF
Naringenin
Gen-7-gluc
740
Loadings

D

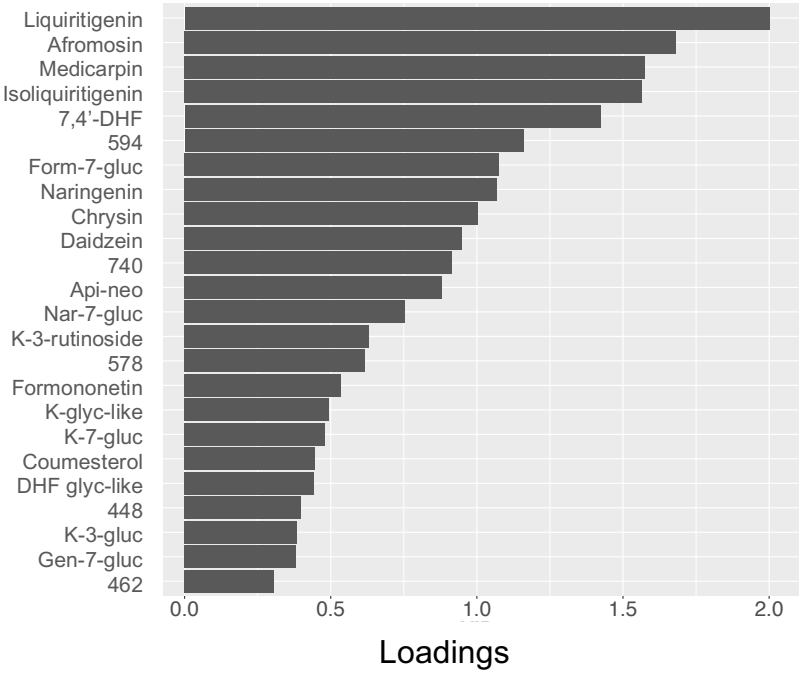
Liquiritigenin
Afromosin
Medicarpin
Isoliquiritigenin
7,4'-DHF
594
Form-7-gluc
Naringenin
Chrysin
Daidzein
740
Api-neo
Nar-7-gluc
K-3-rutinoside
578
Formononetin
K-glyc-like
K-7-gluc
Coumesterol
DHF glyc-like
448
K-3-gluc
Gen-7-gluc
462
Loadings

Figure 3.5: OPLS-DA analyses and the corresponding loading plots of flavonoid responses (log_{10} concentrations) of *Medicago truncatula* cv. 2HA infected with *Meloidogye javanica*. **(A)** Discrimination of flavonoid responses in infected plants based on the time factor. $R^2Y= 0.42$, $Q^2Y= 0.21$. **(B)** Discrimination of flavonoid responses in uninfected and infected plants based on the treatment factor at 24 hours and 4 weeks post inoculation. $R^2Y= 0.895$, $Q^2Y= 0.746$. **(C)** OPLS-DA loadings for the discrimination of flavonoid responses in infected plants based on the time factor. **(D)** OPLS-DA loadings for the discrimination of flavonoid responses in uninfected and infected plants based on the treatment factor at 24 hours and 4 weeks post inoculation.

3.4. Discussion

3.4.1 LC-ESI-QTOF-MS/MS for flavonoid quantification

Flavonoids have different solubilities due to the diversity of their structural conformation and polarity. The solubility of aglycones in organic solvents depends on the torsion angle θ caused by the absence or presence of a double bond between C2 and C3 (Chebil et al., 2007). In contrast, glycosylation increases water solubility and stability of flavonoids by changing flavonoid polarity (Plaza et al., 2014). In our experiment, we tested different aqueous mixtures of methanol or DMSO or both as solvents to solubilise 28 flavonoid standards fully. Although DMSO provided the best solubilisation, it caused ion suppression, as shown by low peak area counts (Figure 3.1). The ion suppression by DMSO may be attributed to its aprotic nature, high viscosity and high boiling point, which likely resulted in poor column separation efficiency, or less uniform droplet sizes or the reduction in flavonoid desolvation efficiency. DMSO has the highest viscosity at 1.996 compared with water at 0.89 and methanol at 0.594 cP, when measured at 25ºC, and the highest boiling point, at 189ºC in comparison with water and methanol at 100ºC and 64.7ºC respectively. Nevertheless, the use of aqueous mixtures of methanol, ethanol or acetone are the preferred solvents in mass spectrometry of flavonoids (de Rijke et al., 2006, Robards, 2003) and in our experiment, aqueous 80% methanol was the most effective solvent.

Flavonoids have been successfully detected in both positive and negative ion polarity modes with the latter reportedly producing higher sensitivity (de Rijke et al., 2006). Ideally, flavonoids should always be tested in both ion polarity modes, depending on the target flavonoids to obtain the optimum detection, as demonstrated by Farag et al. (2006) and Farag et al. (2007), although the mechanisms behind it are unclear and there are differences between flavonoid metabolites. For example, it was found here that biochanin A was better detected in negative ionisation regardless of solvent, whereas 7,4'-DHF was only better detected in negative ionisation in a mixture of aqueous methanol and DMSO (Figure 3.1). Hence, it is important to consider the combined effects of solvents and ionisation mode used when undertaking flavonoid mass spectrometry.

Currently, the main challenge in flavonoid research is their structural diversity. As previously discussed, the large array of flavonoids requires a lot of fine-tuning in separation and detection methods to comprehensively cover as many flavonoids as possible. To date, there are more than 10,000 described flavonoid structures in the literature (Dixon and Steele, 1999, Winkel-Shirley, 2001). In addition, it is impossible to obtain commercial standards for all flavonoids, particularly flavonoid glycosides, as they are not well described and difficult to synthesise. Furthermore, flavonoid diversity in plants is species dependent (Koes et al., 2005). To circumvent the lack of standards for flavonoid glycosides, available flavonoid databases such as Massbank, Metlin and Phenol-Explorer were used to generate a list of tentative flavonoids (Table 3.2). It was possible to narrow down the identity of some tentative glycosides based on matching their most abundant product ions to the protonated aglycone. However, eight tentative compounds with MS/MS fragmentations were also discovered that did not match any known database (Table 3.2). In addition, competitive fragmentation modelling, CFM-ID (available at http://cfmid.wishartlab.com/) was used to identity these compounds, but this was unsuccessful.

The next step in confirming their identity would be to fractionate high concentrations of these compounds using a preparative HPLC and to use NMR for structural confirmation. Due to time constraints, this was not possible as part of this project.

3.4.2 Flavonoid regulation during nematode infection

There were no observed significant changes in flavonoid concentrations at the early time points, i.e. pre-infection, 30 minutes, and 6 hours p.i..

At the pre-infection time point, the lack of changes in flavonoid concentrations (Figure 3.4) indicated that there was no diffusible signal exchange occurring between the incoming J2s and the root to elicit the flavonoid pathway. Nematodes do secrete pheromones that can be perceived by plants as shown by Manosalva et al. (2014), who described picomolar to micromolar ;eve;s of ascaroside secretion from *M. hapla, M. incognita* and *M. javanica* induced the expression of genes associated with plant basal immunity, mitogen-activated protein kinases, salicylic acid and jasmonic acid pathways in *Arabidopsis* under *in vitro* settings. It is plausible that the inoculation of ~15 J2s did not amount to a high enough nematode secretion that is within plant detection threshold. Furthermore, the nematodes are unlikely to produce such high amounts of pico-micromolar concentrations of ascarosides or pheromones in the soil, as this will

adversely affect their infection. Nevertheless, there is a possibility that other non-flavonoid, defence-related pathways were induced in this stage. Thus, to substantiate this, expression of defence-related genes, as previously mentioned, and other plant hormones, including ethylene should provide further insight into plant responses at the pre-infection stages (Fudali et al., 2012, Glazer et al., 1986).

Within 30 minutes, the J2s would have started to mechanically and chemically pierce through the root epidermal cells using their stylet action and stylet secretions, and begin to enter the root elongation zone (Holbein et al., 2016, Wyss et al., 1992). By 6 hours, the J2s have fully entered the root, and begin to migrate intercellularly towards the vascular cylinder (Wyss et al., 1992). Whilst there are studies investigating nematode secretion of plant cell wall degrading enzymes (Jaubert et al., 2005, Rosso et al., 2011), not much is known about the plant defences or how nematodes evade plant immune responses at these stages. Based on the flavonoid quantifications presented here, there is no evidence that the the flavonoid pathway yields sufficient changes in metabolites that can be detected (Figure 3.4). It is possible that while flavonoid pathway gene expression is induced, it does not lead to significant increases in metabolites within the same time frame, or that small increases in flavonoid metabolites in a few cells are not detectable when whole root segments are extracted as was done here. It may be possible to detect changes in flavonoid induction in small area of the root using imaging mass spectrometry

The earliest observed significant change in flavonoid levels occurred at 24 hours post inoculation (Figure 3.4), which coincided with the end of intercellular migration and the beginning of feeding site induction (Wyss et al., 1992). The J2 secrete numerous effectors to manipulate extensive cell functions, such as cell metabolism, cell-cycle progression, water and solute transport, cell division and differentiation and plant immunity (Bird, 2004, Holbein et al., 2016, Williamson and Gleason, 2003). The flavonoid groups elicited during nematode infection were the chalcone, flavanones, and specific flavonols, flavones and isoflavonoids, including its subgroup, the pteocarpans and some tentative flavonoids (Figure 3.4).

The first committed step for flavonoid biosynthesis begins with the chalcone synthase enzyme which converts p-coumaroyl-CoA and malonyl coA into the chalcones, isoliquiritigenin or naringenin chalcone. Isoliquiritigenin levels dramatically increased

in infected plants compared with control plants at 24 hours p.i. (Figure 3.4 and Supplementary Figure 3.2). In addition, isoliquiritigenin levels remained high throughout the next stages of infections at 4 days, 2 weeks and 4 weeks (Figure 3.4), presumably to maintain the high levels of flavonoid production. Chalcone synthase gene expression has been reported to be higher in resistant plants in *Meloidogyne* and other plant-parasitic nematodes infections to increase flavonoid production (Baldridge et al., 1998, Edens, 1995 #198). Isoliquiritigenin is unlikely to have any bioactivity against nematodes as 20- 200 μg/ml isoliquiritigenin did not affect *Radopholus similis* chemotaxis, motility and egg hatching (Wuyts et al., 2006b). However, it may affect other species of nematodes.

Flavonoid induction at 24 hours included flavonoids downstream of isoliquiritigenin biosynthesis, i.e. the flavonones, liquiritigenin, naringenin and nar-7-gluc, showing that the increased pool of upstream flavonoids were converted into other downstream flavonoids with different bioactivities. As shown in Figure 3.4, there were multiple downstream flavonoids which were increased at 24 hours p.i., such as 7,4'-DHF, DHF-glyc-like, form-7-gluc, daidzein, k-3-gluc and k-7-gluc. The increase in daidzein was likely converted to formononetin, and subsequently to form-7-gluc, thereby by-passing the pathway to coumesterol (Figure 3.4).
Although coumesterol was found to accumulate in lima bean and snap bean roots during *Pratylenchus scribneri* infection and inhibited *P. scribneri* motility in the range of mg/ml concentrations, our study did not find evidence of its involvement in response to *M. javanica*. The differences in flavonoid profiles in different nematode species and host species suggest that flavonoid induction is species-specific. As formononetin levels remained consistently similar between uninfected and infected plants (Figure 3.4 and Supplementary Figure 3.4), the flux was specifically directed towards form-7-gluc, perhaps as a storage form for reversible conversion into medicarpin or for subsequent conversion of form-7-gluc into formononetin-7-*O*-glucoside-6"-*O*-malonate. Whilst formononetin-7-*O*-glucoside-6"-*O*-malonate was not measured in this study, this flavonoid may be upregulated in response to root-knot nematodes. This is based on studies by Cook et al. (1995) and Edwards et al. (1995) who discovered that formononetin, formononetin glucoside (the authors did not specify which glycosylation, 3-*O*- or 7-*O*-*)* and formononetin-7-*O*-glucoside-6"-*O*-malonate accumulated in the roots of legumes resistant to the stem nematode, *Ditylenchus dipsaci*.

Flavones are also likely to be involved in plant-nematode interactions, as apigenin glycosides and luteolin glycoside were induced in nematode- infected plants (Soriano et al., 2004), although there have not been any other studies extending to 7,4'-DHF. Flavonols may be increased to perform two functions: 1) as auxin transport inhibitors and/or as 2) defense compounds. Kaempferol and quercetin were demonstrated to act as auxin transport inhibitors based on the displacement of artificial auxin efflux inhibitors (Jacobs and Rubery, 1988). Based on this analysis, kaempferol levels were below the detection limit, and quercetin concentrations were found to be below 1.5ng/g and 2.5ng/g, respectively (Table 3.2). Nevertheless, the detectable k-3-gluc and k-7-gluc suggests that these glycosides may be used as auxin transport inhibitors, likely at the nematode feeding site for giant cell organogenesis. We have also attempted to detect kaempferol 3-*O*-rhamnoside-7-*O*-rhamnoside, which was recently discovered to function as an auxin transport inhibitor in *Arabidopsis* (Yin et al., 2014) using the strategy described in Section 3.3.1.3, but it was not detected. Although flavonols such as kaempferol and quercetin were shown to repel and inhibit the motility of *M. incognita* J2s (Wuyts et al., 2006b), and quercetin and quercetin-3-*O*-rutinoside possessed nematicidal activities against *Heterodera zeae* (Faizi et al., 2011), high levels of these flavonols were not detected in this study.

At 4 days p.i., the infecting nematodes would still be continuously feeding and growing in the gall (Bird, 1959b). At this time point, flavonoid production was found to be somewhat stagnant, except for form-7-gluc, which exhibited a significant increase. The reasons for changes in form-7-gluc have been discussed earlier, although the relationship between its temporal production and function is unknown.

By 2 weeks, most nematodes would have begun moulting successively from J2 into J3, J4 and finally into an adult (Bird, 1959b). Liquiritigenin, naringenin, afromosin, medicarpin and compound 578 showed large increases at 2 weeks p.i. when compared with uninfected samples (Figure 3.4). As previously discussed, the increased levels of liquiritigenin and naringenin most likely reflected the increased flavonoid flux to synthesise downstream and more specific flavonoids, which in this case were afromosin and medicarpin. Medicarpin has been implicated as an antimicrobial against fungi, e.g. *Fusarium oxysporum* in chickpea (Stevenson et al., 1997), and oomyctes, e.g. *Phytophthora medicaginis* in alfalfa (Blount et al., 1992) and when stressed with methyl jasmonate (Naoumkina et al., 2007). In relation to defence against nematodes,

Cook et al. (1995) and Edwards et al. (1995) found that medicarpin and its glycoside, medicarpin-3-*O*-glucoside-6"-*O*-malonate were elicited in white clover and lucerne, respectively, during stem nematode (*Ditylenchus dipsaci*) infection, whereas Baldridge et al. (1998) reported the accumulation of medicarpin in plants resistant to *Pratylenchus penetrans*. In the same study by Baldridge et al. (1998), medicarpin inhibited *P. penetrans* motility in a concentration-dependent manner at µg/ml concentrations. Hence, it is likely that medicarpin and its glycosides were accumulated in roots as part of a defence response against *M. javanica*. On the other hand, there has been no research into the role of afromosin as an antimicrobial, but based on its comparable accumulation pattern to medicarpin, afromosin may also act in a defence response against *M. javanica*. These flavonoids were likely to be either absorbed through the cuticle or ingested during feeding. The accumulation of afromosin and medicarpin may coincide with nematode moulting stages due to the ability of the plant immunity to detect the nematode as the nematode sheds its cuticle, or perhaps the recommencement of feeding in female adults resulted in a different set of plant machinery manipulation.

At 4 weeks post inoculation, adult female nematodes would have started to produce eggs and galls would be fully-matured and have reached their maximum size (Bird, 1959b). Flavonoid profiles at the late stage at 4 weeks were distinctly different from the early infection stage at 24 hours (Figure 3.5 B and D), mainly due to the induction of liquiritigenin, afromosin, medicarpin and isoliquiritigenin. Afromosin and medicarpin concentrations with infected roots were further increased to 120-150 ng/g compared to infected roots at 2 weeks p.i. (Figure 3.4 and Supplementary Figure 3.4). Although afromosin and medicarpin were increased to high concentrations, the adult females apparently tolerated it, as they were able to survive and produced eggs. This feat may be achieved by modifying these flavonoids into inactive forms. Fungi such as *Botrytis* and *Collectotrichum* can hydroxylate medicarpin into 6a,7-dihydroxymedicarpin with decreased antifungal activity (Ingham, 1976). There is some evidence that nematodes can also modify flavonoids. Potato cyst nematodes, *Globera rostochiensis* and *G. pallida* were able to modify quercetin and kaempferol into quercetagetin that conferred their yellow colouration (Vlachopoulos and Smith, 1993). Nonetheless, further *in vitro* and *in planta* experiments to investigate the effects of modifications in afromosin and medicarpin levels on the *M. javanica* fitness will be required to elucidate their functions. Unlike the 2 weeks time point, the increase in afromosin and medicarpin was

not preceded by increase in liquiritigenin and naringenin, although the concentrations of these compounds were still considerably higher in infected roots compared with uninfected roots (Figure 3.4). This was, instead preceded by an increase in form-7-gluc (Figure 3.4). It appeared that the accumulation of afromosin and medicarpin does not solely depend on upstream precursors such as liquiritigenin and naringenin, and intermediates such as form-7-gluc acted as alternative precursors for the biosynthesis of medicarpin (Figure 3.4). It is plausible that another intermediate that was not targeted here acted as the alternative precursor for afromosin. Several unidentified compounds such as 462 and 594 were also significantly increased, but future studies will be required to identify these, possibly through purification and NMR studies.

3.5 Conclusion

LC-ESI-QTOF-MS/MS is a robust technique for reliable separation and sensitive detection of flavonoids. This approach revealed that the use of aqueous methanol and positive ionisation could detect a large population of flavonoids in one run. Several metabolites within the mass range of flavonoids were also uncovered as highly induced using this approach, however, their identification will require further work.

Flavonoid regulation during *M. javanica* infection is time-dependent, with distinct differences in levels of upstream flavonoids such as isoliquiritigenin and liquirtigenin and downstream compounds such as afromosin and medicarpin at early and late infection stages. The main groups of flavonoids that were increased during infection were the chalcones, flavanones, and isoflavonoids, with differential regulation at 24 hours and 4 weeks p.i. in infected roots. Specific kaempferol glycosides from the flavonol group and 7,4'-DHF were also upregulated at 24 hours post inoculation. Upstream flavonoids were increased presumably to act as precursors to increase downstream flavonoid biosynthesis as they have limited activities against nematodes. It is likely that the isoflavonoids, particularly afromosin and medicarpin were synthesised as defence compounds, whereas the kaempferol glycosides may be involved in auxin transport regulation in the gall.

3.6. Supplementary Figures

Analyte name	MS/MS fragmentation spectrum
Kaempferol 3-*O*-rutinoside	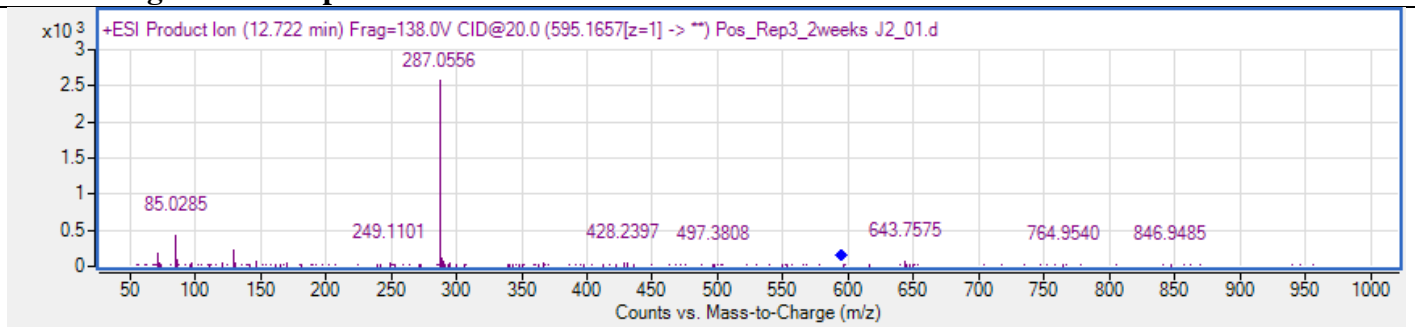
Kaempferol glycoside-like	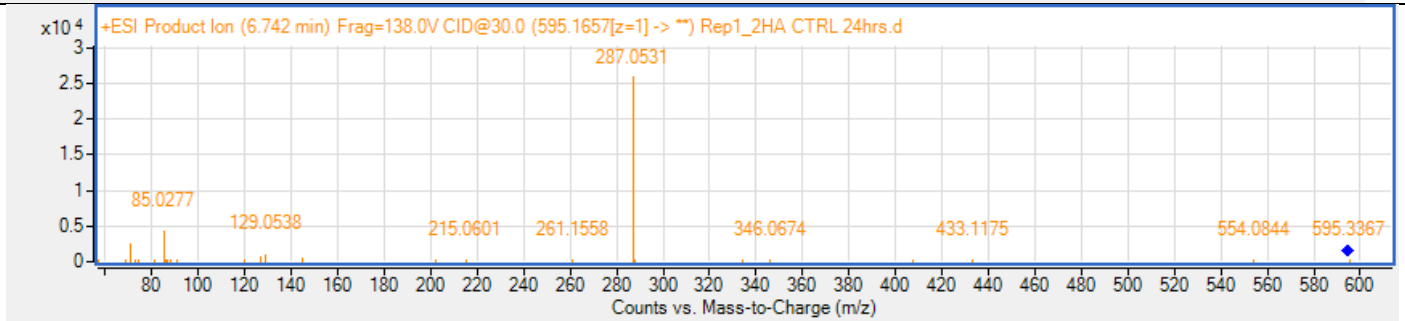

Kaempferol 3-*O*-glucosyl-rhamnosyl-galactoside **OR** Kaempferol 3-*O*-glucosyl-rhamnosyl-glucoside	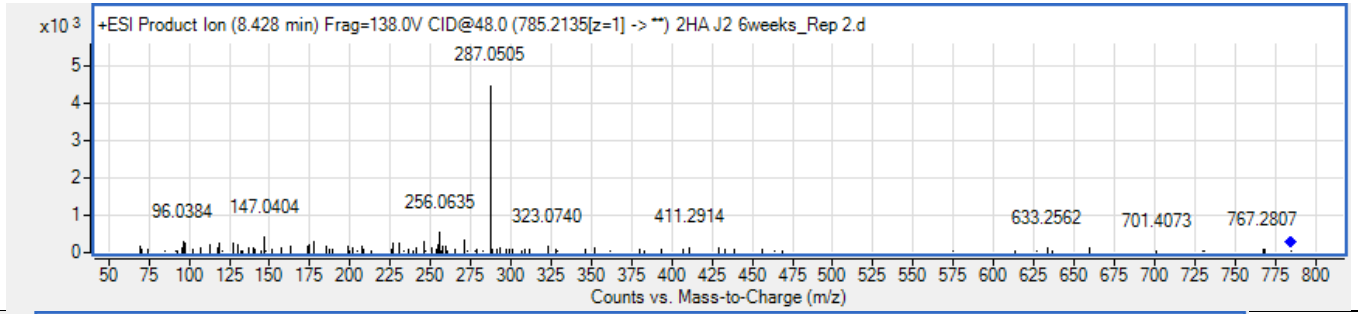
Dihydoroxyflavone glycoside-like	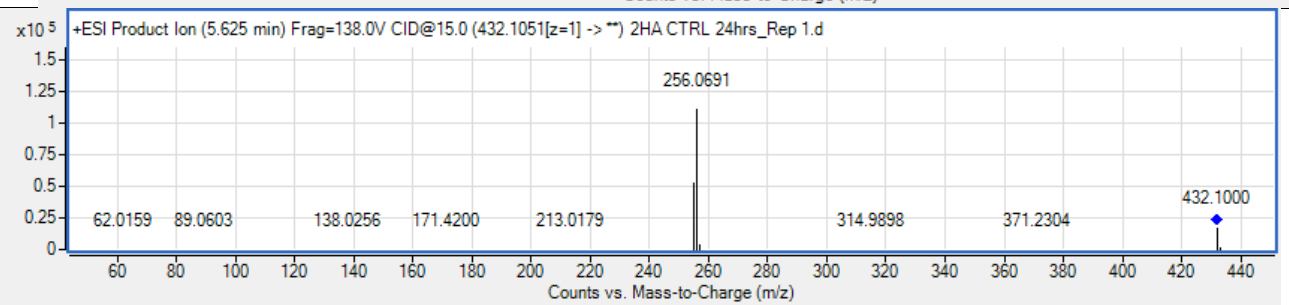
Methoxyisoflavone glycoside-like 1	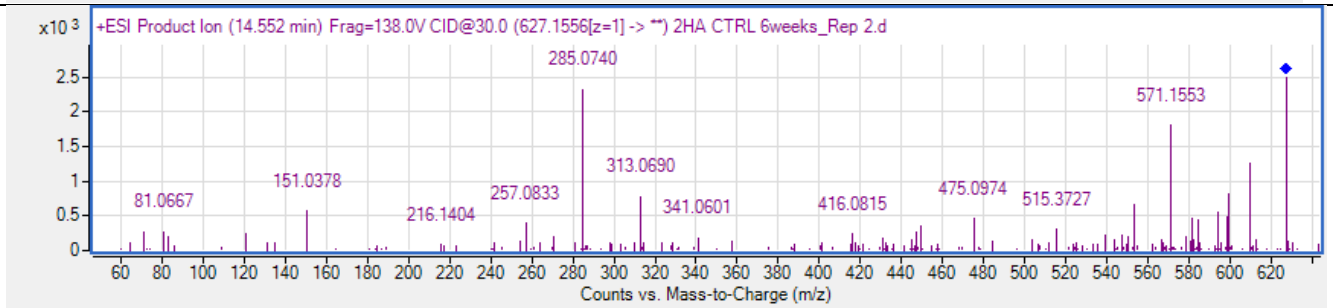

Methoxyisoflavone glycoside-like 2	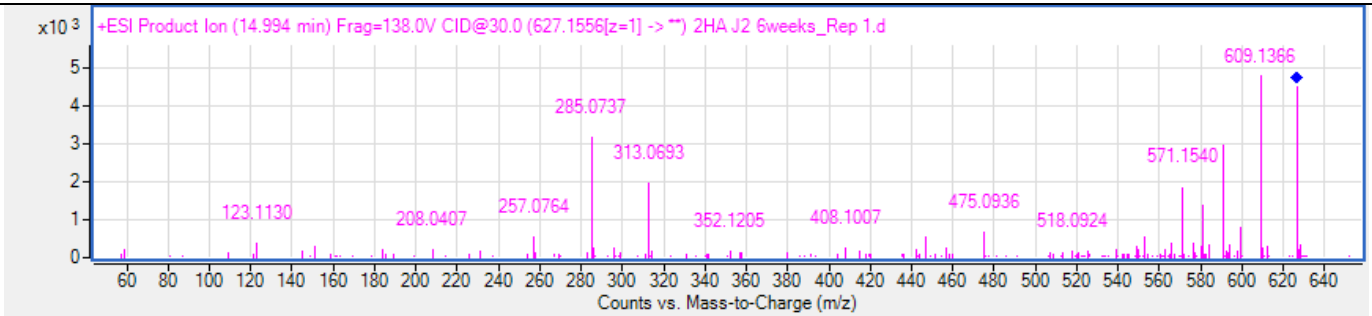
448	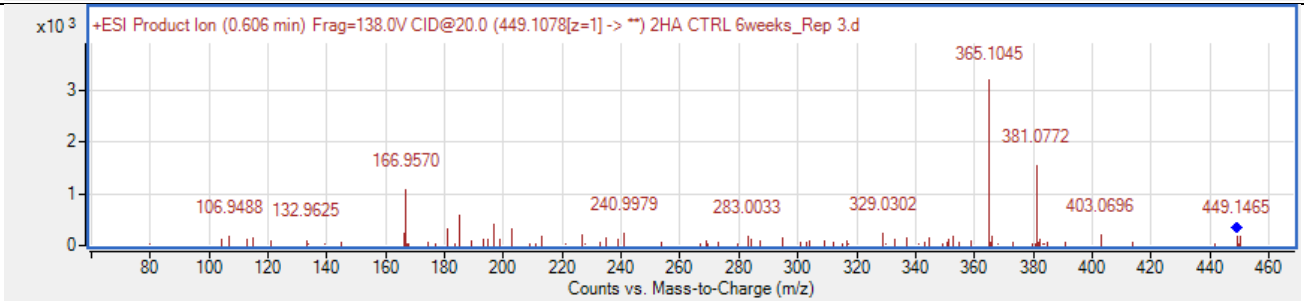
462	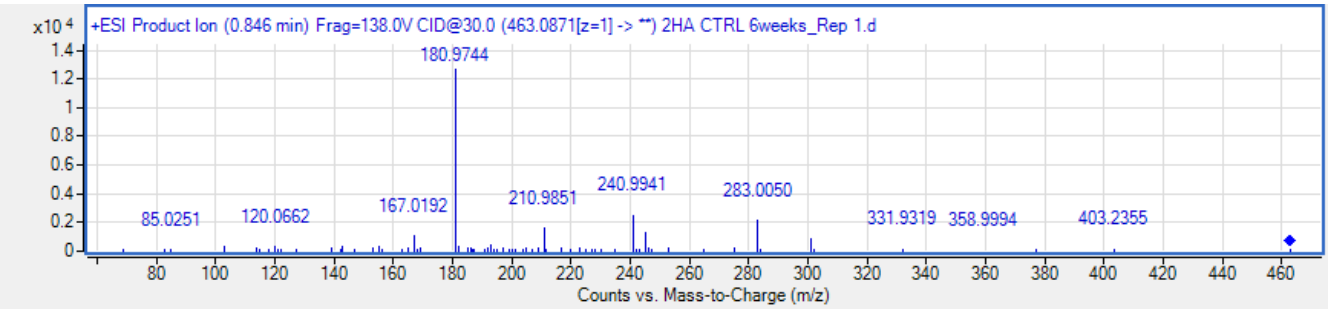

464	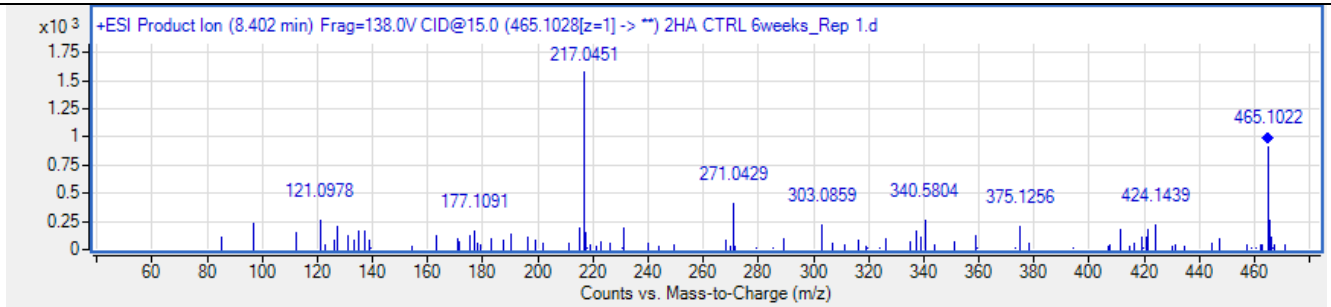 x10 3 +ESI Product Ion (8.402 min) Frag=138.0V CID@15.0 (465.1028[z=1] -> **) 2HA CTRL 6weeks_Rep 1.d 217.0451 465.1022 271.0429 121.0978 177.1091 303.0859 340.5804 375.1256 424.1439 Counts vs. Mass-to-Charge (m/z)
578	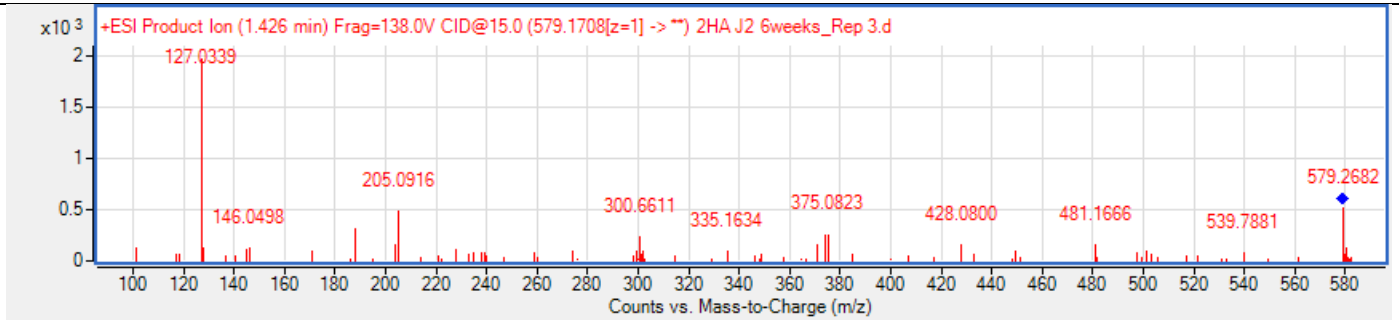 x10 3 +ESI Product Ion (1.426 min) Frag=138.0V CID@15.0 (579.1708[z=1] -> **) 2HA J2 6weeks_Rep 3.d 127.0339 205.0916 579.2682 146.0498 300.6611 335.1634 375.0823 428.0800 481.1666 539.7881 Counts vs. Mass-to-Charge (m/z)
594	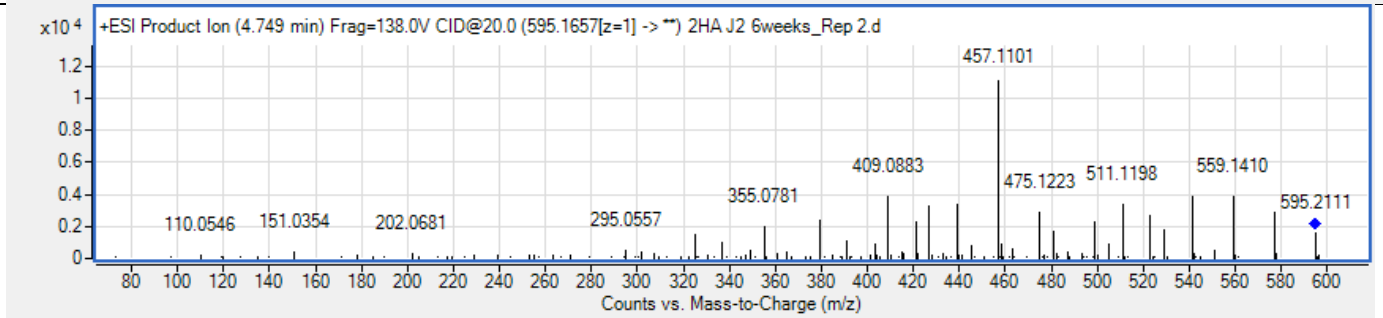 x10 4 +ESI Product Ion (4.749 min) Frag=138.0V CID@20.0 (595.1657[z=1] -> **) 2HA J2 6weeks_Rep 2.d 457.1101 409.0883 475.1223 511.1198 559.1410 355.0781 595.2111 110.0546 151.0354 202.0681 295.0557 Counts vs. Mass-to-Charge (m/z)

610	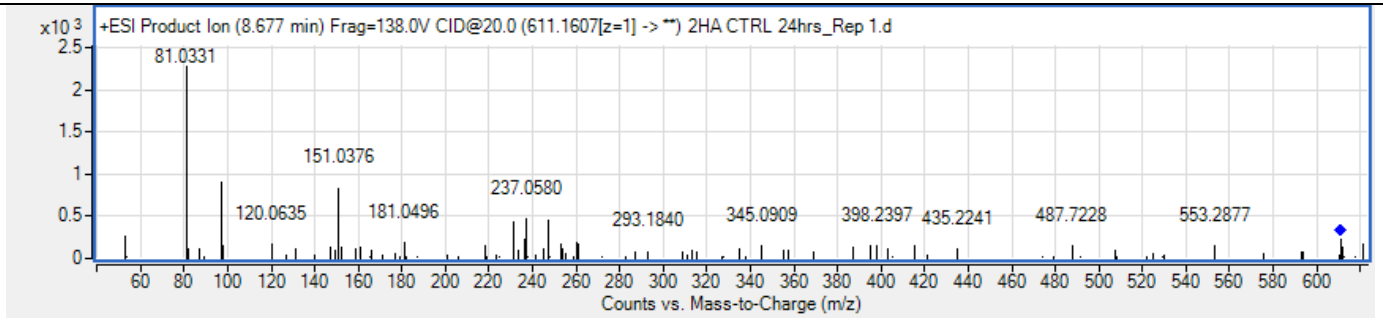 x10 3 +ESI Product Ion (8.677 min) Frag=138.0V CID@20.0 (611.1607[z=1] -> **) 2HA CTRL 24hrs_Rep 1.d 81.0331 151.0376 237.0580 120.0635 181.0496 293.1840 345.0909 398.2397 435.2241 487.7228 553.2877 Counts vs. Mass-to-Charge (m/z)
626	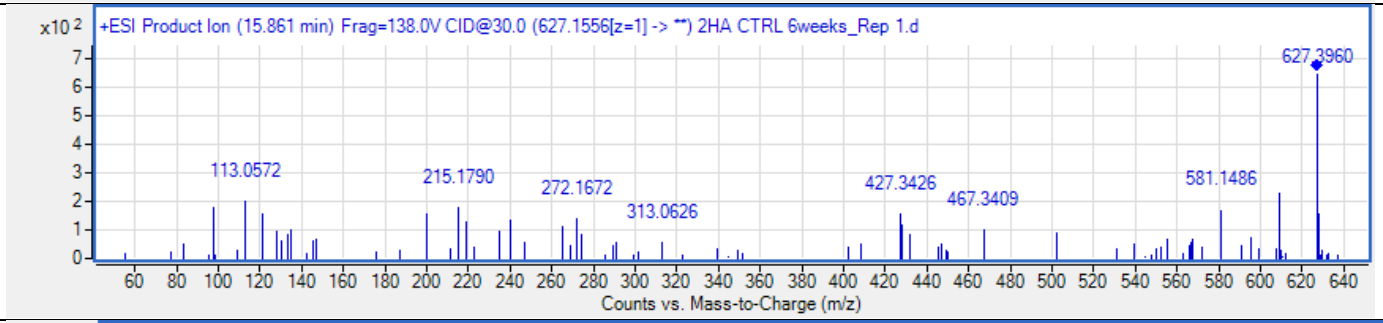 x10 2 +ESI Product Ion (15.861 min) Frag=138.0V CID@30.0 (627.1556[z=1] -> **) 2HA CTRL 6weeks_Rep 1.d 627.3960 113.0572 215.1790 272.1672 313.0626 427.3426 467.3409 581.1486 Counts vs. Mass-to-Charge (m/z)
740	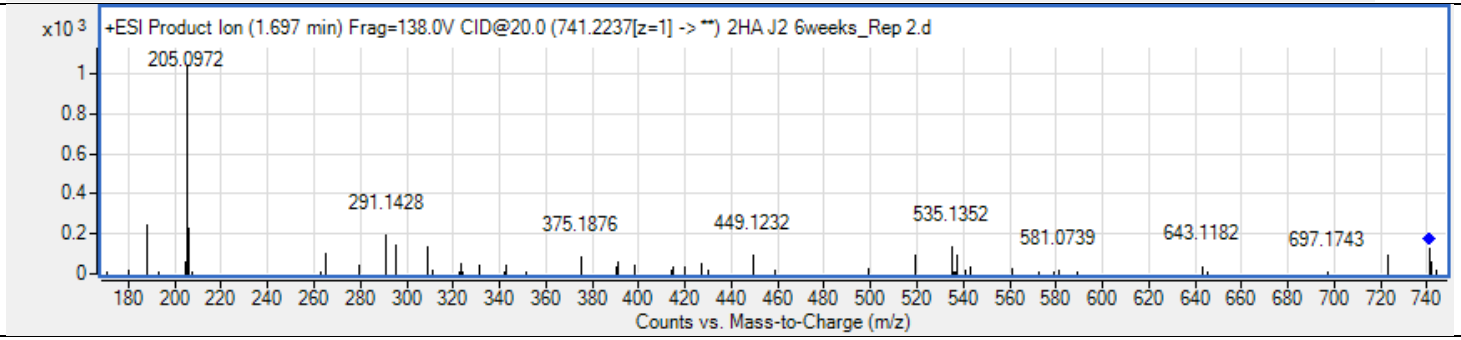 x10 3 +ESI Product Ion (1.697 min) Frag=138.0V CID@20.0 (741.2237[z=1] -> **) 2HA J2 6weeks_Rep 2.d 205.0972 291.1428 375.1876 449.1232 535.1352 581.0739 643.1182 697.1743 Counts vs. Mass-to-Charge (m/z)

784	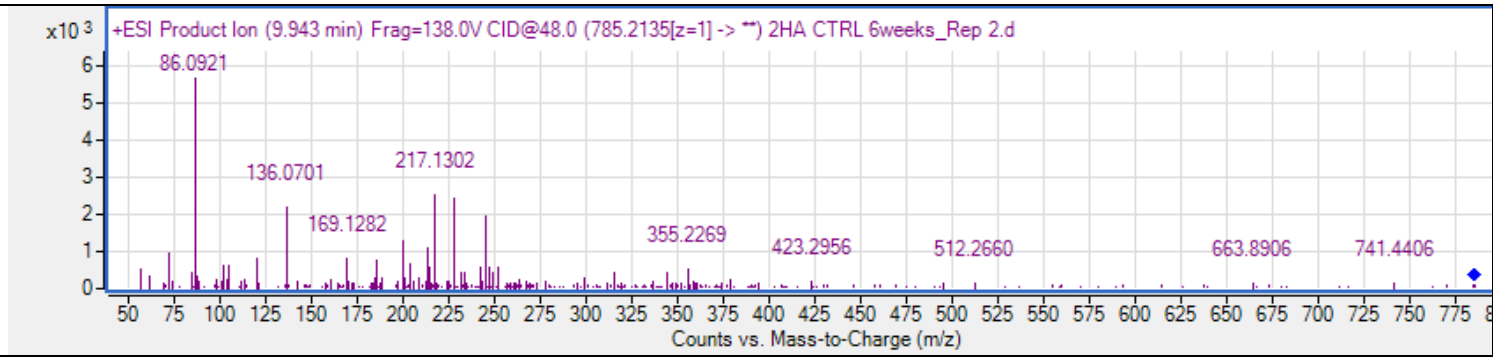

Supplementary Figure 3.1: MS/MS spectra of the analytes detected in *Medicago truncatula* root extracts without commercial standards on positive ionisation on LC-ESI-QTOF MS/MS. Blue diamonds depict the parent ion.

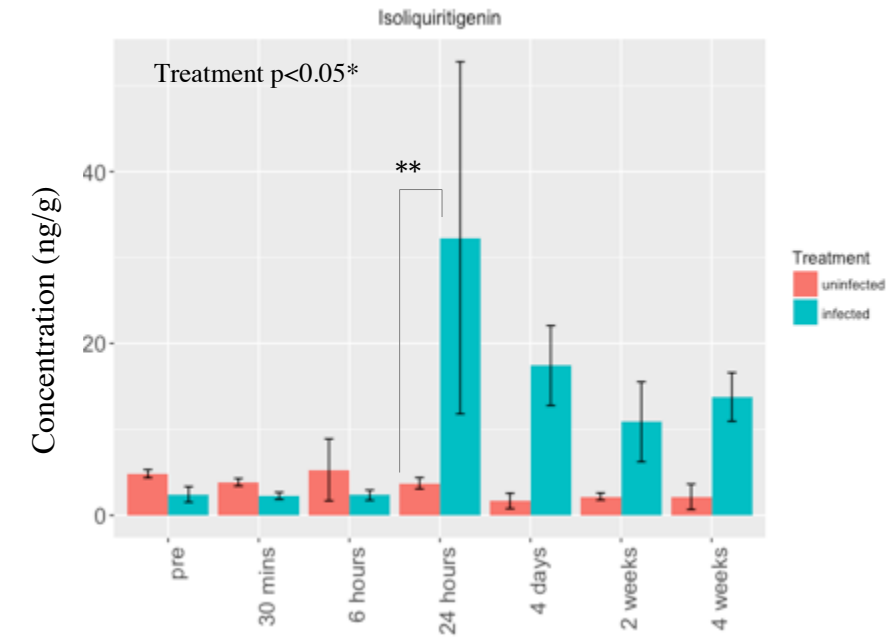
Isoliquiritigenin
Treatment p<0.05*
**
Concentration (ng/g)
0
20
40
pre
30 mins
6 hours
24 hours
4 days
2 weeks
4 weeks
Treatment
uninfected
infected

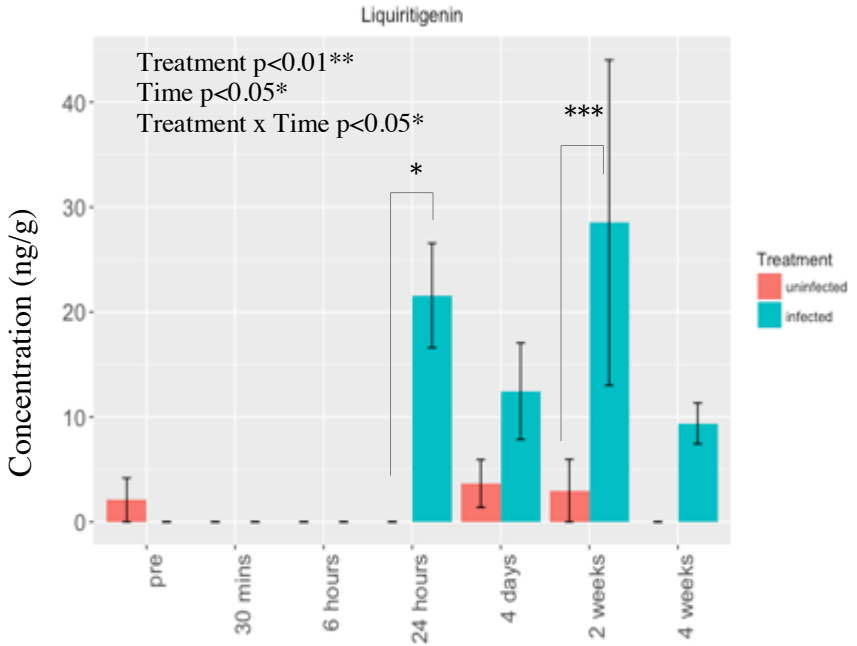
Liquiritigenin
Treatment p<0.01**
Time p<0.05*
Treatment x Time p<0.05*
*
***
Concentration (ng/g)
0
10
20
30
40
pre
30 mins
6 hours
24 hours
4 days
2 weeks
4 weeks
Treatment
uninfected
infected

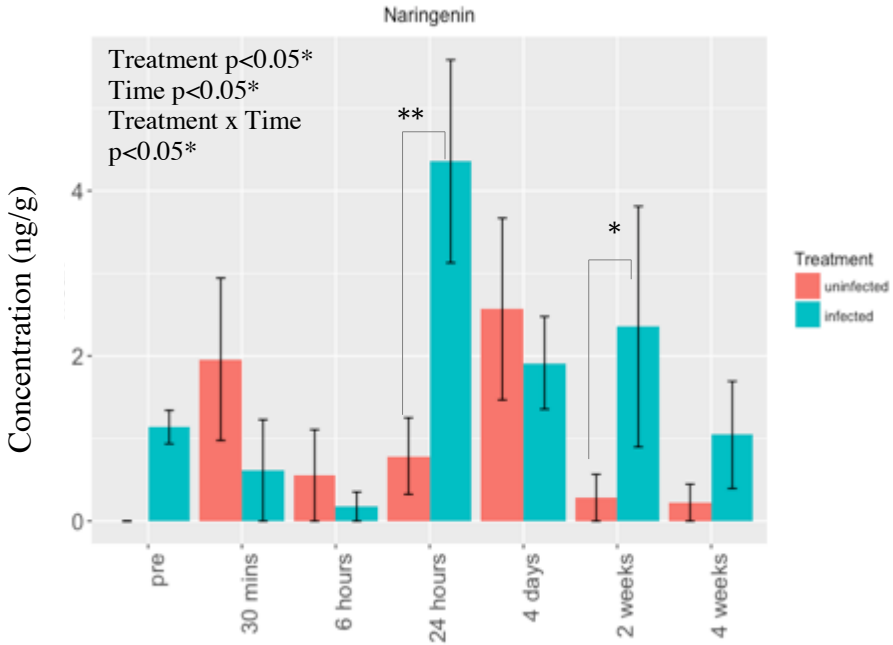
Naringenin
Treatment p<0.05*
Time p<0.05*
Treatment x Time
p<0.05*
**
*
Concentration (ng/g)
0
2
4
pre
30 mins
6 hours
24 hours
4 days
2 weeks
4 weeks
Treatment
uninfected
infected

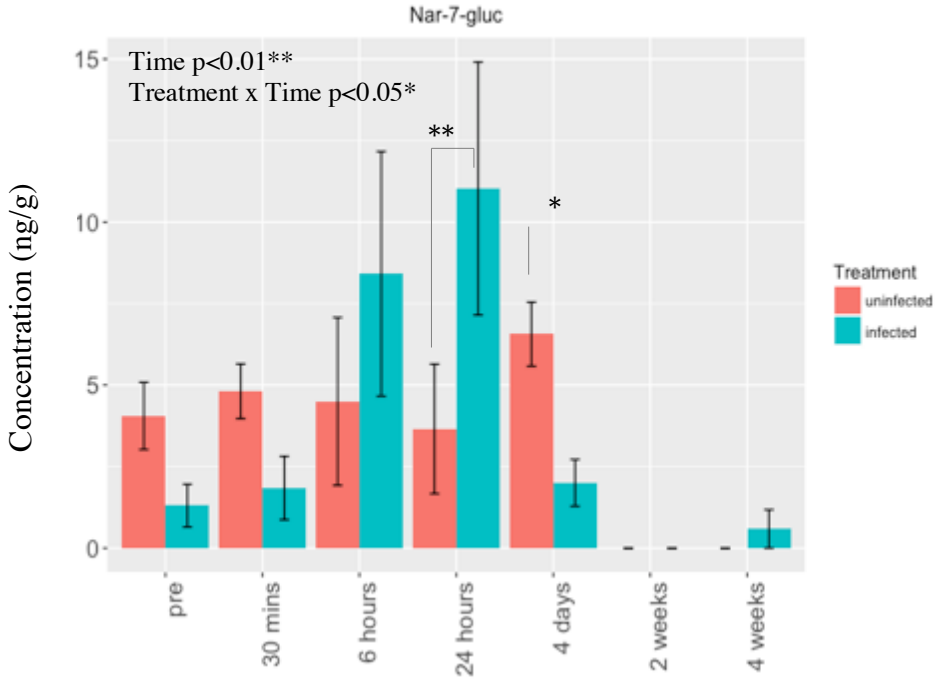
Nar-7-gluc
Time p<0.01**
Treatment x Time p<0.05*
**
*
Concentration (ng/g)
0
5
10
15
pre
30 mins
6 hours
24 hours
4 days
2 weeks
4 weeks
Treatment
uninfected
infected

Supplementary Figure 3.2: Concentrations of flavonoids positioned in the early stages flavonoid biosynthesis pathway, the chalcone, isoliquiritigenin, the flavanones, liquiritigenin, naringenin, and nar-7-gluc in uninfected and *Meloidogyne javanica*-infected roots of *Medicago truncatula* cv. 2HA at pre-infection, 30 minutes, 6 hours, 24 hours, 4 days, 2 weeks and 4 weeks post inoculation. Statistical analyses were based on linear mixed analysis to test the effects of time and treatment factors and the interactions between these factors. Columns represent mean and error bars represent standard errors. Asterisks denote statistically significant results, $p<0.05$. (N=3)

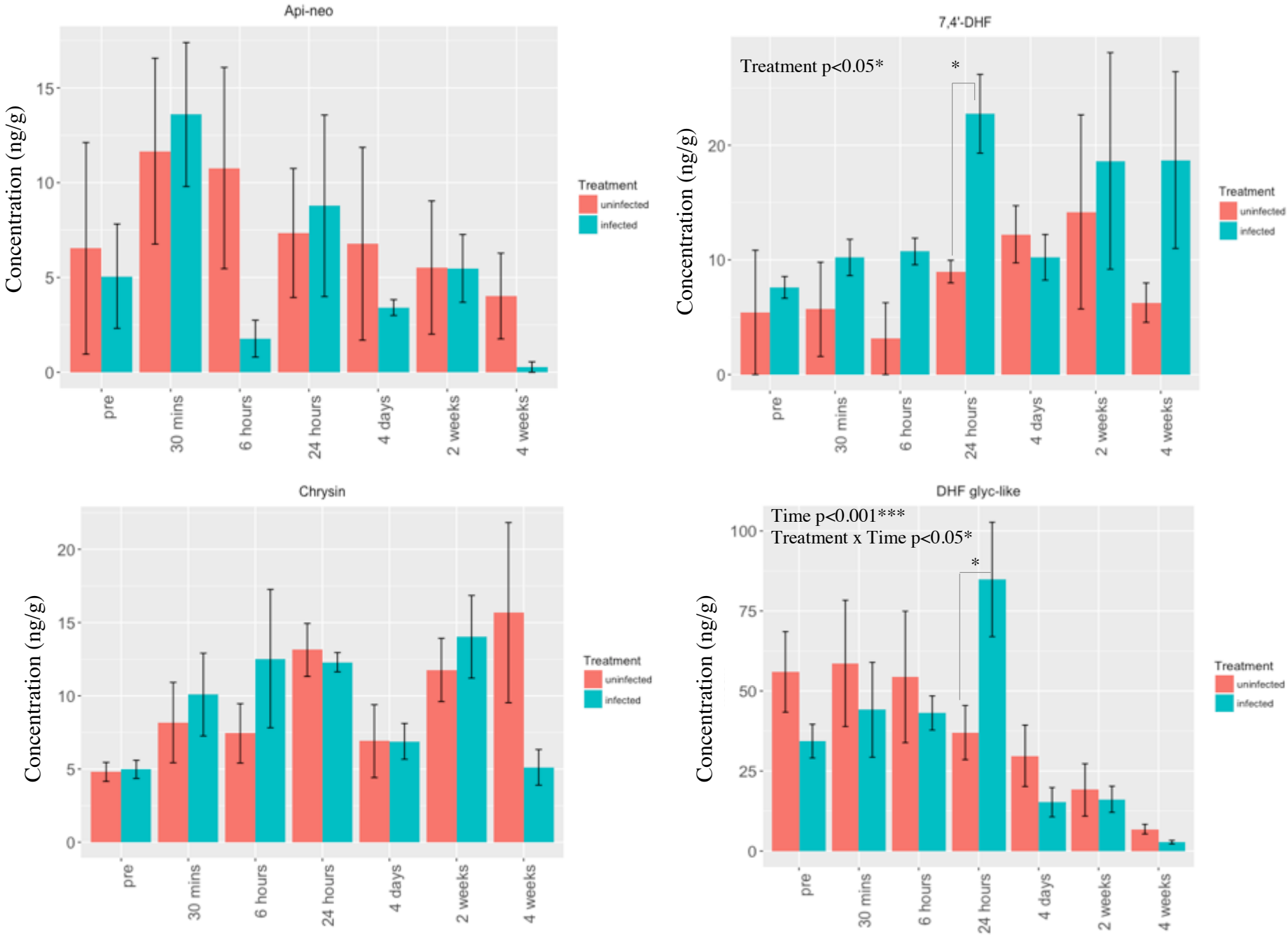
Api-neo
Concentration (ng/g)
15
10
5
0
pre
30 mins
6 hours
24 hours
4 days
2 weeks
4 weeks
Treatment
uninfected
infected
7,4'-DHF
Treatment p<0.05*
*
Concentration (ng/g)
20
10
0
pre
30 mins
6 hours
24 hours
4 days
2 weeks
4 weeks
Treatment
uninfected
infected
Chrysin
Concentration (ng/g)
20
15
10
5
0
pre
30 mins
6 hours
24 hours
4 days
2 weeks
4 weeks
Treatment
uninfected
infected
DHF glyc-like
Time p<0.001***
Treatment x Time p<0.05*
*
Concentration (ng/g)
100
75
50
25
0
pre
30 mins
6 hours
24 hours
4 days
2 weeks
4 weeks
Treatment
uninfected
infected

Supplementary Figure 3.3: Concentrations of the flavones api-neo, 7,4'-DHF, chrysin and the putative DHF-glyc-like in uninfected and *Meloidogyne javanica*-infected roots of *Medicago truncatula* cv. 2HA at pre-infection, 30 minutes, 6 hours, 24 hours, 4 days, 2 weeks and 4 weeks post inoculation. Statistical analyses were based on linear mixed analysis to test the effects of time and treatment factors and the interactions between these factors. Columns represent mean and error bars represent standard errors. Asterisks denote statistically significant results, $p<0.05$. (N=3)

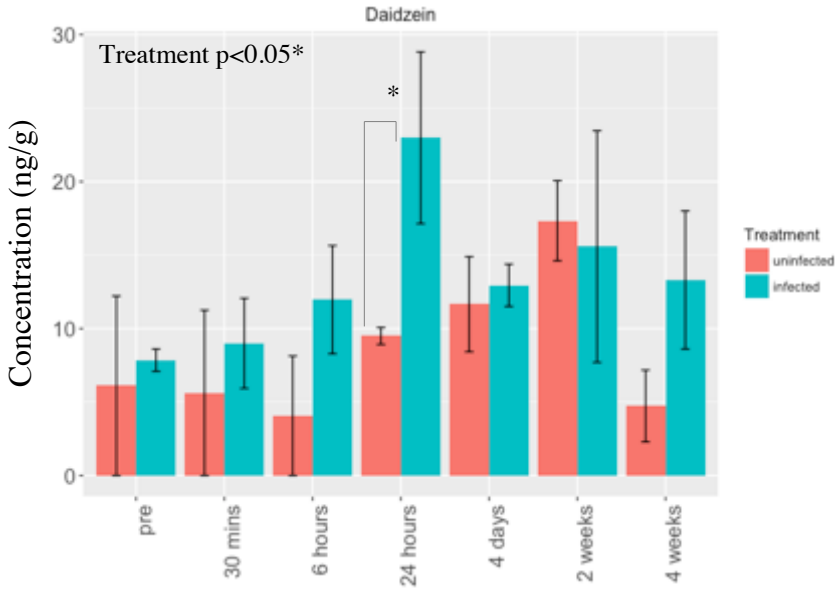
Daidzein
Treatment p<0.05*
Concentration (ng/g)
Treatment
uninfected
infected
pre
30 mins
6 hours
24 hours
4 days
2 weeks
4 weeks

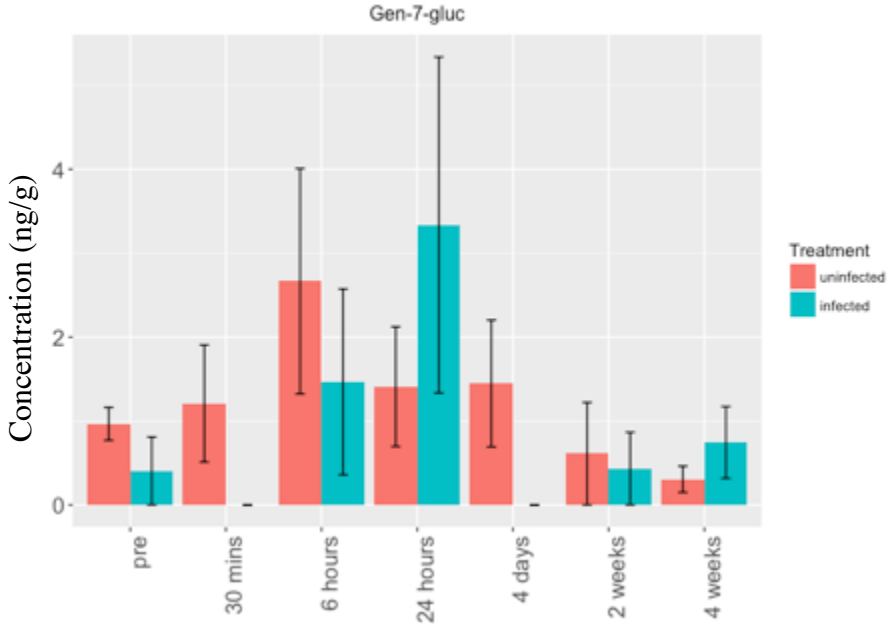
Gen-7-gluc
Concentration (ng/g)
Treatment
uninfected
infected
pre
30 mins
6 hours
24 hours
4 days
2 weeks
4 weeks

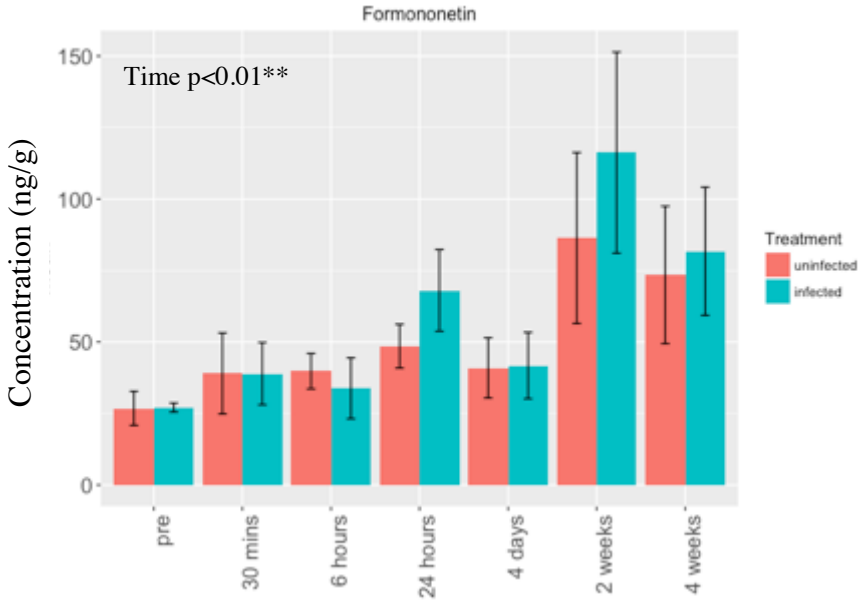
Formononetin
Time p<0.01**
Concentration (ng/g)
Treatment
uninfected
infected
pre
30 mins
6 hours
24 hours
4 days
2 weeks
4 weeks

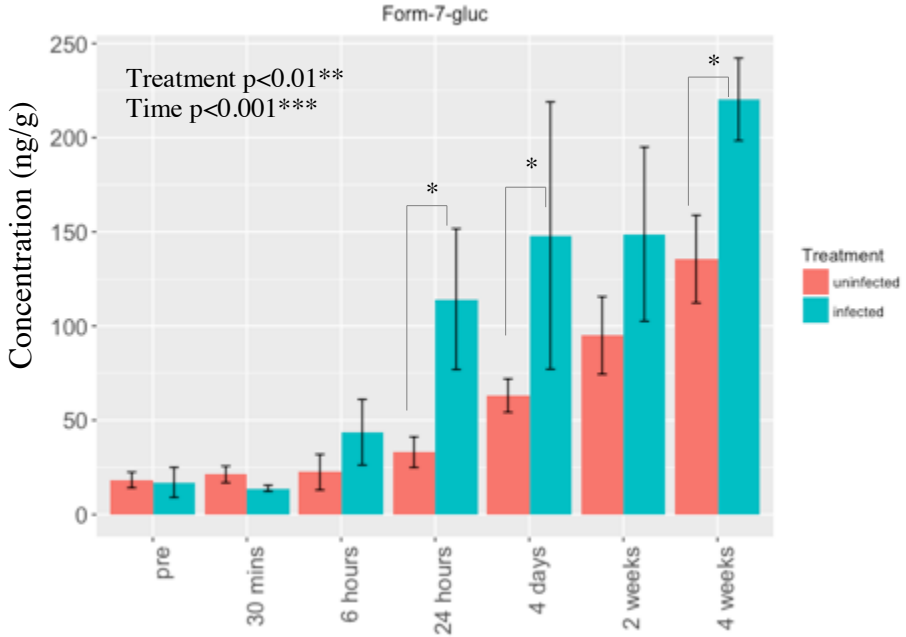
Form-7-gluc
Treatment p<0.01**
Time p<0.001***
Concentration (ng/g)
Treatment
uninfected
infected
pre
30 mins
6 hours
24 hours
4 days
2 weeks
4 weeks

Supplementary Figure 3.4: Concentrations of the isoflavonoids daidzein, gen-7-gluc, formononetin and form-7-gluc in uninfected and *Meloidogyne javanica*-infected roots of *Medicago truncatula* cv. 2HA at pre-infection, 30 minutes, 6 hours, 24 hours, 4 days, 2 weeks and 4 weeks post inoculation. Statistical analyses were based on linear mixed analysis to test the effects of time and treatment factors and the interactions between these factors. Columns represent mean and error bars represent standard errors. Asterisks denote statistically significant results, $p<0.05$. Asterisks above columns represent statistically significant differences between uninfected and infected groups at a given time. (N=3)

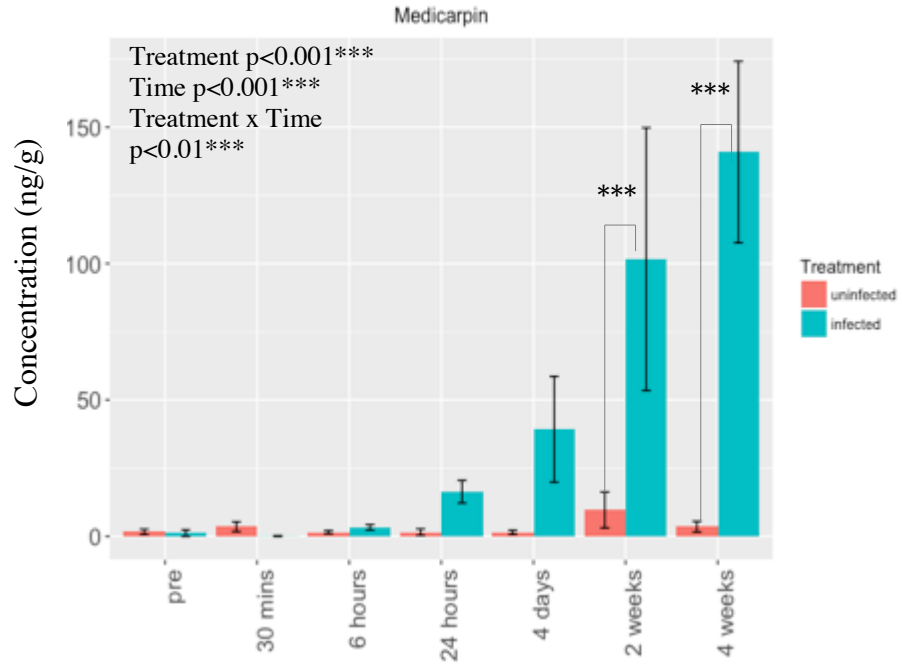
Medicarpin
Treatment p<0.001***
Time p<0.001***
Treatment x Time
p<0.01***
Concentration (ng/g)
150
100
50
0
***
***
pre
30 mins
6 hours
24 hours
4 days
2 weeks
4 weeks
Treatment
uninfected
infected

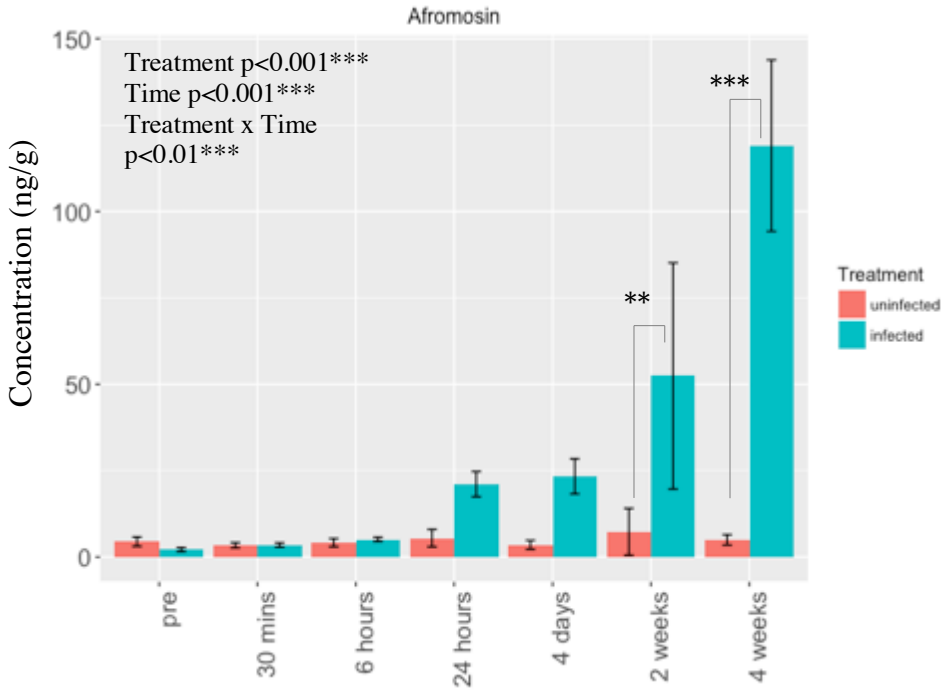
Afromosin
Treatment p<0.001***
Time p<0.001***
Treatment x Time
p<0.01***
Concentration (ng/g)
150
100
50
0
**
***
pre
30 mins
6 hours
24 hours
4 days
2 weeks
4 weeks
Treatment
uninfected
infected

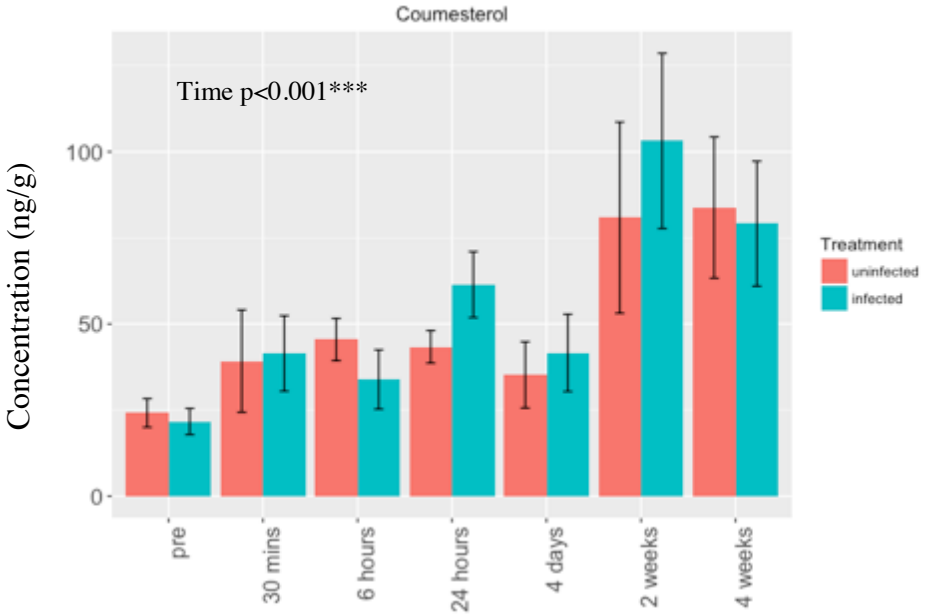
Coumesterol
Time p<0.001***
Concentration (ng/g)
100
50
0
pre
30 mins
6 hours
24 hours
4 days
2 weeks
4 weeks
Treatment
uninfected
infected

Supplementary Figure 3.5: Concentrations of the pterocarpan medicarpin, the isoflavonoid afromosin and the coumestan coumestrol in uninfected and *Meloidogyne javanica*-infected roots of *Medicago truncatula* cv. 2HA at pre-infection, 30 minutes, 6 hours, 24 hours, 4 days, 2 weeks and 4 weeks post inoculation. Statistical analyses were based on linear mixed analysis to test the effects of time and treatment factors and the interactions between these factors. Columns represent mean and error bars represent standard errors. Asterisks denote statistically significant results, $p<0.05$. Asterisks above columns represent statistically significant differences between uninfected and infected groups at a given time. (N=3)

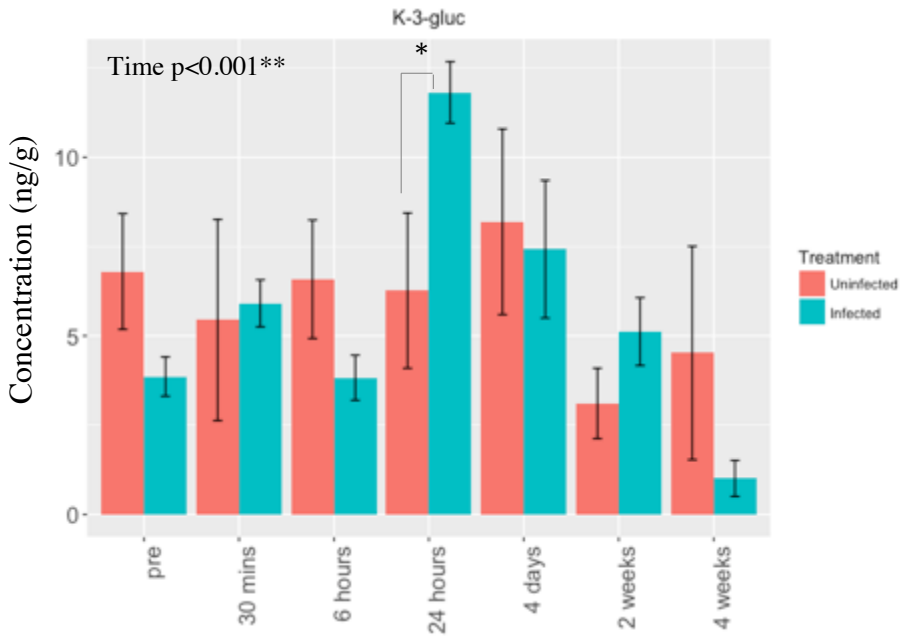
K-3-gluc
Time p<0.001**
*
Concentration (ng/g)
10
5
0
pre
30 mins
6 hours
24 hours
4 days
2 weeks
4 weeks
Treatment
Uninfected
Infected

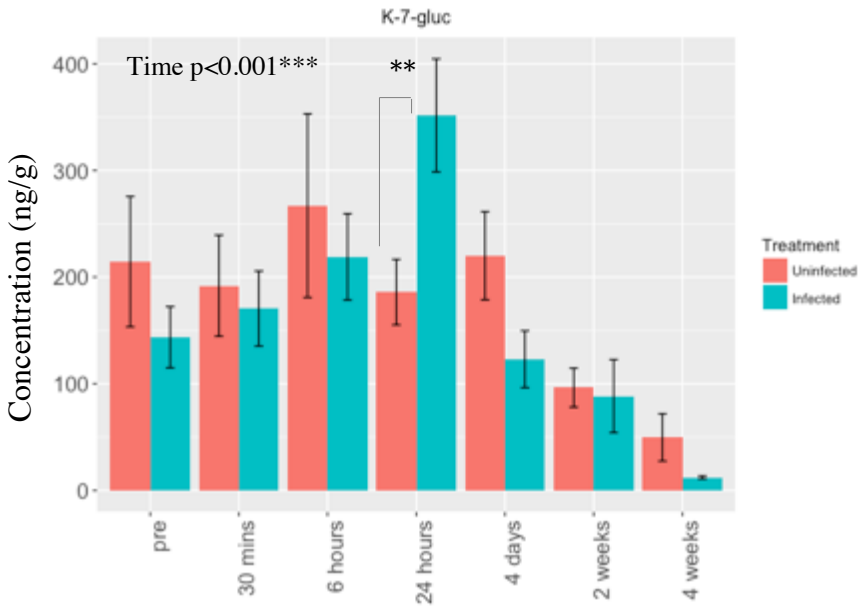
K-7-gluc
Time p<0.001***
**
Concentration (ng/g)
400
300
200
100
0
pre
30 mins
6 hours
24 hours
4 days
2 weeks
4 weeks
Treatment
Uninfected
Infected

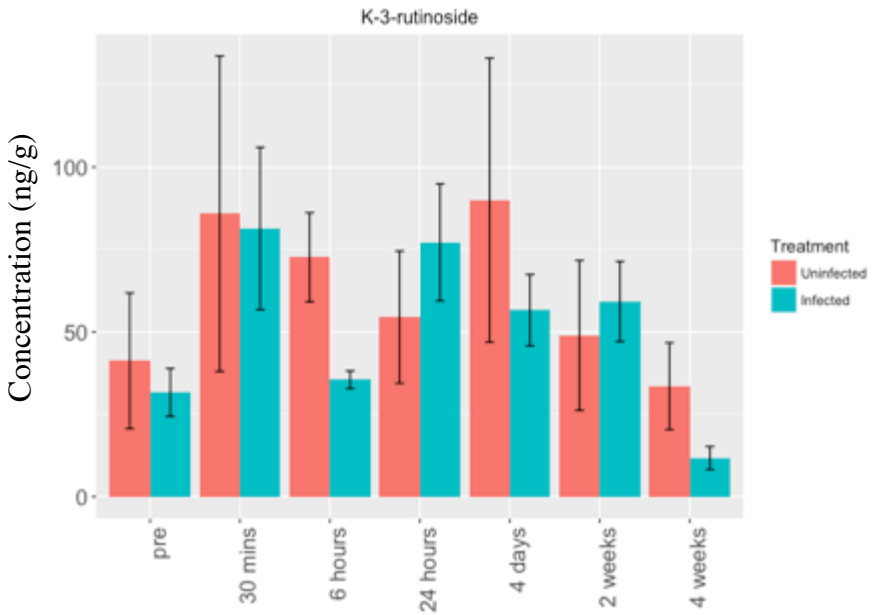
K-3-rutinoside
Concentration (ng/g)
100
50
0
pre
30 mins
6 hours
24 hours
4 days
2 weeks
4 weeks
Treatment
Uninfected
Infected

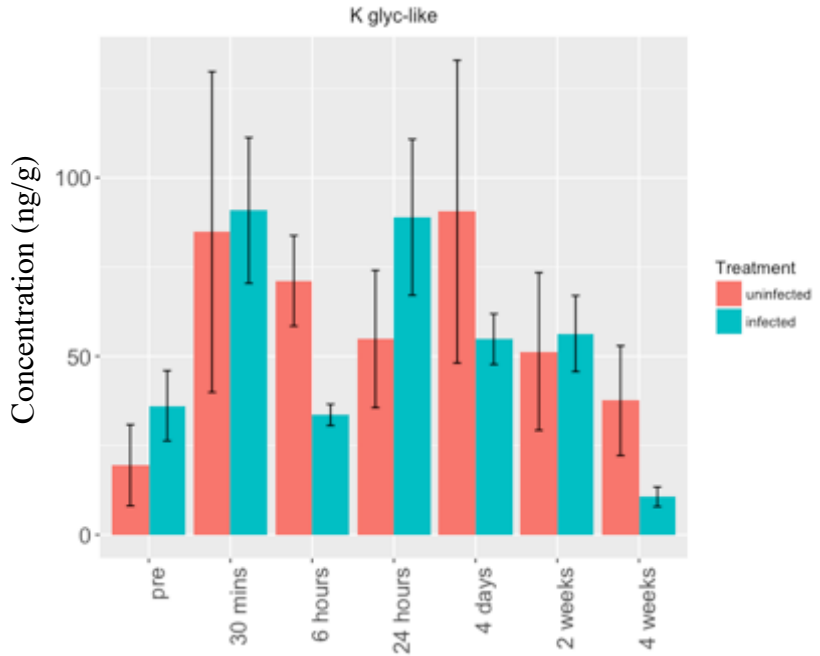
K glyc-like
Concentration (ng/g)
100
50
0
pre
30 mins
6 hours
24 hours
4 days
2 weeks
4 weeks
Treatment
uninfected
infected

Supplementary Figure 3.6: Concentrations of flavonols, K-3-gluc, K-7-gluc, K-3-rutinoside and a putative K-glyc-like in uninfected and *Meloidogyne javanica*-infected roots of *Medicago truncatula* cv. 2HA at pre-infection, 30 minutes, 6 hours, 24 hours, 4 days, 2 weeks and 4 weeks post inoculation. Statistical analyses were based on linear mixed analysis to test the effects of time and treatment factors and the interactions between these factors. Columns represent mean and error bars represent standard errors. Asterisks denote statistically significant results, $p<0.05$. (N=3)

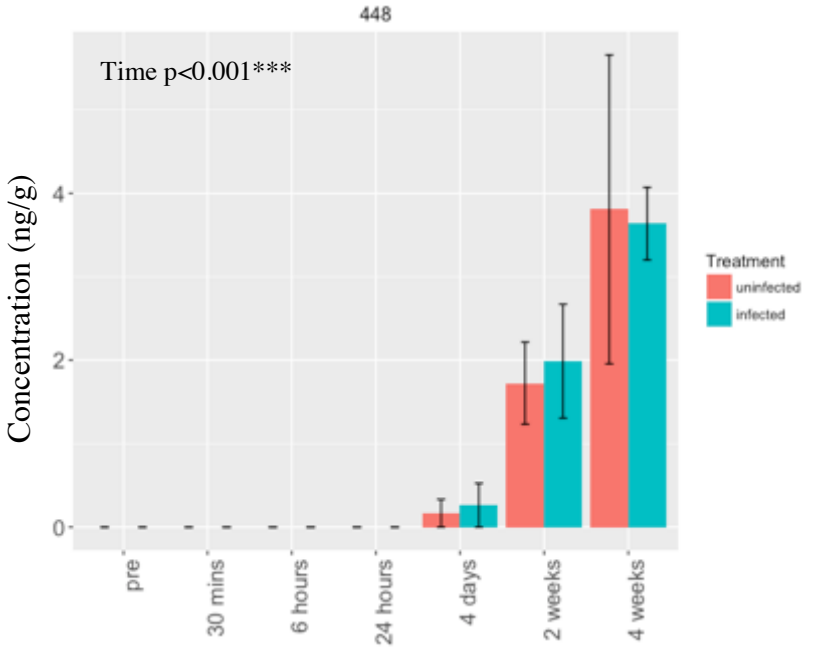
448
Time p<0.001***
Concentration (ng/g)
0
2
4
pre
30 mins
6 hours
24 hours
4 days
2 weeks
4 weeks
Treatment
uninfected
infected

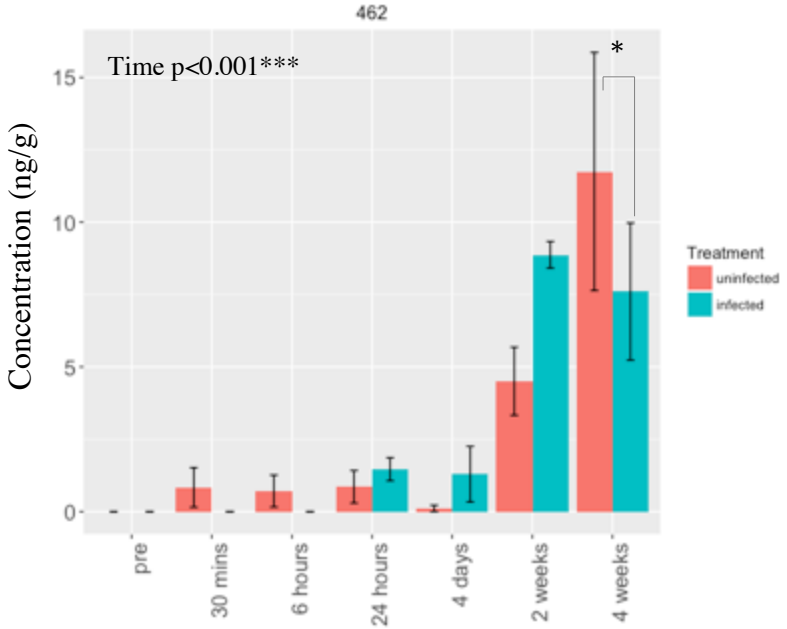
462
Time p<0.001***
*
Concentration (ng/g)
0
5
10
15
pre
30 mins
6 hours
24 hours
4 days
2 weeks
4 weeks
Treatment
uninfected
infected

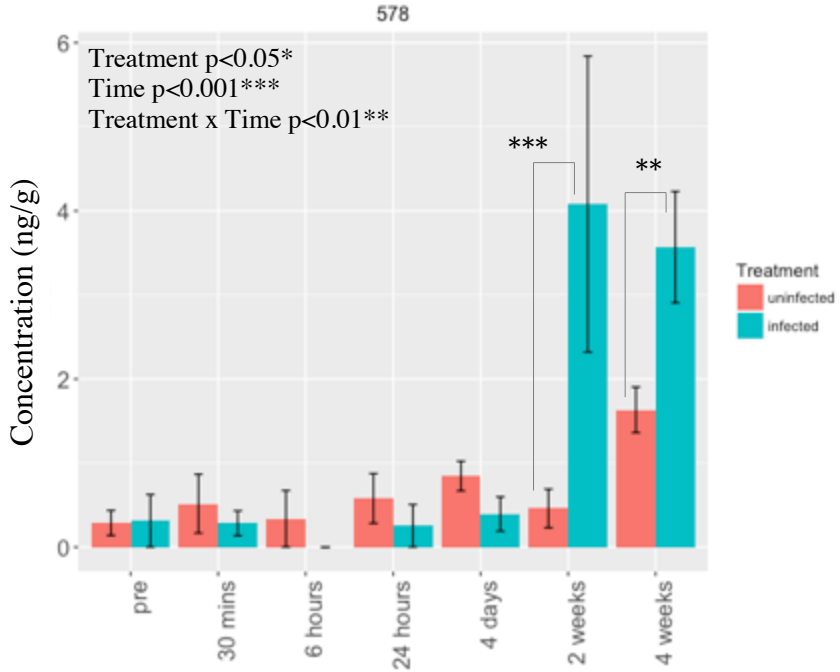
578
Treatment p<0.05*
Time p<0.001***
Treatment x Time p<0.01**
***
**
Concentration (ng/g)
0
2
4
6
pre
30 mins
6 hours
24 hours
4 days
2 weeks
4 weeks
Treatment
uninfected
infected

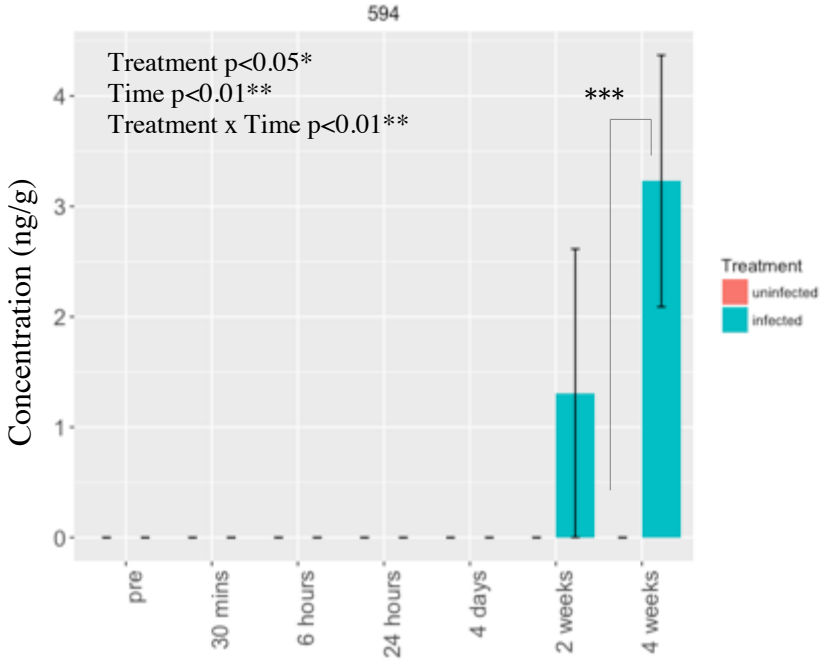
594
Treatment p<0.05*
Time p<0.01**
Treatment x Time p<0.01**
***
Concentration (ng/g)
0
1
2
3
4
pre
30 mins
6 hours
24 hours
4 days
2 weeks
4 weeks
Treatment
uninfected
infected

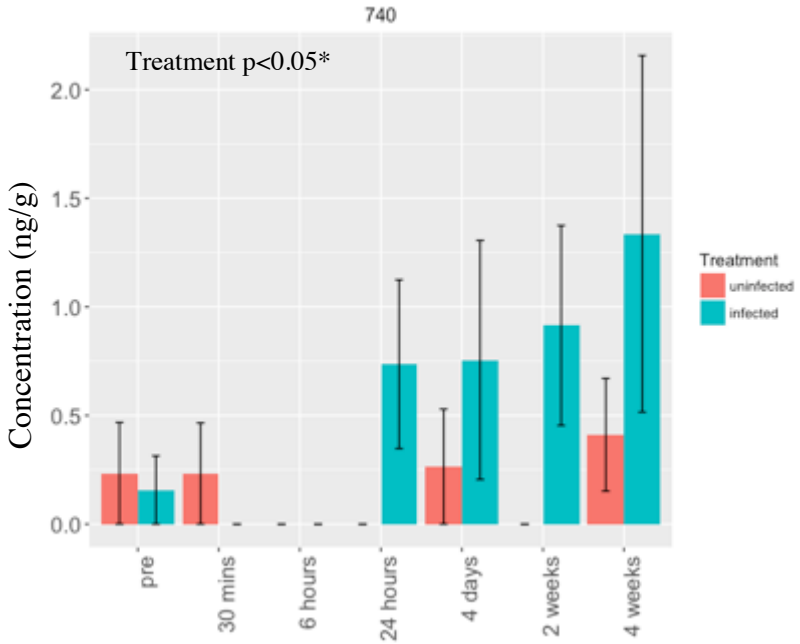

Supplementary Figure 3.7: Concentrations of tentative compounds, 448, 462, 578, 594 and 740 in uninfected and *Meloidogyne javanica*-infected roots of *Medicago truncatula* cv. 2HA at pre-infection, 30 minutes, 6 hours, 24 hours, 4 days, 2 weeks and 4 weeks post inoculation. Statistical analyses were based on linear mixed analysis to test the effects of time and treatment factors and the interactions between these factors. Columns represent mean and error bars represent standard errors. Asterisks denote statistically significant results, $p<0.05$. Asterisks above columns represent statistically significant differences between uninfected and infected groups at a given time. (N=3)

Chapter 4: Functional analysis of flavonoids in defence against root-knot nematodes

4.1 Abstract

The role of flavonoids in defence against nematodes was investigated by varying *in planta* flavonoid production either by the use of readily available cultivars and accessions, and by genetically modifying the *isoflavone synthase* (*IFS*) genes via RNA interference (RNAi) silencing and promoter over-expression. These experiments were also complemented with *in vitro* motility assays and chemotaxis assays of flavonoids and root exudates on the pre-parasitic J2 stage. Afromosin and medicarpin showed the best motility inhibition and repellence. Nevertheless, high levels of *in planta* afromosin did not appear to reduce nematode infection, whereas early accumulation of *in planta* medicarpin at 24 hours post infection may reduce infection severity, as observed in *IFS* over-expression plants. Certain flavonols and isoflavonoids were weak to moderate motility inhibitors and repellents. Although the chalcone isoliquiritigenin was induced during nematode infection, it was a poor motility inhibitor and did not repel J2s and thus, is likely to be involved in other roles.

4.2 Introduction

Flavonoids play a multitude of roles in the plant, from acting as UV protectants, pigments, auxin transport inhibitors, signalling molecules, to one of the more important roles in protecting the plant against pathogens (Winkel-Shirley, 2002). The activities of flavonoids as defence compounds are broad-spectrum, and specificity is derived from the ability of a pathogen to detoxify the flavonoid (Dixon, 2001, Mierznak et al., 2014). This is used to regulate reactive oxygen species homeostasis generated by both the plant and pathogen during infection (Mierznak et al., 2014). In addition, flavonoids can induce hypersensitive response and callus formation when incorporated into the cells and cell walls of infected cells and those adjacent to them. As defence compounds, they are often categorised into two groups: the phytoanticipins and phytoalexins (Treutter, 2005). The former is pre-formed during normal plant development and are often stored in vacuoles and rapidly released during a pathogen attack, whereas the latter is induced and synthesised in concentrations sufficient to be antimicrobial in response to pathogenesis. Nevertheless, these terms are often indistinguishable as the same flavonoids are interchangeable as phytoanticipins and phytoalexins in different plant species (Dixon, 2001). Moreover, it is difficult to definitively quantify the true concentrations of a flavonoids as well as ascertaining the sufficient bioactive concentrations *in vivo*. As a result, we refrain from using these terminologies and classify them broadly as defence compounds when their detected levels significantly increased due to infection and when they exhibit *in vitro* bioactivities against nematodes.

The subgroups isoflavonoids and pterocarpans have been well described as defence compounds, although individual flavonoids from other subgroups can play similar roles. The pterocarpan medicarpin is induced in different plants such as alfalfa and pea in response to the pathogenic fungi *Rhizoctonia solani* and *Phoma medicaginis* (He and Dixon, 2000, Guenoune et al., 2001). On the other hand, some pterocarpans are specific to one species, such as pisatin in pea (Perrin and Bottomley, 1961) and glyceollin in soybean (Kaplan et al., 1980a). Although numerous studies demonstrated the induction of flavonoids during PPN infection (previously reviewed in Chapter 1), no studies have targeted an extensive list of flavonoids metabolites

(most focussed on up to six metabolites) nor complemented their studies with multiple approaches, with authors using single approach of transcriptomic, metabolomics or *in vitro* assays. Furthermore, there is a lack of comparative studies into conserved flavonoid induction in plants with different genotypes and susceptibilities to nematode infection.

The elucidation of flavonoids as defence compounds in the interaction of *M. truncatula* with *M. javanica* encompassed *in planta* and *ex planta* strategies. The *in planta* approach involved nematode infection in seven different *M. truncatula* genotypes which included two accessions, two cultivars and three *IFS* modified transgenics with different flavonoid contents. This experiment was split into two groups, the cultivars/accessions group, which included the cultivars 2HA, A17, the accessions DZA045 and F83005 and the other being the transgenics group, which targeted *IFS* through both RNAi and over-expression to silence and increase gene expression, respectively with the inclusion of wild-type 2HA. The isoflavonoid pathway was selected based on results from Chapter 3, in which isoflavonoids and the isoflavonoid-derived flavonoids, pterocarpans were highly induced in response to infection. For the first experiment, the two accessions, DZA045 and F83005 were selected based on the study by Dhandaydham et al. (2008) which reported that the former accession was more resistant to *M. incognita, M. hapla* and *M. arenaria,* whereas the latter accession was more susceptible to the afromentioned nematodes based on galling severity. The resistance mechanism was not fully understood, and the authors excluded a hypersensitive-based resistance mechanism and differences in J2 migration in the root. The two cultivars selected were the readily available and closely related *M. truncatula* Jemalong cv. 2HA and cv. A17. As for the transgenics, *M. truncatula* Jemalong cv. 2HA was transformed with an RNAi silencing construct, with two *IFS* silenced (IFSi) lines selected, IFSi 101-2 and IFSi 42-7 and a 35S promoter::*IFS* over-experession cassette, with one *IFS* over-expression (IFSOE) line, IFSOE 10-3 being selected. Subsequently, these seven genotypes were infected with *M. javanica* J2s and infection phenotypes such as gall number, gall size (2 dimensional), and nematode eggs were measured.

Ex planta strategies such as motility and chemotaxis assays have been developed to inform on how the pre-parasitic J2 stage of *M. javanica* are likely to in the root rhizosphere when it is locating its host. Several chemotaxis assays have been

employed, varying from complex and expensive labyrinth setups with specialised microchannels (Hida et al., 2015, Reynolds et al., 2011) to simpler agar filled dishes (Dalzell et al., 2011, Diez and Dusenbery, 1989, Wuyts et al., 2006b). The selected chemotaxis setup in this project included the use of agar filled dishes. The tested compound placed in the centre of the dish and J2s were evenly distributed across the dish. The change in their distribution in response to the compound in the dish was recorded based on concentric ring grids (Figure 2.2). As for the motility assay, a high-throughput technique was developed with the use of a computer software, WormAssay to calculate the number of body bends over time in response to selected flavonoids (Marcellino et al., 2012).

The aims of this chapter are summarised as below:

1) Investigate whether the differing susceptibilities of four *M. truncatula* genotypes to *M. javanica* is associated with their root flavonoid content.
2) Examine the effects of *in planta* up and down-regulation of isoflavonoids on nematode infection using *M. truncatula* transgenics.
3) Determine the bioactivity of selected flavonoids and root exudates on *in vitro* nematode chemotaxis and motility.

4.3 Results

4.3.1. Nematode infection in *Medicago truncatula* cultivars/accessions with different *Meloidogyne* susceptibilities

4.3.1.1. Nematode infection phenotypes

M. truncatula cultivars 2HA, A17, and accessions DZA045 and F83005 were infected with *M. javanica* J2s at one week old. Next, these plants were monitored over the duration of 6 weeks and infection phenotypes were observed. These included 1) gall phenotypes- number of galls per plant and gall size, and 2) number of eggs per plant.

All four genotypes had similar number of galls, with an average of about 4 galls per plant (Figure 4.1). However, the sizes of their galls varied significantly ($p<0.01$) (Figure 4.1). DZA045 galls were significantly smaller than 2HA and A17 galls, with the average size of 3.4 mm^2, compared to 2HA's galls which measured 4.4 mm^2 and A17's galls that were 4.1 mm^2(Figure 4.1). F83005 galls were slightly larger than DZA045 galls with an average size of 4 mm^2 (Figure 4.1).

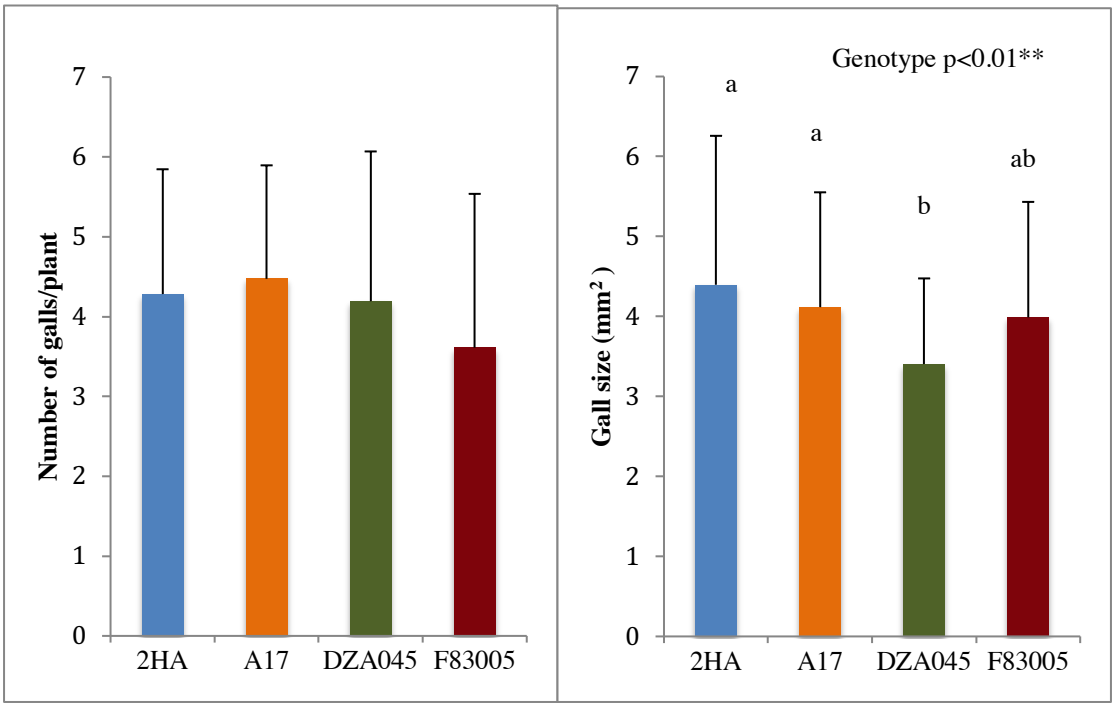

Figure 4.1: Gall phenotypes observed in four *Medicago truncatula* cultivars/accessions, 2HA, Jemalong A17, DZA045 and F83005 at 6 weeks post inoculation with *Meloidogyne javanica*. Genotype effect was tested using linear mixed analysis. Letters represent statistically significant differences amongst groups using Tukey pairwise comparison. Columns represent means and error bars represent standard errors. (N=4)

In addition to gall phenotypes, the number of eggs produced by adult female nematodes were harvested from egg sacs on mature eggs and the eggs were counted. Plant genotype influenced egg production ($p<0.05$) (Figure 4.2). Nematodes infecting DZA045 plants produced the most eggs, with an average of 1720 eggs per plant, which was in contrast to egg production in F83005 plants, in which adult females produced significantly less eggs, at 344 eggs per plant (Figure 4.2). On the other hand, egg production in 2HA and A17 plants did not vary significantly to other genotypes, with average egg numbers per plant at 1335 and 1549, respectively (Figure 4.2).

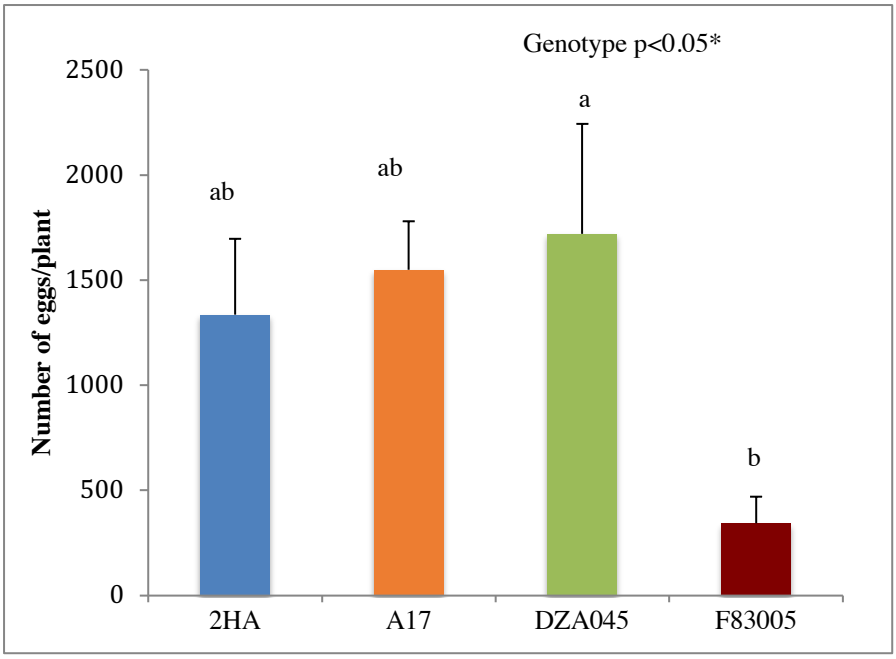

Figure 4.2: Number of eggs per plants in four *Medicago truncatula* cultivars/accessions, 2HA, Jemalong A17, DZA045 and F83005 at 6 weeks post inoculation with *Meloidogyne javanica*. Genotype effect was tested using linear mixed analysis. Letters represent statistically significant differences amongst groups using Tukey pairwise comparison. Columns represent means and error bars represent standard errors. (N=3)

4.3.1.2. Flavonoid phenotypes

Flavonoids were extracted from root segments of uninfected and infected plants of *M. truncatula* 2HA, A17, DZA045 and F83005 at 24 hours and 6 weeks post inoculation. These were subsequently separated and detected on the LC-ESI-Q-TOF-MS/MS and analysed with OPLS-DA. 48.2% (R^2Y= 0.482) of flavonoid responses in these four genotypes were separated based on nematode treatment variable, and 38.8% of flavonoid responses can be accurately predicted based on the treatment variable (Q^2Y= 0.388) (Figure 4.3A). The flavonoid responses that were heavily influenced by nematode infection at 24 hours and 6 weeks post inoculation were afromosin, isoliquiritigenin, naringenin, rutin, 740, k-gluc-rham, 784, methoxyisoflav 2 and liquiritigenin (Figure 4.3C).

OPLS-DA modelling on the same sets of flavonoid responses (both uninfected and infected data) based on genotype factor showed a less robust model with R^2Y= 0.46, Q^2Y= 0.289 (Figure 4.3B). All four genotypes showed similarities in flavonoid responses for daidzein, DHF glyc-like, k-3-rutinoside, luteolin, liquiritigenin, medicarpin, glycetein, gen-7-gluc and genistein (Figure 4.3D), regardless of infection status. Generally, A17 and 2HA genotypes showed the highest similarities to each other (Figure 4.3B), which was expected as both cultivars were derived from the Jemalong background (Rose et al., 1999, Rose, 2008). On the other hand, the French accession F83005 and Algerian accessions DZA045 showed similarities in flavonoid responses (Figure 4.3B), which may indicate common lineages.

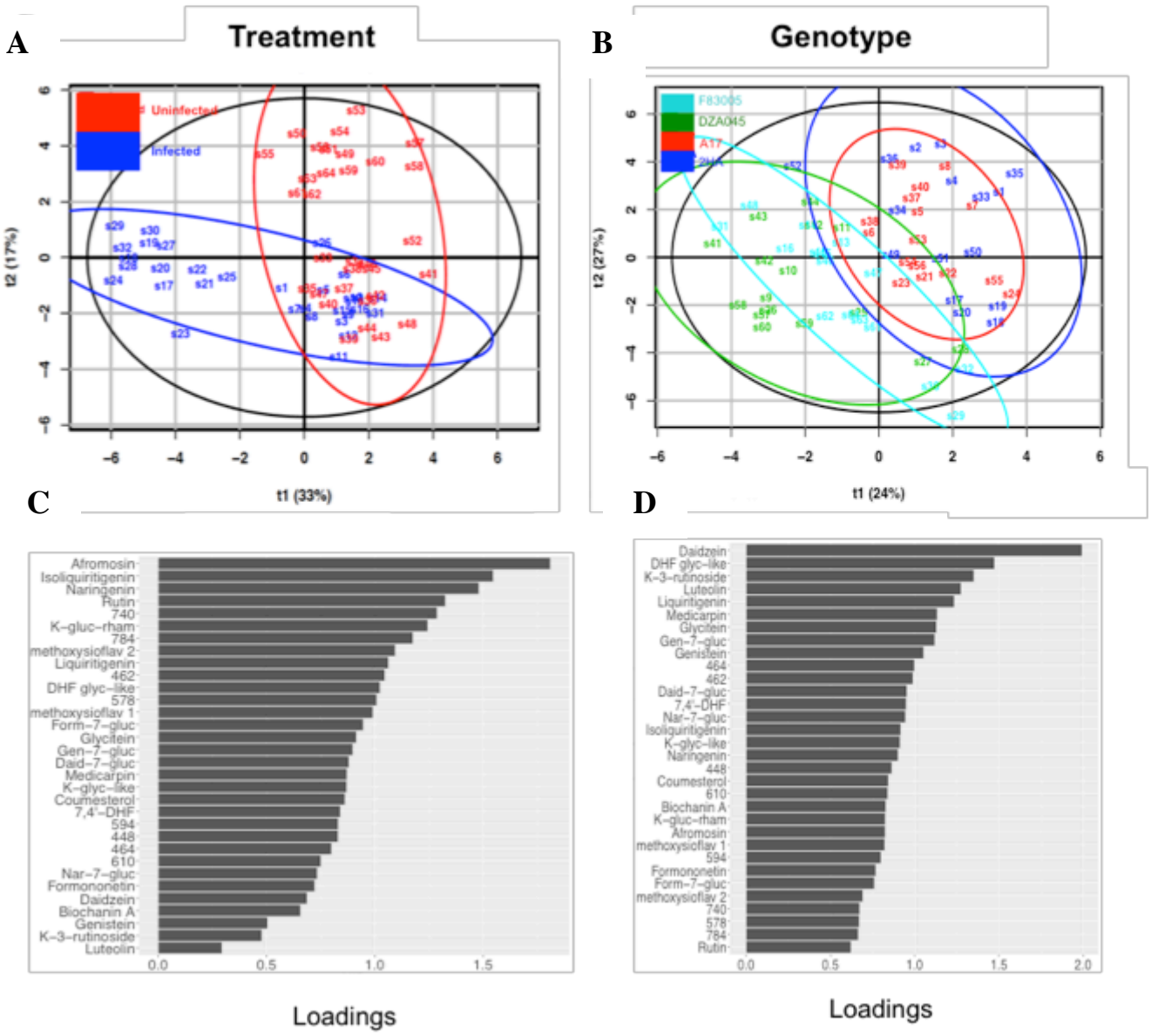

Figure 4.3: OPLS-DA analyses and the corresponding loading plots of flavonoid responses (log 10 concentrations) of four *Medicago truncatula* cultivars/accessions (2HA, Jemalong A17, DZA045 and F83005) in control plants and nematode infected plants at 24 hours and 6 weeks post inoculation. **(A)** Discrimination of flavonoid responses based on the treatment factor. $R^2Y= 0.482$, $Q^2Y= 0.388$. **(B)** Discrimination of flavonoid responses based on genotype factor. $R^2Y= 0.46$, $Q^2Y= 0.289$. **(C)** OPLS-DA loadings for the discrimation of flavonoid responses based on the treatment factor. (**D**) OPLS-DA loadings for the discrimination of flavonoid responses based on genotype factor.

The fold changes in flavonoid concentrations between infected and uninfected groups were calculated and plotted as a heatmap (Figure 4.4). Isoliquiritigenin was increased in all four lines at 24 hours and 6 weeks post inoculation time points (Figure 4.4). The flavanones, liquiritigenin, naringenin and nar-7-gluc showed variable accumulation at 24 hours, particularly nar-7-gluc which showed reduction in A17 and 2HA plants, but were mostly increased at 6 weeks (Figure 4.4). Flavonols showed slight fold changes or were unchanged between uninfected and infected groups at 24 hours (Figure 4.4). However, at 6 weeks, the flavonol responses diverged into reductions for k-gluc, k-3-rutinoside (with the exception of 2HA plants showing an increase), and k-glyc-like and increases for k-gluc-rham and rutin (Figure 4.4). The flavones, luteolin and 7,4'-DHF levels oscillated up and down at 24 hours and 6 weeks, whereas DHF glyc-like and glycitein were mostly unchanged at 24 hours but were mostly decreased at 6 weeks (Figure 4.4). Methoxyisoflav 1 and methoxyisoflav 2 were consistently unchanged in all lines at 24 hours but by 6 weeks, methoxyisoflav 1 was reduced in all lines but 2HA, whereas methoxyisoflav 2 was increased in all lines (Figure 4.4). At 24 hours, isoflavonoids were mostly unchanged or slightly increased or decreased (Figure 4.4). At 6 weeks, the isoflavonoid profiles in A7 plants were the outliers amongst the other three genotypes, whereby isoflavonoids in A17 were reduced, whereas these were increased in other genotypes (Figure 4.4). Medicarpin and afromosin were mostly increased at both time points, whereas coumesterol was decreased in DZA045 plants at 24 hours and A17 plants at 6 weeks (Figure 4.4). Variable trends were also observed for unidentified compounds at 24 hours (Figure 4.4). However, at 6 weeks, compound 784 was consistently increased in all lines (Figure 4.4). In addition, A17 plants also showed decreased unidentified compounds at 6 weeks, which was in contrast to other genotypes (Figure 4.4).

Statistical analysis using linear mixed model found that the changes in flavonoid concentrations in isoliquiritigenin, liquiritigenin, naringenin, nar-7-gluc, k-gluc-rham, rutin, 7'4'-DHF, methoxyisoflav 1, methoxyisoflav 2, daidzein, form-7-gluc, medicarpin, afromosin and 784 were attributable to nematode infection (Figure 4.4 and Supplementary Table 4.2). On the other hand, flavonoids such as k-3-rutinoside, k-glyc-like, formononetin, afromosin, coumesterol and 784 were significantly influenced by the interactions between time, genotype and infection treatment (Figure 4.4 and Supplementary Table 4.2).

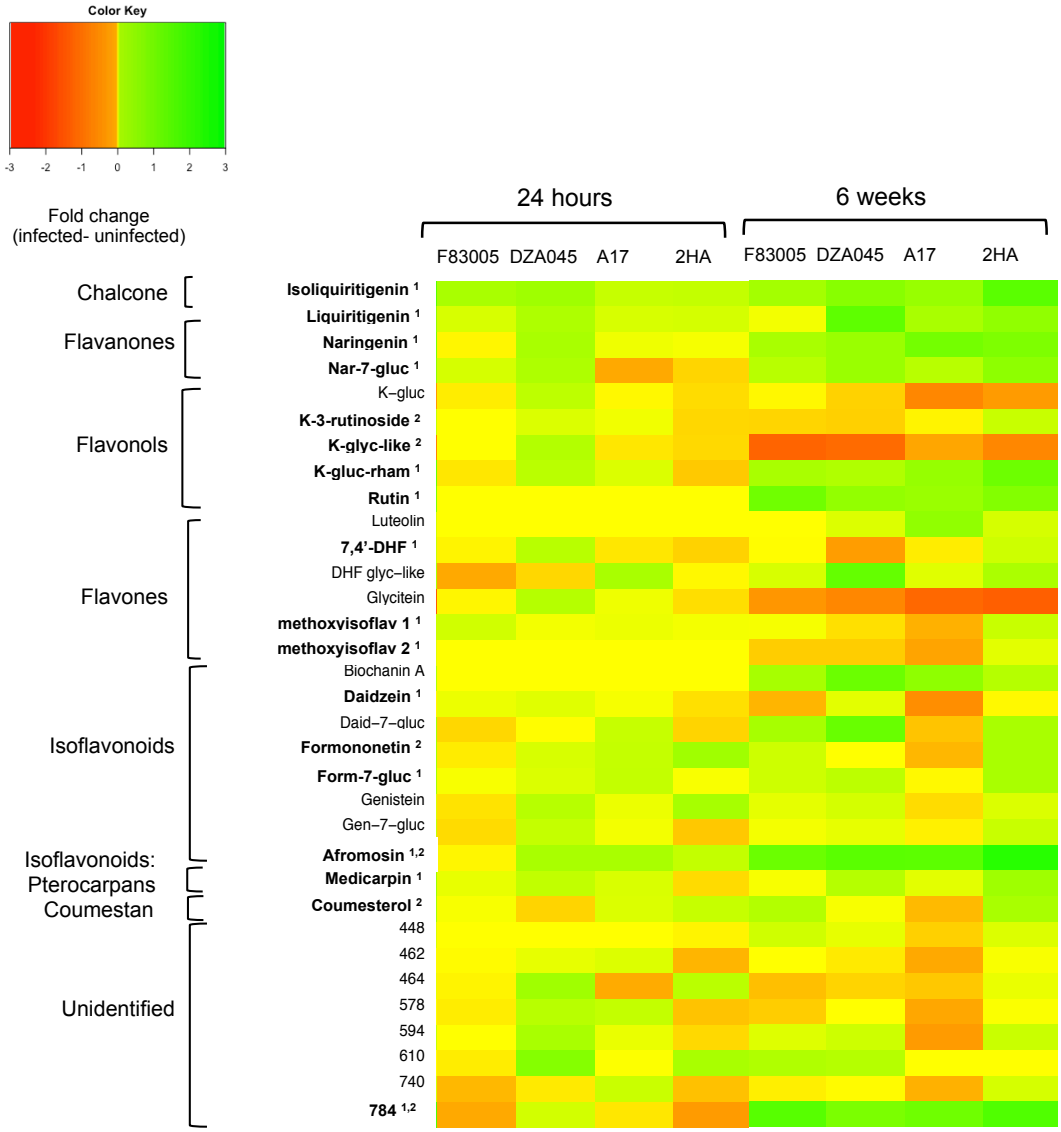

Figure 4.4: Fold changes in flavonoid concentrations (log10) between uninfected and *Meloidogyne javanica* infected roots of *Medicago truncatula* cultivars/accessions 2HA, A17, DZA045 and F83005 at 24 hours and 6 weeks post inoculation. Flavonoids in highlighted in bold showed statistically significant effects for treatment (indicated by the subscript number 1) and for time x treatment (infection) x genotype factors (indicated by the subscript number 2) based on linear mixed model analysis on flavonoid concentrations (full description of linear mixed model results available on Supplementary Table 4.1).

4.3.1.3. The link between infection and flavonoid phenotypes

To test for a possible correlation between infection phenotypes and flavonoid phenotypes, simple regressions between gall size or egg number (measured at 6 weeks post inoculation) with flavonoid concentrations at 6 weeks were performed (Supplementary Table 4.2). Gall number phenotype was excluded, as this phenotype was similar in all genotypes. Gall size in the four accessions/cultivars showed positive linear relationships with liquiritigenin, naringenin and 784 concentrations ($p<0.05$) (Figure 4.5 and Supplementary Table 4.2). As for egg number per plant phenotype, there was no linear relationship with any of the quantified flavonoids (Supplementary Table 4.2).

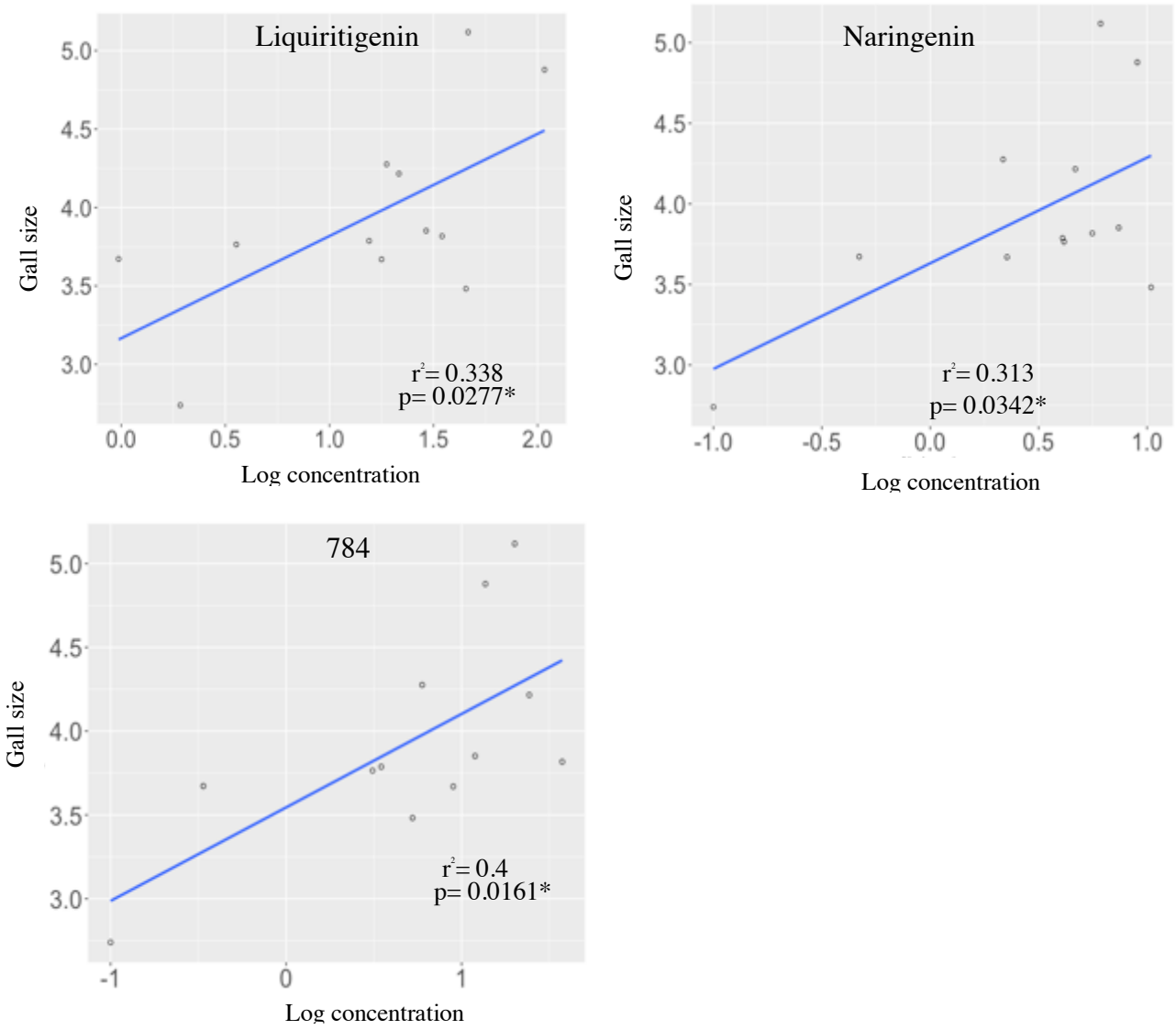

Figure 4.5: Scatter plots of flavonoid concentrations with statistically significant positive linear relationships with the gall size in infected *Medicago truncatula* cultivars, 2HA, A17, DZA045 and F83005 at 6 weeks post inoculation with *Meloidogyne javanica*. Asterisks indicate $p<0.05$.

4.3.2. Nematode infection in *Medicago truncatula* transgenics with silenced or over-expressed isoflavone synthase

4.3.2.1. Generation of *M. truncatula* IFS transgenics

M. truncatula cv. Jemalong, genotype 2HA plants were transformed using *Agrobacterium tumafaciens* mediated transformation as described by (Chabaud et al., 2007). Based on results on Chapter 3 (Section 3.3.2.), the isoflavonoid and flavonols pathways were selected for modification (Figure 1.3). *Isoflavone synthase (IFS*) gene members, *IFS 1* and three others (designated as XM_013601477.2, XM_0.13601742.2 and putative *IFS*) were silenced using the pk7WIWG2D(II) vector (Karimi et al., 2002) or over-expressed through the over-expression of *IFS* 1 using 35S promoter in pK7WG2D vector (Karimi et al., 2002). Likewise, three *flavone synthase (FLS)* gene members, designated as XM_003614733, BT146097.1 and XM_003614732.3 were silenced, whereas *FLS* gene (MTR_5g059140) was over-expressed.

Flavonol transgenics did not survive past the rooting of shoots stage likely as a result of essential functions of flavonols in plant development in auxin transport regulation (Brown et al., 2001). As for isoflavonoid transgenics, 11 IFSi lines and two IFSOE lines successfully regenerated. Subsequently, two IFSi lines, IFSi 42-7 and IFSi 101-2 and one IFS-OE line, IFSOE 10-3 were determined to be positive homozygotes by segregation analysis using DNA genotyping of the transformation marker, kanamycin resistance gene, *nptII* (Supplementary Figure 4.1.).

Empty vector plants for both silencing and over-expressions were also generated but these did not regenerate. Therefore, untransformed *M. truncatula* cv. 2HA plants were selected as controls.

The selected three transgenics, IFSi 42-7, IFSi 101-2 and IFSOE 10-3 plants showed higher *nptII* (transformation marker) expressions (Figure 4.6) compared to untransformed wild-type 2HA plants (based on housekeeping gene, *GAPDH* levels in all lines). IFSi 42-7 plants showed significantly less *CHS* transcripts than IFSi 101-2

and IFSOE 10-3 plants (Figure 4.6). This trend was similar for *IFS* gene expression, although the reduction in *IFS* transcript in IFSi 42-7 was insignificant.

In addition, these transgenics were phenotyped based on their flavonoid profiles and were compared to wild-type 2HA plants (Figures 4.6 and 4.7). For metabolite phenotypying, flavonoids in roots were extracted from an aliquot (100 mg) of the whole root system, whereas flavonoids in exudates were extracted from the plant growth media, Fåhraeus media.

IFSOE 10-3 plants produced the highest levels of isoliquiritigenin in the root and root exudates compared to 2HA, IFSi 101-2 and IFSi 42-7 (Figure 4.7). On the other hand, the flavanones, naringenin and liquiritigenin were produced at similar levels to 2HA and IFSi 42-7 in the root (Figure 4.7). Nonetheless, IFSOE 10-3 root exuded the least naringenin, whereas liquiritigenin was exuded at the highest levels compared to all plants (Figure 4.7). As for isoflavonoids, IFSOE 10-3 plants produced the most formononetin and medicarpin in roots and root exudates (Figure 4.8). Although IFSOE 10-3 plants produced significantly more daidzein in roots than other lines, IFSOE 10-3 roots exudated the least daidzein (Figure 4.8). On the other hand, afromosin was produced in IFSOE 10-3 roots at similar concentration to other plants but was exuded at the highest concentration (Figure 4.8).

Both IFSi lines, IFSi 101-2 and IFSi 42-7 plants produced varied amounts of upstream flavonoids, ie. isoliquiritigenin, naringenin and liquiritigenin, with IFSi 101-2 roots producing less of these flavonoids and exuded less compared to IFSi 42-7 (Figure 4.7). Moreover, the production of these upstream flavonoids in IFSi 42-7 roots was unaffected by gene silencing, as these roots produced the same amount of upstream flavonoids compared to 2HA roots (Figure 4.7). However, IFSi 42-7 roots showed variation to 2HA roots in exudation of these compound, in which IFSi 42-7 roots exuded more flavonoids (Figure 4.7). IFSi 101-2 and IFSi 42-7 roots produced comparable amounts of isoflavonoids in the root but varied in exudation (Figure 4.8). IFSi 42-7 roots exuded more formononetin and daidzein but less medicarpin compared to IFSi 101-2 root exudate (Figure 4.8).

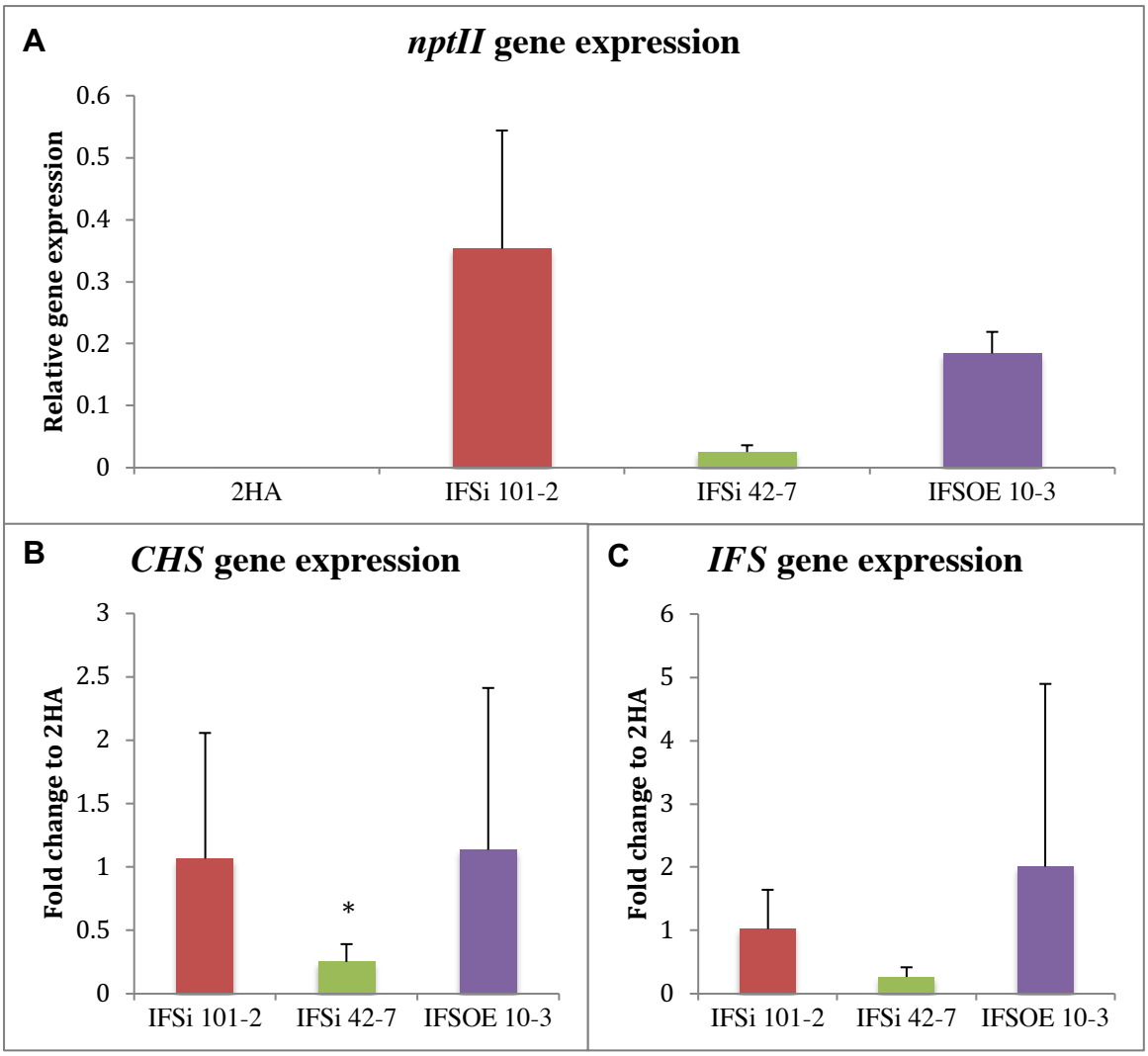

Figure 4.6: Gene expression changes in roots of 6 weeks old *Medicago truncatula* wild-type, cv. 2HA and isoflavone synthase transgenics, silenced lines, IFSi 101 and IFSi 42 and over-expression line, IFSOE 10. Gene expressions were normalised to *M. truncatula GAPDH* transcript levels. **(A)** Relative gene expressions of neomycin phosphotransferase gene (*nptII*), **(B)** *CHALCONE SYNTHASE (CHS)* and **(C)** *ISOFLAVONE SYNTHASE (IFS)*. Data are the means of 5-6 plants and error bars represent standard deviations. Mann-Whitney tests were performed to compare wild-type 2HA and isoflavone synthase transgenics for *CHS* and *IFS* gene expressions. This was excluded for *nptII* gene expression because wild-type 2HA did not exhibit gene expression change for *nptII*. Asterisks denote statistically significant difference compared to wild-type 2HA ($p<0.05$).

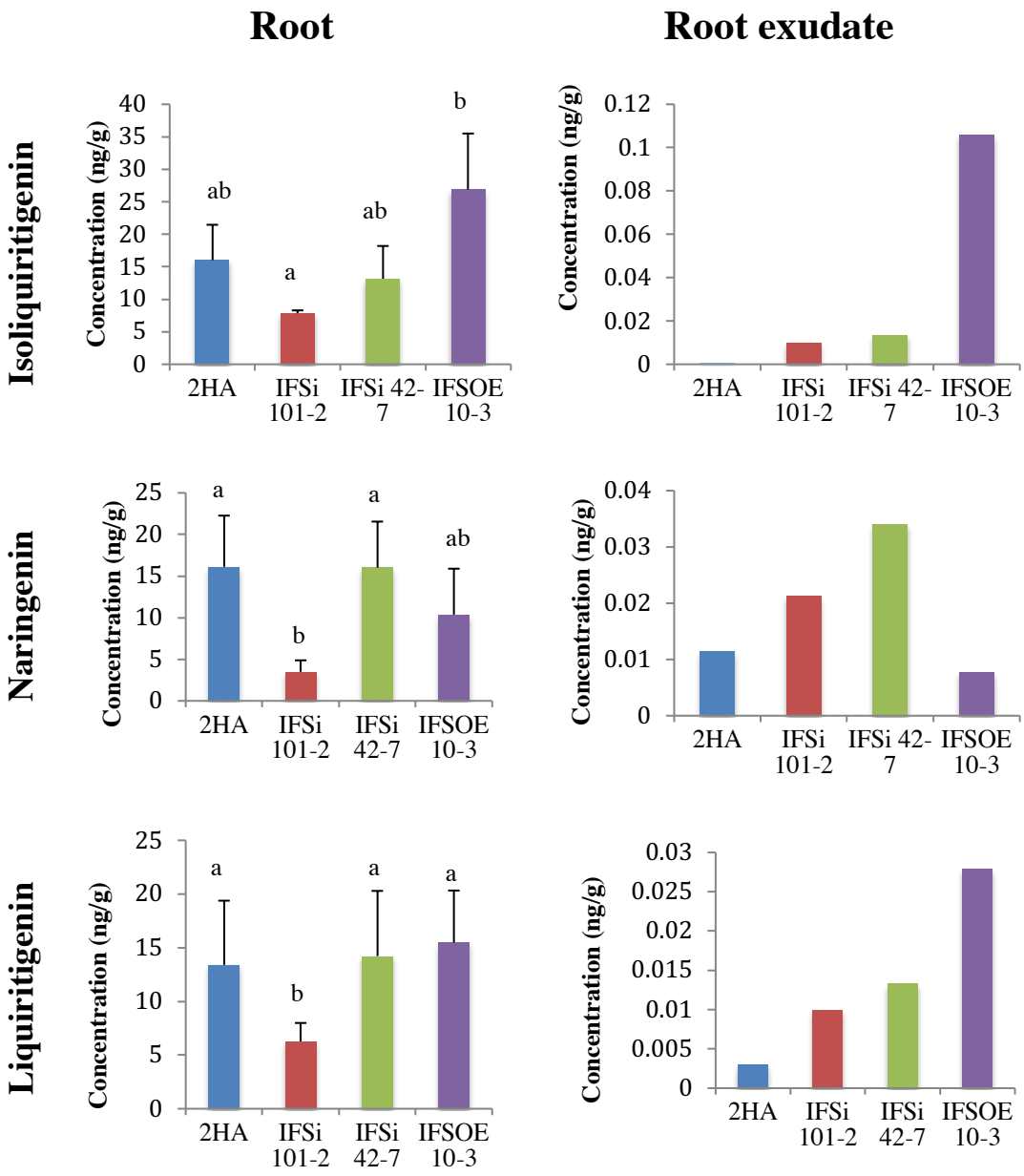

Figure 4.7: Flavonoid content changes of chalcone (isoliquiritigenin) and flavanones (naringenin and liquiritigenin) in uninfected roots and root exudates of 6 weeks old *Medicago truncatula* wild-type, cv. 2HA and isoflavone synthase transgenics, silenced lines, IFSi 101-2 and IFSi 42-7 and over-expression line, IFSOE 10-3. Flavonoids were quantified using LC-QTOF, with ~100 mg fresh weight root samples of each 5-6 plants and ~200 g media with root exudates of 5-6 plants. Columns represent means. Error bars represent standard deviation for root data. No standard deviation data for root exudates as root exudates from individual plants were indistinguishable in the media. One-way ANOVA analysis was performed on root data, with letters denoting statistically significant differences ($p<0.05$) between genotypes.

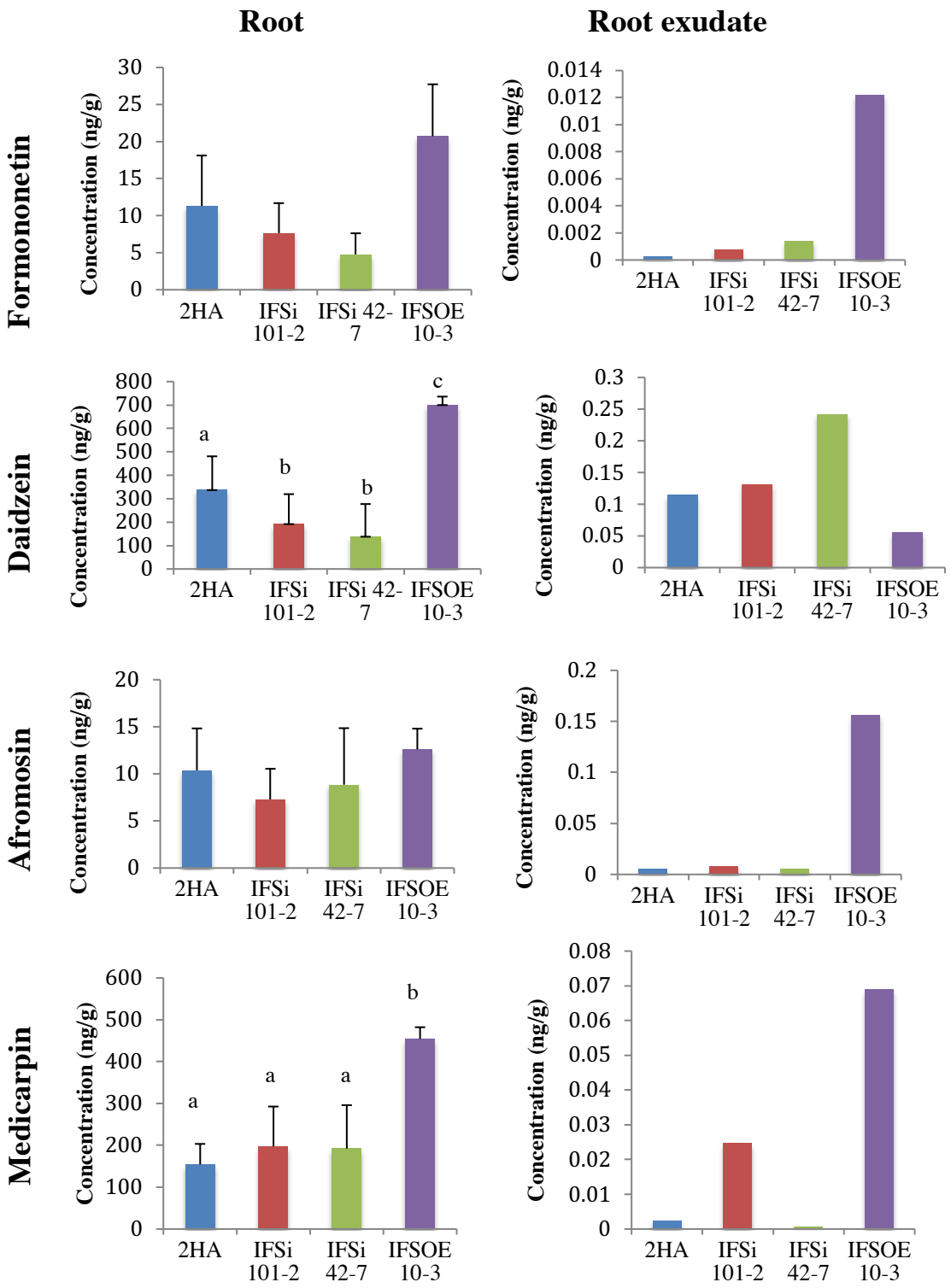

Figure 4.8: Flavonoid content changes of isoflavonoids (formononetin and daidzein) and pteocarpans (afromosin and medicarpin) in uninfected roots and root exudates of 6 weeks old *Medicago truncatula* wild-type, cv. 2HA and isoflavone synthase transgenics, silenced lines, IFSi 101-2 and IFSi 42-7 and over-expression line, IFSOE 10-3. Flavonoids were quantified using LC-QTOF, with ~100mg fresh weight root samples of each 5-6 plants and ~200g media with root exudates of 5-6 plants. Columns represent means. Error bars represent standard deviation for root data. No

standard deviation data for root exudates as root exudates from individual plants were indistinguishable in the media. One-way ANOVA analysis was performed on root data, with letters denoting statistically significant differences ($p<0.05$) between genotypes.

4.3.2.2. Nematode infection in *M. truncatula* IFS transgenics

4.3.2.2.1. Nematode infection phenotypes

Isoflavone synthase transgenics, IFSi 101-2, IFSi 42-7 and IFSOE 10-3, as well as wild-type 2HA plants were infected with *M. javanica* J2s at one week old. At 6 weeks post inoculation, infection phenotypes were measured. These included: 1) gall phenotypes, ie. number of galls and gall size, 2) number of eggs per plant, 3) plant wet weights, ie. overall weight, shoot weight and root weight and 4) lateral root numbers.

The observed gall phenotypes included the measurements of number of galls per plant and gall sizes. For both gall phenotypes, plant genotype exerted statistically significant influences ($p<0.01$) (Figure 4.9). Nematode infected IFSi 42-7 plants produced the most number of galls per plant, 3.4 galls per plant and were closely followed by 2HA plants, at 3 galls per plant, and subsequently IFSi 101-2 plants at 2.5 galls per plant, and finally IFSOE 10-3 plants at 2.3 galls per plant (Figure 4.9). The gall counts for IFSi 42-7 plants were significantly higher compared to IFSi 101-2 and IFSOE 10-3 plants, but not when compared to 2HA plants (Figure 4.9). Galls produced by 2HA plants were distinctively larger at an average size of 6.84 mm^2 compared to IFSi 101-2, IFSi 42-7 and IFSOE 10-3 galls with average sizes ranging from 5.85 mm^2 to 5.25 mm^2 (Figure 4.9).

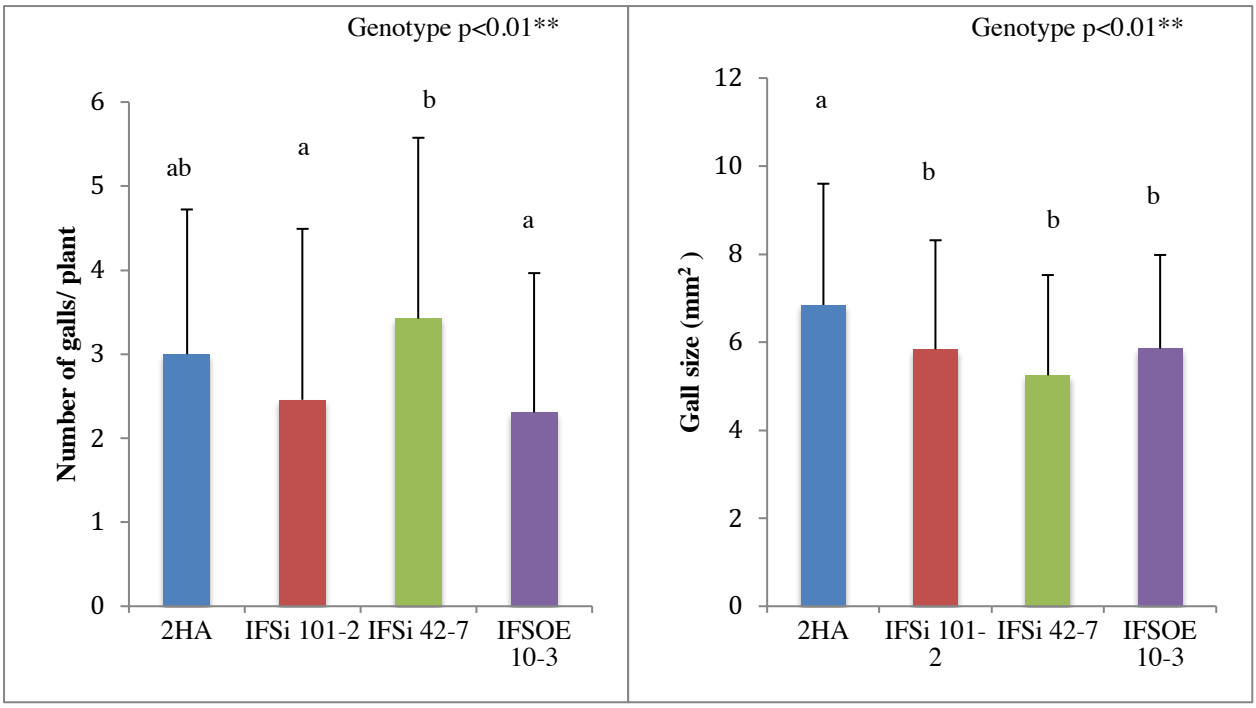

Figure 4.9: Gall phenotypes observed in *Medicago truncatula* wild-type cv. 2HA and isoflavone synthase transgenics, silenced lines, IFSi 101-2 and IFSi 42-7 and over-expression line, IFSOE 10-3 at 6 weeks post inoculation with *Meloidogyne javanica*. Genotype effect was tested using linear mixed analysis. Letters represent statistically significant differences amongst groups using Tukey pairwise comparison. Columns represent means. Error bars represent standard deviations. (N=3)

At 6 weeks post inoculation, the egg masses produced by adult female nematodes were harvested and dissolved in 1% sodium hypochlorite to release eggs from their gelatinous sacs. Plant genotype had a statistically significant effect on egg production ($p<0.01$) (Figure 4.10). Adult female nematodes that infected 2HA plants produced the most eggs, at an average of 3162 eggs per plant, and were trailed by IFSi 42-7 plants with 2821 eggs per plant, IFSOE 10-3 plants with 1239 eggs per plant and lastly, IFSi 42-7 plants with significantly fewer eggs compared to 2HA, at 769 eggs per plant (Figure 4.10).

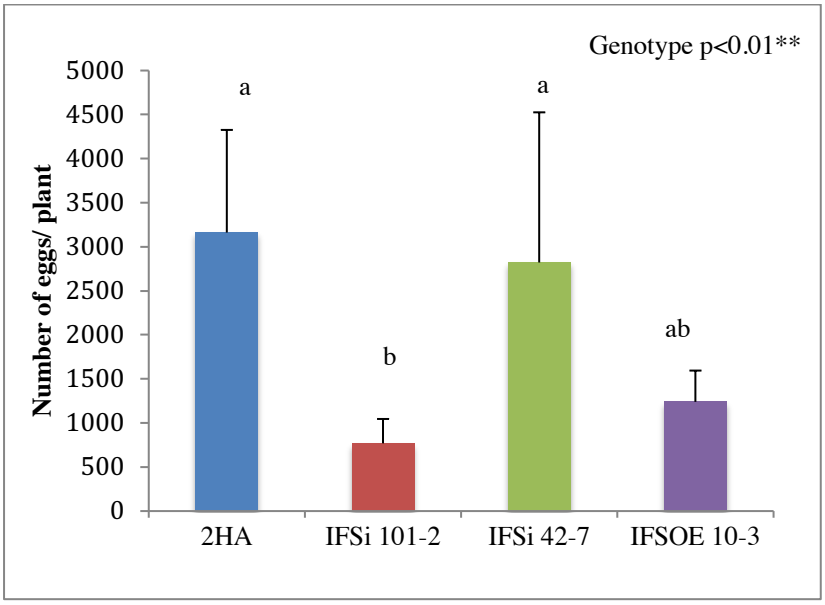

Figure 4.10: Number of eggs per plant in *Medicago truncatula* wild-type cv. 2HA and isoflavone synthase transgenics, silenced lines, IFSi 101-2 and IFSi 42-7 and over-expression line, IFSOE 10-3 at 6 weeks post inoculation with *Meloidogyne javanica*. Genotype effect was tested using linear mixed analysis. Letters represent statistically significant differences amongst groups using Tukey pairwise comparison. Columns represent means. Error bars represent standard deviations. (N=3)

Plant weights, including the overall, shoot tissue and root tissue weights were measured to observe the effects of nematode infection on host fitness. The overall plant weight was influenced by genotype ($p<0.01$) and nematode treatment ($p<0.05$) (Figure 4.11). 2HA plants had the heaviest average overall weight when uninfected and infected, at 0.41 g and 0.3 g respectively, with a significant 35% reduction in overall weight due to infection (Figure 4.11 and Table 4.1). IFSi 101-2 plants had the second heaviest average overall weight, with uninfected weight at 0.34 g and infected weight at 0.24 g, with a very significant 40% reduction in overall weight due to infection (Figure 4.11 and Table 4.1). IFSi 42-7 plants were the third heaviest plants, with average uninfected weight at 0.34g and infected weight at 0.23 g, with a very significant weight loss due to infection, at 45% (Figure 4.11 and Table 4.1). Lastly, IFSOE 10-3 plants had the lowest uninfected weight at 0.33 g, but showed the least weight reduction due to nematode infection, with 19% weight loss to 0.28 g (Figure 4.11 and Table 4.1).

As for shoot weights, 2HA plants exhibited the heaviest weights, with uninfected shoots weighing 0.23 g and infected shoots weighing 0.16 g (Figure 4.11). However, 2HA plants experienced the most significant weight loss due to infection, with 41% weight reduction (Table 4.1). IFSi 101-2, IFSi 42-7 and IFSOE 10-3 plants had comparable shoot weights; with uninfected shoot tissues ranging around 0.18 g and infected shoot tissues ranging from 0.13-0.14 g (Figure 4.11). IFSi 101-2 shoots showed 38% weight reduction due to infection, followed by IFSi 42-7 shoots with 32% loss and IFSOE 10-3 shoots with 30% loss (Table 4.1).

Uninfected 2HA roots were the heaviest at 0.18 g, followed by IFSi 101-2 roots, which weighed 0.16 g, IFSi 42-7 roots at 0.15g and IFSOE 10-3 roots at 0.14 g (Figure 4.11). Nevertheless, this ranking was changed for infected roots, with 2HA roots weighing 0.14 g, followed by IFSOE 10-3 roots at 0.13 g, IFSi 101-2roots at 0.11 g and IFSi 42-7 roots at 0.09 g (Figure 4.11). Consequently, the weight reduction due to nematode infection was the highest for IFSi 42-7 roots (65%), followed by IFSi 101-2 roots (42%), 2HA roots (28%) and IFSOE 10-3 (7%) (Table 4.1). In general, root weights were strongly influenced by nematode infection ($p<0.001$) (Figure 4.11).

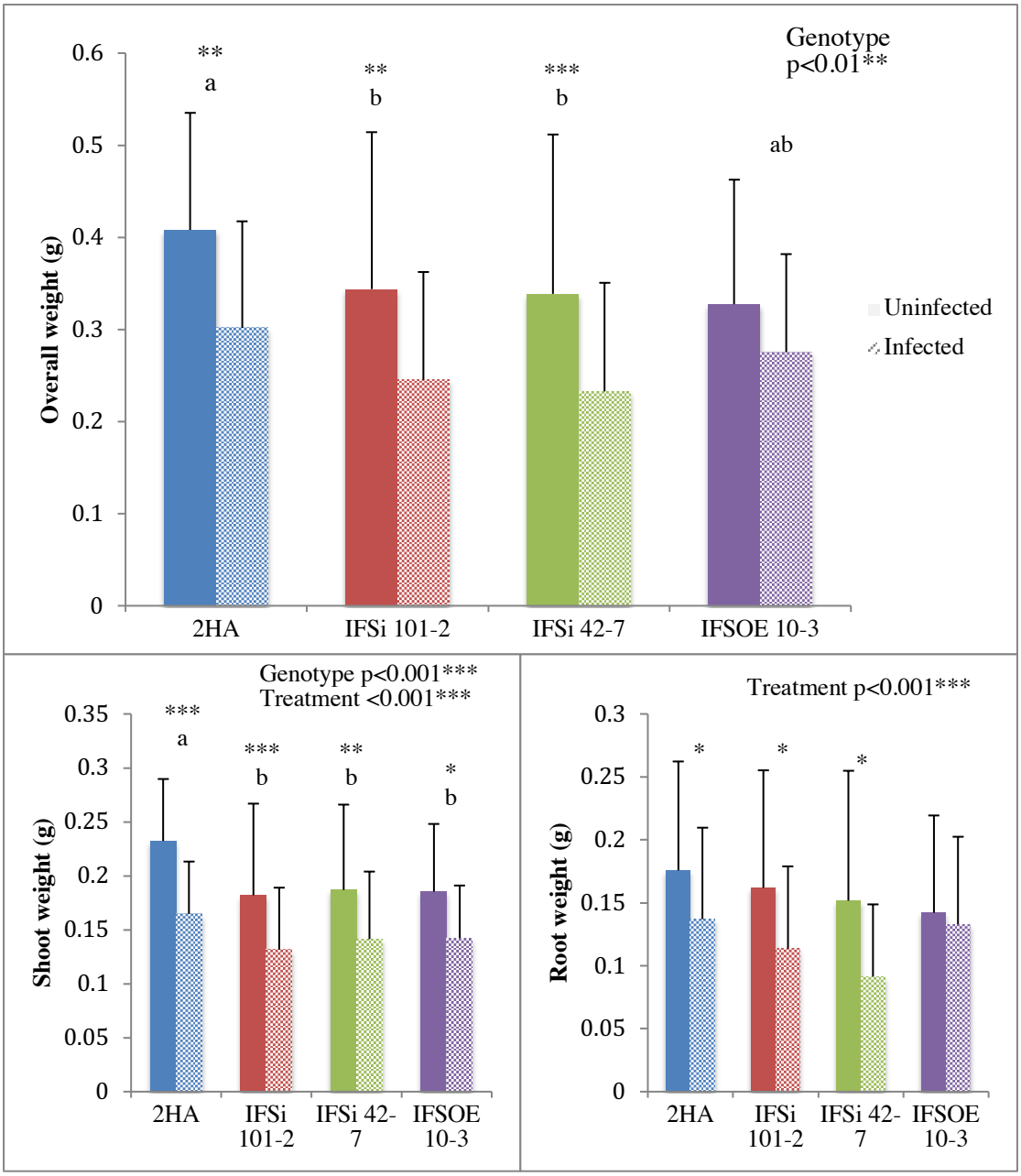

Figure 4.11: Fresh plant weights of uninfected and *Meloidogyne javanica*-infected *Medicago truncatula* wild-type cv. 2HA and isoflavone synthase transgenics, silenced lines, IFSi 101-2 and IFSi 42-7 and over-expression line, IFSOE 10-3 at 6 weeks post inoculation. Solid bar graphs represent uninfected plants, whereas patterned bar graphs represent infected plants. Statistical analysis was done using linear mixed analysis to test the effects of genotype, treatment and the combination of genotype and treatment. Tukey pairwise comparison was done to compare between uninfected and infected groups within the same genotype (denoted by asterisks) and between genotype groups based on averaged levels of treatment (denoted by letters). Columns represent means. Error bars represent standard deviations. (N=3)

Phenotype	**% change due to infection**			
	2HA	**IFSi 101-2**	**IFSi 42-7**	**IFSOE 10-3**
Overall weight	-35.2 **	-40.1 **	-45.4 ***	-18.9
Shoot weight	-41.1 ***	-38.3 ***	-32.2 **	-30.1 *
Root weight	-28.2 *	-42.4 *	-65.9 *	-6.8
Lateral root number	37.9 ***	31.8 ***	30 *	55.8 ***

Table 4.1: Effect of nematode infection on the overall weight, shoot weight, root weight and lateral root numbers in terms of percentage change of infected plants to uninfected plants on *Medicago truncatula* wild-type cv. 2HA and isoflavone synthase transgenics, silenced lines, IFSi 101-2 and IFSi 42-7 and over-expression line, IFSOE 10-3 at 6 weeks post inoculation. Tukey pairwise comparison was done to compare between uninfected and infected groups within the same genotype (denoted by asterisks) (same analysis for Figures 4.7 and 4.8) ($p < 0.05$ *; $p < 0.01$**; $p < 0.0001$***).

Additionally, the root phenotype, lateral roots in infected and uninfected wild-type 2HA and transgenics, IFSi 101-2, IFSi 42-7 and IFSOE 10-3 plants was counted. Nematode infection significantly increased the number of lateral roots across all plant genotypes ($p<0.001$) and different genotypes grew significantly different numbers of lateral roots ($p<0.001$) (Figure 4.12). In uninfected roots, IFSi 101-2 roots exhibited the most lateral roots, with an average of 12.2 lateral roots per plant (Figure 4.12). This number very significantly increased to 17.9 lateral roots per plant (31.8% increase) when the plant was infected with nematodes (Figure 4.12 and Table 4.1). Uninfected 2HA roots had similar number of lateral roots to IFSi 101-2 plants, with 12.1 lateral roots per plant (Figure 4.12). Nematode infection in 2HA resulted in a highly significant 37.9% increase of lateral roots to 19.5 lateral roots per plant (Figure 4.12 and Table 4.1). Next, uninfected IFSi 42-7 roots had 9.3 lateral roots which significantly increased by 30% to 13.3 lateral roots per plant during nematode infection (Figure 4.12 and Table 4.1). Lastly, whilst IFSOE 10-3 roots initially showed the least number of lateral roots when uninfected, with 6.9 lateral roots per plant, these plants showed the highest increase in number of lateral roots during nematode infection, with 55.8% increase to 15.6 lateral roots per plant (Figure 4.12 and Table 4.1).

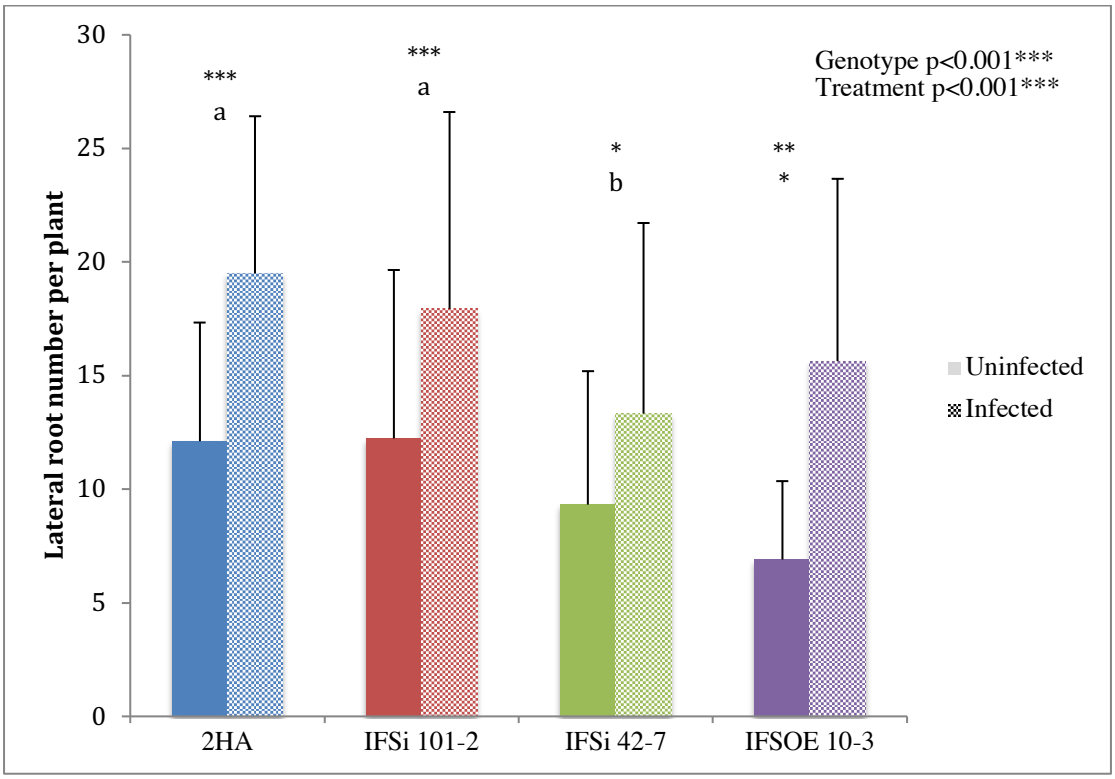

Figure 4.12: Lateral root number per plant of uninfected and *Meloidogyne javanica*-infected *Medicago truncatula* wild-type cv. 2HA and isoflavone synthase transgenics, silenced lines, IFSi 101-2 and IFSi 42-7 and over-expression line, IFSOE 10-3 at 6 weeks post inoculation. Solid bar graphs represent uninfected plants, whereas patterned bar graphs represent infected plants. Statistical analysis was done using linear mixed analysis to test the effects of genotype, treatment and the combination of genotype and treatment. Tukey pairwise comparison was done to compare between uninfected and infected groups within the same genotype (denoted by asterisks) and between genotype groups based on averaged levels of treatment (denoted by letters). Columns represent means. Error bars represent standard deviations. (N=3)

4.3.2.2.2. Flavonoid phenotypes

Flavonoids were extracted from root segments of uninfected and infected plants of *M. truncatula* 2HA and transgenics, IFSi 101-2, IFSi 42-7 and IFSOE 10-3 at 24 hours and 6 weeks post inoculation. These were separated and detected on the LC-ESI-Q-TOF-MS/MS. Next, flavonoid responses in uninfected and nematode infected plants at 24 hours and 6 weeks post inoculation were modelled using OPLS-DA. OPLS-DA based on the treatment factor demonstrated that although some flavonoid responses were distinct between uninfected and infected plants, there were some overlapping responses ($R^2Y= 0.58$, $Q^2Y= 0.47$) (Figure 4.13A). The flavonoids with the top loadings for this model were isoliquiritigenin, afromosin, liquiritigenin, k-gluc-rham, 784, luteolin, naringenin and apigenin (Figure 4.13B).
Additionally, no statistical model could be generated based on genotype factor, indicating that the flavonoid responses were only subtly different across genotypes. These subtle differences in flavonoids profiles were previously described in Section 4.3.2.1.

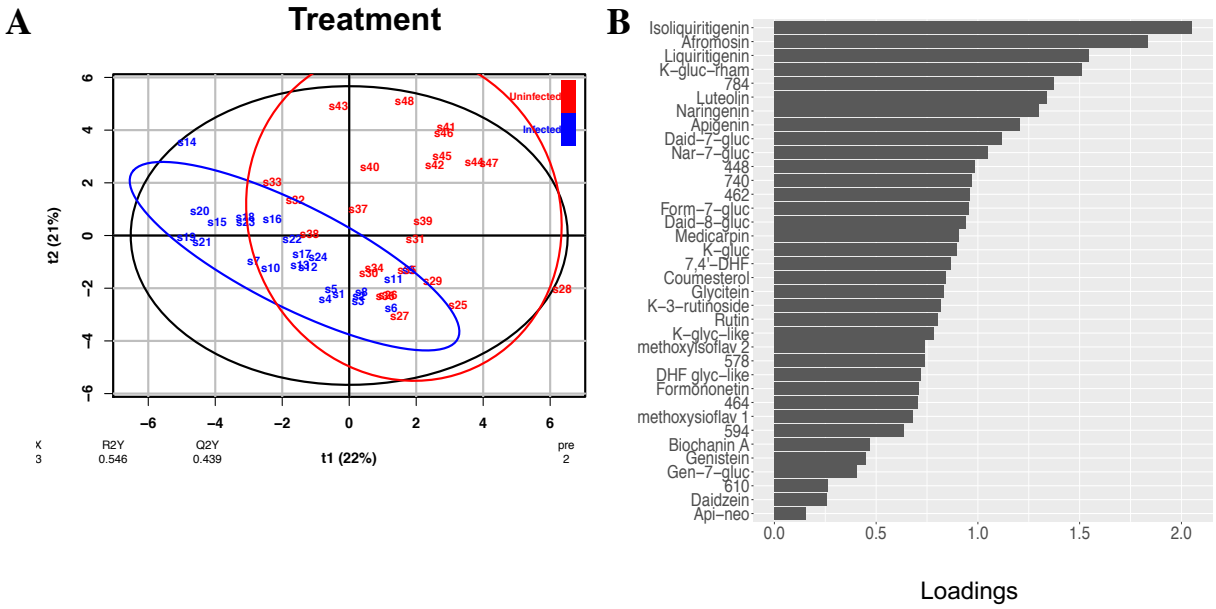

Figure 4.13: OPLS-DA analyses and the corresponding loading plots of flavonoid responses (log 10 concentrations) of *Medicago truncatula* wild-type cv. 2HA and isoflavone synthase transgenics, silenced lines, IFSi 101-2 and IFSi 42-7 and over-expression line, IFSOE 10-3 at 24 hours and 6 weeks post inoculation with *Meloidogyne javanica* for treatment variable. Flavonoid responses refer to log10 concentrations of 39 flavonoids measured using LC-ESI-Q-TOF-MS. Loading values are arbitrary values. **(A)** Discrimination of flavonoid responses based on the treatment factor. $R^2Y = 0.58$, $Q^2Y = 0.47$. **(C)** OPLS-DA loadings for the discrimination of flavonoid responses based on the treatment factor.

Fold-change of flavonoid concentrations based on comparison between infected and uninfected samples at 24 hours and 6 weeks post inoculation for all four genotypes were illustrated in a heatmap (Figure 4.14). At 24 hours post inoculation, the chalcone, flavanones, flavonols, flavones and isoflavonoids were generally increased in all infected plant genotypes with the exception of IFSi 101-2 plants that showed different (decreased or unchanged) flavonoid concentrations (Figure 4.14). These flavonoids include isoliquiritigenin, liquiritigenin, naringenin, nar-7-gluc, k-gluc, k-3-rutinoside, k-glyc-like, k-gluc-rham, apigenin, api-neo, luteolin (also increased in IFSi 101-2 plants), 7,4'-DHF, DHF-glyc-like, form-7-gluc, genistein, medicarpin (also increased in IFSi 101-2 plants), afromosin, 448, 462, and 610 (Figure 4.14). Some flavonoids showed consistently unchanged concentrations in all genotypes, such as methoxyisoflavone glycoside-like (methoxyisoflav) 1, methoxyisoflav 2, daid-8-gluc, 454, 578 and 594 (Figure 4.14). Other interesting patterns included an increase in compound 784 in infected IFSOE 10-3 roots and a decrease in biochanin A and formononetin in infected 2HA roots (Figure 4.14).

At 6 weeks post inoculation, distinct patterns were observed between three plant genotypes, 2HA, IFSi 101-2 and IFSi 42-7, and IFSOE 10-3, whereby the first three genotypes often showed decreased concentrations of some flavonoids during infection, whereas IFSOE 10-3 roots showed increased concentrations of those flavonoids (Figure 4.14). This included k-glyc-like, apigenin, DHF-glyc-like, daidzein, daid-8-gluc and 454 (Figure 4.14). Moreover, flavonoids in IFSOE 10-3 roots were mostly increased, with some remaining unchanged, as opposed to other genotypes which decreased flavonoids (Figure 4.14). Flavonoids that were increased across all genotypes due to nematode infection were isoliquiritigenin, liquiritigenin, naringenin, nar-7-gluc, k-gluc-rham, rutin, methoxyisoflav 1, methoxyisoflav 2, afromosin, compound 578 and compound 784 (Figure 4.14).

Flavonoids which were found to be statistically upregulated based on linear mixed model analysis as a consequence of nematode infection were isoliquiritigenin, liquiritigenin, naringenin, k-gluc-rham, rutin, luteolin, methoxyisoflav 1, methoxyisoflav 2, form-7-gluc, afromosin, 578 and 784 (Figure 4.14). Some of these flavonoids were upregulated in 24 hours and 6 weeks time points in most genotypes.

These were isoliquiritigenin, liquiritigenin, naringenin, k-gluc-rham, form-7-gluc and afromosin (Figure 4.14). On the other hand, some flavonoids only showed increases during later stages of infection, at 6 weeks p.i., eg. rutin, methoxyisoflav 1, methoxyisoflav 2, 578 and 784 (Figure 4.14). Luteolin was increased in all infected genotypes at 24 hours, but was only increased by IFSi 42-7 and IFSOE 10-3 genotypes at 6 weeks (Figure 4.14). The flavonoids which were important in all three interactions, ie. time, genotype and treatment, were isoliquiritigenin, liquiritigenin, k-gluc-rham, apigenin, gen-7-gluc and compound 784 (Figure 4.14). Most of these were also involved in treatment only interaction as previously described, except for apigenin and gen-7-gluc. Apigenin increased across most genotypes at 24 hours but was decreased at 6 weeks post inoculation (Figure 4.14), whereas gen-7-gluc was only increased in 2HA and IFSi 42-7 plants at 24 hours and was unchanged in all genotypes at 6 weeks post inoculation (Figure 4.14).

Based on these flavonoid profiles, although both IFSi 101-2 and IFSi 42-7 lines were silenced for isoflavone synthase genes, they demonstrated different flavonoid regulation, particularly at 24 hours post inoculation (Figure 4.14). In contrast, IFSOE 10-3 plants exhibited upregulation of most flavonoids, which were prominent in 6 weeks post inoculation (Figure 4.14).

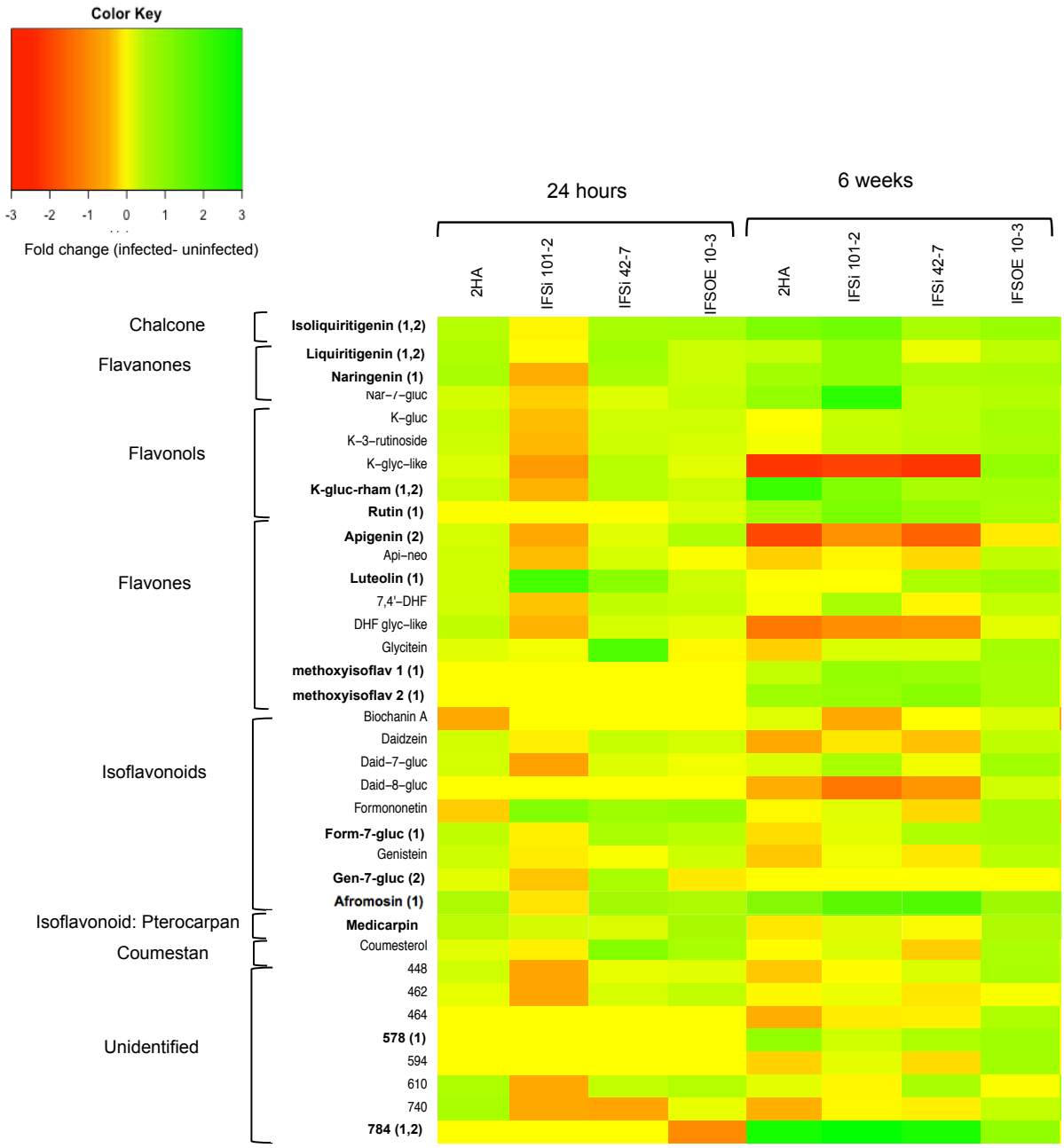

Figure 4.14: Fold change between uninfected and *Meloidogyne javanica* infected roots of *Medicago truncatula* wild type cv. 2HA and isoflavone synthase transgenics, silenced lines, IFSi 101-2 and IFSi 42-7 and over-expression line, IFSOE 10-3 at 24 hours and 6 weeks post inoculation. Flavonoids highlighted in bold showed statistically significant results for treatment (indicated by the number 1) and for time x treatment x genotype factors (indicated by the number 2) based on linear mixed model analysis on flavonoid concentrations (full description of linear mixed model results available in Supplementary Table 4.1).

4.3.2.2.3. The link between infection and flavonoid phenotypes

Simple linear regressions were performed for each 35 flavonoids targeted in the LC-ESI-Q-TOF-MS/MS against five measured phenotypes, which were overall plant weight (excluded root and shot weights as overall weight provided a general overview), lateral root number, gall number per plant, gall size and egg number per plant for infected samples at 6 weeks post inoculation.

Overall plant weight was negatively correlated with methoxyisoflav 1 and methoxyisoflav 2 concentrations, with r^2 values of 0.35 and 0.3, respectively ($p<0.05$) (Figure 4.15 and Supplementary Table 4.4). Lateral root numbers positively correlated with DHF glyc-like level (r^2 value of 0.35, $p<0.05$) (Figure 4.16 and Supplementary Table 4.4). Gall number per plant phenotype showed positive linear relationship with six flavonoids, isoliquiritigenin, liquiritigenin, naringenin, and compounds 462, 578 and 784 (p values ranging from <0.05 and < 0.01) with r^2 values ranging from 0.35 to 0.58 (Figure 4.19 and Supplementary Table 4.4). As for gall size, negative linear relationships were calculated to two similar flavonoids, methoxyisoflav 1 and methoxyisoflav 2 ($p<0.05$) with r^2 values of 0.39 (Figure 4.18 and Supplementary Table 4.4). Lastly, three flavonoids, isoliquiritigenin, liquiritigenin and compound 578 were positively correlated with egg number per plant phenotype ($p<0.05$) with r^2 values of 0.27 to 0.39 (Figure 4.17 and Supplementary Table 4.4).

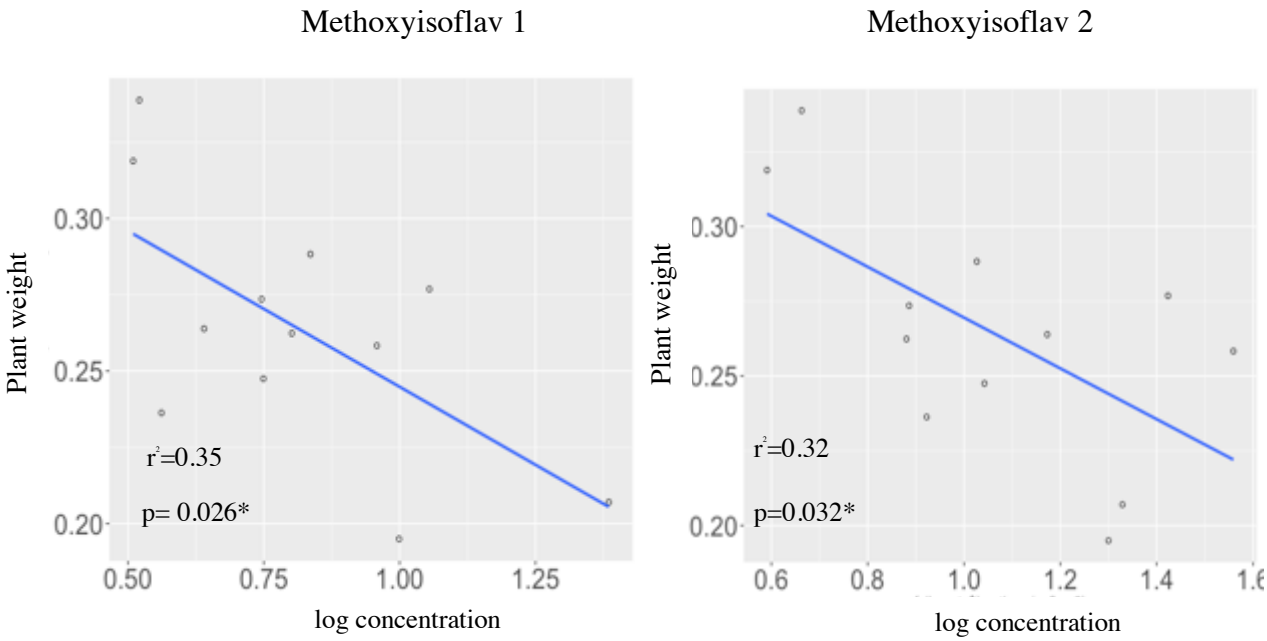

Figure 4.15: Scatter plots of flavonoids with statistically significant negative linear relationships with the overall plant weight in infected *Medicago truncatula* cv. 2HA and isoflavone synthase transgenics, silenced lines, IFSi 101-2 and IFSi 42-7 and over-expression line, IFSOE 10-3 at 6 weeks post inoculation with *Meloidogyne javanica*.

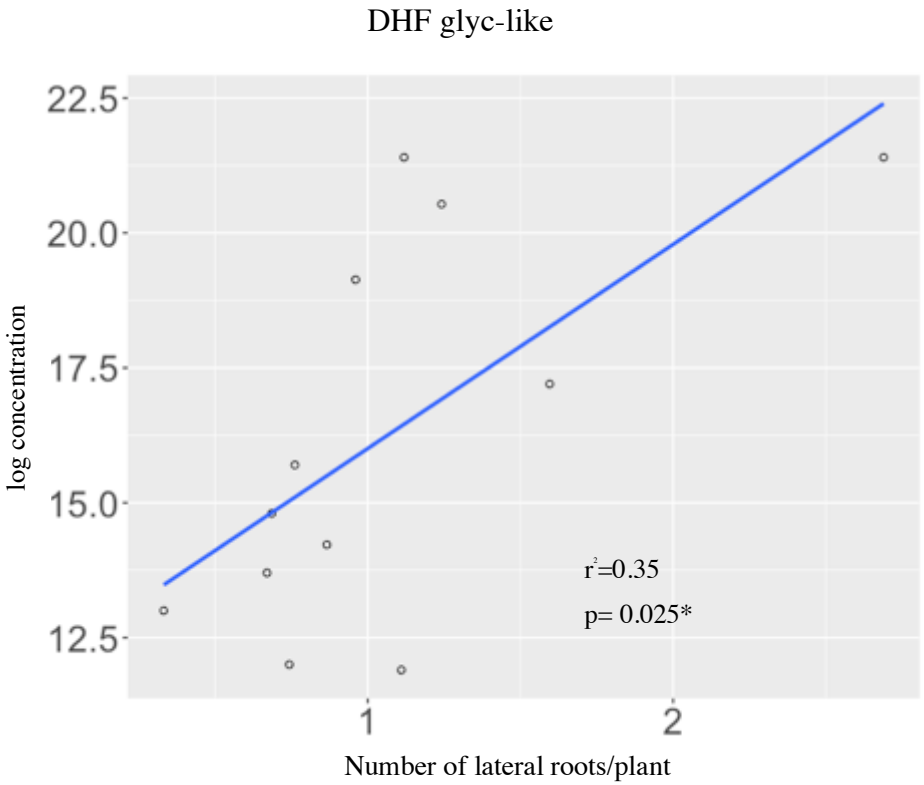

Figure 4.16: Scatter plots of DHF glyc-like with statistically significant positive linear relationship with the number of lateral roots per plant in infected *Medicago truncatula* cv. 2HA and isoflavone synthase transgenics, silenced lines, IFSi 101-2 and IFSi 42-7 and over-expression line, IFSOE 10-3 at 6 weeks post inoculation with *Meloidogyne javanica*.

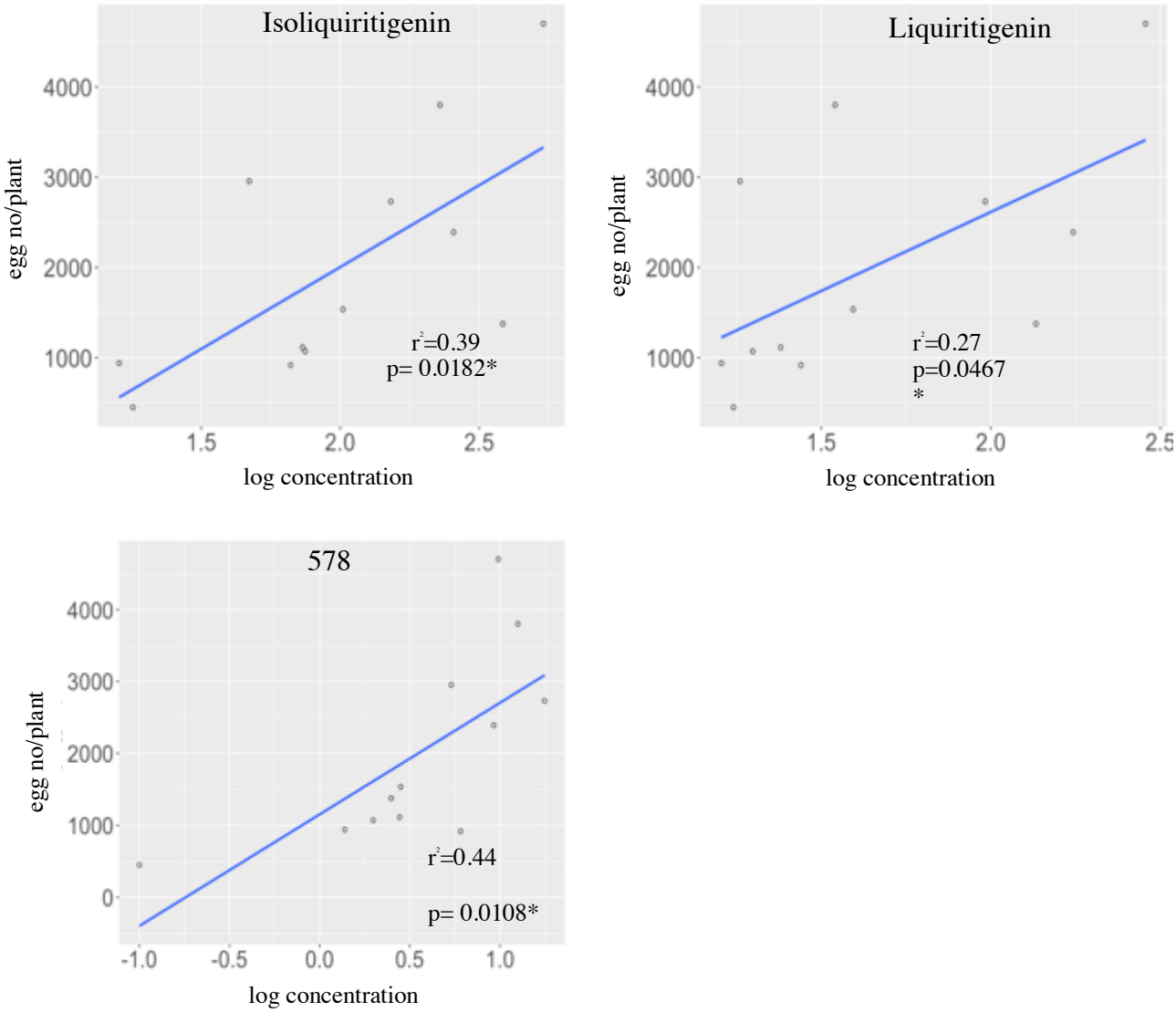

Figure 4.17: Scatter plots of flavonoids with statistically significant positive linear relationships with the production of nematode eggs per plants in infected *Medicago truncatula* cv. 2HA and isoflavone synthase transgenics, silenced lines, IFSi 101-2 and IFSi 42-7 and over-expression line, IFSOE 10-3 at 6 weeks post inoculation with *Meloidogyne javanica*.

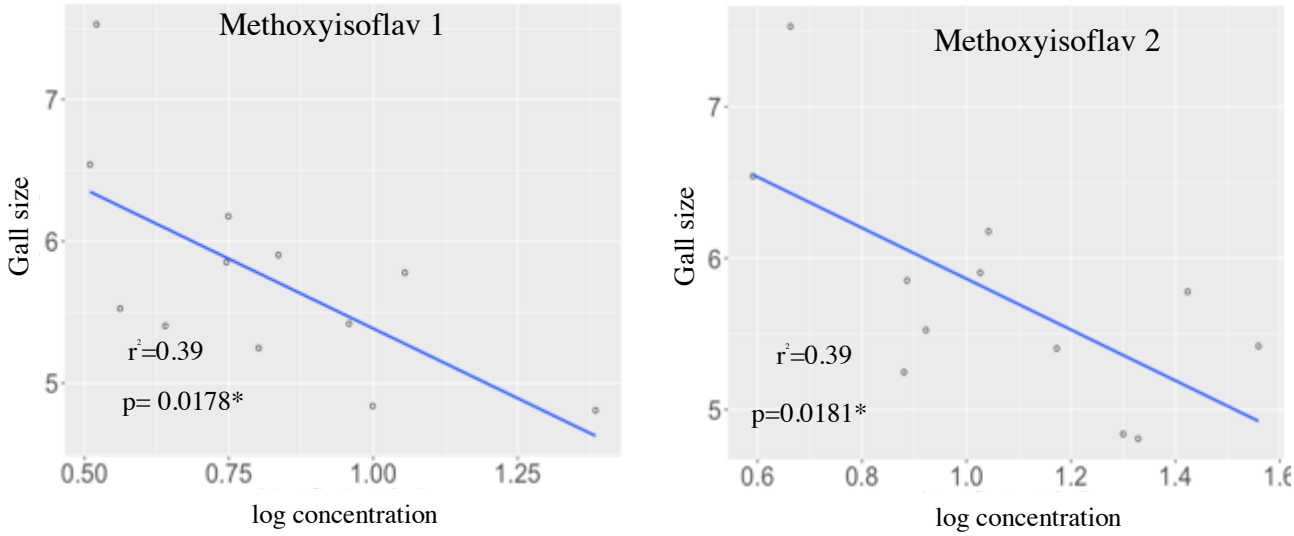

Figure 4.18: Scatter plot of flavonoids with statistically significant negative linear relationship with gall size in infected *Medicago truncatula* cv. 2HA and isoflavone synthase transgenics, silenced lines, IFSi 101-2 and IFSi 42-7 and over-expression line, IFSOE 10-3 at 6 weeks post inoculation with *Meloidogyne javanica*.

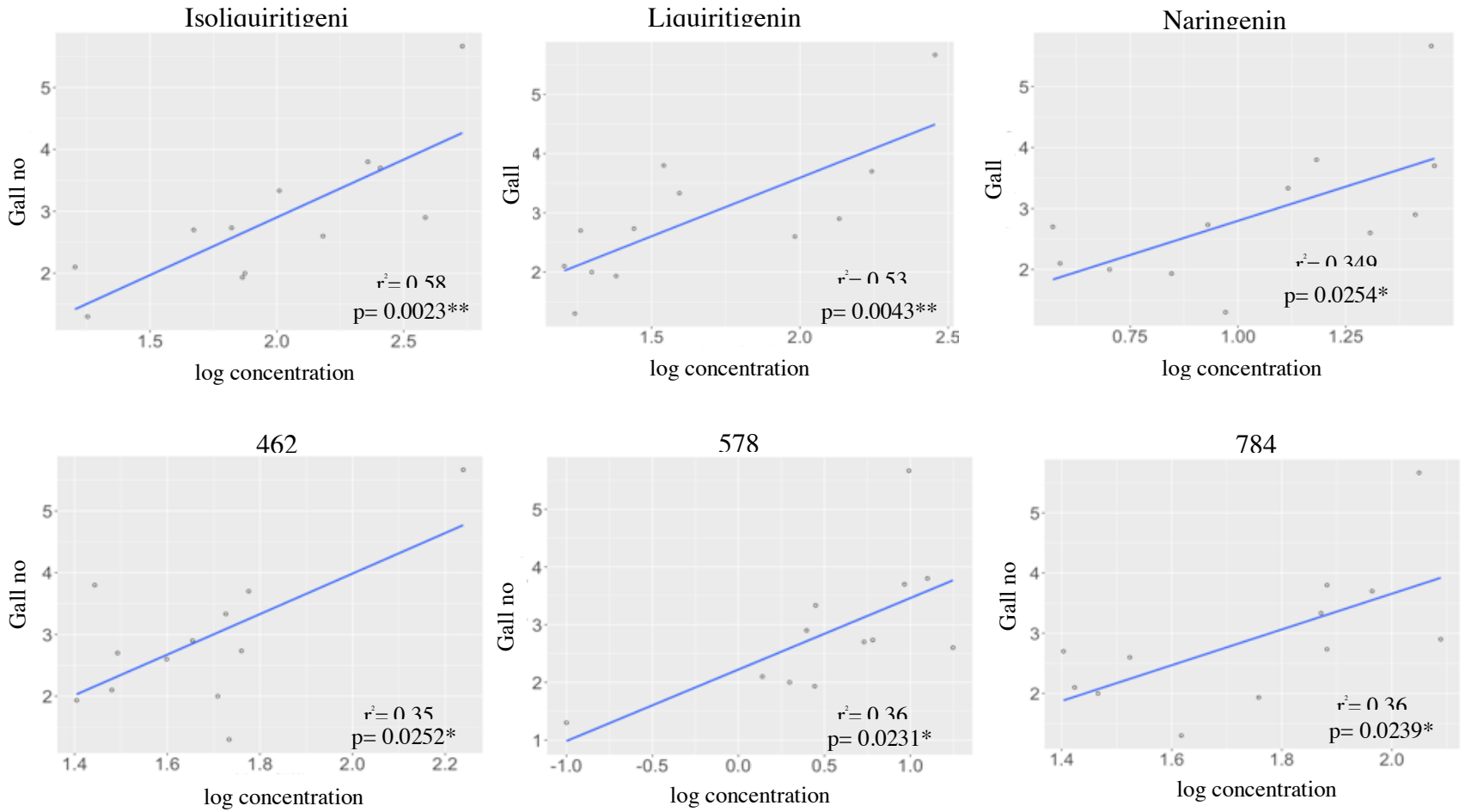

Figure 4.19: Scatter plots of flavonoids with statistically significant positive linear relationships with the production of galls per plant in infected *Medicago truncatula* cv. 2HA and isoflavone synthase transgenics, silenced lines, IFSi 101-2 and IFSi 42-7 and over-expression line, IFSOE 10-3 at 6 weeks post inoculation with *Meloidogyne javanica*.

4.3.3. *In vitro* effects of purified flavonoids and root exudates of *M. truncatula* IFS transgenics on J2 motility and chemotaxis

4.3.3.1. Motility assay

An *in vitro* motility assay was performed on pre-parasitic J2s of *M. javanica*, by the direct application of purified flavonoids or root exudates of *M. truncatula* wild-type 2HA and IFS transgenics. Body bends were measured by using WormAssay (Marcellino et al., 2012) and percentage motility inhibition after compound application was calculated. The selected ten flavonoids were based on flavonoids which were significantly upregulated during nematode infection in *M. truncatula* 2HA (Section 3.3.2.2.), *M. truncatula* accessions/cultivars (Section 4.3.1.) and *M. truncatula* IFS transgenics (Section 4.3.2.). These included isoliquiritigenin (upregulated in all sections), 7,4'-DHF (upregulated in Sections 3.3.2.2. and 4.3.1.), daidzein (upregulated in Section 3.3.2.2. and 4.3.1.), form-7-gluc (upregulated in all sections), medicarpin (upregulated in Sections 3.3.2.2. and 4.3.1.) and afromosin (upregulated in all sections). In addition, formononetin was included as it was upregulated due to infection in Section 4.3.2. and to test the differences in bioactivity between the aglycone and its glycoside in bioactivies. The glycosides for genistein, kaempferol and quercetin were excluded as most of their glycosides were not readily available and due to time constraints.

All ten flavonoids produced different response curve trends, with the exceptions of formononetin and its glucoside, form-7-gluc sharing similar sinusoidal trends (Figure 4.20). Quercetin, 7,4'-DHF, daidzein, formononetin, form-7-gluc, medicarpin and afromosin inhibited nematode motility at all tested concentrations, raning from 10^{-11} to 10^{-5} M (Figure 4.20). On the other hand, the bioactivities as of isoliquiritigenin, kaempferol, and genistein were concentration dependent, resulting in either motility stimulation or inhibition (Figure 4.20). Isoliquiritigenin inhibited nematode motility at concentrations of 10^{-11} M, 10^{-10} M, 10^{-7} M and 10^{-6} M, with the optimum inhibition of 78%, occurring at 10^{-11} M (Figure 4.20). Isoliquiritigenin

stimulated motility at 10^{-9} M and 10^{-8} M concentrations, with optimum stimulation at 10^{-9} M resulting in 85% increased movement (Figure 4.20). The flavonol kaempferol was a moderate motility inhibitor, with the maximum inhibition of 48% at 10^{-7} M concentrations and was a weak stimulator with increased nematode movements up to 23% when 10^{-11} M was used (Figure 4.20). Another flavonol, quercetin, was also a moderate motility inhibitor, with maximum inhibition of 61% at 10^{-11} M (Figure 4.20). Similarly, 7,4'-DHF was also a moderate inhibitor, with maximum inhibition at 63% at 10^{-7} M concentration (Figure 4.20). Genistein was a good inhibitor, with maximum inhibition of 89% at 10^{-11} M , but was a weak stimulator, with 26% stimulation at 10^{-9} M concentration (Figure 4.20). Daidzein inhibited nematode motility to a maximum of 71% at 10^{-6} M (Figure 4.20). Formononetin and form-7-gluc demonstrated similar optimum inhibition at 66% and 63%, respectively, but at different concentrations, the former at 10^{-10} M and the latter, at 10^{-6} M (Figure 4.20). Although medicarpin was a consistent inhibitor at all six concentrations, it was a moderate inhibitor, with maximum inhibition of 58% at 10^{-11} M (Figure 4.20). Afromosin was a strong inhibitor at lower concentrations of 10^{-11} M, 10^{-10} M and 10^{-9} M, with inhibition ranging from 82-88% (Figure 4.20).

Thereafter, the inhibition activities of the ten flavonoids were ranked using their upper 90th quantile values (based on the frequency distribution of inhibition values) to determine which flavonoids were the best inhibitors. Afromosin at 10^{-11} M was the best inhibitor, followed closely by genistein (10^{-11} M) (Figure 4.21). Subsequently, isoliquiritigenin (10^{-11} M), form-7-gluc (10^{-6} M), daidzein (10^{-6} M), formononetin (10^{-10} M), medicarpin (10^{-11} M), quercetin (10^{-11} M), 7,4'-DHF (10^{-7} M) and kaempferol (10^{-7} M) trailed behind, with significantly lower 90th quantile values compared to afromosin (Figure 4.21).

Additionally, these flavonoids were ranked as worst nematode motility inhibitors based on their lower 10th quantile values. The worst inhibitor was isoliquiritigenin (10^{-9} M), followed by genistein (10^{-9} M), kaempferol (10^{-11} M), form-7-gluc (10^{-8} M), quercetin (10^{-6} M), medicarpin (10^{-8} M), 7,4'-DHF (10^{-9} M), formononetin (10^{-8} M), daidzein (10^{-11} M) and afromosin (10^{-7} M) (Figure 4.22).

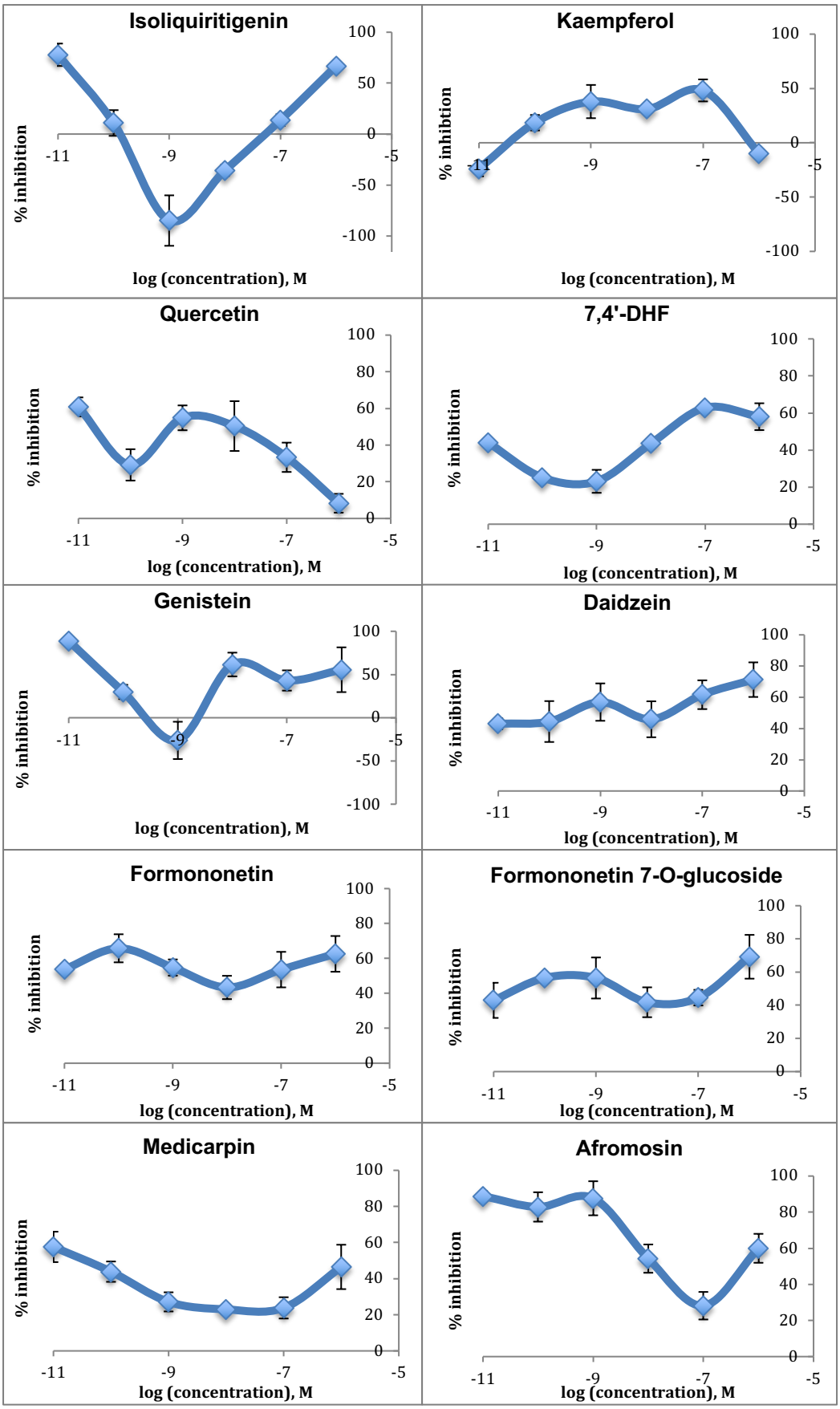

Figure 4.20: Percentage inhibition of ten flavonoids on nematode motility compared to solvent control. Six concentrations, ranging from 10^{-11} to 10^{-5} M was tested. Each data points represent mean values. Error bars represent standard deviations. (N=3)

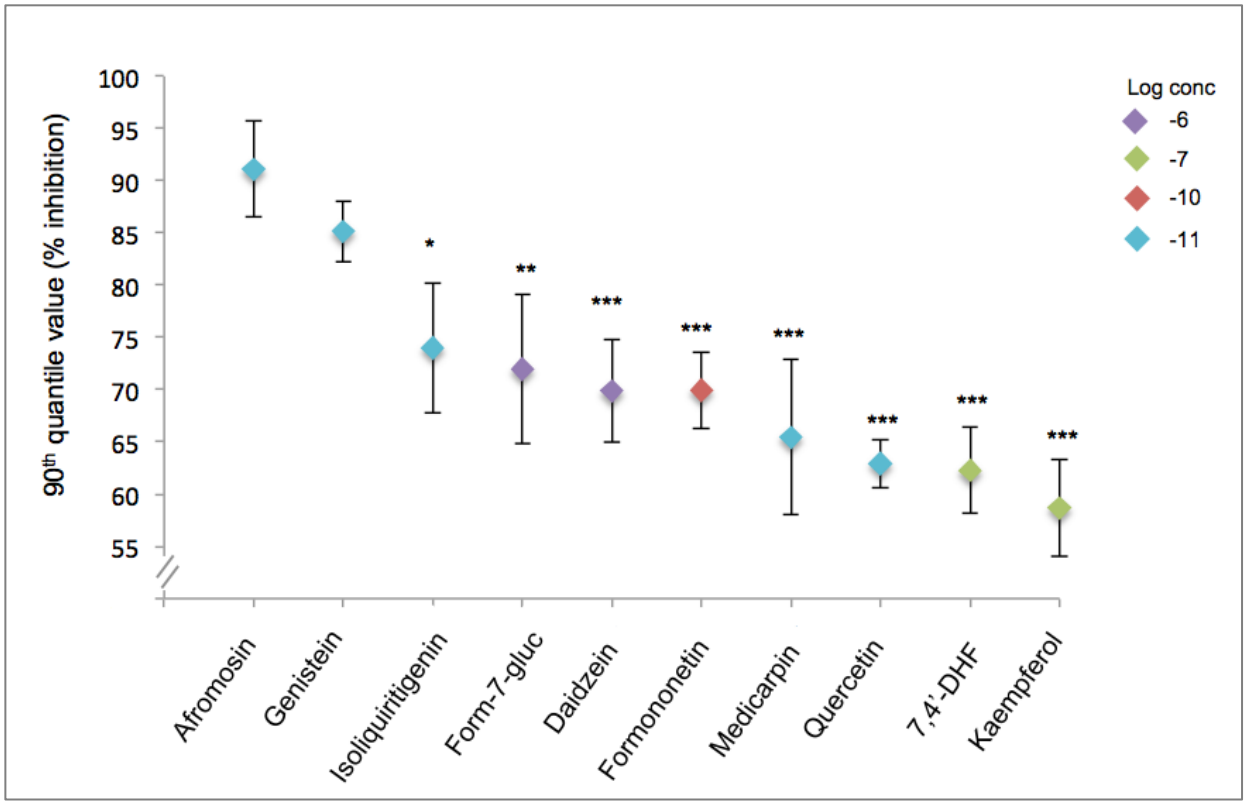

Figure 4.21: Rankings of ten flavonoids as best nematode motility inhibitors. Rankings were weighed based on their upper 90th quantile values for percentage inhibition with their corresponding concentrations. Upper quantile comparisons between afromosin and nine remaining flavonoids were done to compare differences in maximum inhibition values (extensive lists of pairwise comparisons available in Appendix Table). Asterisks indicate p values <0.05. Scatter plots represent the 90th quantile values, whereas the error bars represent standard errors.

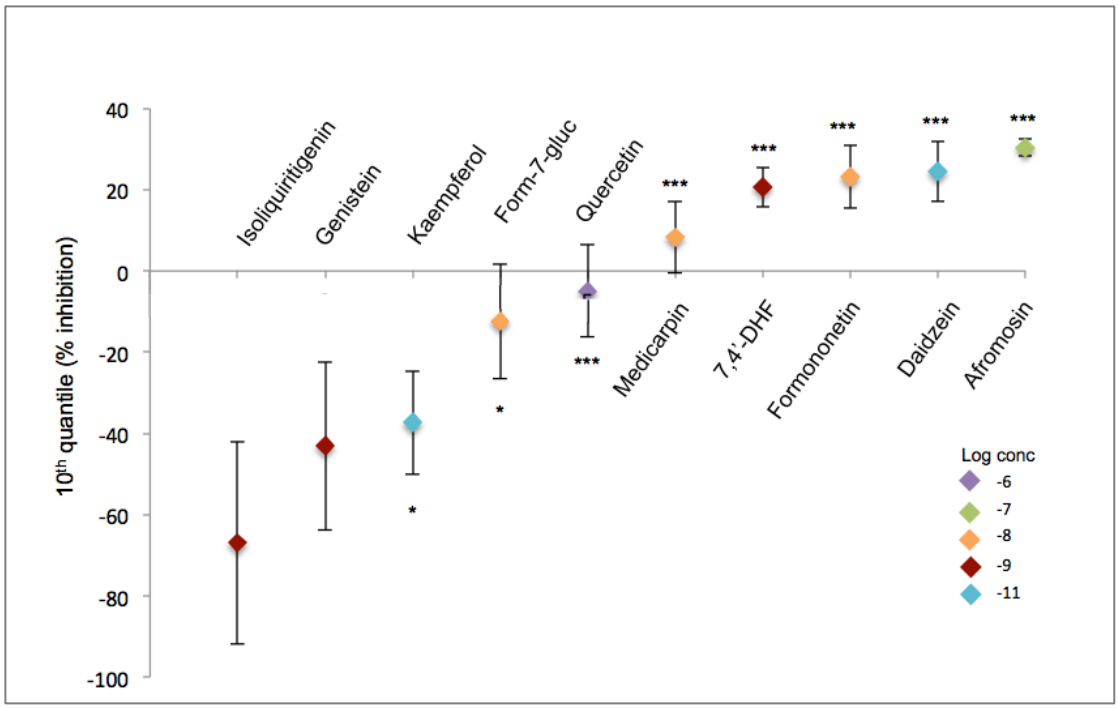

Figure 4.22: Rankings of ten flavonoids as worst nematode motility inhibitors. Rankings were weighed based on their lower 10th quantile values for percentage inhibition with their corresponding concentrations. Lower quantile comparisons between isoliquiritigenin and nine remaining flavonoids were done to compare differences in minimum inhibition values (extensive lists of pairwise comparisons available in Appendix Table). Asterisks indicate p values <0.05. Scatter plots represent the 10th quantile values, whereas the error bars represent standard errors.

Root exudates of *M. truncatula* 2HA, IFSi 101-2, IFSi 42-7 and IFSOE 10-3 were extracted from the growth media (same as Figures 4.6 and 4.7) and were further diluted by 10^{2} to 10^{6}. Dilutions were used because the exact concentrations of individual flavonoids and the full composition of root exudates were difficult to ascertain. Next, these root extracts were used in motility assays using same methods as aforementioned. All transgenic root exudates inhibited nematode motility at all dilutions, whereas 2HA root exudate stimulated or inhibited nematode motility depending on its dilution (Figure 4.23). 2HA root exudate highly stimulated nematode movement to 130% at 10^{6}-fold dilution, whilst the 10^{4}-fold dilution only caused a very weak 18% motility stimulation (Figure 4.23). 2HA root exudate inhibited nematode motility at 10^{5}-, 10^{3}- and 10^{2}-fold dilutions, with 42%, 17% and 23%, respectively (Figure 4.23). IFSi 101-2 root exudate showed highest motility inhibition activity at 73% at 10^{4}-fold dilution, and the lowest at 11% at 10^{2}-fold dilution (Figure 4.23). IFSi 42-7 root exudate was the best motility inhibitor, with 90% motility inhibition at 10^{2}-fold and ~80% inhibitions at 10^{6}-fold and 10^{5}-fold dilutions (Figure 4.23). IFSOE 10-3 root exudate had similar inhibitor activity as IFSi 101-2 exudate, at 72% when 10^{2}-fold dilution was used (Figure 4.23).

Rankings of root exudate based on 90th quantile values showed that IFSi 42-7 root exudate was the best motility inhibitor at 10^{2}-fold dilution, followed by IFSi 101-2, IFSOE 10-3 and 2HA root exudates (Figure 4.24). As for the worst motility inhibitor (or best motility stimulator), 10^{6}-fold diluted 2HA root exudate was the worst motility inhibitor, followed by IFSi 42-7, IFSOE 10-3 and IFSi 101-2 root exudates (Figure 4.25).

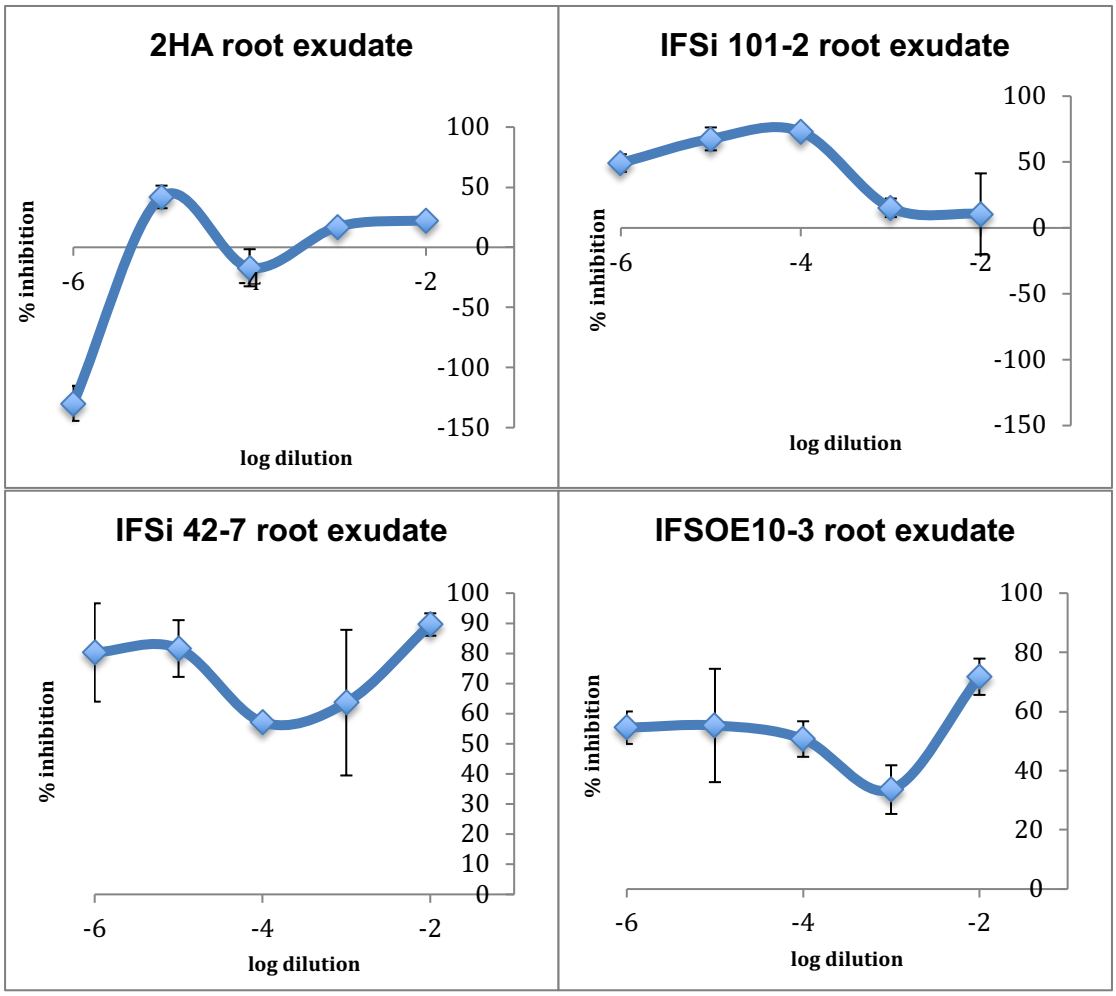

Figure 4.23: Percentage inhibition of four root exudates from 2HA, IFSi 101, IFSi 42 and IFSOE 10-3 on nematode motility compared to solvent control. Five dilutions of the original root exudate extracts, ranging from 10^{-6} to 10^{-4} fold were tested. Each data point represents a mean value. Error bars represent standard deviations. (N=3).

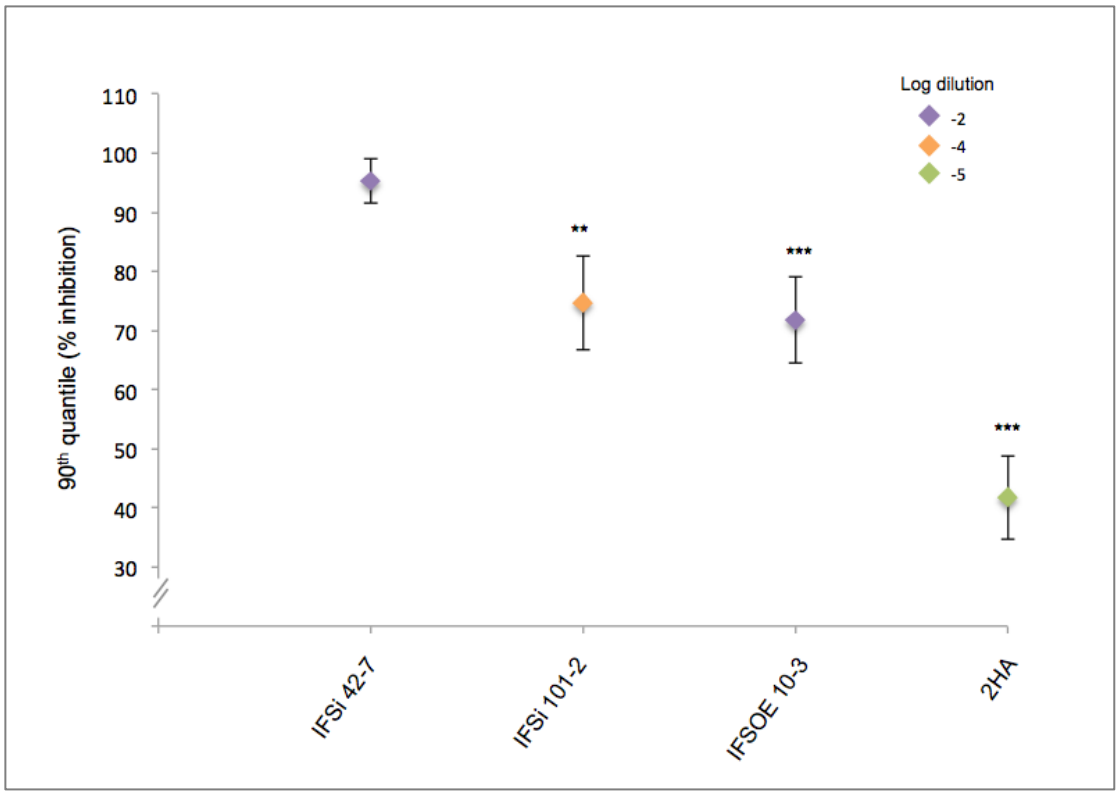

Figure 4.24: Rankings of root exudates from wild-type *Medicago truncatula* cv. 2HA and transgenics IFSi 101-2, IFSi 42-7 and IFSOE 10-3 as best nematode motility inhibitors. Rankings were weighed based on their upper 90th quantile values for percentage inhibition with their corresponding concentrations. Upper quantile comparisons between root exudate of IFSi 42 and other plants were done to compare differences in maximum inhibition values (extensive lists of pairwise comparisons available in Appendix Table). Asterisks indicate p values <0.05. Scatter plots represent the 90th quantile values, whereas the error bars represent standard errors.

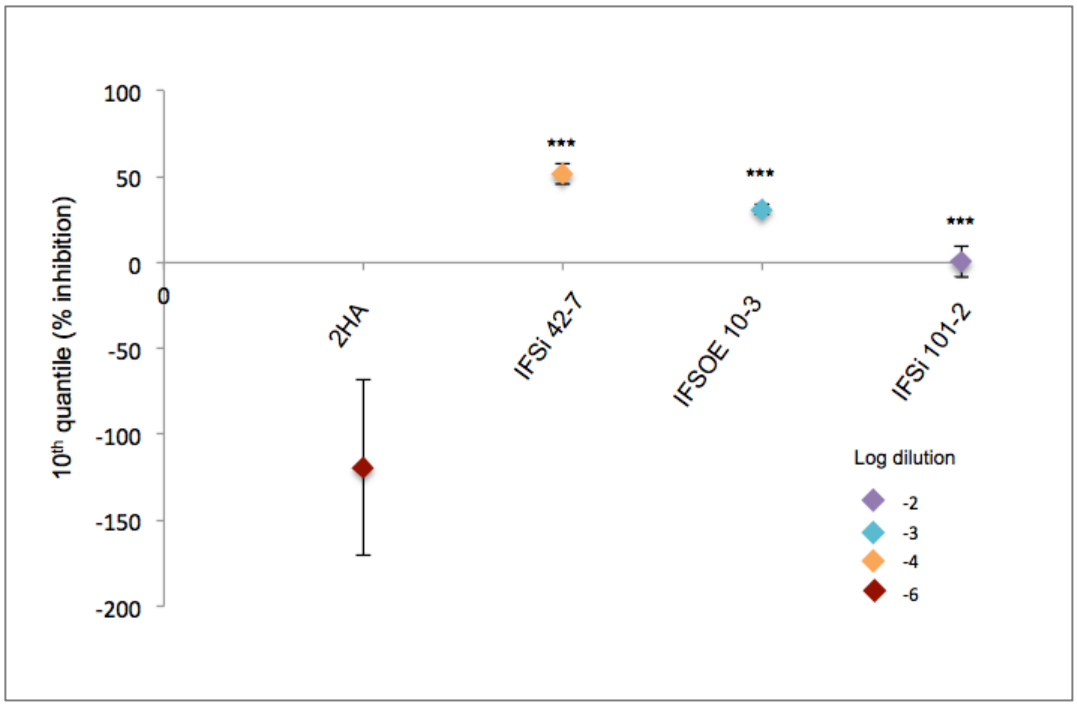

Figure 4.25: Rankings of root exudates from wild-type *Medicago truncatula* cv. 2HA and transgenics IFSi 101-2, IFSi 42-7 and IFSOE 10-3 as worst nematode motility inhibitors. Rankings were weighed based on their lower 10th quantile values for percentage inhibition with their corresponding concentrations. Lower quantile comparisons between root exudate of 2HA and other plants were done to compare differences in minimum inhibition values (extensive lists of pairwise comparisons available in Appendix Table). Asterisks indicate p values <0.05. Scatter plots represent the 10th quantile values, whereas the error bars represent standard errors.

4.3.3.2. Chemotaxis assay

Nine flavonoids, ie. isoliquiritigenin, kaempferol, quercetin, 7,4'-DHF, formononetin, daidzein, genistein, afromosin, and medicarpin, and four root exudates from *M. truncatula* 2HA and IFS transgenics were tested for their effects on J2 chemotaxis. For flavonoids, three concentrations (or dilutions for exudates) were selected based on concentrations that exerted effects on motility, either stimulating or inhibiting motility (Section 4.3.3.1.). As for root exudates, the same dilutions were used as the motility assays (Section 4.3.3.1.). J2s were randomly distributed in a water pluronic gel plate and each compound was place in the centre of the plate. This resulted in three outcomes, whereby 1) the J2s did not respond, 2) the J2s were attracted therefore moved towards the centre and 3) the J2s were repelled, hence moved away from the centre (For examples of responses, see Supplementary Figure 4.15).

None of the tested flavonoids were attractive to J2s. Isoliquiritigenin, 7,4'-DHF, formononetin and genistein had no effect on nematode chemotaxis as shown by the even distribution of nematodes across the plate, with relative density of ~0.2-0.3 (Figure 4.26). Furthermore, statistical analysis using linear mixed analysis found that nematode densities in different positions for these compounds were similar to each other. The remaining five flavonoids, kaempferol, quercetin, daidzein, afromosin and medicarpin repelled nematodes (Figure 4.26). This was demonstrated by increased nematode densities in positions further away from the centre, resulting in significantly higher relative densities at positions 4 and 5 (Figure 4.26). The change in compound concentration did not affect repellent activities of kaempferol, quercetin, daidzein and medicarpin, whereas repellent activity for afromosin was concentration dependent, with afromosin being the most repellent at 10^{-7}M concentration (Figure 4.26). Medicarpin showed the highest repellence activity, followed by afromosin, kaempferol, daidzein and quercetin based on nematode densities in positions 4 and 5 (Figure 4.27).

Similar to flavonoids, root exudates did not attract J2s (Figure 4.28). Only IFSi 101-2 root exudate was slightly repellent at all three dilutions, with statistically significant differences in density values based different positions ($p<0.05$), whereas

root exudates from 2HA, IFSi 42-7 and IFSOE 10-3 did not affect nematode chemotaxis (Figure 4.28).

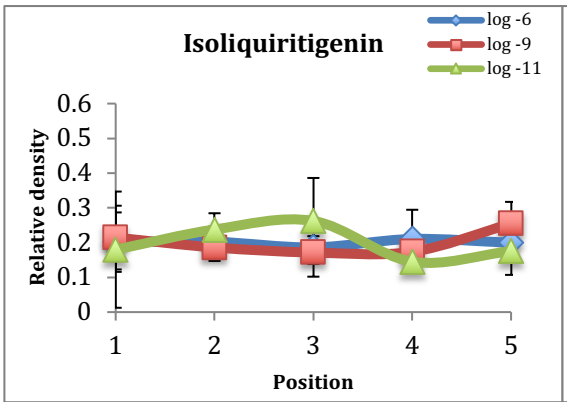
Isoliquiritigenin
log -6
log -9
log -11
Relative density
0.6
0.5
0.4
0.3
0.2
0.1
0
1
2
3
4
5
Position

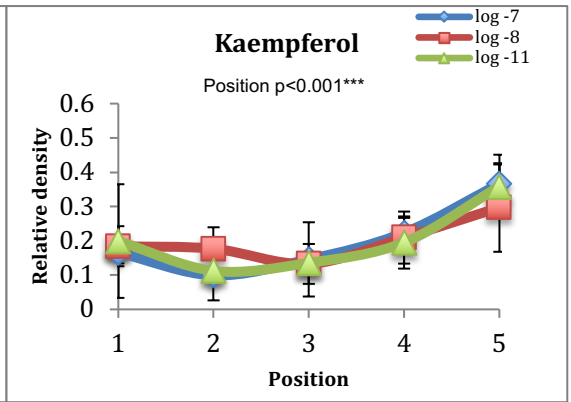
Kaempferol
log -7
log -8
log -11
Position p<0.001***
Relative density
0.6
0.5
0.4
0.3
0.2
0.1
0
1
2
3
4
5
Position

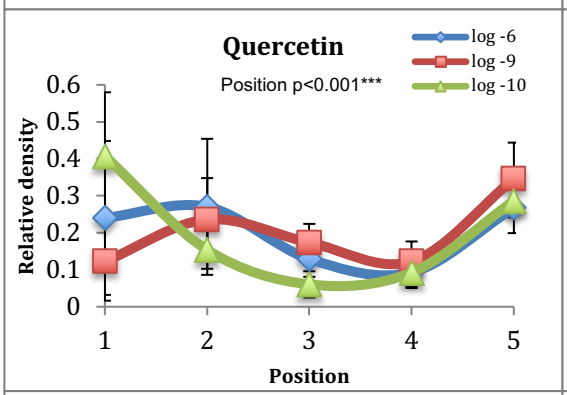
Quercetin
log -6
log -9
log -10
Position p<0.001***
Relative density
0.6
0.5
0.4
0.3
0.2
0.1
0
1
2
3
4
5
Position

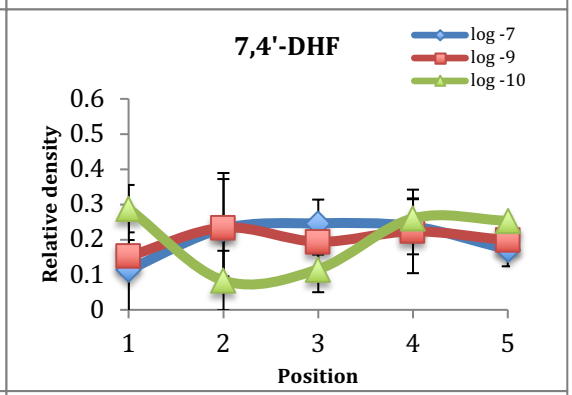
7,4'-DHF
log -7
log -9
log -10
Relative density
0.6
0.5
0.4
0.3
0.2
0.1
0
1
2
3
4
5
Position

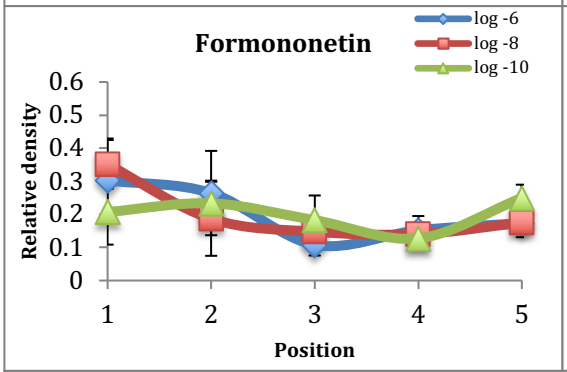
Formononetin
log -6
log -8
log -10
Relative density
0.6
0.5
0.4
0.3
0.2
0.1
0
1
2
3
4
5
Position

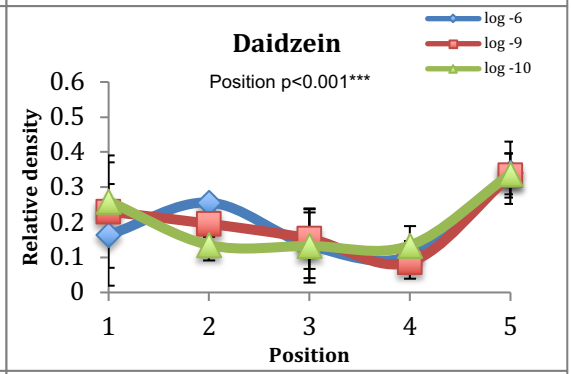
Daidzein
log -6
log -9
log -10
Position p<0.001***
Relative density
0.6
0.5
0.4
0.3
0.2
0.1
0
1
2
3
4
5
Position

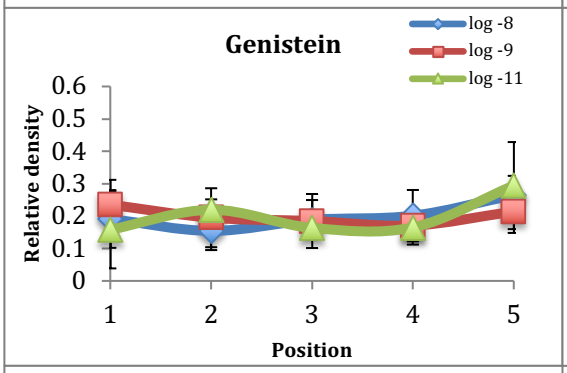
Genistein
log -8
log -9
log -11
Relative density
0.6
0.5
0.4
0.3
0.2
0.1
0
1
2
3
4
5
Position

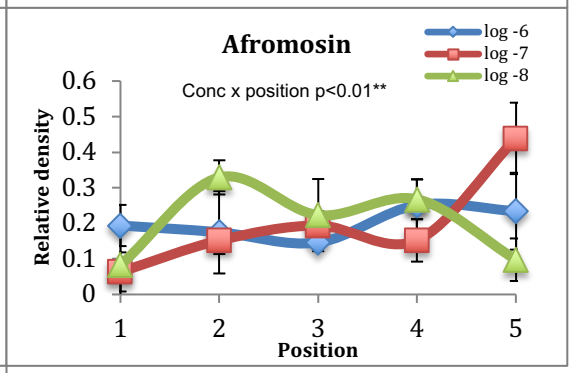
Afromosin
log -6
log -7
log -8
Conc x position p<0.01**
Relative density
0.6
0.5
0.4
0.3
0.2
0.1
0
1
2
3
4
5
Position

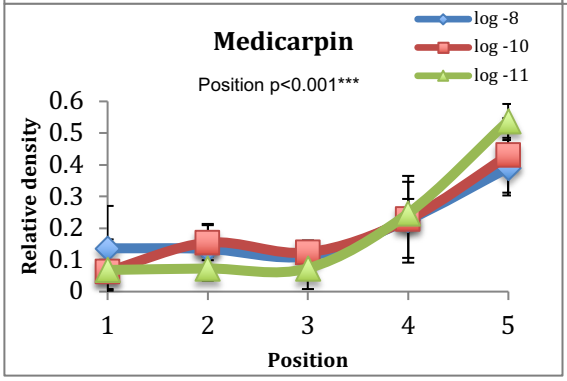
Medicarpin
log -8
log -10
log -11
Position p<0.001***
Relative density
0.6
0.5
0.4
0.3
0.2
0.1
0
1
2
3
4
5
Position

Figure 4.26: Effect of nine flavonoids at three concentrations on *Meloidogyne javanica* J2 chemotaxis. Relative density is nematode density per position normalised to the total number of nematodes per plate (on average ~100 J2s per plate). Position 1 is the centre of the late where each compound/exudate was applied, whereas position 5 is the outermost circle of the chemotaxis plate. Thus, relative densities of nematodes in positions 4 and 5 indicate repellent activity of the test compound. Scatterplots represent average values. Error bars represent standard deviations. Statistical analysis was performed with linear mixed model analysis for compound, position and concentration factors. (N=3)

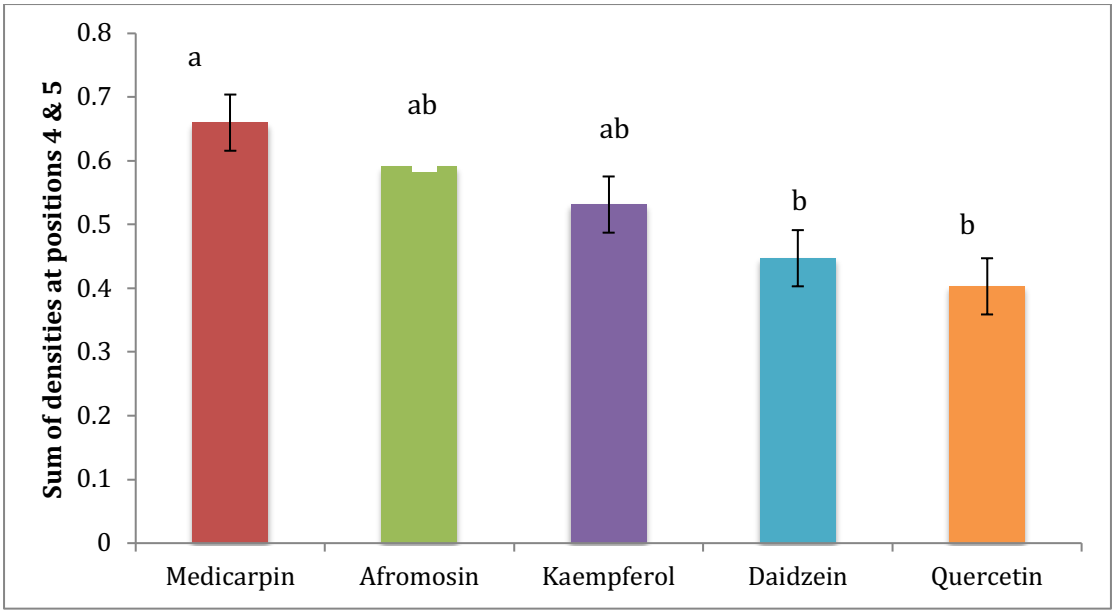

Figure 4.27: Rankings of nine flavonoids with repellent bioactivities based on the sum of nematode densities at positions 4 and 5. The sum of densities at positions 4 and 5 for each flavonoid was averaged across three concentrations, except afromosin, which only included values at 10^{-7} M concentration (hence, the lack of error bar). Error bars represent standard errors. Statistical analysis was done using ANOVA to compare the sum values across different flavonoids, with letter representing statistically significant comparisons.

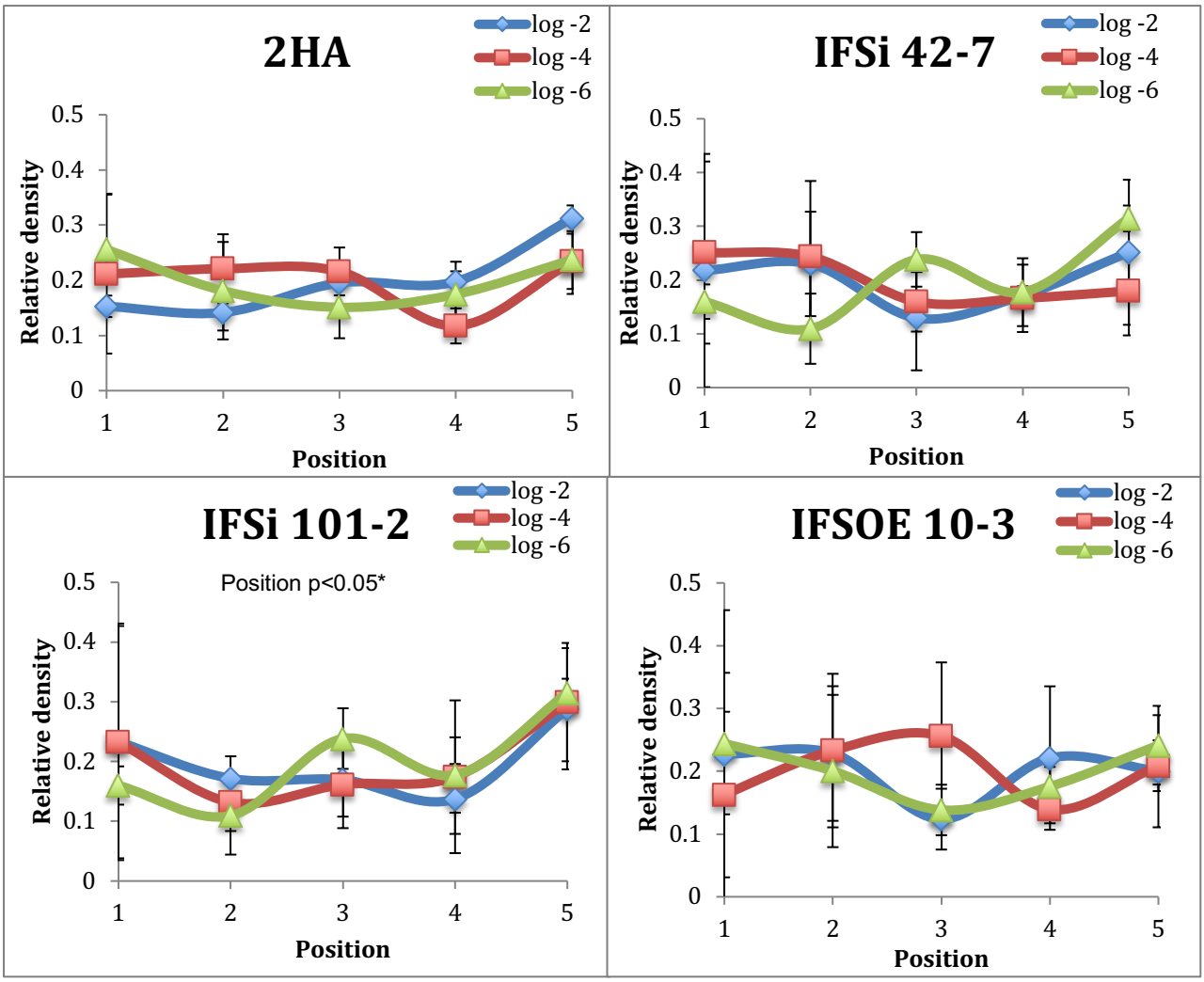

Figure 4.28: Effect of root exudates at three dilutions, 10^{-2}, 10^{-4} and 10^{-6}-fold, originating from wild-type *Medicago truncatula* cv. 2HA and transgenic *M. truncatula* IFSi 101, IFSi 42 and IFSOE 10 on the *Meloidogyne javanica* J2 chemotaxis. Relative density is normalised nematode density per position to the total number of nematodes per plate. Scatterplots represent averaged values. Error bars represent standard deviations. (N=3)

4.4. Discussion

4.4.1 Flavonoid gene experession in isoflavone synthase transgenics did not correlate with metabolite levels.

In Figure 4.6, *CHS* gene expressions were similar between IFSi 101-2 and IFSOE 10-3 roots. However, this was contrasted by isoliquiritigenin concentrations, whereby IFSi 101-2 roots produced significantly less isoliquiritigenin compared with IFSOE 10-3 roots (Figure 4.7). Although *IFS* gene expressions for IFSi 101-2 and IFSOE 10-3 roots were similar (Figure 4.6), the concentrations of the isoflavonoids daidzein and formononetin were lower in IFSi 101-2 roots than IFSOE 10-3 roots (Figure 4.8).

The differences in transcriptomic and metabolomics results may be attributed to temporal gaps that occur between RNA translation to synthase production to metabolite synthesis, as the duration for these processes are unclear. The quantification of flavonoids will also be affected by concentrations produced by *in vivo* synthesis and flavonoids stored in cytosol, vacuole, endoplasmic reticulum, chloroplast, nucleus and small vesicles (Zhao and Dixon, 2009). Moreover, epigenetic regulation of flavonoids in plants has not been well studied. The promiscuity of flavonoid enzymes also obscures the correlation between transcriptomics and metabolomics. Flavonoid enzymes can often produce more than product and/or be involved in multiple catalysis. For instance, the CHS enzyme catalyses malonyl- CoA and p-coumaroyl CoA into isoliquiritigenin or naringenin chalcone (Figure 1.3). In addition to CHS, chalcone reductase (CHR) can also catalyse the same precursors into isoliquiritigenin. Therefore, accurate representations of flavonoid regulation for the chalcones require transcript quantification of both CHS and CHR, as well as metabolite quantification of isoliquiritigenin and naringenin chalcone. Furthermore, flavonoid biosynthetic genes in *M. truncatula* are highly duplicated with multiple gene members, with 28 *CHS* genes, 10 *CHR* gene members and 11 *CHI* genes (Young et al., 2011), which suggest that gene members can complement each other. In addition, flavonoid production can be influenced by the accumulation of downstream products, either resulting in a negative feedback

inhibition of the corresponding pathway (Yin et al., 2012) and/or the re-channeling of metabolites into a different pathway (Onkokesung et al., 2014)

The quantification of flavonoid synthase transcripts and flavonoid concentrations is not straightforward and require the careful considerations of enzyme promiscuity, redundant roles of gene members, the effects of downstream product accumulation, as well as other unknown transcriptional processes that affect flavonoid synthesis. Hence, the

4.4.2 How did the change in *in planta* flavonoid production alter nematode infection?

In planta variations in flavonoid production were obtained by using existing different cultivars and accessions and by genetically modifying flavonoid biosynthesis genes. The cultivars 2HA and A17, and accessions F83005 and DZA045 mainly differed in daidzein, DHF glyc-like, k-3-rutinoside, luteolin, liquiritigenin, medicarpin, glycitein, gen-7-gluc and genistein concentrations (Figure 4.3). We were unable to clearly find a distinction in flavonoid productions based on flavonoid groups. The differences in these flavonoid concentrations resulted in changes in nematode infection phenotypes, notably in accessions DZA045 and F83005, with the former producing the smallest galls, but the most eggs and the latter had the least eggs (Figure 4.29). The flavonoids positively correlated with the gall sizes were liquiritigenin, naringenin and compound 784 (Figure 4.5), for each of which DZA045 plants produced the lowest concentrations (Supplementary Figures 4.2, 4.3 and 4.4). However, linear regressions of 33 flavonoid concentrations with egg numbers failed to show any correlation between individual flavonoid concentrations and egg numbers. It is possible that combinations of several compounds have an effect on egg numbers, but this was not further tested here. Alternatively, egg numbers could be affected by non-flavonoid-related changes. For example, it could be due to differences in other biochemical pathways such as jasmonic acid, salicylic acid, and ethylene in cultivars and accessions, which are also induced in response to nematode infection (Goverse and Smant, 2014, Holbein et al., 2016). Currently, there is no information about global gene expression changes or other signals between these cultivars.

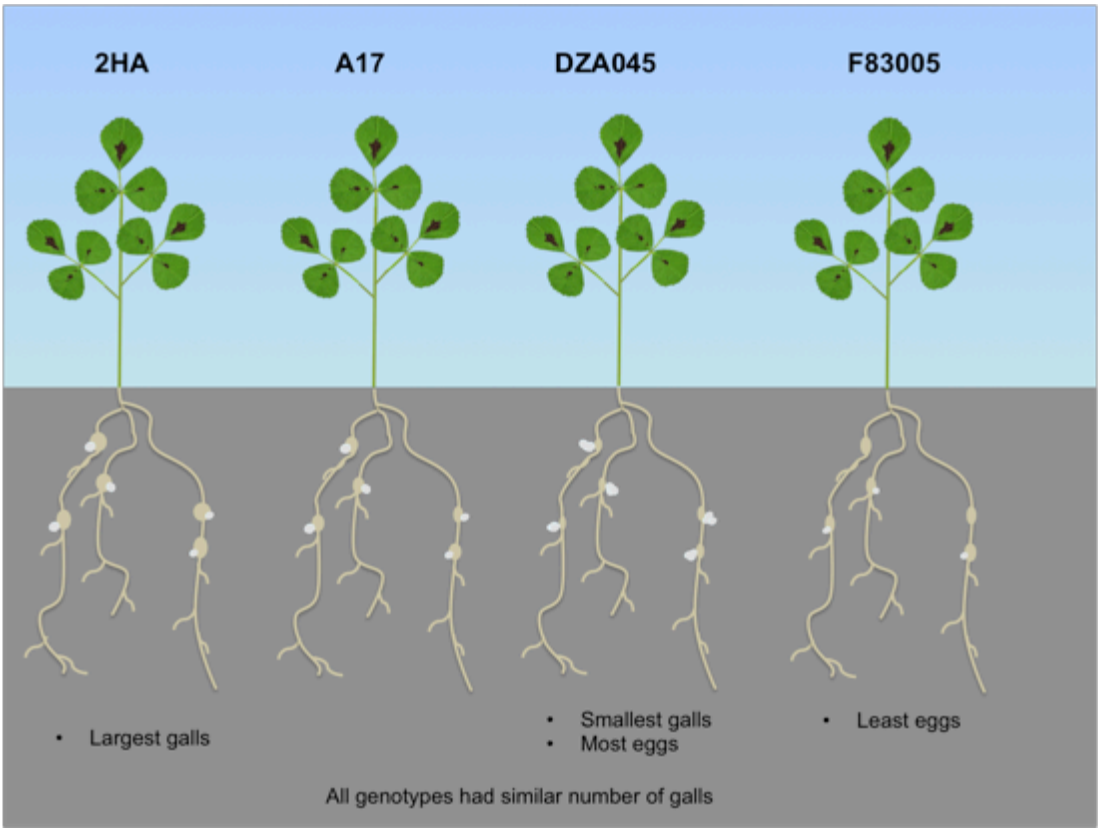

Figure 4.29: A summary infection phenotypes observed in four *Medicago truncatula* cultivars/accessions, 2HA, A17, DZA045 and F83005 during *Meloidogyne javanica* infection. Drawings are not to scale.

On the other hand, genetically modified IFS transgenics plants mainly showed differences in isoflavonoids and pterocarpan concentrations, particularly IFSOE 10-3, which over-produced formononetin, daidzein, afromosin and medicarpin either in roots or in root exudates or in both samples (Figure 4.8), although measurements of root exudates would have to be repeated for statistical analysis. Interestingly, IFSi lines, IFSi 101-2 and IFSi 42-7 did not show noticeable differences in isoflavonoid production, with the exception of significantly reduced daidzein production in the root (Figure 4.8). This may be the result of compensation of reduced flavonoid production by the redirection of flavonoids from other pathways or incomplete silencing of *IFS* gene members, possibly due to off-target RNAi. In addition, IFSi 101-2 and IFSi 42-7 plants exhibited non-identical flavonoid profiles (Figures 4.6 and 4.7), which likely further indicates transgene insertion into different sites and/or transgene insertion with different numbers of copies. In contrast, overexpression of IFS in IFSOE 10-3 did result in higher accumulation of some isoflavonoids and pterocarpan (Figure 4.8).

IFSOE 10-3 plants showed the best outcome by experiencing the least biomass loss from nematode infection and smaller galls (Figure 4.30). In contrast, IFSi 42-7 had the poorest outcome, with the highest biomass loss from infection and most galls (Figure 4.30). Overall infected plant weight (but not biomass loss) was negatively correlated with methoxyisoflav 1 and methoxyisoflav 2 concentrations (Figure 4.15). Additionally, the same flavonoids were also negatively correlated with gall size (Figure 4.18). IFSi 42-7 plants had the second highest concentration of methoxyisoflav 1 (Supplementary Figure 4.5) and the highest concentration of methoxyisoflav 2 (Supplementary Figure 4.6), which correlated with this genotype's lowest overall weight and smaller gall sizes. However, we were unable to correlate biomass loss with flavonoid concentrations. The reduced biomass loss in IFSOE 10-3 may be the result of highest increase in lateral roots compared to other genotypes to help compensate for reduced root function as a result of nematode infection (Figure 4.30 and Table 4.1). Although numbers of lateral roots were related to DHF glyc-like concentrations (Figure 4.16) (2HA plants which had the highest levels of DHF glyc-like had the most lateral roots), we couldn't ascertain what contributed to high relative increase of lateral roots in IFSOE 10-3 plants. IFSi 101-2 plants produced the least eggs, which was correlated with low accumulations of isoliquiritigenin, liquiritigenin and compound 578 (Figure 4.17 and Supplementary Figures 4.8, 4.9 and 4.10). Unlike accessions and cultivars, liquiritigenin, naringenin and compound 784 as well as additional isoliquiritigenin, compound 462 and compound 578 were linked to gall number in transgenics (Figure 4.19). IFSi 42-7 plants with the most galls tended to either produce the highest or second highest concentrations of these flavonoids (Supplementary Figures 4.8, 4.9, 4.10, 4.11, 4.12 and 4.13). Nonetheless, the correlations of flavonoid concentrations with infection phenotypes do not necessarily indicate cause or effect. It is possible that higher concentrations of particular flavonoids in mature galls correlate with gall numbers, for example, just because the flavonoid accumulates in galls and thus roots with more galls per tissue weight would yield in higher flavonoid concentrations, even in the absence of any activity of the flavonoid on the infection process. However, the correlations may be useful in future studies that aim overexpress specific flavonoid end products to test more directly whether these compounds would have an effect on infection phenotypes.

In terms of *ex planta* nematode behaviours, generally, exudates of IFS transgenics were better J2 motility inhibitor than those of wild-type 2HA (Figure 4.23) and IFSi 101-2 exudate was the only repellent root exudate (Figure 4.28). Nevertheless, motility inhibition by root exudates would have been overcome by J2s because although IFSi 42-7 exudate at 10^{2}-fold dilution was the most repellent (Figure 4.24), this genotype was the most infected, with most galls (Figure 4.9) and most nematode eggs (Figure 4.10). IFSi 101-2 plants in comparison were not as affected by nematode infection, perhaps as a result of reduced re-infections by J2s. IFSOE plants were neither particularly effective at repelling nor inhibiting J2 motility, suggesting that *in planta* flavonoids played bigger roles in influencing infection outcomes. Nevertheless, the best test for flavonoid bioactivities as motility inhibitors and chemo-repellants will require further testing in soil conditions, which accounts for realistic spatial proximity between nematodes and host roots.

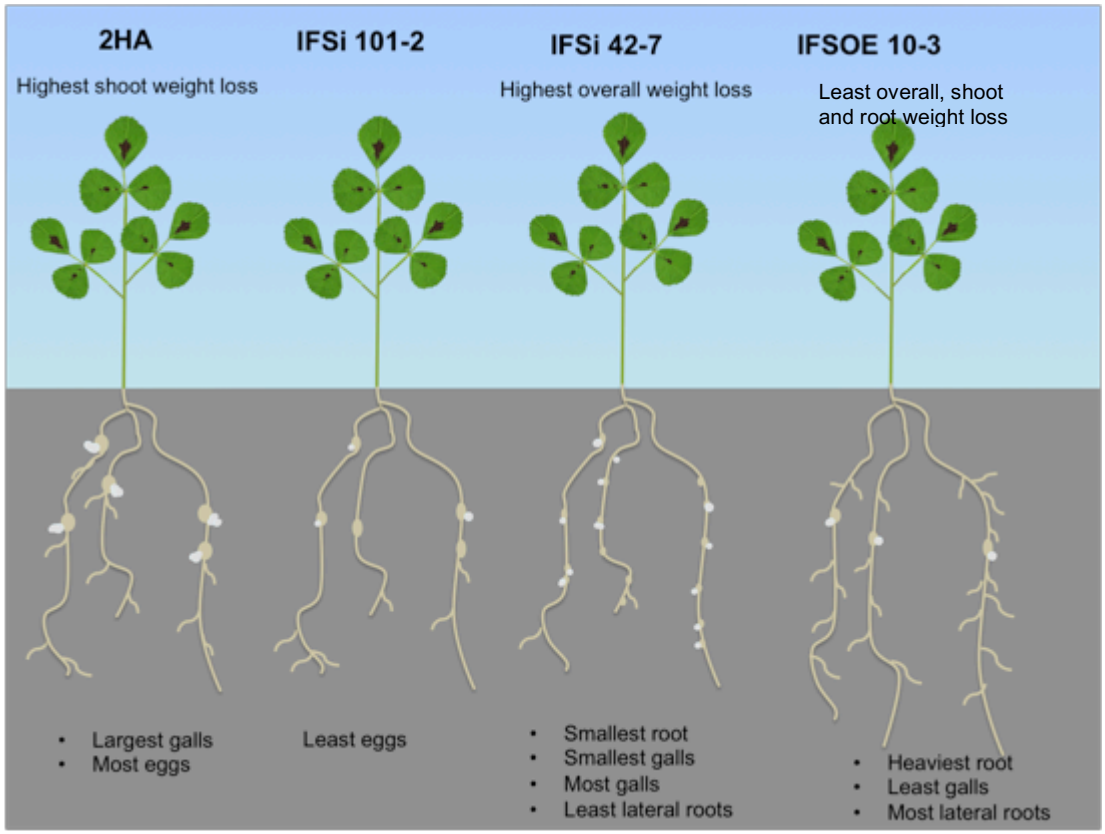

Figure 4.30: *Meloidogyne javanica* nematode infection phenotype summaries for *Medicago truncatula* wild-type cv. 2HA and isoflavone synthase transgenics, silenced lines, IFSi 101-2 and IFSi 42-7 and over-expression line, IFSOE 10-3. Drawings are not to scale.

In general, both experiments showed conflicting flavonoid correlations with infection phenotypes. This could reflect the limitations of simple linear regressions in correlation analysis, as flavonoids may interact synergistically and antagonistically to exert one or multiple effects. Moreover, there are numerous biochemical, hormonal and defence pathways eg. cytokinin, gibberellins, jasmonic acid, salicylic acid, ethylene, reactive oxygen species involved in plant-nematode interactions (Bird, 1974, Caillaud et al., 2008, Kyndt et al., 2013) which may affect infection and gall formation. The comparison of the top 12 influencers from OPLS-DA models based on nematode treatment variable at 6 weeks post inoculation in accessions/cultivars and transgenics revealed seven overlapping flavonoids which were influenced by nematode infection, regardless of the plant genotype (Figure 4.31). These were isoliquiritigenin, liquiritigenin, naringenin, afromosin, k-gluc-rham, compounds 740 and 784, which were highly upregulated across all genotypes at 6 weeks, with the exception of 740, which increased and decreased in different genotypes (Figures 4.4 and 4.13).

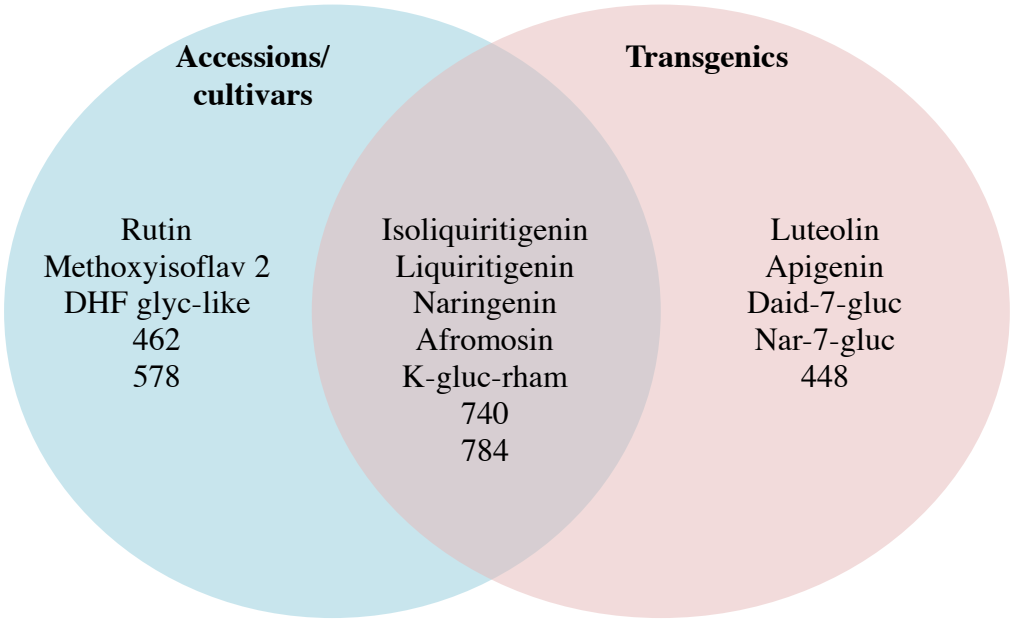

Figure 4.31: The list of top 12 flavonoids influencing OPLS-DA models based on nematode treatment factor (in no particular order) for two experiments involving *M. truncatula* accessions/ cultivars (2HA, A17, DZA045 and F83005) and transgenics (wild-type 2HA, IFSi 101-2, IFSi 42-7 and IFSOE 10-3).

4.4.3 Which flavonoids were likely involved in defence against nematodes?

Afromosin showed the strongest bioactivities against pre-parasitic J2s of *M. javanica*. It exhibited the strongest nematode motility inhibition out of the ten tested flavonoids, with 80- 90% inhibitions at 10^{-11} to 10^{-9} M concentrations (Figures 4.19) as well as being a moderate repellent, particularly at 10^{-7} M concentration (Figure 4.26). *In planta* experiments with *M. truncatula* cultivars, accessions and IFS transgenics showed that afromosin was upregulated at 24 hours and 6 weeks post inoculation (Figures 4.4 and 4.13) and was one of the top flavonoids influenced by nematode treatment based on OPLS-DA (Figure 4.31). Nevertheless, high amounts of afromosin *in planta* appeared to be less effective against parasitic stages of *M. javanica* eg. J3, J4 and adult as IFSi 42-7 plants produced the most galls and eggs, despite making the highest amount of afromosin compared to IFSi 101-2, IFSOE 10-3 and 2HA (Supplementary Figure 4.19). Likewise, in the accessions and cultivars experiment, although 2HA plants produced highest level of afromosin at 6 weeks post inoculation (Supplementary Figure 4.17); they still produced the largest galls (Figure 4.29). However, the mode of action and metabolism of afromosin in nematodes is still unknown.

Medicarpin was the most effective J2 repellent, at various concentrations of 10^{-11}, 10^{-10} and 10^{-8} M (Figures 4.25 and 4.26). However, it was a moderate motility inhibitor, ranking 7th out of the ten tested flavonoids with maximum inhibition of ~65% (Figure 4.21). High levels of *in planta* medicarpin may have protected F83005 from infection, as this genotype produced the highest amounts of medicarpin at 24 hours and 6 weeks post inoculation compared to 2HA, A17, and DZA045 genotypes (Supplementary Figure 4.20). IFSOE 10-3 plants produced the most medicarpin compared to other transgenics and 2HA at 24 hours inoculation, but by 6 weeks, they produced the least medicarpin (Supplementary Figure 4.21). It is possible that early induction of medicarpin at 24 hours post inoculation is more crucial in reducing nematode infection compared to late induction, possibly by interfering with nematode development. Several studies have also suggested medicarpin in defense against other plant parasitic nematodes such as stem nematode and root lesion nematode, as

medicarpin and its conjugate accumulated in infection sites either at 48 hours or 10 days post inoculation (Baldridge et al., 1998, Cook et al., 1995, Edwards et al., 1995). Whilst, the mechanism behind medicarpin's bioactivity is unclear, a study on the effects of medicarpin and its conjugate, 4-hydroxymedicarpin on *C. elegans* (LD_{50} of 25μg/ml) revealed that these compounds inhibited oxygen consumption in *C. elegans* (Stadler et al., 1994). Medicarpin may also are exuded into the soil by nematode-infected plants to reduce new infections.

The flavonols, kaempferol and quercetin were moderate J2 repellents (Figure 4.27) and poor motility inhibitors (Figures 4.20 and 4.21). It is possible that flavonol aglycones were not primarily used in defence as kaempferol and quercetin aglycones were undetected in our experiments (data not shown). Moreover, the host root will need to exude up to 10^{-7} M concentration of kaempferol and up to 10^{-11} M concentration of quercetin, which would be physiologically difficult given the low abundance foud in roots. In contrast, flavonol conjugates such as k-gluc-rham and rutin were detected. K-gluc-rham was significantly influenced by nematode infection based on linear mixed analysis and OPLS-DA (Supplementary Tables 4.1 and 4.3 and Figure 4.31), suggesting that conjugated kaempferol may be the preferred form against nematodes and may exhibit stronger bioactivities on nematodes. Likewise, rutin was also significantly influenced by nematode infection (Supplementary Tables 4.1 and 4.3). Whilst the role of flavonol aglycones as auxin transport inhibitors had been described, some flavonol conjugates have also been demonstrated to inhibit auxin transport (Buer et al., 2013, Kuhn et al., 2016, Yin et al., 2014). In contrast, in *C. elegans,* uptake of flavonols such as kaempferol and quercetin prolonged its lifespan by reducing oxidative stress (Grünz et al., 2012, Kampkötter et al., 2007).

Isoflavonoids such as daidzein moderately repelled and moderately inhibited motility of J2s, whereas formononetin and form-7-gluc were moderately inhibitory to J2 motility but had no effect on chemotaxis (Figures 4.20 and 4.26). Although daidzein concentrations was discriminable based on genotypes in accessions and cultivars with different nematode susceptibilities (Figure 4.3), daidzein does not appear to be central in defence against *M. javanica*. In accessions and cultivars, daidzein concentrations did not accumulate and in some genotypes, was reduced during infection (Figure 4.4). Other studies on different PPN species found that daidzein (in μM concentrations) repelled *Radopholus similis* juveniles but did not

inhibit their motility and that formononetin and its conjugates accumulated in stem-nematode infected plant tissues (Cook et al., 1995, Edwards et al., 1995, Wuyts et al., 2006b). Whilst the induction of isoflavonoids in root exudates in response to nematode infection had not been tested, isoflavonoids are likely exuded in high amounts into the rhizosphere by nodulating plants, including *M. truncatula,* because nodulating plants exude large amounts of isoflavonoids to symbiotic bacteria and other pathogens (Dakora and Phillips, 1996, Liu and Murray, 2016). Nonetheless, these isoflavonoids did not consistently accumulated in the roots of in *M. truncatula* accessions, cultivars and transgenics (Figures 4.4 and 4.13). This is possibly due to high conversions of these isoflavonoids into downstream flavonoids such as afromosin and medicarpin, which are more effective in repelling and inhibiting J2s, as previously discussed. Alternatively, they may be exuded out from the roots into the soil to moderately inhibit motility and repel J2s. Interestingly, formononetin and form-7-gluc had similar response curves for nematode motility inhibition (Figure 4.20). This suggests the presence of flavonoid receptors in *M. javanica* J2s that bind to the backbone structure of flavonoids. In addition, the differences in motility inhibition between formononetin and form-7-gluc also suggests that glycosylation could possibility alter flavonoid adsorption or permeability into nematode cuticle by increasing flavonoid solubility.

The chalcone isoliquiritigenin inhibited J2 motility at 10^{-11} M concentration but stimulated nematode motility at 10^{-9} M concentration (Figures 4.20 and 4.21). As isoliquiritigenin is an important flavonoid during plant-nematode interaction (Figure 4.31), higher concentration at 10^{-9} M that stimulated J2 movement may promote J2s to move towards the root faster. However, pure isoliquiritigenin at the same 10^{-9} M concentration did not attract J2s. This may indicate that sets of receptors and/or neurons or sensory transduction were utilised for motility and chemotaxis. Moreover, J2 chemotaxis and motility is likely to be influenced by combinations of pH, volatiles, soluble sugars, amino acids, organic acids, phenolics, proteins, redox potential, microbes and etc, present in root exudates and rhizosphere, with the integration of multiple signals ultimately driving its behaviour (Bird, 1959a, Čepulytė et al., 2018, Prot, 1980, Wang et al., 2009a). *In planta,* isoliquiritigenin may not directly alter nematode infection. Instead, isoliquiritigenin was likely used as a precursor for downstream flavonoids with more specific bioactivities. Alternatively,

isoliquiritigenin may be directly metabolised by *M. javanica* to reduce oxidative stress, although this has only been tested in *C. elegans* using *Glycyrrhizae radix* extract which purportedly contained high levels of isoliquiritigenin (Ruan et al., 2016).

The flavanones naringenin and liquiritigenin were also primarily influenced by nematode infection but their exact roles are contentious, much like isoliquiritigenin. Similar to the study by Ruan et al. (2016), naringenin was conjugated by *C. elegans* and resulted in reduced reactive oxygen species and prolonged lifespan.

Several ambiguous compounds such as methoxyisoflav 1, methoxyisoflav 2, DHF glyc-like, and compounds 462, 578 and 784 appeared to be important in *in planta* plant-nematode interactions. These are likely involved in plant developmental regulation, instead of behaving as defence compounds as they were correlated to phenotypes such as lateral root numbers, gall numbers, and gall sizes. Methoxyisoflav 1 and methoxyisoflav 2 are types *O*-methylated isoflavones similar to biochanin A and glycitein (same backbones based on protonated ion of 285.07). To date, not much is known about the roles of *O*-methylated isoflavones on plant development. DHF glyc-like is a type of flavone, similar to 7,4'-DHF and chrysin (same backbones based on protonoated ion of 255.06). A derivative of 7,4'-DHF and free DHF were reported to strongly reduce auxin breakdown by peroxidase, resulting in auxin accumulation (Mathesius, 2001). Hence, DHF glyc-like may possibly be used to accumulate auxin at lateral root primordial for lateral root organogenesis (Blilou et al., 2005, Casimiro et al., 2001, Casimiro et al., 2003).

4.5. Conclusion

The isoflavonoid afromosin and pterocarpan medicarpin showed characteristics of defence compounds against nematodes, by repelling J2s and inhibited J2 motility and by accumulating high concentrations during infection. High levels of *in planta* afromosin did not necessarily result in better infection outcomes across the tested *M. truncatula* genotypes, whereas high concentrations of *in planta* medicarpin at 24 hours post inoculation may be for crucial in reducing nematode infection. The flavonols kaempferol and quercetin, isoflavonoids genistein, formononetin and daidzein, and the flavone, 7,4-DHF tested here were moderate to weak defence compounds, which suggest that they are likely to play different roles in plant-nematode interactions. Upstream flavonoids such as isoliquiritigenin, liquiritigenin and naringenin were important during nematode infection as alterations of these flavonoids were linked to changes in gall numbers, egg numbers and gall size. These flavonoids may play non-specific roles as precursors and reflect the general increase in flavonoid production. In addition, there were several ambiguous compounds found to be linked to nematode infection phenotypes, but their roles were postulated to be in plant development, instead of plant defence. Future studies are required to modify the flavonoid pathway in more specific ways to test the effect of these individual flavonoid candidates in plant-nematode infection, as the transgenic plants generated here had more wide-ranging changes in flavonoid composition than the targeted pathway.

4.6 Supplementary Figures

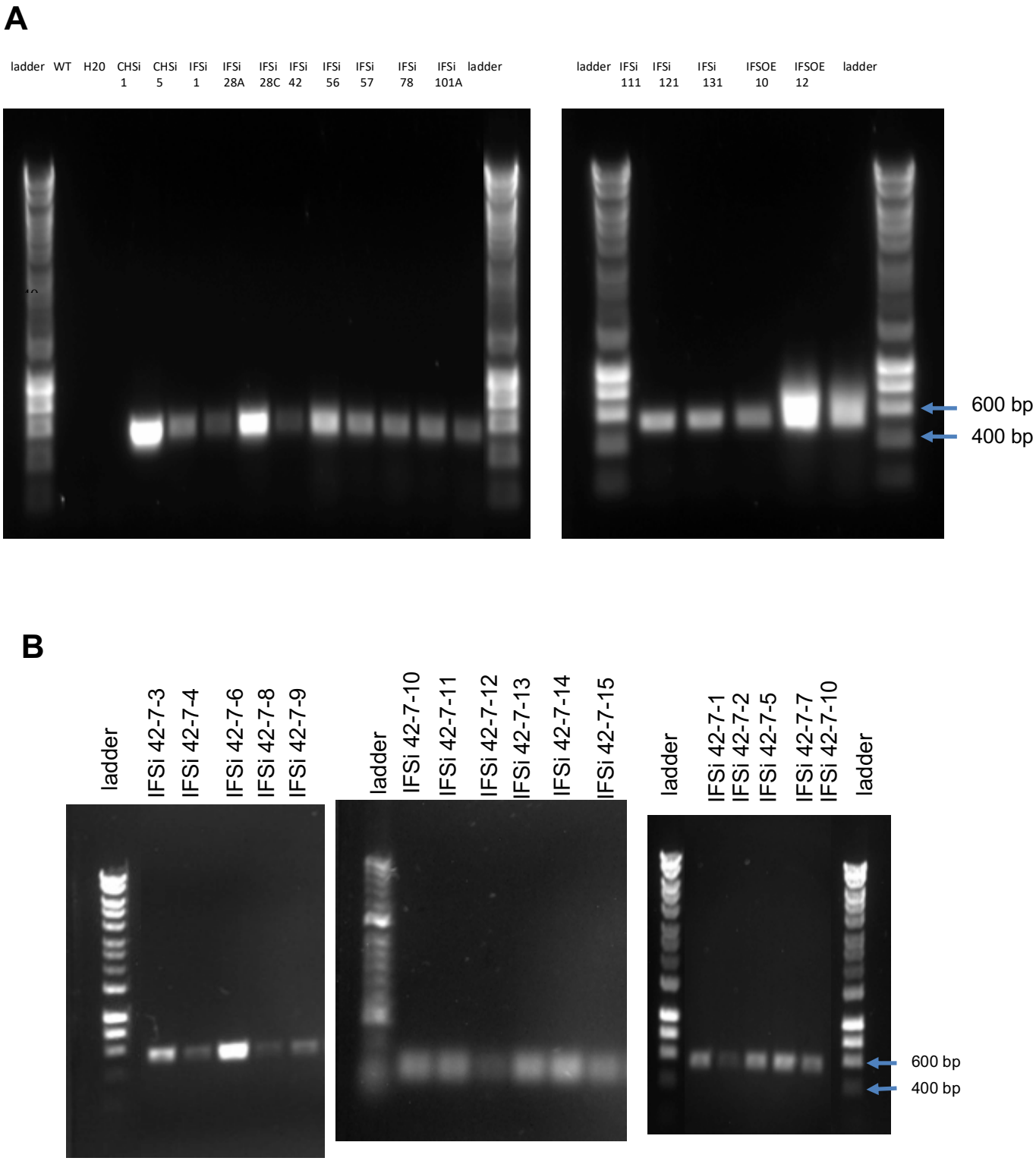

C
ladder
IFSi 101A-2-1
IFSi 101A-2-2
IFSi 101A-2-3
IFSi 101A-2-4
IFSi 101A-2-5
IFSi 101A-2-6
IFSi 101A-2-7
IFSi 101A-2-8
ladder
IFSi 101A-2-9
IFSi 101A-2-10
IFSi 101A-2-11
IFSi 101A-2-12
ladder
600 bp
400 bp

D
ladder
IFS OE 10-3-1
IFS OE 10-3-2
IFS OE 10-3-3
IFS OE 10-3-4
IFS OE 10-3-5
IFS OE 10-3-6
IFS OE 10-3-7
IFS OE 10-3-8
IFS OE 10-3-9
IFS OE 10-3-10
IFS OE 10-3-11
IFS OE 10-3-12
IFS OE 10-3-13
ladder
ladder
IFS OE 10-3-14
IFS OE 10-3-15
ladder
600bp
400 bp

Supplementary Figure 4.1: PCR- based DNA genotyping of transgenic *M. truncatula* via *nptII* transgene.

(A) Positive T_0 regenerants of IFSi and IFS-OE lines.

(B) The positive homozygote IFSi 42-7 with 15 T_3 progenies showing positive *nptII* insertion.

(C) The positive homozygote IFSi 101A-2 with 12 T_3 progenies showing positive *nptII* insertion.

(D) The positive homozygote IFS-OE with 15 T_3 progenies showing positive *nptII* insertion.

The expected *nptII* amplicon size is 453 bp.

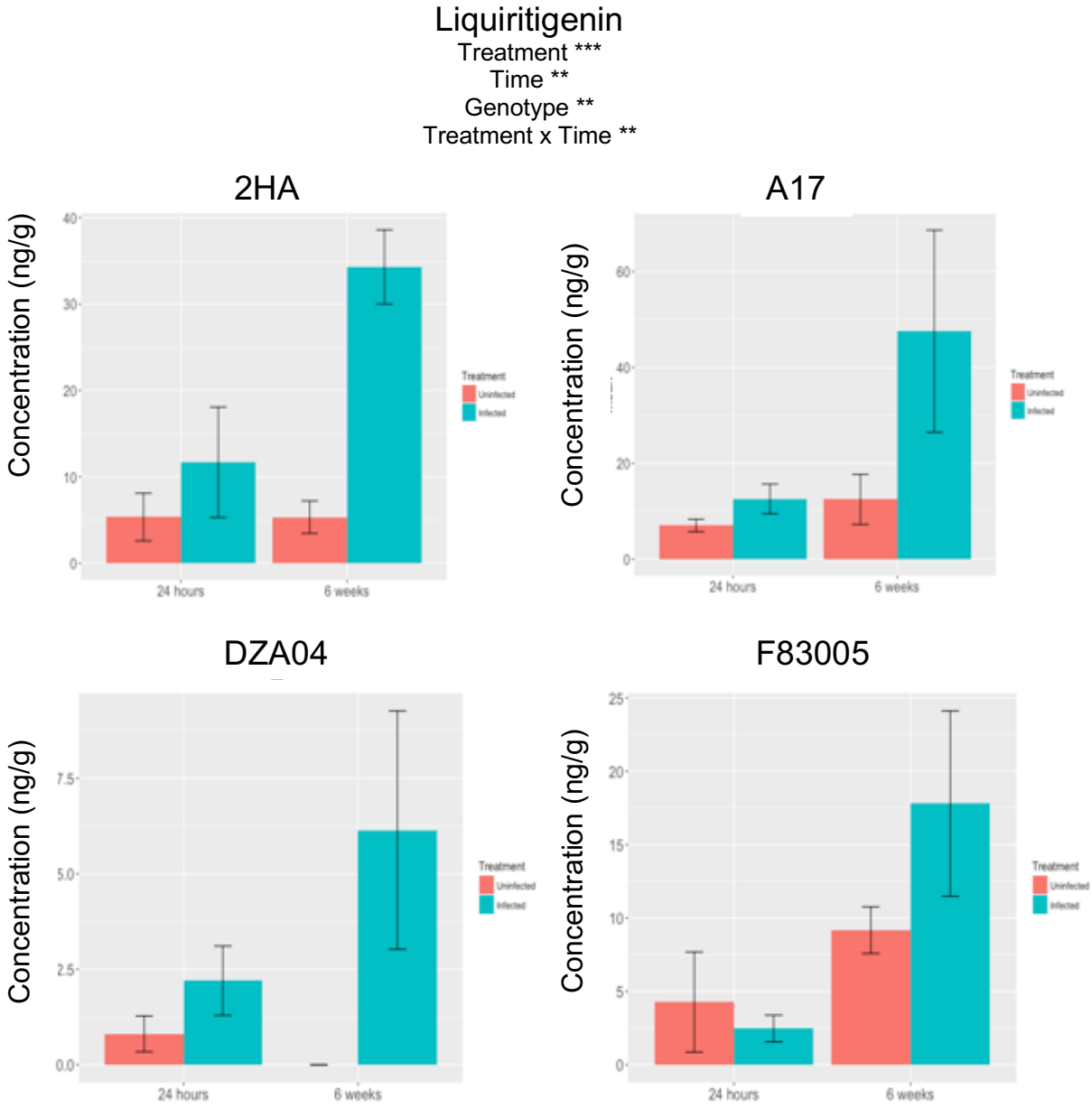

Supplementary Figure 4.2: Liquiritigenin concentrations based on fresh weight in root segments of uninfected and *Meloidogyne javanica* infected roots (galls) of *Medicago truncatula* cultivars, 2HA, A17, DZA045 and F83005. Statistical analysis is based on linear mixed analysis to test the effects of genotype, time, treatment factors and the interactions between these factors. Columns represent means and error bars represent standard errors. (N=4)

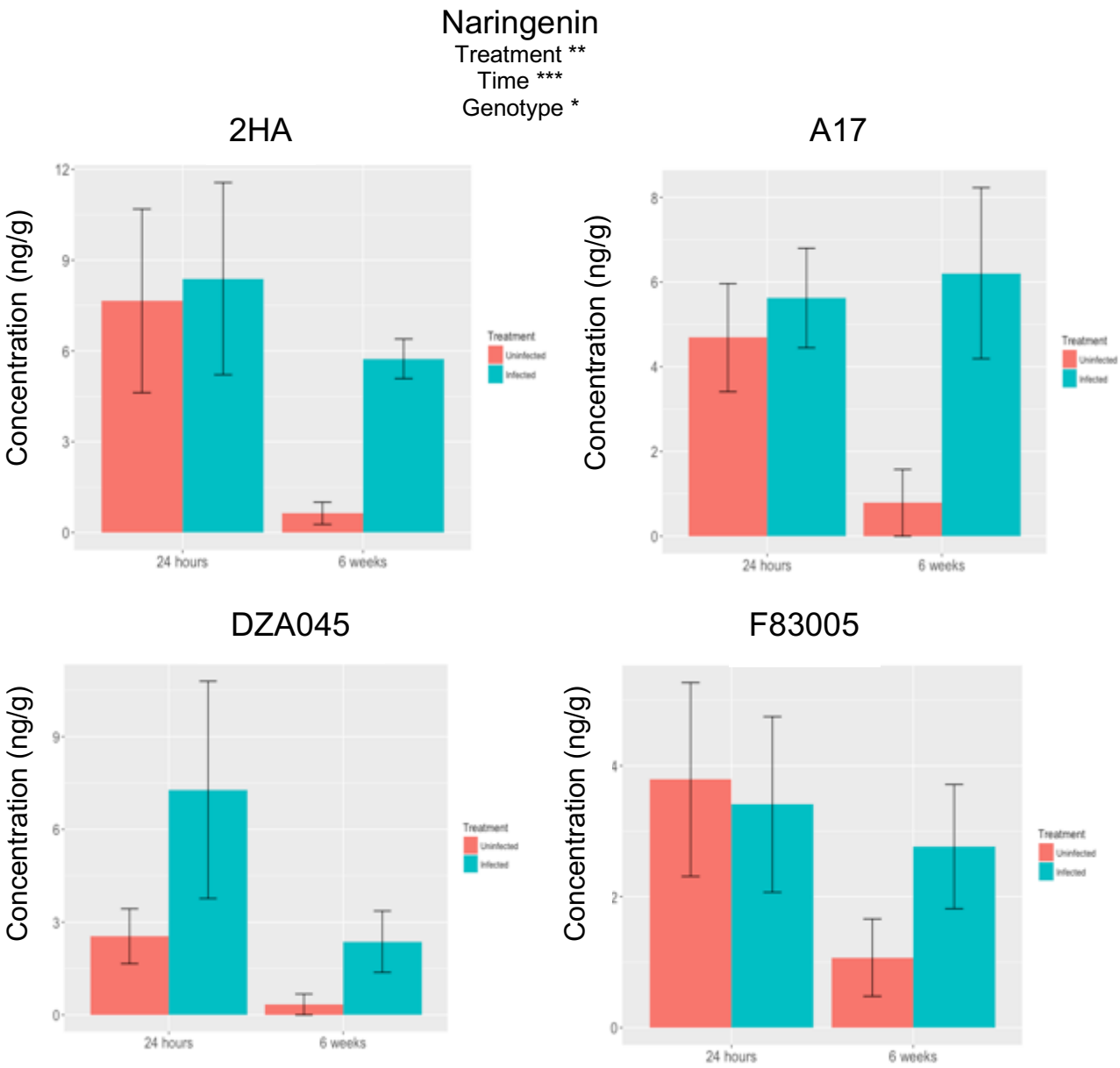

Supplementary Figure 4.3: Naringenin concentrations based on fresh weight in root segments of uninfected and *Meloidogyne javanica* infected roots (galls) of *Medicago truncatula* cultivars, 2HA, A17, DZA045 and F83005. Statistical analysis is based on linear mixed analysis to test the effects of genotype, time, treatment factors and the interactions between these factors. Columns represent means and error bars represent standard errors. (N=4)

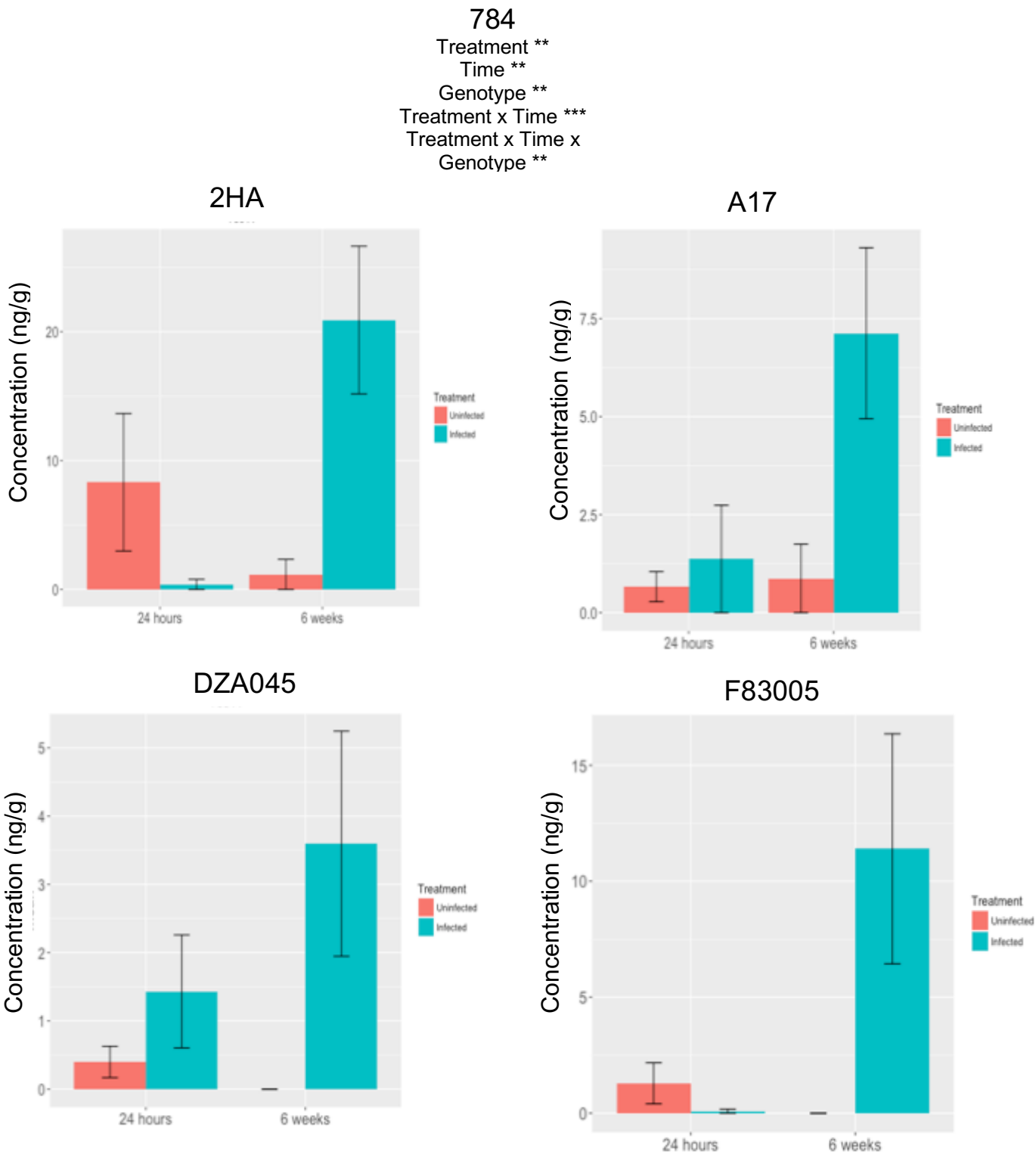

Supplementary Figure 4.4: Compound 784 concentrations based on fresh weight in root segments of uninfected and *Meloidogyne javanica* infected roots (galls) of *Medicago truncatula* cultivars, 2HA, A17, DZA045 and F83005. Statistical analysis is based on linear mixed analysis to test the effects of genotype, time, treatment factors and the interactions between these factors. Columns represent means and error bars represent standard errors. (N=4)

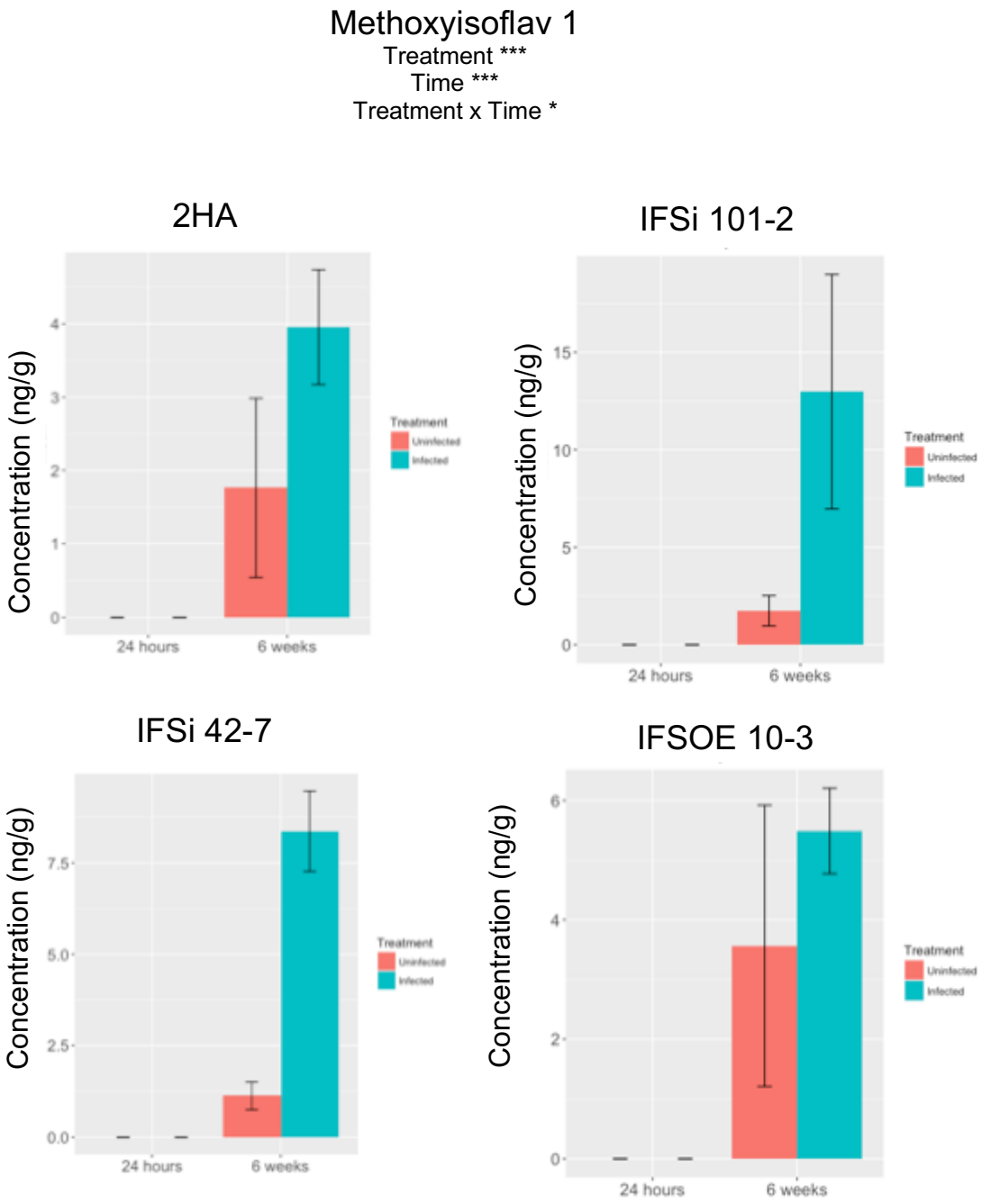

Supplementary Figure 4.5: Methoxyisoflav 1 concentrations based on fresh weight in root segments of uninfected and *Meloidogyne javanica* infected roots (galls) of *Medicago truncatula* wild type cv. 2HA and isoflavone synthase transgenics, silenced lines, IFSi 101-2 and IFSi 42-7 and over-expression line, IFSOE 10-3. Statistical analyses were based on linear mixed analysis to test the effects of genotype, time, treatment factors and the interactions between these factors. Columns represent means. Error bars represent standard errors. (N=3)

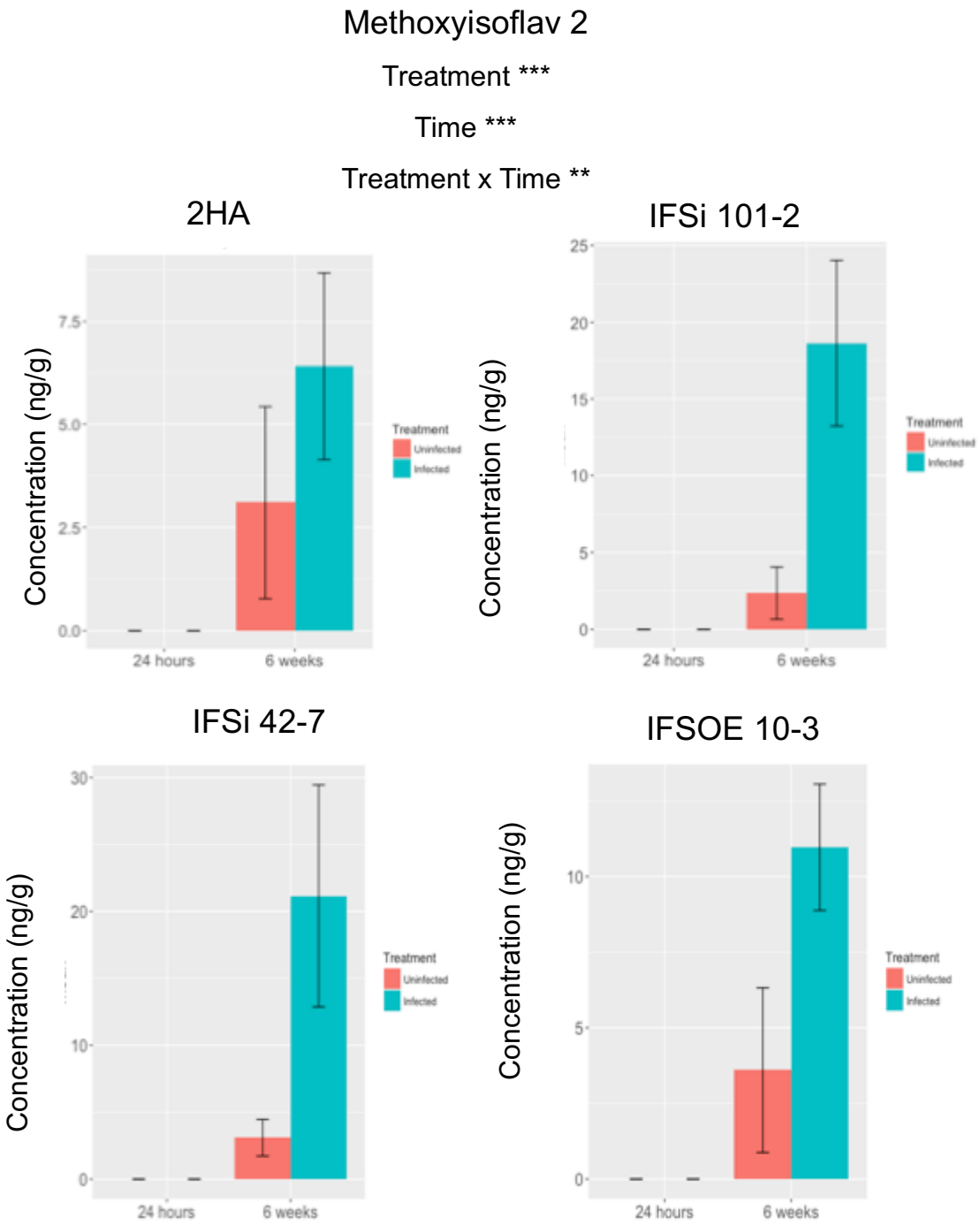

Supplementary Figure 4.6: Methoxyisoflav 2 concentrations based on fresh weight in root segments of uninfected and *Meloidogyne javanica* infected roots (galls) of *Medicago truncatula* wild type cv. 2HA and isoflavone synthase transgenics, silenced lines, IFSi 101-2 and IFSi 42-7 and over-expression line, IFSOE 10-3. Statistical analyses were based on linear mixed analysis to test the effects of genotype, time, treatment factors and the interactions between these factors. Columns represent means. Error bars represent standard errors. (N=3)

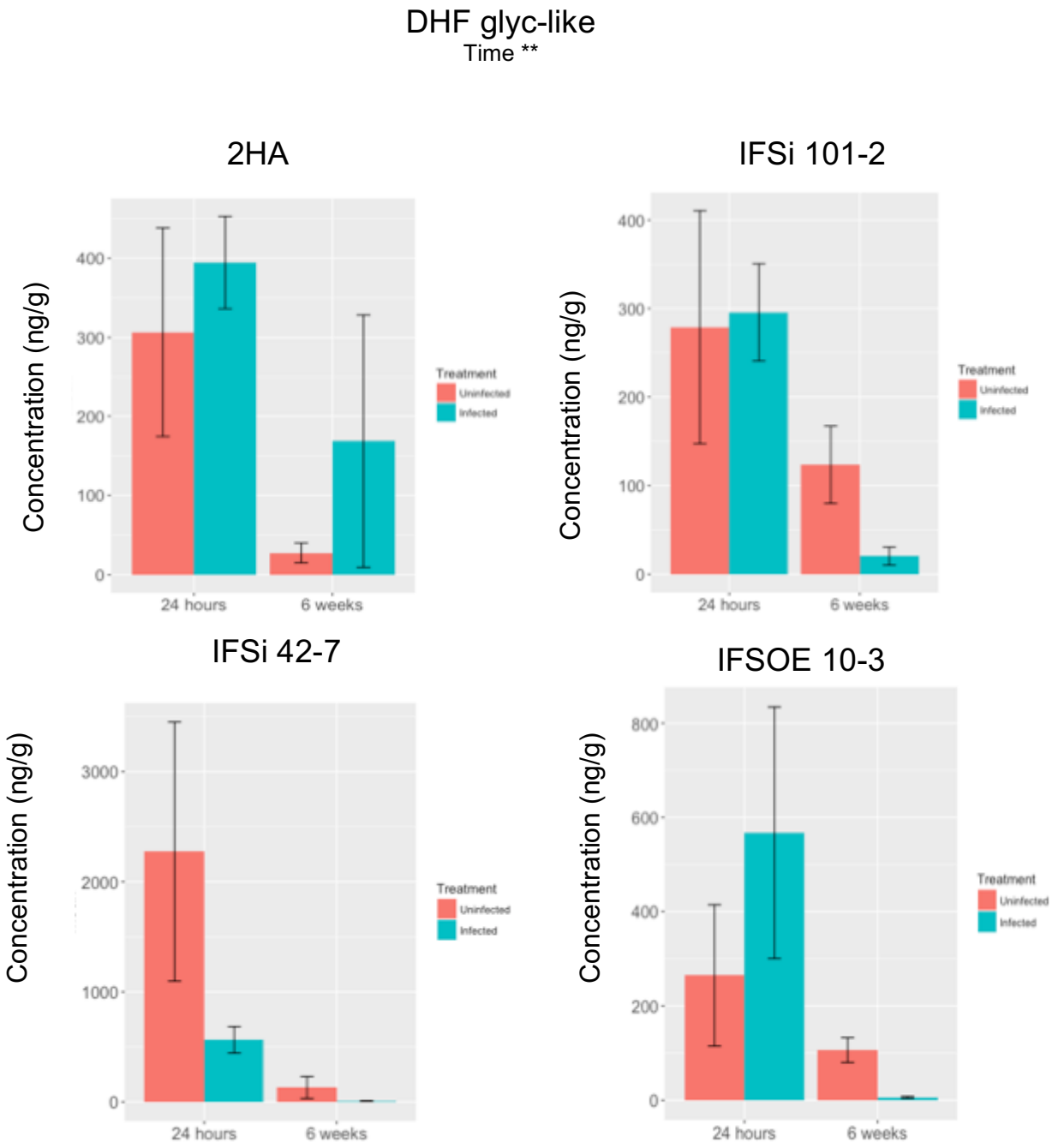

Supplementary Figure 4.7: DHF glyc-like concentrations based on fresh weight in root segments of uninfected and *Meloidogyne javanica* infected roots (galls) of *Medicago truncatula* wild type cv. 2HA and isoflavone synthase transgenics, silenced lines, IFSi 101-2 and IFSi 42-7 and over-expression line, IFSOE 10-3. Statistical analyses were based on linear mixed analysis to test the effects of genotype, time, treatment factors and the interactions between these factors. Columns represent means. Error bars represent standard errors. (N=3)

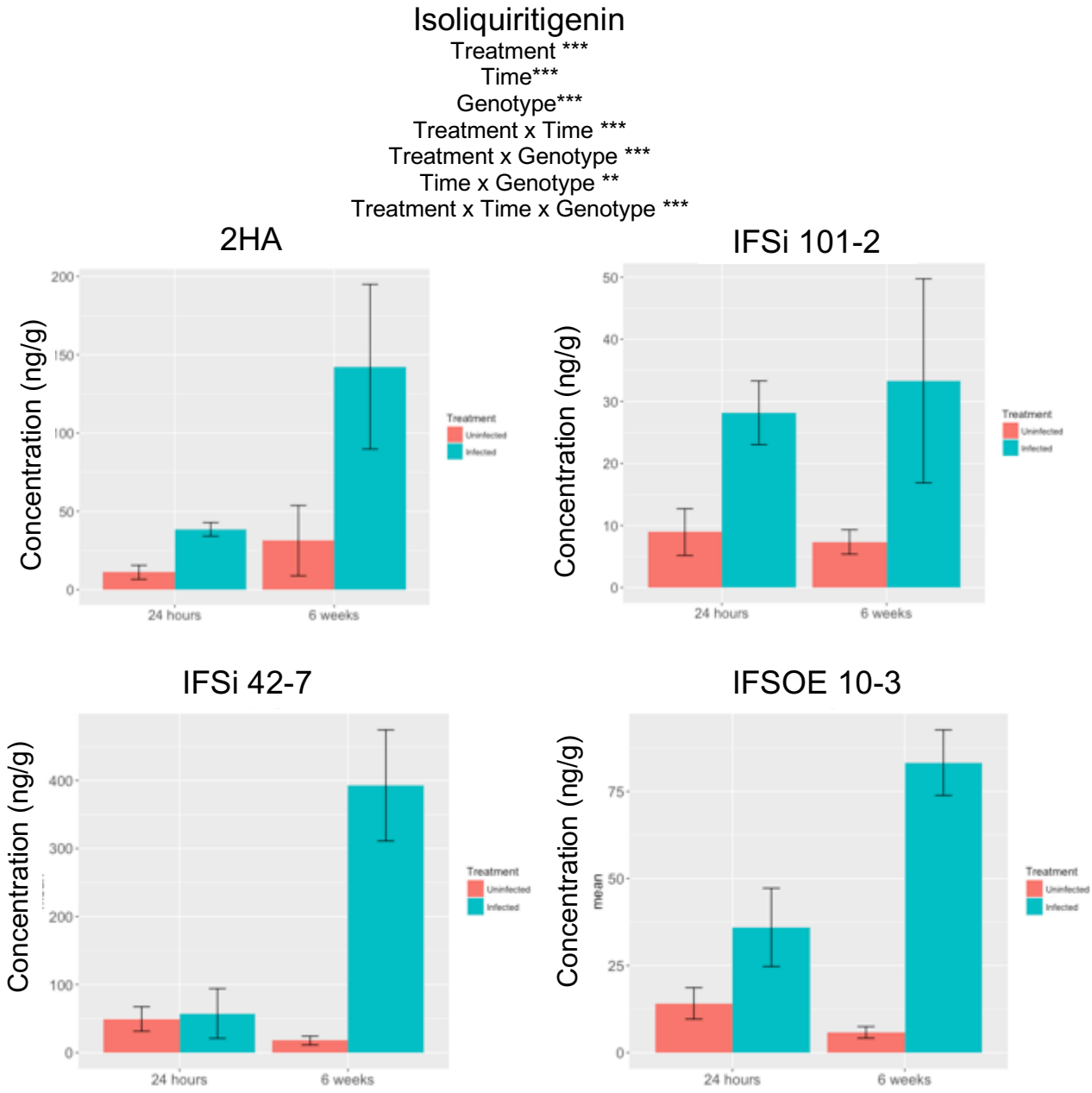

Supplementary Figure 4.8: Isoliquiritigenin concentrations based on fresh weight in root segments of uninfected and *Meloidogyne javanica* infected roots (galls) of *Medicago truncatula* wild type cv. 2HA and isoflavone synthase transgenics, silenced lines, IFSi 101-2 and IFSi 42-7 and over-expression line, IFSOE 10-3. Statistical analyses were based on linear mixed analysis to test the effects of genotype, time, treatment factors and the interactions between these factors. Columns represent means. Error bars represent standard errors. (N=3)

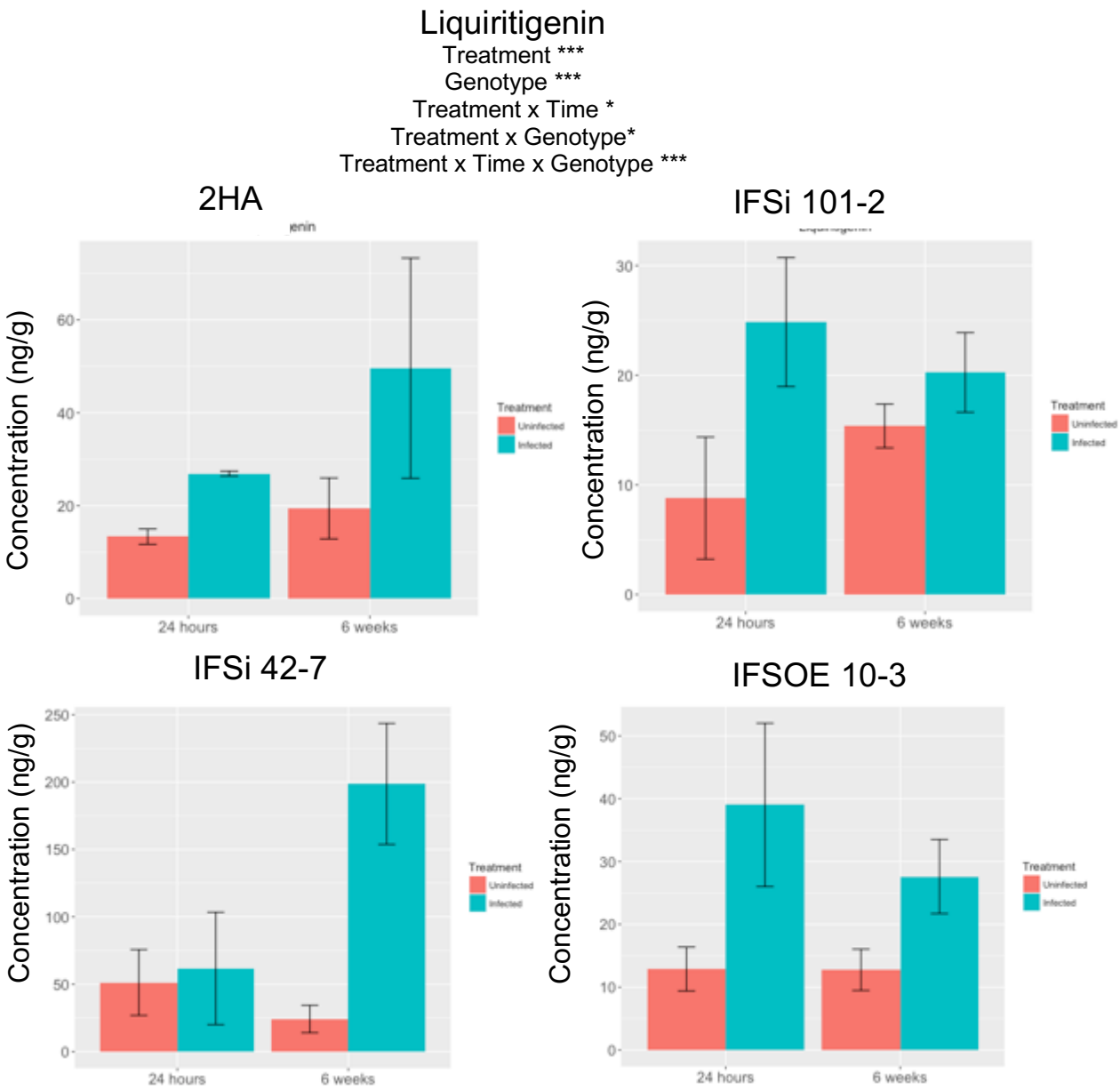

Supplementary Figure 4.9: Liquiritigenin concentrations based on fresh weight in root segments of uninfected and *Meloidogyne javanica* infected roots (galls) of *Medicago truncatula* wild type cv. 2HA and isoflavone synthase transgenics, silenced lines, IFSi 101-2 and IFSi 42-7 and over-expression line, IFSOE 10-3. Statistical analyses were based on linear mixed analysis to test the effects of genotype, time, treatment factors and the interactions between these factors. Columns represent means. Error bars represent standard errors. (N=3)

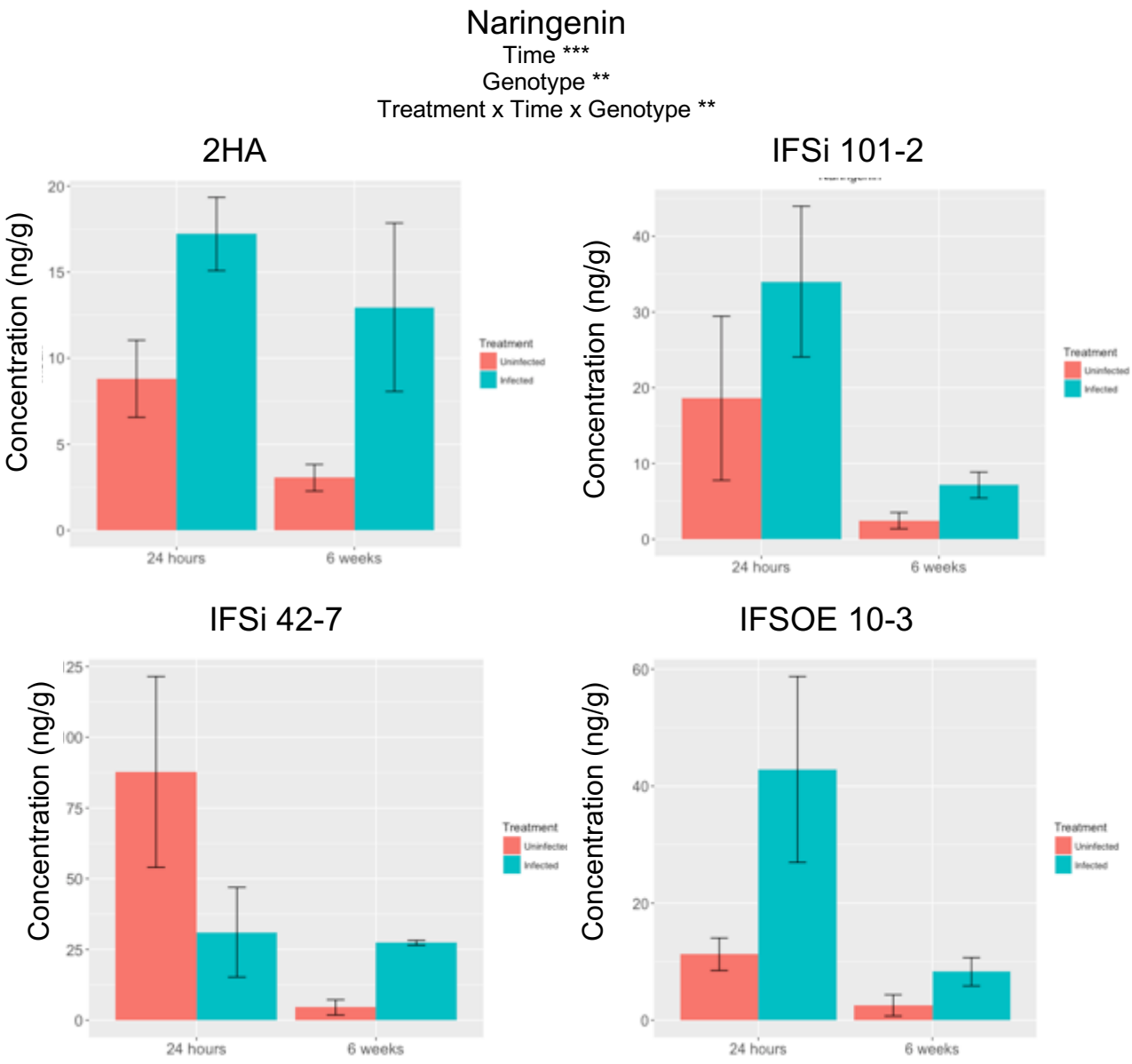

Supplementary Figure 4.10: Naringenin concentrations based on fresh weight in root segments of uninfected and *Meloidogyne javanica* infected roots (galls) of *Medicago truncatula* wild type cv. 2HA and isoflavone synthase transgenics, silenced lines, IFSi 101-2 and IFSi 42-7 and over-expression line, IFSOE 10-3. Statistical analyses were based on linear mixed analysis to test the effects of genotype, time, treatment factors and the interactions between these factors. Columns represent means. Error bars represent standard errors. (N=3)

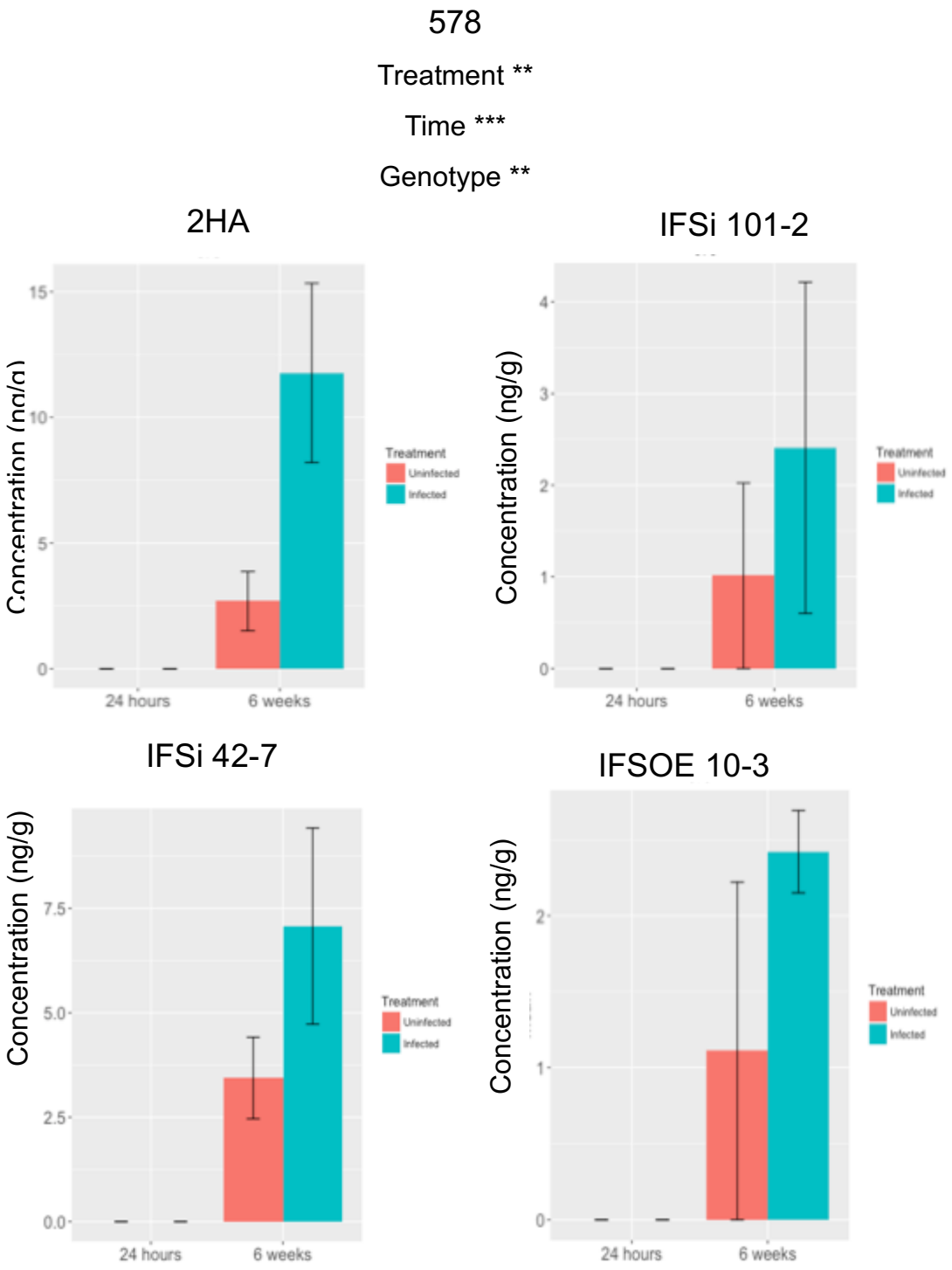

Supplementary Figure 4.11: Compound 578 concentrations based on fresh weight in root segments of uninfected and *Meloidogyne javanica* infected roots (galls) of *Medicago truncatula* wild type cv. 2HA and isoflavone synthase transgenics, silenced lines, IFSi 101-2 and IFSi 42-7 and over-expression line, IFSOE 10-3. Statistical analyses were based on linear mixed analysis to test the effects of genotype, time, treatment factors and the interactions between these factors. Columns represent means. Error bars represent standard errors. (N=3)

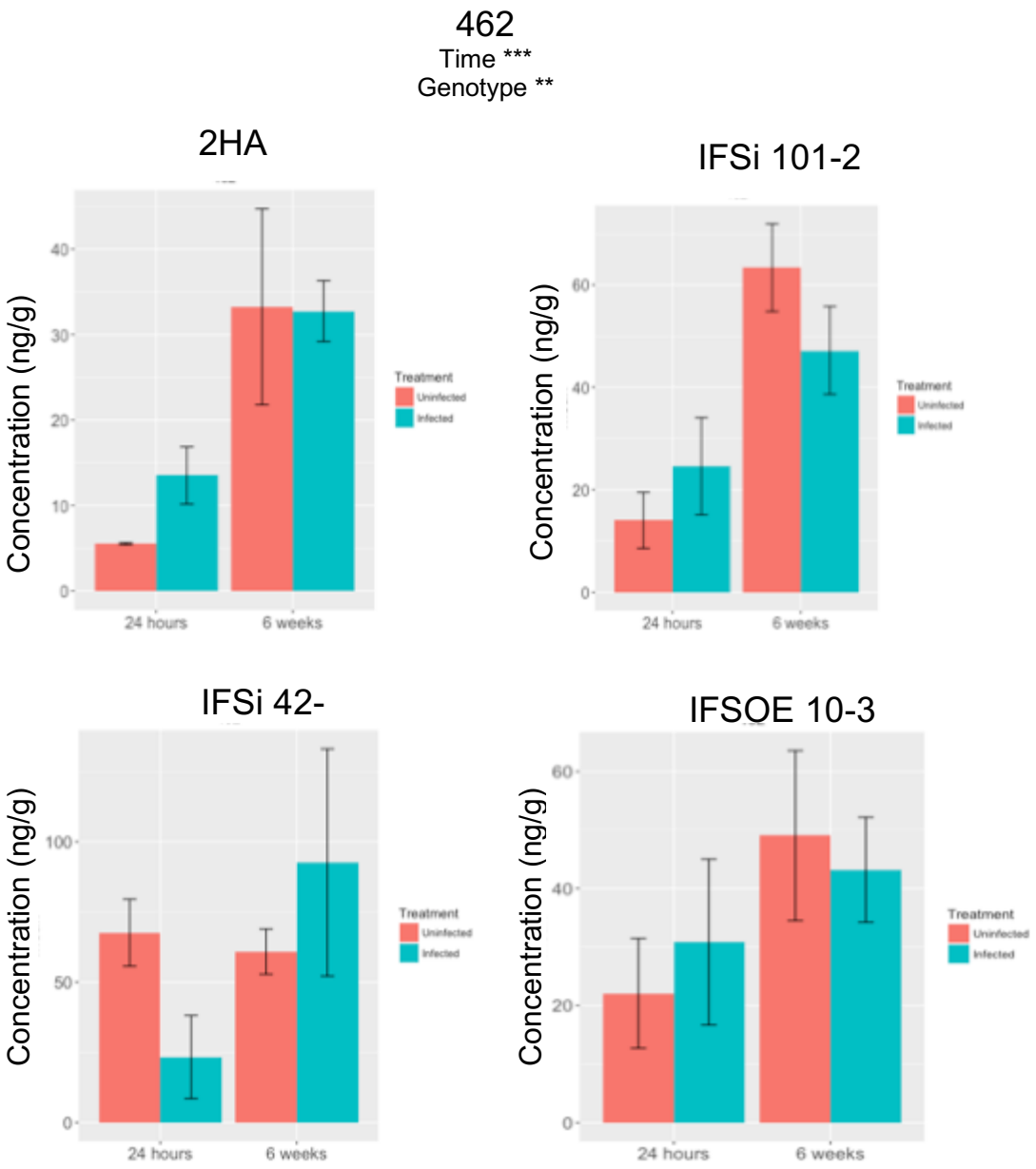

Supplementary Figure 4.12: Compound 462 concentrations based on fresh weight in root segments of uninfected and *Meloidogyne javanica* infected roots (galls) of *Medicago truncatula* wild type cv. 2HA and isoflavone synthase transgenics, silenced lines, IFSi 101-2 and IFSi 42-7 and over-expression line, IFSOE 10-3. Statistical analyses were based on linear mixed analysis to test the effects of genotype, time, treatment factors and the interactions between these factors. Columns represent means. Error bars represent standard errors. (N=3)

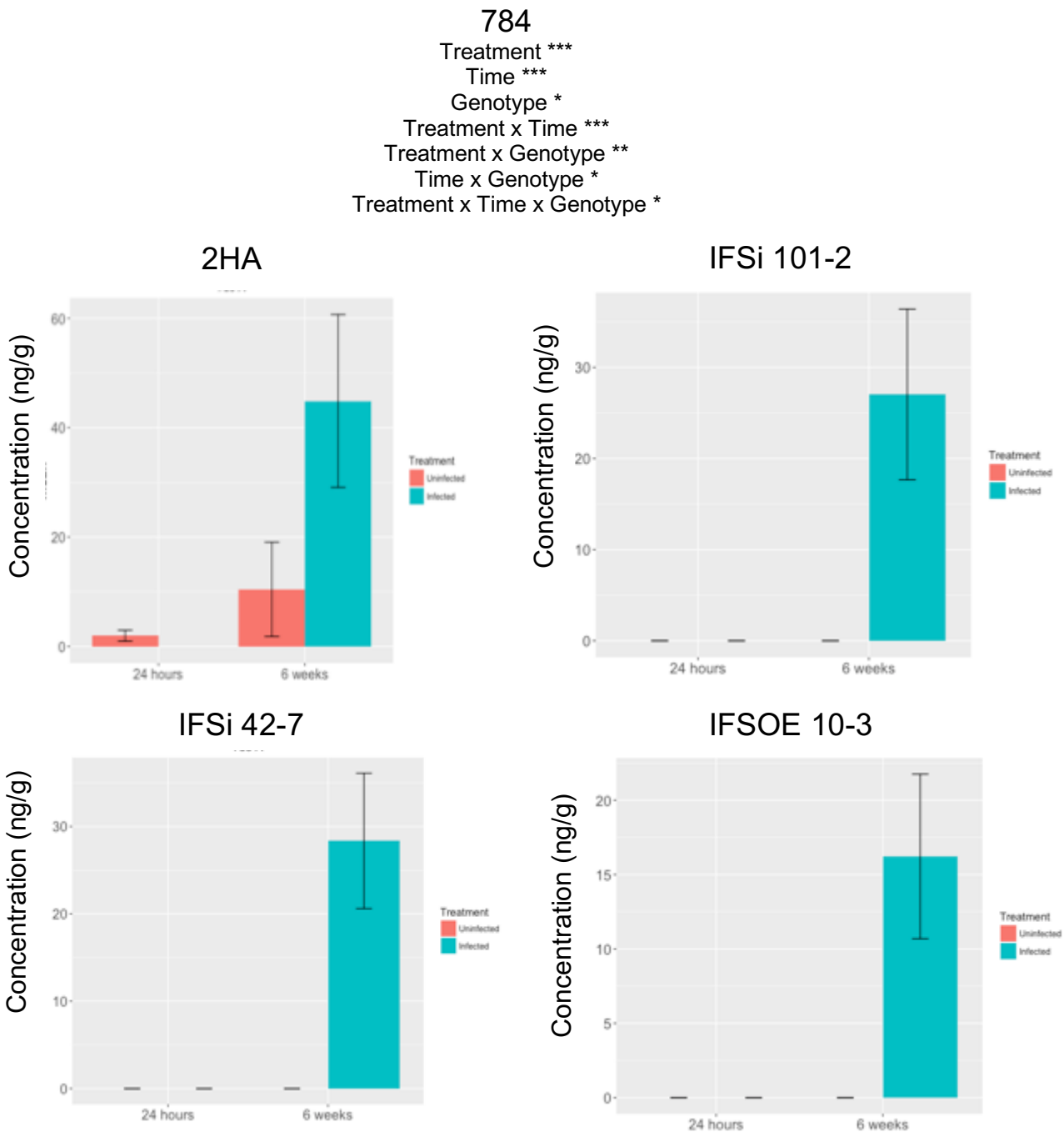

Supplementary Figure 4.13: Compound 784 concentrations based on fresh weight in root segments of uninfected and *Meloidogyne javanica* infected roots (galls) of *Medicago truncatula* wild type cv. 2HA and isoflavone synthase transgenics, silenced lines, IFSi 101-2 and IFSi 42-7 and over-expression line, IFSOE 10-3. Statistical analyses were based on linear mixed analysis to test the effects of genotype, time, treatment factors and the interactions between these factors. Columns represent means. Error bars represent standard errors. (N=3)

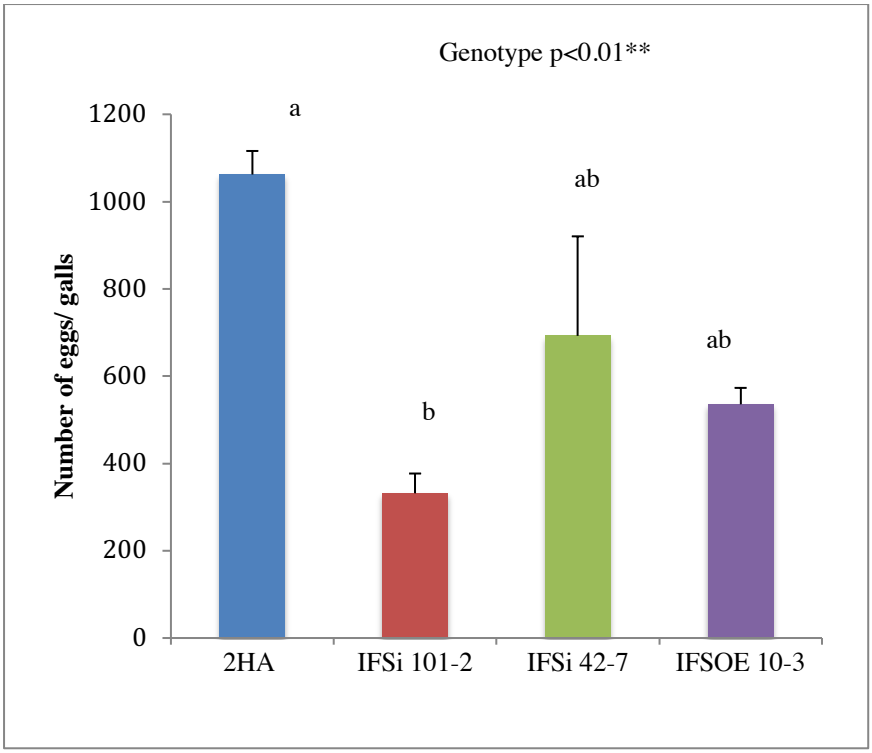

Supplementary Figure 4.14: Number of eggs per galls in *Medicago truncatula* wild-type cv. 2HA and isoflavone synthase transgenics, silenced lines, IFSi 101-2 and IFSi 42-7 and over-expression line, IFSOE 10-3 at 6 weeks post inoculation with *Meloidogyne javanica*. Genotype effect was tested using linear mixed analysis. Letters represent statistically significant differences amongst groups using Tukey pairwise comparison. Columns represent means. Error bars represent standard deviations. (N=3)

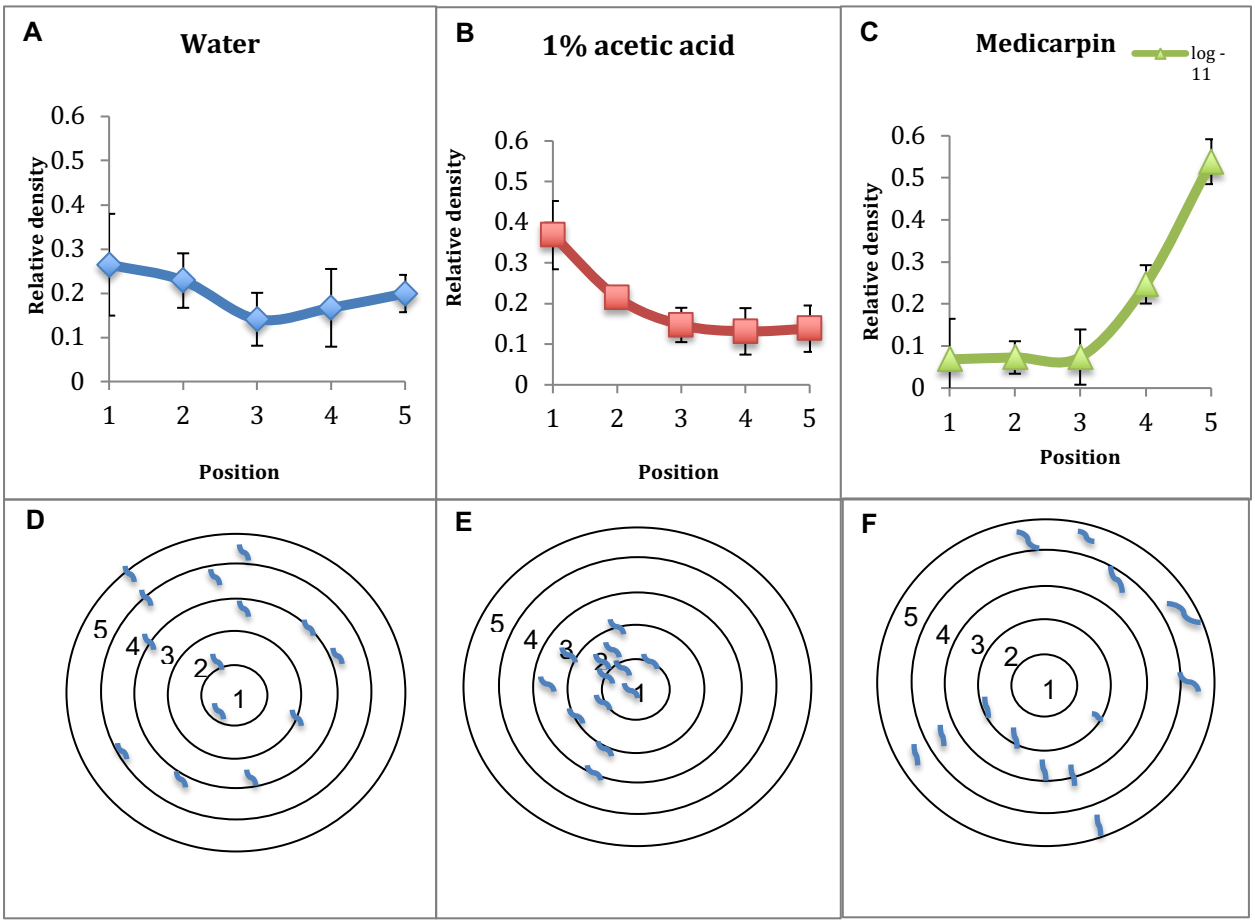

Supplementary Figure 4.15: Examples of *Meloidogyne javanica* J2 chemotaxis responses. (**A**) Chemotaxis response when the compound, water produced nil effect, resulting in even distribution across the plate, (**B**) when the compound, 1% acetic acid was an attractant, which resulted in higher nematode densities in positions 1 and 2 and, (**C**) when the compound, log-11M medicarpin was a repellent, which resulted in higher nematode densities in positions 4 and 5. **(D)** A cartoon illustration showing an even nematode distribution on the plate. **(E)** A cartoon illustration showing a biased nematode distribution towards the tested compound, 1% acetic acid. Higher nematode densities were observed in positions 1 and 2. **(F)** A cartoon illustration showing a biased nematode distribution away from the tested compound, medicarpin. Higher nematode densities were observed in positions 4 and 5. Cartoons in (D-F) show approximate nematode numbers. Scatterplots represent average values. Error bars represent standard deviations (N=3).

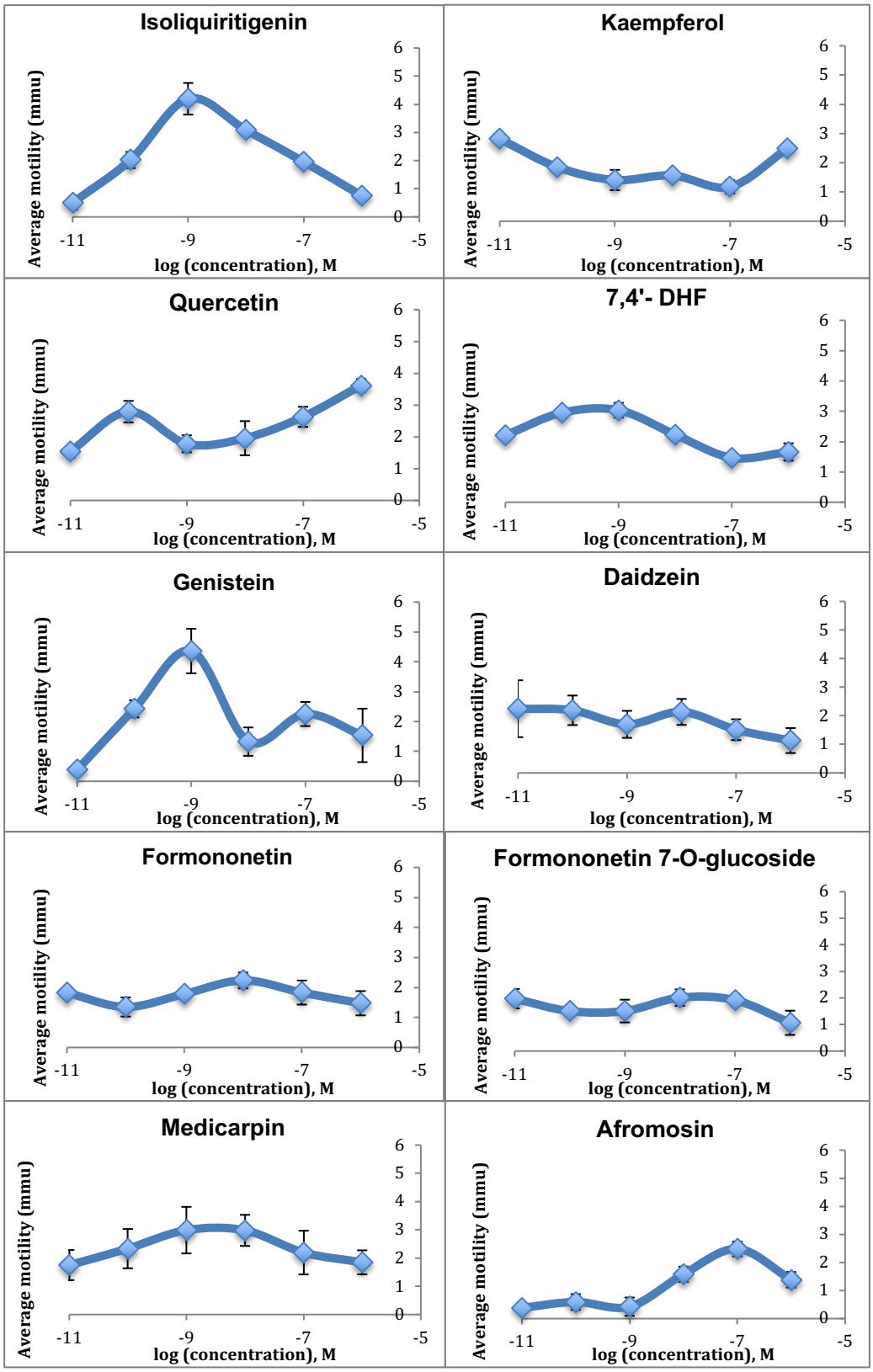

Supplementary figure 4.16: Average motility of *Meloidogyne javanica* J2s based on mean motility movement against ten purified flavonoids. mmu= mean motility unit (arbitrary value). Each data points represent mean values. Error bars represent standard deviations. (N=3) The average motility unit for solvent control (0.004% methanol) is 2.744.

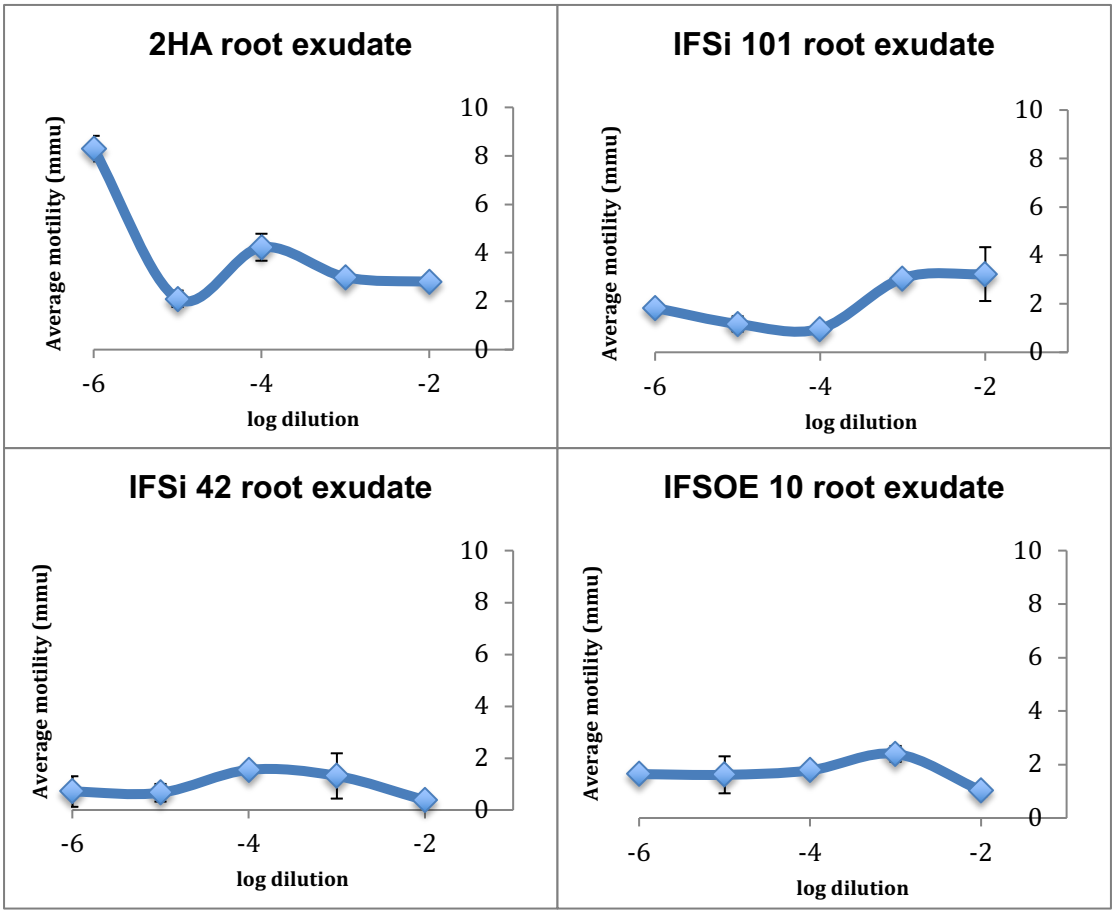

Supplementary figure 4.17: Average motility of *Meloidogyne javanica* J2s based mean motility movement against root exudates of *Medicago truncatula* wild type cv. 2HA and transgenics IFSi 101, IFSi 42 and IFSOE 10. mmu= mean motility unit (arbitrary value). Each data points represent mean values. Error bars represent standard deviations. (N=3). The average motility unit for solvent control (8% methanol) is 3.611.

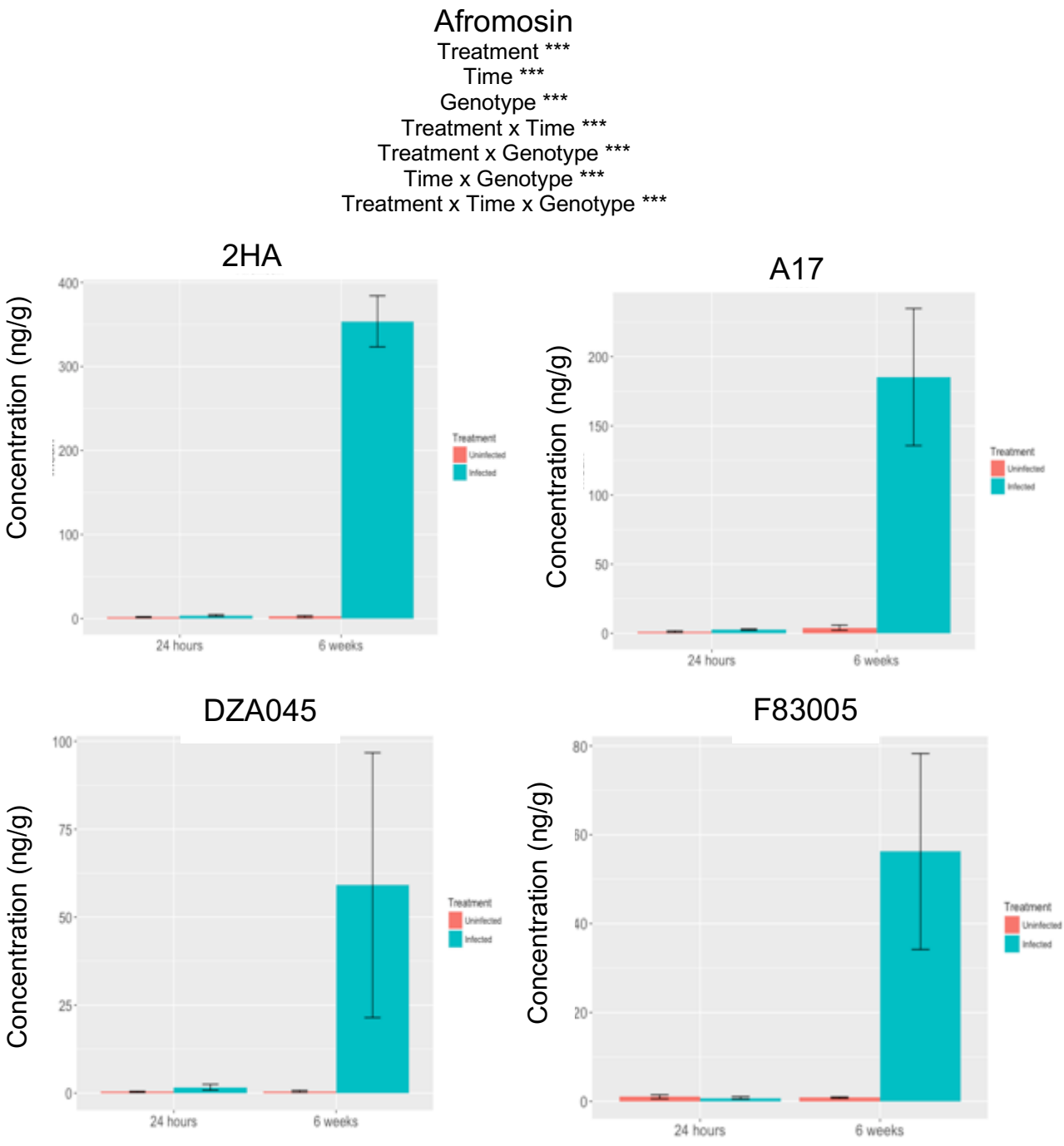

Supplementary Figure 4.18: Afromosin concentrations based on fresh weight in root segments of uninfected and *Meloidogyne javanica* infected roots (galls) of *Medicago truncatula* cultivars, 2HA, A17, DZA045 and F83005. Statistical analysis is based on linear mixed analysis to test the effects of genotype, time, treatment factors and the interactions between these factors. Columns represent means and error bars represent standard errors. (N=4)

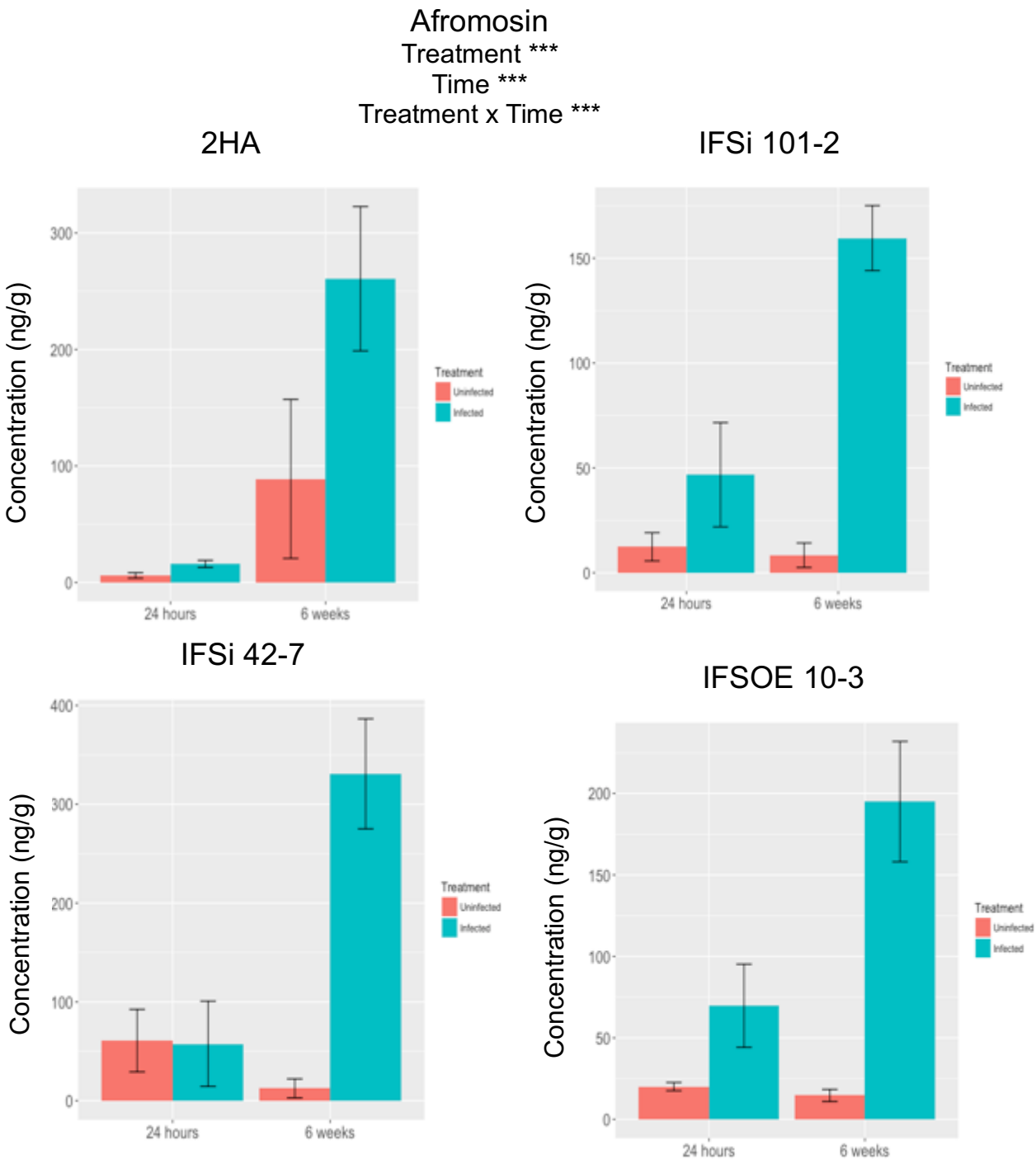

Supplementary Figure 4.19: Afromosin concentrations based on fresh weight in root segments of uninfected and *Meloidogyne javanica* infected roots (galls) of *Medicago truncatula* wild type cv. 2HA and isoflavone synthase transgenics, silenced lines, IFSi 101-2 and IFSi 42-7 and over-expression line, IFSOE 10-3. Statistical analyses were based on linear mixed analysis to test the effects of genotype, time, treatment factors and the interactions between these factors. Columns represent means. Error bars represent standard errors. (N=3)

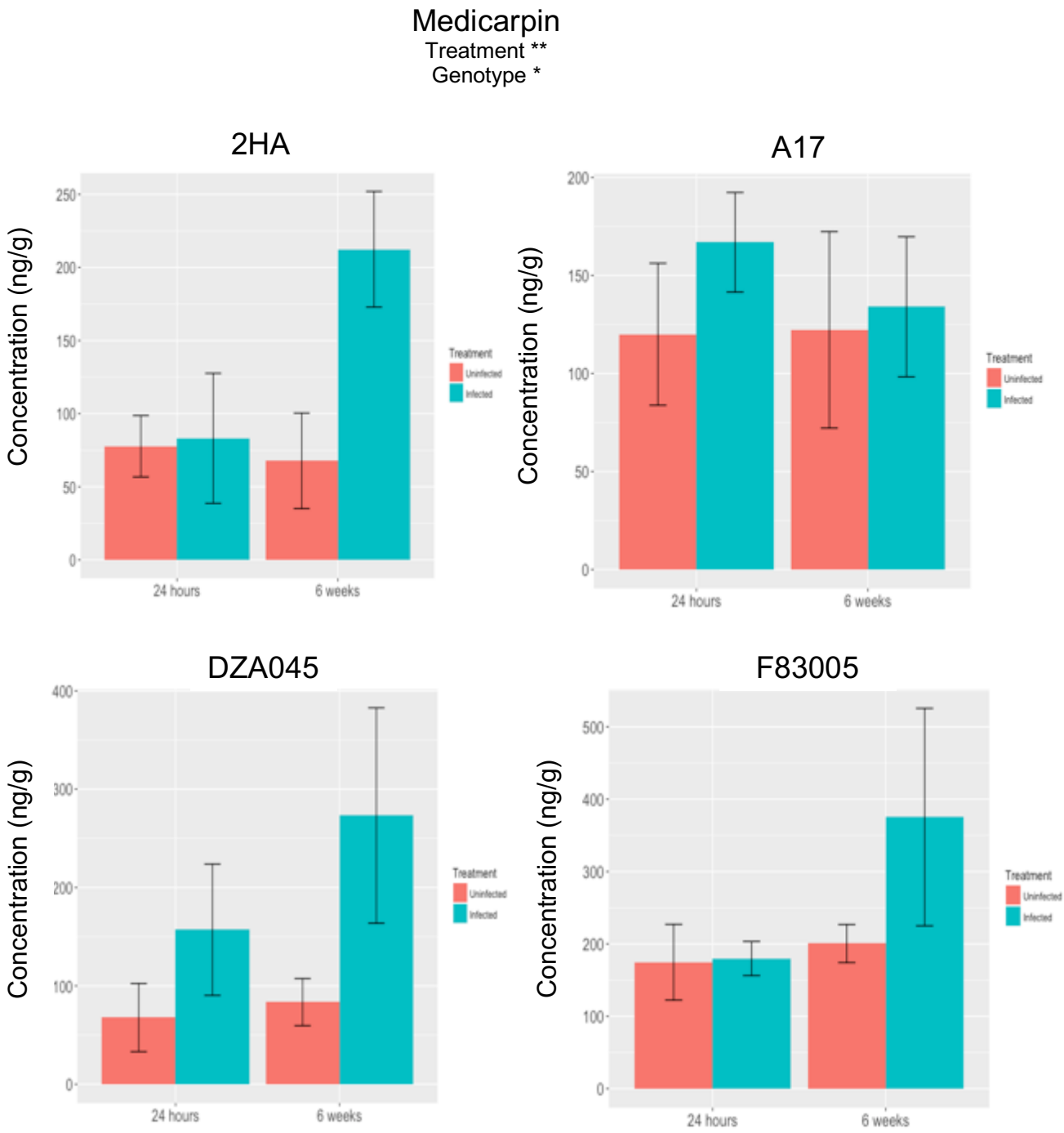

Supplementary Figure 4.20: Medicarpin concentrations based on fresh weight in root segments of uninfected and *Meloidogyne javanica* infected roots (galls) of *Medicago truncatula* cultivars, 2HA, A17, DZA045 and F83005. Statistical analysis is based on linear mixed analysis to test the effects of genotype, time, treatment factors and the interactions between these factors. Columns represent means and error bars represent standard errors. (N=4)

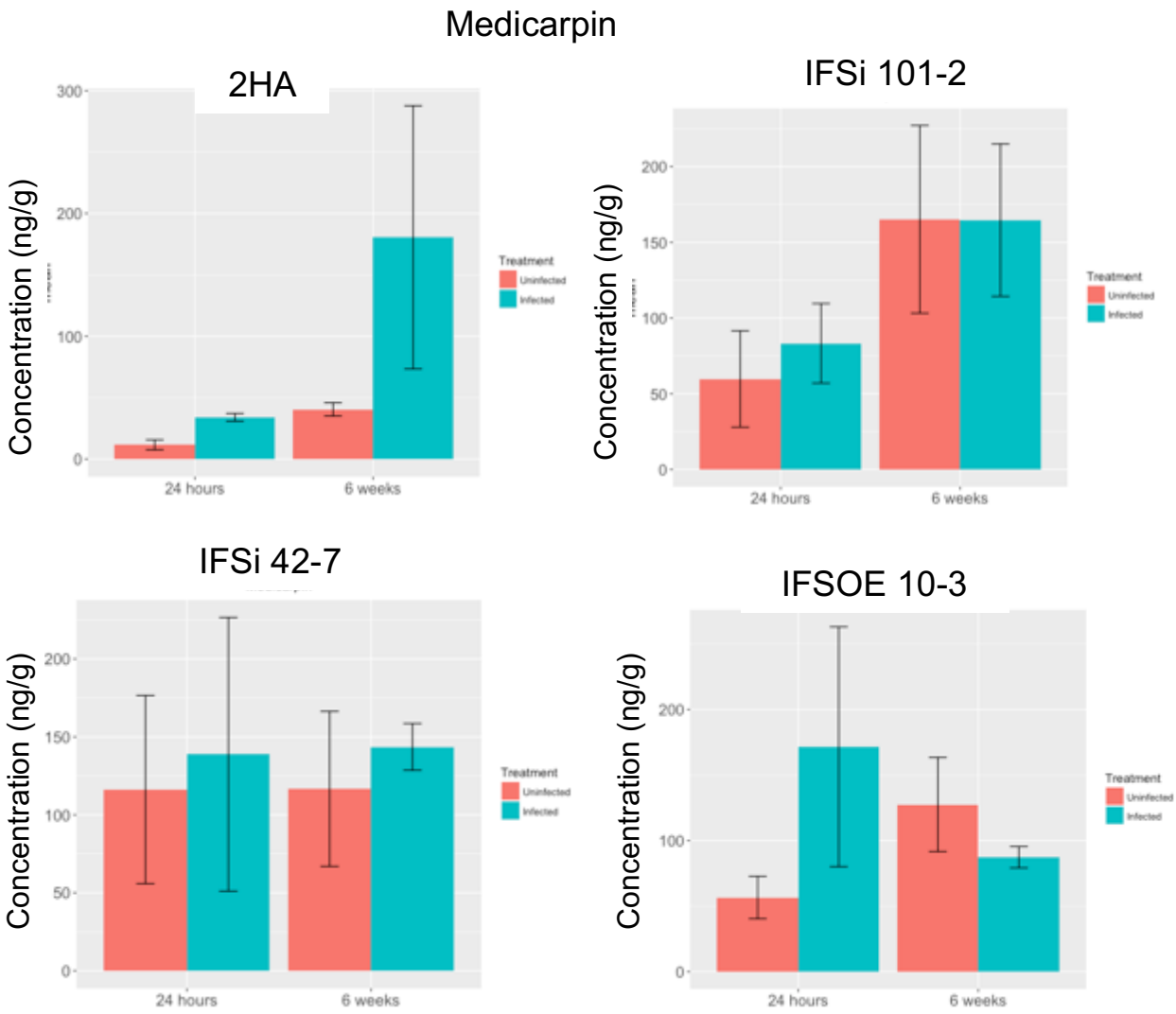

Supplementary Figure 4.21: Medicarpin concentrations based on fresh weight in root segments of uninfected and *Meloidogyne javanica* infected roots (galls) of *Medicago truncatula* wild type cv. 2HA and isoflavone synthase transgenics, silenced lines, IFSi 101-2 and IFSi 42-7 and over-expression line, IFSOE 10-3. Statistical analyses were based on linear mixed analysis to test the effects of genotype, time, treatment factors and the interactions between these factors. Columns represent means. Error bars represent standard errors. (N=3)

Flavonoid group	Constituent flavonoid	Linear mixed model on factor						
		Treatment	Time	Genotype	Treatment x Time	Treatment x Genotype	Time x Genotype	Time x Genotype x Treatment
Chalcone	Isoliquiritigenin	***	***	*	***			
Flavanones	Liquiritigenin	***	**	**	**			
	Naringenin	**	***	*				
	Nar-7-gluc	*		*	*			
Flavonols	K-gluc		***	***			***	
	K-gluc-rham	***	**		***			
	K-glyc-like		***					
	K-3-rutinoside						***	*
	Rutin	***	***		***			
Flavones	Luteolin		*	**				
	7,4'-DHF	*	*	**	**			
	DHF glyc-like		***	***			***	
	Glycitein		**					
	Methoxyisoflav 1	*	***		*			
	Methoxyisoflav 2	**	**		**			
Isoflavonoids	Biochanin A		*					
	Daidzein	*	***	***			***	
	Daid-7-gluc		**					

	Formononetin		***			**		**
	Form-7-gluc	**	***		*			
	Genistein		*	*			*	
	Gen-7-gluc			**	*		*	
	Afromosin	***	***	***	***	***	***	***
Isoflavonoids: pterocarpans	Medicarpin	**		*				
Coumestan	Coumesterol		***			**		**
Unknowns	448		***					
	462		***					
	464		***					
	578		***					
	594		***	*				
	610		***				*	
	740		***					
	784	**	**	**	***			**

Supplementary Table 4.1: Flavonoids with statistically significant changes in concentrations (indicated by asterisk, $p<0.05$) based on linear mixed analysis derived from the root segments of uninfected and *Meloidogyne javaniva* infected *Medicago truncatula* cultivars/accessions, 2HA, A17, DZA045 and F83005 at 24 hours and 6 weeks post inoculation.

Flavonoid group	Constituent flavonoid	Gall size	Egg no/ plant
Chalcone	Isoliquiritigenin	0.073	0.479
Flavanones	Liquiritigenin	0.0277*	0.634
	Naringenin	0.03419*	0.359
	Nar-7-gluc	0.0504	0.629
Flavonols	K-gluc	0.472	0.411
	K-3-rutinoside	0.8359	0.8025
	K-glyc-like	0.8949	0.7012
	K-gluc-rham	0.4333	0.5308
	Rutin	0.075	0.501
Flavones	Luteolin	0.953	0.328
	7,4'-DHF	0.244	0.701
	DHF glyc-like	0.4738	0.5549
	Glycitein	0.216	0.295
	Methoxyisoflav 1	0.3265	0.5828
	Methoxyisoflav 2	0.9171	0.7457
Isoflavonoids	Biochanin A	0.479	0.874
	Daidzein	0.0888	0.454
	Daid-7-gluc	0.099	0.34
	Formononetin	0.374	0.663
	Form-7-gluc	0.272	0.556
	Genistein	0.401	0.433
	Gen-7-gluc	0.1513	0.32
	Afromosin	0.0679	0.513
Isoflavonoids: Pterocarpan	Medicarpin	0.719	0.664
Coumestan	Coumesterol	0.331	0.805
Unknowns	448	0.494	0.296
	462	0.5573	0.4454
	464	0.3572	0.488
	578	0.6471	0.631
	594	0.4066	0.696
	610	0.786	0.742
	740	0.385	0.676
	784	0.0161*	0.739

Supplementary Table 4.2: P-values of simple linear regressions of the relationship between flavonoid responses in infected plants and the nematode infection phenotypes observed/measured in four *Medicago truncatula* accessions/cultivars, 2HA, A17, DZA045 and F83005 at 6 weeks post inoculation with *Meloidogyne javanica*. Asterisks indicate statistically significant results ($p<0.05$). Flavonoid responses refer to flavonoid concentrations (log10) measured using LC-ESI-Q-TOF-MS/MS. Gall number was excluded from linear regression analysis, as there was no distinct difference in gall number across accessions/cultivars.

Flavonoid group	Constituent flavonoid	Linear mixed model on factor						
		Treatment	Time	Genotype	Treatment x Time	Treatment x Genotype	Time x Genotype	Time x Genotype x Treatment
Chalcone	Isoliquiritigenin	***	***	***	***	***	**	***
Flavanones	Liquiritigenin	***		***	*	*		**
	Naringenin	**	***	*				
	Nar-7-gluc		***	***		*	*	
Flavonols	K-gluc		***	*			*	
	K-3-rutinoside		***	*		*	**	
	K-glyc-like							
	K-gluc-rham	*			*	*	**	*
	Rutin	**	***	*	**		*	
Flavones	Apigenin		**	*		*	*	*
	Api-neo		***	*			*	
	Luteolin	**	**	*				
	7,4'-DHF							
	DHF glyc-like		**				*	
	Glycitein		**					
	Methoxyisoflav 1	**	***		**			
	Methoxyisoflav 2	***	***		***			
Isoflavonoids	Biochanin A							
	Daidzein		***	***			***	
	Daid-7-gluc				*			

	Daid-8-gluc		**					
	Formononetin		***					
	Form-7-gluc	*	***					
	Genistein							
	Gen-7-gluc		***	**		*	**	*
	Afromosin	***	***		***			
Isoflavonoids: pterocarpan	Medicarpin							
Coumestan	Coumesterol		***					
Unknowns	448			*				
	462		***	**				
	464		**					
	578	**	***	**	**		**	
	594		***					
	610		*				*	
	740		**					
	784	***	***	*	***	**	*	*

Supplementary Table 4.3: Flavonoids with statistically significant changes in concentrations (indicated by asterisk, $p<0.05$) based on linear mixed model analysis derived from the root segments of uninfected and *Meloidogyne javaniva* infected *Medicago truncatula* wild-type cv. 2HA and isoflavone synthase transgenics, IFSi 101-2, IFSi 42-7 and IFSOE 10-3 at 24 hours and 6 weeks post inoculation.

Flavonoid group	Constituent flavonoid	Plant weight	Lateral root number	Gall no/plant	Gall size	Egg no/plant
Chalcone	Isoliquiritigenin	0.4283	0.0701	0.00023**	0.309	0.0182*
Flavanones	Liquiritigenin	0.699	0.0887	0.0043**	0.319	0.0467*
	Naringenin	0.433	0.1181	0.0254*	0.272	0.0781
	Nar-7-gluc	0.58	0.1346	0.118	0.287	0.0933
Flavonols	K-gluc	0.759	0.333	0.9655	0.981	0.609
	K-3-rutinoside	0.435	0.8	0.782	0.528	0.739
	K-glyc-like	0.172	0.139	0.8	0.296	0.586
	K-gluc-rham	0.709	0.742	0.322	0.704	0.16
	Rutin	0.913	0.185	0.792	0.471	0.448
Flavones	Apigenin	0.5162	0.236	0.921	0.614	0.48
	Api-neo	0.227	0.216	0.996	0.367	0.476
	Luteolin	0.698	0.209	0.1688	0.741	0.534
	7,4'-DHF	0.223	0.38	0.773	0.425	0.4
	DHF glyc-like	0.2236	0.025*	0.5329	0.325	0.905
	Glycetein	0.375	0.164	0.938	0.319	0.459
	Methoxyisoflav 1	0.026*	0.6712	0.649	0.0178*	0.221
	Methoxyisoflav 2	0.032*	0.213	0.731	0.0181*	0.166
Isoflavonoids	Daidzein	0.232	0.132	0.895	0.388	0.567
	Daid-7-gluc	0.342	0.422	0.677	0.527	0.329
	Daid-8-gluc	0.164	0.119	0.837	0.279	0.524
	Formononetin	0.268	0.145	0.615	0.489	0.413
	Form-7-gluc	0.99	0.149	0.3805	0.84	0.8004
	Genistein	0.214	0.122	0.886	0.354	0.587
	Biochanin A	0.873	0.774	0.436	0.545	0.322
	Medicarpin	0.767	0.266	0.8533	0.903	0.9888
Isoflavonoid: Pterocarpan	Afromosin	0.590	0.512	0.107	0.438	0.165
Coumestan	Coumesterol	0.313	0.167	0.515	0.499	0.368

Unknowns	448	0.383	0.225	0.7483	0.63	0.456
	462	0.5994	0.108	0.0252*	0.139	0.262
	464	0.8	0.2327	0.8544	0.973	0.638
	578	0.0616	0.8175	0.0231*	0.093	0.011*
	594	0.727	0.532	0.3026	0.701	0.103
	610	0.55	0.429	0.803	0.564	0.794
	740	0.976	0.58	0.641	0.888	0.606
	784	0.0556	0.369	0.0239*	0.128	0.366

Supplementary Table 4.4: P-values of simple linear regressions of the relationship between flavonoid responses in infected plants and the nematode infection phenotypes observed/measured in *Medicago truncatula* wild-type cv. 2HA and isoflavone synthase transgenics, silenced lines, IFSi 101-2 and IFSi 42-7 and over-expression line, IFSOE 10-3 at 6 weeks post inoculation with *Meloidogyne javanica*. Asterisks indicate statistically significant results ($p<0.05$). Flavonoid responses refer to flavonoid concentrations (log10) measured using LC-ESI-Q-TOF-MS.

Pairwise comparison		Lower 10th quantile	Upper 90th quantile
7,4'-DHF	Afromosin	0.073	0***
	Daidzein	0.54	0.0095
	Formononetin	0.763	0.045*
	Formononetin-7-*O*-glucoside	0.214	0.211
	Genistein	0.011*	0.019*
	Isoliquiritigenin	0***	0.136
	Kaempferol	0***	0.666
	Medicarpin	0.071	0.656
	Quercetin	0.055	0.754
Afromosin	7,4'-DHF	0.073	0***
	Daidzein	0.383	0***
	Formononetin	0.579	0.001**
	Formononetin-7-*O*-glucoside	0.077	0.005**
	Genistein	0.005**	0.195
	Isoliquiritigenin	0***	0.021*
	Kaempferol	0***	0.001**
	Medicarpin	0.005**	0.001**
	Quercetin	0.004**	0***
Daidzein	7,4'-DHF	0.54	0.0095
	Afromosin	0.383	0***
	Formononetin	0.977	0.998
	Formononetin-7-*O*-glucoside	0.155	0.875
	Genistein	0.008**	0.092
	Isoliquiritigenin	0***	0.671
	Kaempferol	0***	0.328
	Medicarpin	0.042*	0.536
	Quercetin	0.036*	0.147
Formononetin	7,4'-DHF	0.763	0.045*
	Afromosin	0.579	0.001**
	Daidzein	0.977	0.998
	Formononetin-7-*O*-glucoside	0.194	0.781
	Genistein	0.014*	0.08
	Isoliquiritigenin	0***	0.598
	Kaempferol	0.001**	0.293
	Medicarpin	0.188	0.406
	Quercetin	0.104	0.07
Formononetin-7-*O*-glucoside	7,4'-DHF	0.214	0.211
	Afromosin	0.077	0.005**
	Daidzein	0.155	0.875

	Formononetin	0.194	0.781
	Genistein	0.343	0.13
	Isoliquiritigenin	0.036*	0.811
	Kaempferol	0.263	0.275
	Medicarpin	0.479	0.444
	Quercetin	0.868	0.253
Genistein	7,4'-DHF	0.011*	0.019*
	Afromosin	0.005**	0.195
	Daidzein	0.008**	0.092
	Formononetin	0.014*	0.08
	Formononetin-7-*O*-glucoside	0.343	0.13
	Isoliquiritigenin	0.455	0.266
	Kaempferol	0.93	0.033*
	Medicarpin	0.064	0.037*
	Quercetin	0.226	0.02*
Isoliquiritigenin	7,4'-DHF	0***	0.136
	Afromosin	0***	0.021*
	Daidzein	0***	0.671
	Formononetin	0***	0.598
	Formononetin-7-*O*-glucoside	0.036*	0.811
	Genistein	0.455	0.266
	Kaempferol	0.276	0.255
	Medicarpin	0***	0.318
	Quercetin	0.021*	0.134
Kaempferol	7,4'-DHF	0***	0.666
	Afromosin	0***	0.001**
	Daidzein	0***	0.328
	Formononetin	0.001**	0.293
	Formononetin-7-*O*-glucoside	0.263	0.275
	Genistein	0.93	0.033*
	Isoliquiritigenin	0.276	0.255
	Medicarpin	0.001**	0.573
	Quercetin	0.106	0.603
Medicarpin	7,4'-DHF	0.071	0.656
	Afromosin	0.005**	0.001**
	Daidzein	0.042*	0.536
	Formononetin	0.188	0.406
	Formononetin-7-*O*-glucoside	0.479	0.444
	Genistein	0.064	0.037*
	Isoliquiritigenin	0***	0.318
	Kaempferol	0.001**	0.573
	Quercetin	0.472	0.746

Supplementary table 4.5: Pairwise comparisons of lower 10th and upper 90th quantiles for the multivariate distributions of percentage nematode motility inhibitions for ten purified flavonoids.

Chapter 5: Dissecting auxin homeostasis in galls and the role of isoflavonoids in auxin transport regulation

5.1 Abstract

Auxin transport, response and concentrations in galls of *M. truncatula* 2HA at early, 24 hours and 4 days and mature stages, 4 weeks were studied. At 24 hours, IAA concentrations were significantly reduced in infected roots. However, the drop in IAA concentrations was neither reflected in the auxin responsive reporter system, *GH3::GUSa*, nor was there significant changes in auxin transport. A strong and local *GH3::GUSa* expression occurred in young galls at 4 days and strong auxin transport inhibition occurred at segments basal to young galls. Despite this, auxin concentrations in young galls were relatively unchanged when compared with control roots. In 4 week-old mature galls, auxin response had susbsided, which was followed by a significant decrease in IAA-Val concentration, whilst auxin transport suppression in tissues basal to the mature galls was still present. Nematode infection in silenced isoflavone synthase (IFS) transgenics resulted in earlier auxin transport suppression at 4 days, which may have contributed to the formation of terminal galls. In contrast, infected over-expression IFS transgenics showed delayed auxin transport suppression, thereby suggesting that isoflavonoids were unlikely key auxin transport inhibitors during gall formation.

5.2 Introduction

The pre-parasitic juveniles of root-knot nematodes (*Meloidogyne* spp.) infect the root and establish a long-term feeding site in the root throughout its lifecycle. The feeding site consists of giant cells and hyperplastic neighbouring cells, thus resulting in the formation of a gall. This is achieved by the injection of effectors into progenitor giant cells, the procambium, which triggers developmental and cell cycle changes to increase the cell metabolism, nutritional content and transfer networks, eventuating in giant cells acting as nutrient sinks (Caillaud et al., 2008, de Almeida Engler et al., 1999, Kyndt et al., 2013). Such orchestration is thought to involve the manipulation of plant hormones and signalling molecules such as auxins, cytokinins, gibberellic acid, brassinosteroids, ethylene, salicyclic acid and jasmonic acid, although the complete extent has not yet been clarified (Cabrera et al., 2015b, Kyndt et al., 2013).

Auxins are responsible for cell division, cell elongation, cell differentiation, trophic responses, growth and formation of new organs (Davies, 1995), and are important for the initiation of galls (Hutangura et al., 1999). Auxin regulation genes such as auxin response and auxin transport protein genes were upregulated during nematode infection (Absmanner et al., 2013, Gheysen and Fenoll, 2002). The auxin indole-acetic acid (IAA) had been previously found in *M. javanica* galls using paper chromatography (Balasubramanian and Rangaswami, 1962) and increase auxin responses were observed using auxin responsive reporters such as *GH3* and *DR5* in young galls (Hutangura et al., 1999, Karczmarek et al., 2004). Exogenous applications the auxin affected nematode infection, by resulting in larger galls (Glazer et al., 1986) and increasing the susceptibilities of previously resistant peach plants to *M. javanica* (Kochba and Samish, 1971). Nematodes infecting the auxin insensitive tomato mutant, *diageotropica* showed arrested development and formed less galls (Richardson and Price, 1984). Auxins have also been detected in juveniles and eggs of *M. incognita* (De Meutter et al., 2005, Yu and Viglierchio, 1964). These studies imply that precise auxin regulation is required for gall formation.

Auxins can be regulated by its biosynthesis, conjugation, turnover, transport and signal transduction (Woodward and Bartel, 2005). Currently, not much is known about auxin homeostasis in the gall, with the exception of a recent study by Kyndt et al. (2016) which suggested auxin accumulation in galls involved auxin transport

redistribution, by the import of auxin through AUX1/LAX3 and the relocalisation and suppression of the auxin efflux proteins, PIN. The manipulation of PIN may be achieved via flavonoids, as the induction of *chalcone synthase (CHS) 1* and *CHS2,* which are enzymes in the first step of flavonoid biosynthesis coincided with the increase of auxin response during early infection in white clover (Hutangura et al., 1999). Flavonoids, particularly the flavonols have been shown to inhibit polar auxin transport by inhibiting PIN proteins as well as regulating auxin turnover (Brown et al., 2001, Murphy et al., 2000a, Peer et al., 2004, Stenlid, 1963, Taylor and Grotewold, 2005). Although flavonoids may be involved in auxin transport regulation in the gall, they are not essential, as flavonoid deficient roots still formed galls, although they were smaller (Wasson et al., 2009). Nevertheless, the effects of root flavonoids on auxin transport and accumulation during gall formation has not been studied. As such, the aims of this chapter are:

1) Examine auxin regulation in nematode-infected roots of *M. truncatula* wild-type 2HA by determining auxin content, expression of an auxin reporter as an indirect assay for auxin responses and polar auxin transport.
2) Determine the effects of altering *in planta* isoflavonoid regulation via IFS transgenics on auxin transport regulation during nematode infection.

To address the first aim, auxins were extracted from the roots of wild-type *M. truncatula* 2HA infected with *M. javanica* and were analysed by tandem mass spectrometry at 6 hours, 24 hours, 4 days, 2 weeks and 4 weeks post inoculation. Eleven types of auxin species that were previously detected in *M. truncatula* (Ng et al., 2015b) were targeted and quantified using LC-ESI-QTOF-MS/MS. These auxins included indole-3-acetic acid (IAA), indole-3-butyric acid (IBA), phenylacetic acid, conjugated IAA, namely, IAA-alanine (IAA-Ala), 4-chloro-IAA (4-Cl-IAA), IAA-aspartate (IAA-Asp), IAA-isoleucine (IAA-Ile), IAA-leucine (IAA-Leu), IAA-phenylalanine (IAA-Phe), IAA- tryptophan (IAA-Trp), and IAA-valine (IAA-Val). Auxin content quantification was complemented with the observations of the soybean auxin responsive promoter, *GH3* fused to the *GUSa* reporter, which is expressed when auxins are present (Hagen et al., 1991, Jefferson, 1987). In addition, acropetal auxin transport in infected roots using radiolabelled IAA at different stages of gall development, early (24 hours and 4 days) and mature stage (4 weeks) was be assayed.

The second aim involved measurements of acropetal auxin transport in infected isoflavone synthase (IFS) transgenics, with silenced lines, IFSi 42-7 and IFSi 101-2 and an over-expression line, IFSOE 10-3. Previous results in chapter 4 suggested high levels of isoflavonoids such as afromosin and medicarpin in the gall were associated in plant defense response, but their roles in auxin transport regulation has yet to be studied.

5.3 Results

5.3.1. Auxin transport in roots and galls of *M. truncatula* wild-type 2HA and IFS transgenics

Auxin transports in uninfected roots of 2HA and IFS transgenics were measured at equivalent times to nematode infected roots at 24 hours, 4 days and 4 weeks post inoculation. At 24 hours, IFSi 42-7 roots showed the highest auxin transport capacity, followed by 2HA, IFSi 101-2 and IFSOE 10-3 roots (Figure 5.1). However, this trend changed at 4 days as 2HA roots increased their auxin transport capacity, and was followed by counts in IFSi 101-2, IFSi 42-7 and IFSOE 10-3 roots (Figure 5.1). Although IFSOE 10-3 roots showed the lowest auxin transport capacities at 24 hours and 4 days, these roots had the highest auxin transport capacity at 4 weeks (Figure 5.1). This was closely followed by IFSi 101-2 and IFSi 42-7 roots, and lastly, 2HA with significantly lower counts compared to the other three genotypes (Figure 5.1).

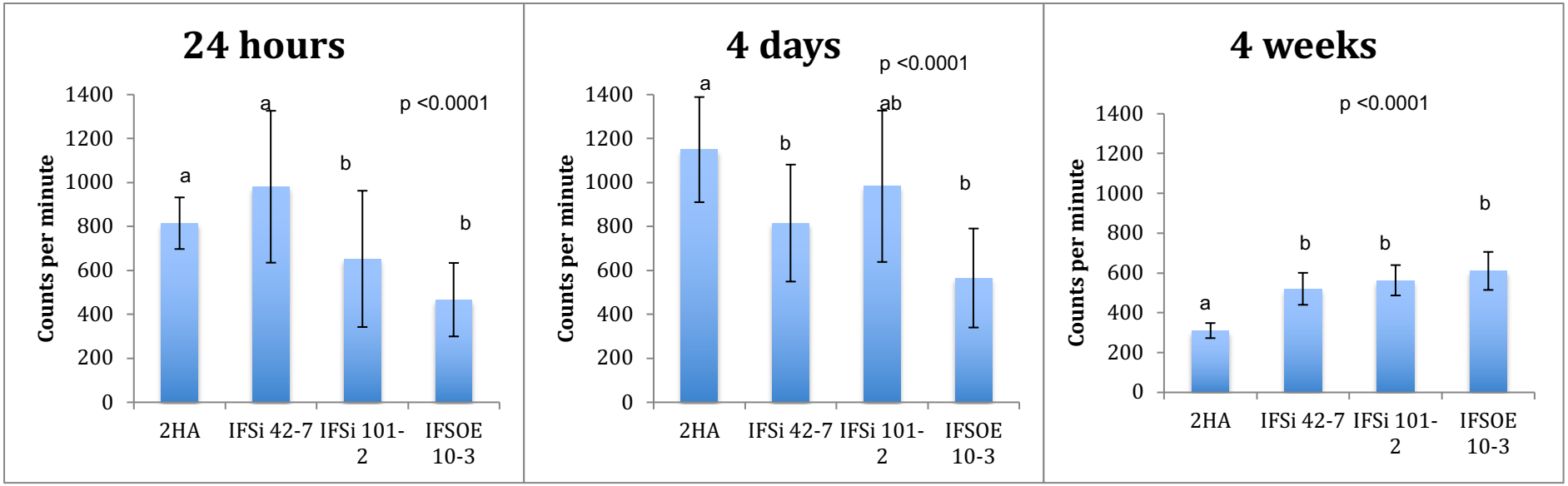

Figure 5.1: Acropetal auxin transport in uninfected roots of wild-type *Medicago truncatula* cv. 2HA and transgenics, isoflavone synthase silenced lines, IFSi 42-7 and IFSi 101-2 and isoflavone synthase over-expression line, IFSOE 10-3 at 24 hours, 4 days and 4 weeks. One-way ANOVA with Tukey-Kramer multiple comparison tests were performed. Letters indicate statistically significant differences at $p<0.05$.

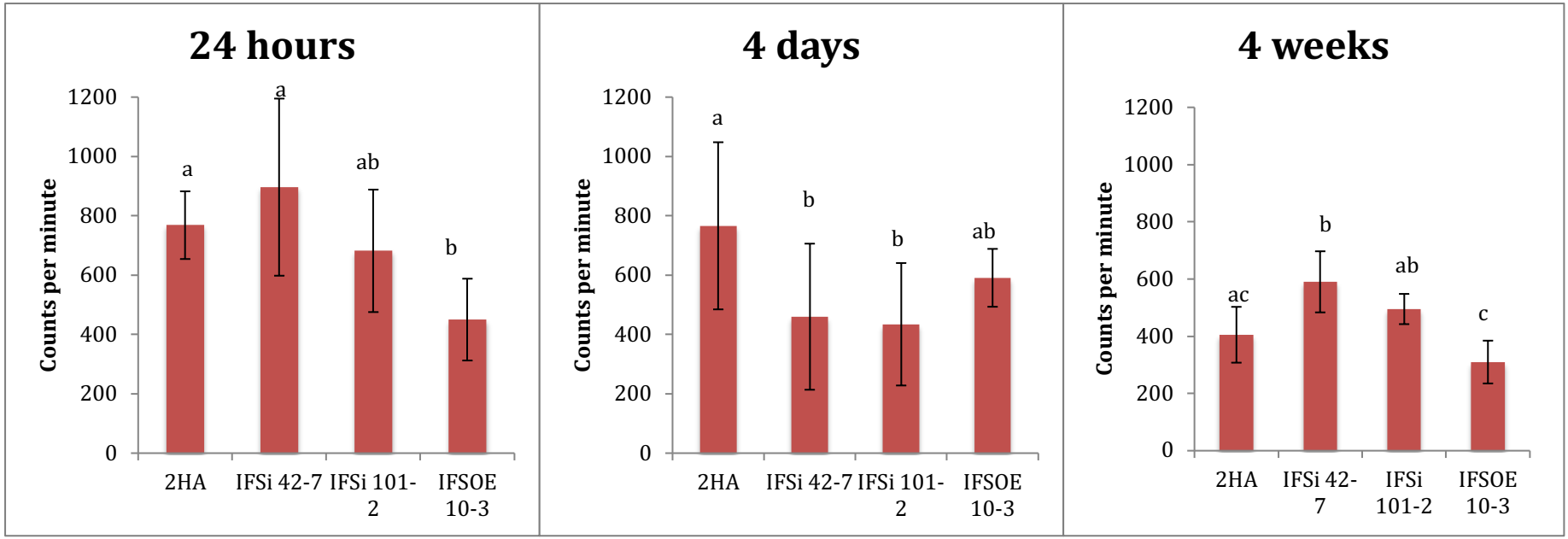

Figure 5.2 : Acropetal auxin transport in infected roots of wild-type *Medicago truncatula* cv. 2HA and transgenics, isoflavone synthase silenced lines, IFSi 42-7 and IFSi 101-2 and isoflavone synthase over-expression line, IFSOE 10-3 at 24 hours, 4 days and 4 weeks. One-way ANOVA with Tukey-Kramer multiple comparison tests were performed. Letters indicate statistically significant differences at $p<0.05$.

Acropetal auxin transport was measured for nematode-infected roots of wild-type 2HA and IFS transgenics, IFSi 42-7, IFSi 101-2 and IFSOE 10-3 plants at 24 hours, 4 days and 4 weeks (illustrated in Figure 2.1). At 24 hours post-inoculation, auxin transport capacities in all genotypes were unaffected by nematode infection (Figures 5.3, 5.4, 5.5 and 5.6). Comparatively across the genotypes, the auxin transport rankings remained similar to uninfected roots (Figures 5.1 and 5.2).

Once the nematodes established their early feeding sites (young galls) at 4 days, there were extremely significant reductions in acropetal auxin transport in infected roots compared to uninfected roots in 2HA (-33.3%), IFSi 42-7 (-43.6%) and IFSi 101-2 (-55.5%), with the exception of IFSOE 10-3 plants, which showed no significant differences between uninfected and infected roots (+4.4%) (Figures 5.3, 5.4, 5.5 and 5.6 and Table 5.1). In infected roots, relative change in auxin transport between nematode inoculated segments and the corresponding downstream segment showed the strongest auxin transport inhibition in young galls of IFSi 101-2 with 86% reduction in auxin transport, followed by IFSi 101-2 with 80% reduction, 2HA with 68% reduction and lastly, IFSOE 10-3 with 37% reduction (Table 5.2). Across genotypes, both IFSi lines, IFSi 42-7 and IFSi 101-2 had similar auxin transport counts in infected roots, which were significantly less than the counts for 2HA roots (Figure 5.2).

By 4 weeks, mature galls had developed. Two types of mature galls formed at 4 weeks post inoculation, ie. terminal and non-terminal galls (Table 5.3). In terminal galls, galls formed at the root tip, which resulted in the growth termination at the root tip. These galls were often accompanied by the presence of multiple short lateral roots and/or a few long lateral root(s). On the other hand, non-terminal galls formed along any part of the root, with the root growing past the gall and the root tip being maintained. Whilst lateral roots also emerged from non-terminal galls, they usually occured less frequently and were often short. Nematode infection in 2HA and IFSOE 10-3 plants resulted in the formation of 100% non-terminal galls (Table 5.3). In contrast, IFSi 42-7 and IFSi 101-2 plants formed 9%-10% terminal galls, with the remaining 91-90% galls turning into non-terminal types (Table 5.3). Chi-square test for independence revealed highly significant association ($p<0.01$) between gall types and plant genotypes. Non- terminal galls of all four genotypes showed strong inhibition of auxin transport in the tissues below the galls, whereas the tissues above

the galls and wherein the galls were showed almost equal auxin redistributions (Figure 5.7).

Infected IFSOE 10-3 roots at 4 weeks showed the extreme auxin transport reduction (49.3%) when compared to uninfected roots (Figure 5.6 and Table 5.1). Auxin transport was also strongly supressed (85%) in tissues basal to the gall in IFSOE 10-3 roots (Table 5.2). In contrast, other genotypes experienced an overall increase or no change in auxin transport capacities in infected roots when compared with uninfected roots (Figures 5.3, 5.4 and 5.5). Despite this, tissues basal of the galls of 2HA, IFSi 42-7 and IFSi 101-2 still exhibited auxin transport suppression (Table 5.2). Comparison across genotypes revealed that the total auxin transport counts in infected IFSi 42-7 and IFSi 101-2 roots were similar and were higher than the counts in 2HA and IFSOE 10-3 roots (Figure 5.2).

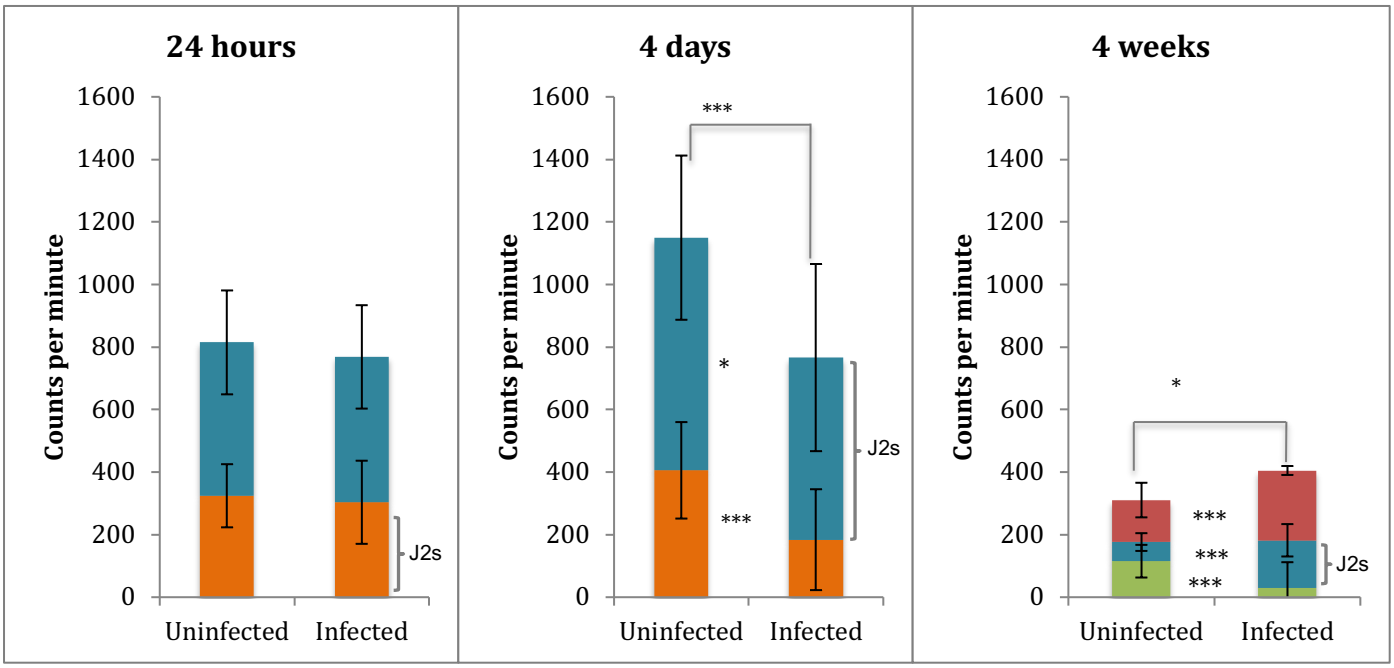

Figure 5.3: Acropetal auxin transport of wild-type *M. truncatula* cv. 2HA at 24 hours, 4 days and 4 weeks post inoculation with *Meloidogyne javanica*. For the 24 hours time point, the orange segments represent the 4 mm of nematode inoculation site with the root tip, whereas the blue segments represent the upstream 4 mm from the root tip. For the 4 days time point, the orange segments represent 4 mm of root tip, whereas the blue segments represent the upstream 4 mm of root tip with the nematode inoculation site as the root grew. For the 4 weeks time point, the green segments represent 4 mm of roots downstream of inoculation site, where a gall had formed, the blue segments represent 4mm of root with a gall(s) and the red segments represent 4mm of roots upstream of the inoculation site. Segments with a bracket indicate nematode inoculated segment. Unpaired t-tests were performed. Asterisks indicate statistically significant difference ($p<0.05$) between uninfected and infected groups for equivalent root segments. Error bars represent standard deviation. (n = 22-33)

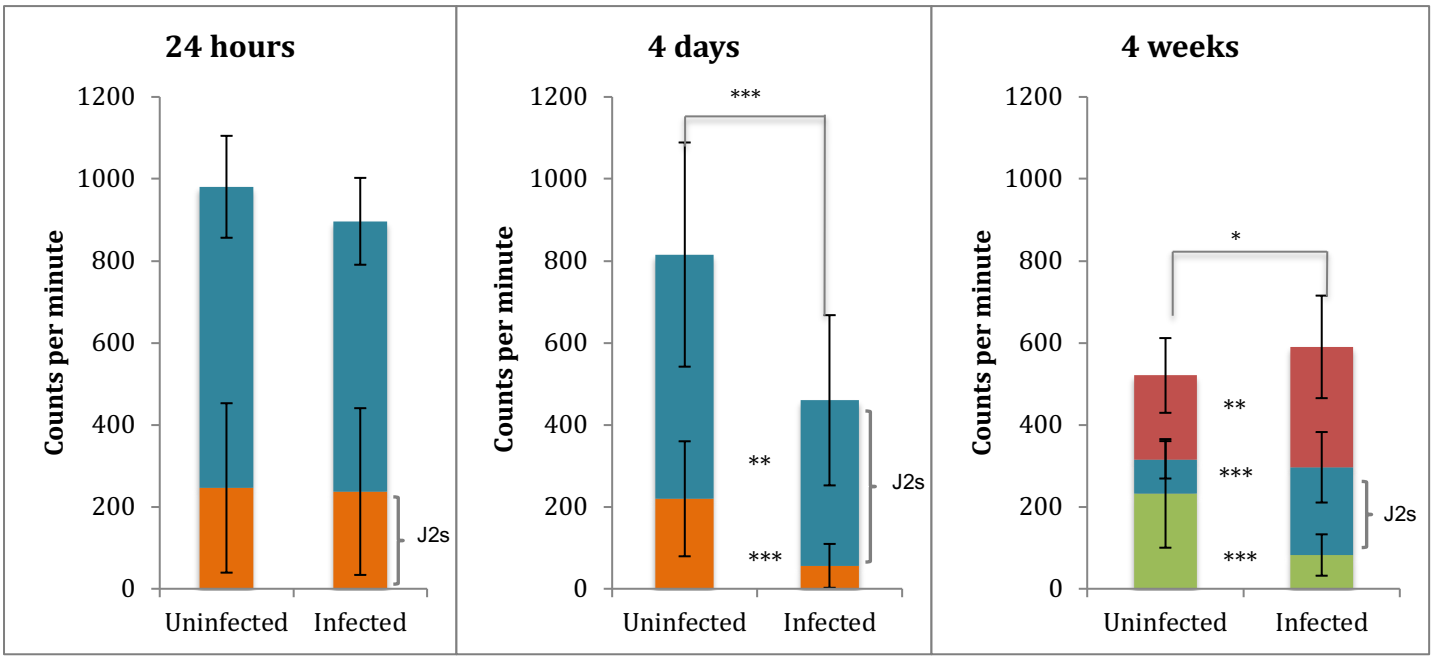

Figure 5.4: Acropetal auxin transport of transgenic *M. truncatula* isoflavone synthase silenced line, IFSi 42-7 at 24 hours, 4 days and 4 weeks post inoculation with *Meloidogyne javanica*. For the 24 hours time point, the orange segments represent the 4 mm of nematode inoculation site with the root tip, whereas the blue segments represent the upstream 4 mm from the root tip. For the 4 days time point, the orange segments represent 4 mm of root tip, whereas the blue segments represent the upstream 4 mm of root tip with the nematode inoculation site as the root grew. For the 4 weeks time point, the green segments represent 4 mm of roots downstream of inoculation site, where a gall had formed, the blue segments represent 4 mm of root with a gall(s) and the red segments represent 4mm of roots upstream of the inoculation site. Segments with a bracket indicate nematode inoculated segment. Unpaired t-tests. Asterisks indicate statistically significant difference ($p<0.05$) between uninfected and infected groups for equivalent root segments. Error bars represent standard deviation. (n= 24-35)

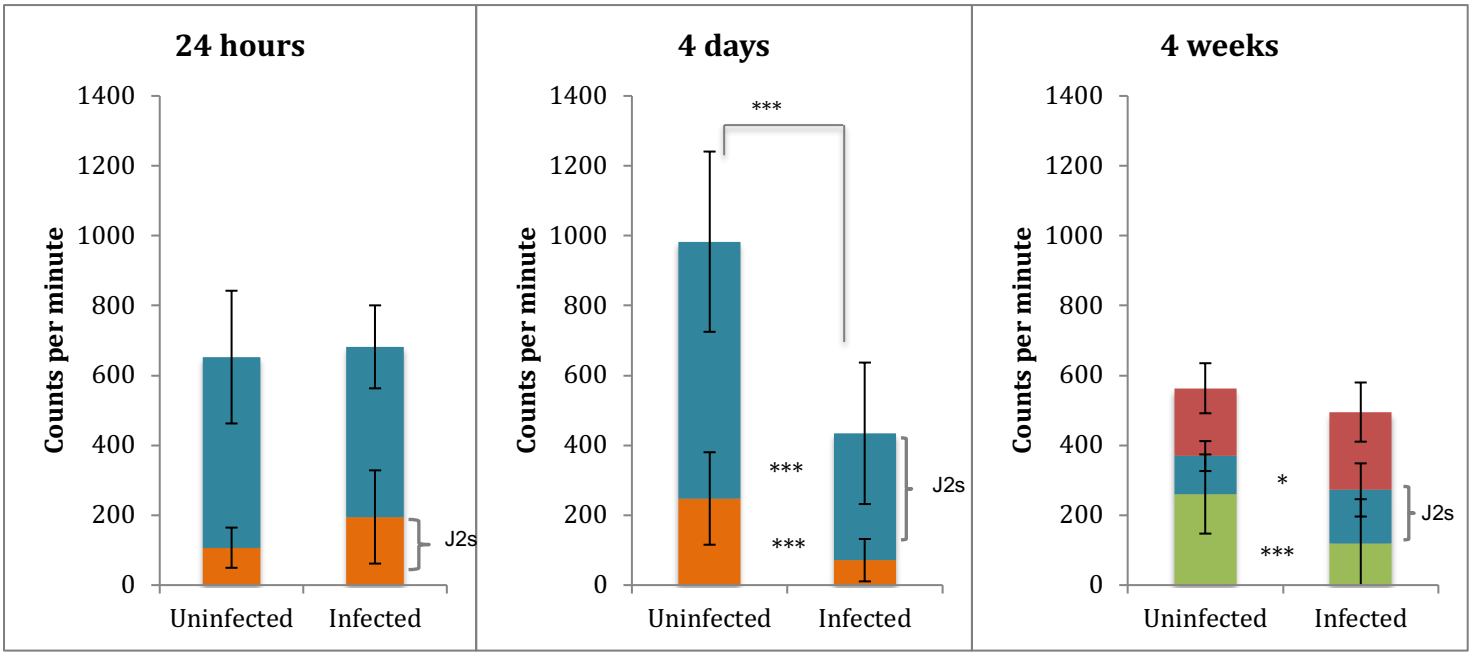

Figure 5.5: Acropetal auxin transport of transgenic *M. truncatula* isoflavone synthase silenced line, IFSi 101-2 at 24 hours, 4 days and 4 weeks post inoculation with *Meloidogyne javanica*. For the 24 hours time point, the orange segments represent the 4 mm of nematode inoculation site with the root tip, whereas the blue segments represent the upstream 4 mm from the root tip. For the 4 days time point, the orange segments represent 4 mm of root tip, whereas the blue segments represent the upstream 4 mm of root tip with the nematode inoculation site as the root grew. For the 4 weeks time point, the green segments represent 4mm of roots downstream of inoculation site, where a gall had formed, the blue segments represent 4mm of root with a gall(s) and the red segments represent 4 mm of roots upstream of the inoculation site. Segments with a bracket indicate nematode inoculated segment. Unpaired t-tests were performed. Asterisks indicate statistically significant difference ($p<0.05$) between uninfected and infected groups for equivalent root segments. Error bars represent standard deviation. (n = 14-23)

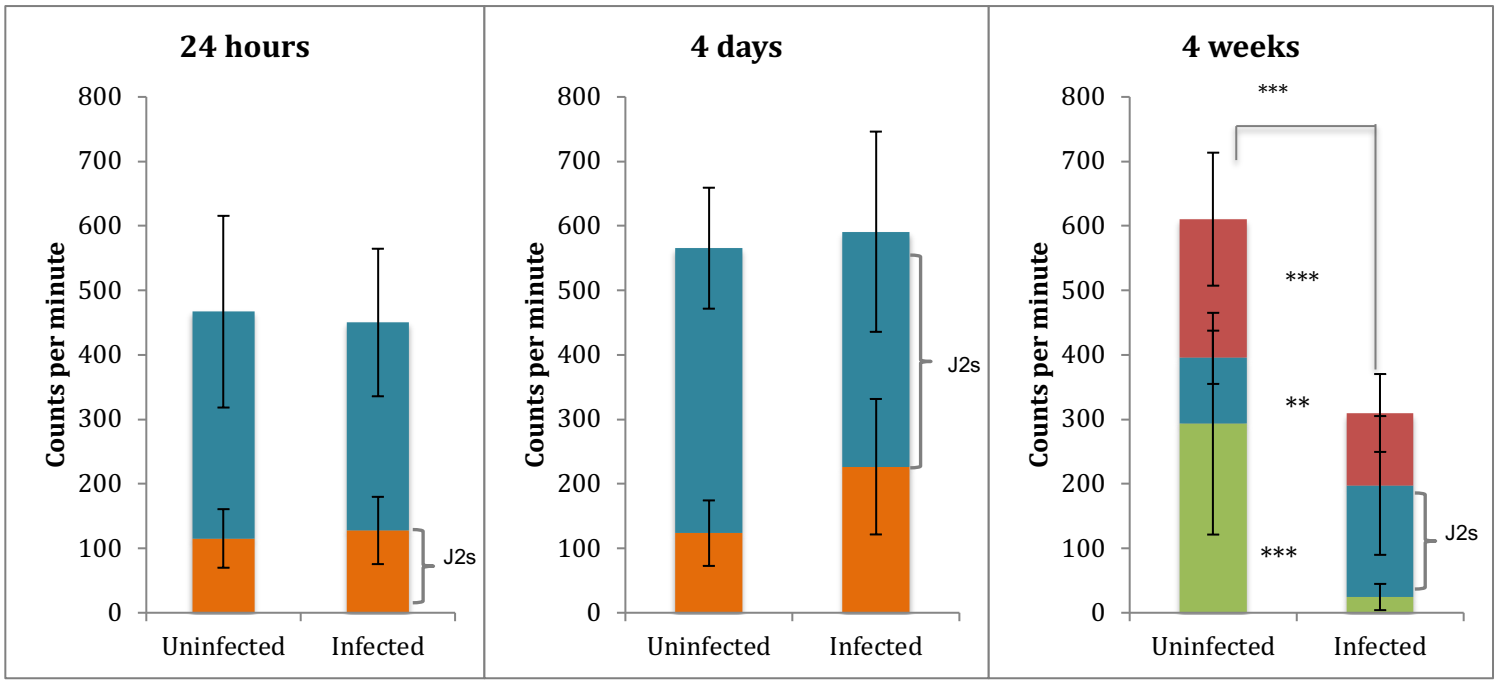

Figure 5.6: Acropetal auxin transport of transgenic *M. truncatula* isoflavone synthase over-expression line, IFSOE 10-3 at 24 hours, 4 days and 4 weeks post inoculation with *Meloidogyne javanica*. For the 24 hours time point, the orange segments represent the 4 mm of nematode inoculation site with the root tip, whereas the blue segments represent the upstream 4 mm from the root tip. For the 4 days time point, the orange segments represent 4 mm of root tip, whereas the blue segments represent the upstream 4 mm of root tip with the nematode inoculation site as the root grew. For the 4 weeks time point, the green segments represent 4 mm of roots downstream of inoculation site, where a gall had formed, the blue segments represent 4mm of root with a gall(s) and the red segments represent 4 mm of roots upstream of the inoculation site. Segments with a bracket indicate nematode inoculated segment. Unpaired t-tests were performed. Asterisks indicate statistically significant difference ($p<0.05$) between uninfected and infected groups for equivalent root segments. Error bars represent standard deviation. (n= 19-23)

% change in auxin transport between uninfected and infected roots	Time point	Genotype			
		2HA	IFSi 42-7	IFSi 101-2	IFSOE 10-3
	4 days	-33.3% ***	-43.6% ***	-55.5% ***	+4.4%
	4 weeks	+30.6% *	+13.5% *	-12.2%	-49.3% ***

Table 5.1: Percentage change in auxin transport between uninfected and infected roots of wild-type *Medicago truncatula* cv. 2HA and transgenics of isoflavone synthase silenced lines, IFSi 42-7, IFSi 101-2, and isoflavone synthase overexpression line, IFSOE 10-3 at 4 days and 4 weeks post inoculation with *Meloidogyne javanica*. Statistical analyses were based on unpaired t-test, similar to Figures 5.4, 5.5, 5.6 and 5.7. Asterisks indicate statistically significant difference ($p<0.05$) between uninfected and infected groups for equivalent root segments. Error bars represent standard deviation.

% change in auxin transport between inoculated segment and downstream segment	Time point	Genotype			
		2HA	IFSi 42-7	IFSi 101-2	IFSOE 10-3
	4 days	-68	-86	-80	-37
	4 weeks	-80	-61	-22	-85

Table 5.2: Percentage change in auxin transport between nematode inoculated segments and corresponding downstream segments in *Medicago truncatula* cv. 2HA and transgenics of isoflavone synthase silenced lines, IFSi 42-7, IFSi 101-2, and isoflavone synthase overexpression line, IFSOE 10-3 at 4 days and 4 weeks post inoculation with *Meloidogyne javanica*.

Gall type	Picture	Description	% gall type formed for each genotype at 4 weeks			
			2HA	IFSi 42-7	IFSi 101-2	IFSOE 10-3
Terminal	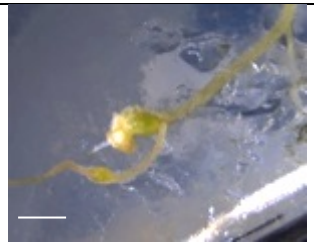	Growth of primary root terminates at the gall. Primary root loses its root tip and root tip morphology is lost. Multiple short lateral root(s) usually emerge from the gall. Often, a single lateral root grows long to compensate for the loss of primary root tip.	0%	9%	10%	0%
Non-terminal	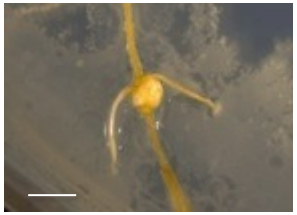 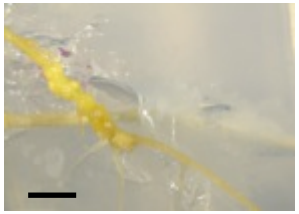	Primary root grows past gall(s) and maintains its root tip. In some galls, lateral root(s) can emerge from the gall but are often short.	100%	91%	90%	100%

Table 5.3: Summary of the types of galls formed at nematode inoculation in wild-type *Medicago truncatula* cv. 2HA and transgenics, isoflavone synthase silenced lines, IFSi 42-7 and IFSi 101-2 and isoflavone synthase over-expression line, IFSOE 10-3 at 4 weeks post inoculation with *Meloidogyne javanica*. Data exclude galls formed at non-inoculated sites. White scale bars represent 2 mm whereas the black scale bar represents 5 mm. Statistical analysis with chi-squared test for independence showed statistically significant result (p=0.0002). (n= 18-23)

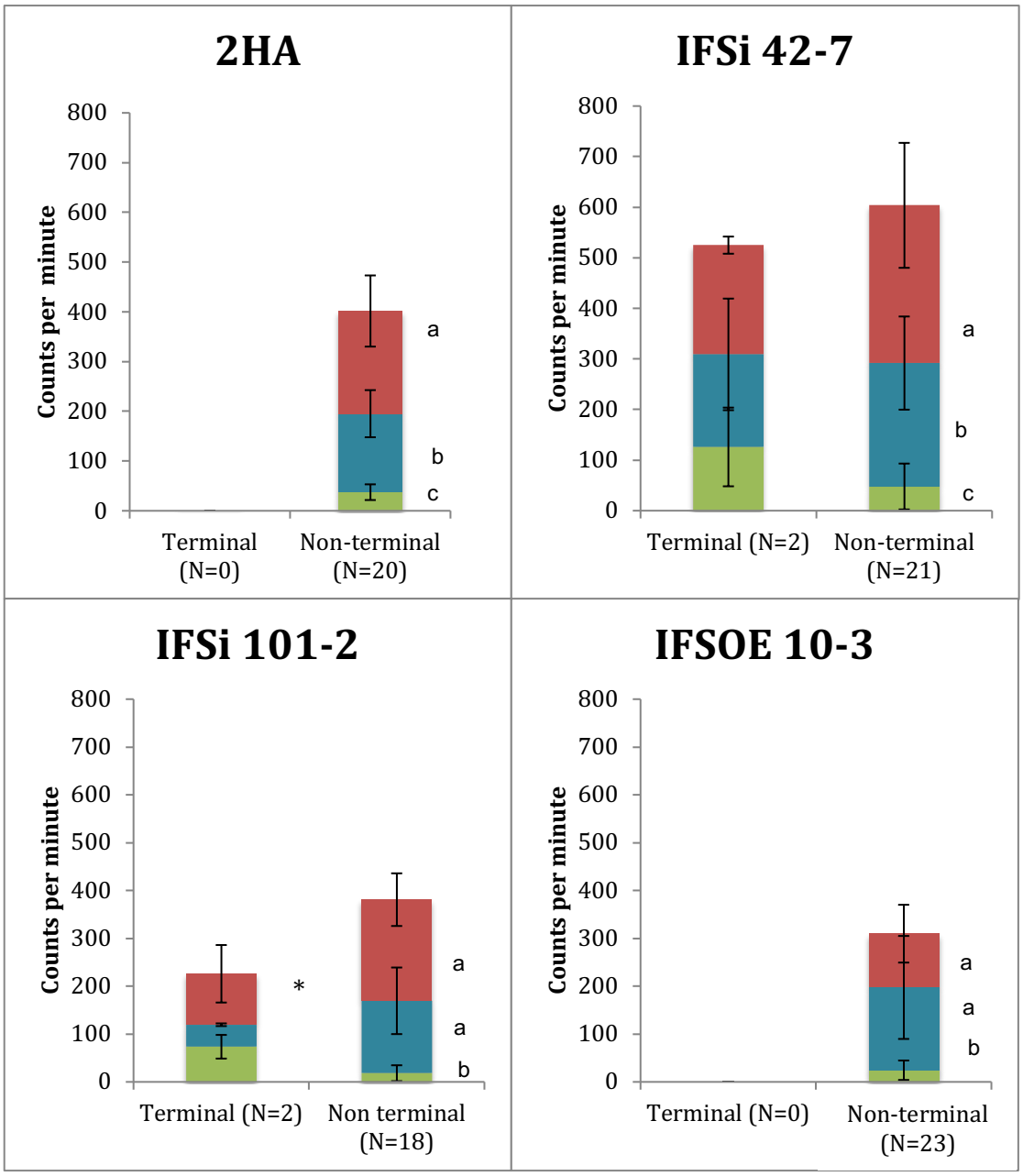

Figure 5.7: Acropetal auxin transport in terminal and non-terminal galls in wild-type *Medicago truncatula* cv. 2HA and transgenics, isoflavone synthase silenced lines, IFSi 42-7 and IFSi 101-2 and isoflavone synthase over-expression line, IFSOE 10-3 at 4 weeks post inoculation with *Meloidogyne javanica*. The blue segments indicate 4mm nematode inoculation site, whereas the green segments correspond with 4mm downstream segment and the red segments correspond with 4mm upstream segment. Striped bar graphs represent root segments with gall(s). Data exclude galls formed at non-inoculated sites. Mann Whitney tests were performed for IFSi 42-7 and IFSi 101-2 data to compare equivalent terminal and non-terminal segments, with asterisk indicating statistically significant result ($p<0.05$). One-way ANOVA with Tukey-Kramer multiple comparison tests were performed for all genotypes to compare variation between root segments of the same gall. Different lower case letters indicate statistically significant results ($p<0.05$). Figures were derived from Figures 5.3-5.6 (auxin transport capacities were summed up in Figures 5.3-5.6).

5.3.2. Auxin quantification in roots and galls of *M. truncatula* 2HA

Only four auxin species, IAA, IAA-Ala, IAA-Trp and IAA-Val were detected out of the targeted 11 auxins. IAA concentrations in uninfected root were higher than in infected roots at 6 hours, 24 hours and 4 days post inoculation, but these differences were only significant at 24 hours (Figure 5.8). Nematode infection gradually increased IAA concentrations from 4 days to 4 weeks post inoculation, whereas this trend was reversed in uninfected roots (Figure 5.8). Overall, IAA levels fluctuated significantly across time and were also affected by the combined effects of time and nematode inoculation ($p<0.05$).

IAA-Ala concentrations in the 2HA roots were initially measured to be around 1-2 ng/g (Figure 5.8). These increased by approximately two times, reaching around 3.3-4 ng/g at 24 hours (Figure 5.8). In the following time points, IAA-Ala levels in uninfected roots continued to decrease from ~0.5 ng/g at 4 days to undetectable levels by 4 weeks, whereas IAA-Ala in infected roots began to increase from 0.2 ng/g at 4 days to 1ng/g at 4 weeks (Figure 5.8). The changes in IAA-Ala levels were found to be significantly dependent on time ($p<0.0001$), but not by nematode inoculation.

IAA-Trp levels were higher in uninfected roots compared to infected roots at early time points such as 6 hours and 24 hours, but again these differences were not significant (Figure 5.8). At 4 days and 2 weeks, both uninfected and infected groups had similar concentrations of IAA-Trp (Figure 5.8). However at 4 weeks, IAA-Trp concentration was significantly lower in infected roots than uninfected roots (Figure 5.8).

As for IAA-Val, infected roots produced minimal amounts of IAA-Val at earlier time points, such as 6 hours, 24 hours and 4 days (Figure 5.8). Prominent differences between uninfected and infected roots were observed at 2 weeks, with significantly lower IAA-Val concentration in infected roots (Figure 5.8).

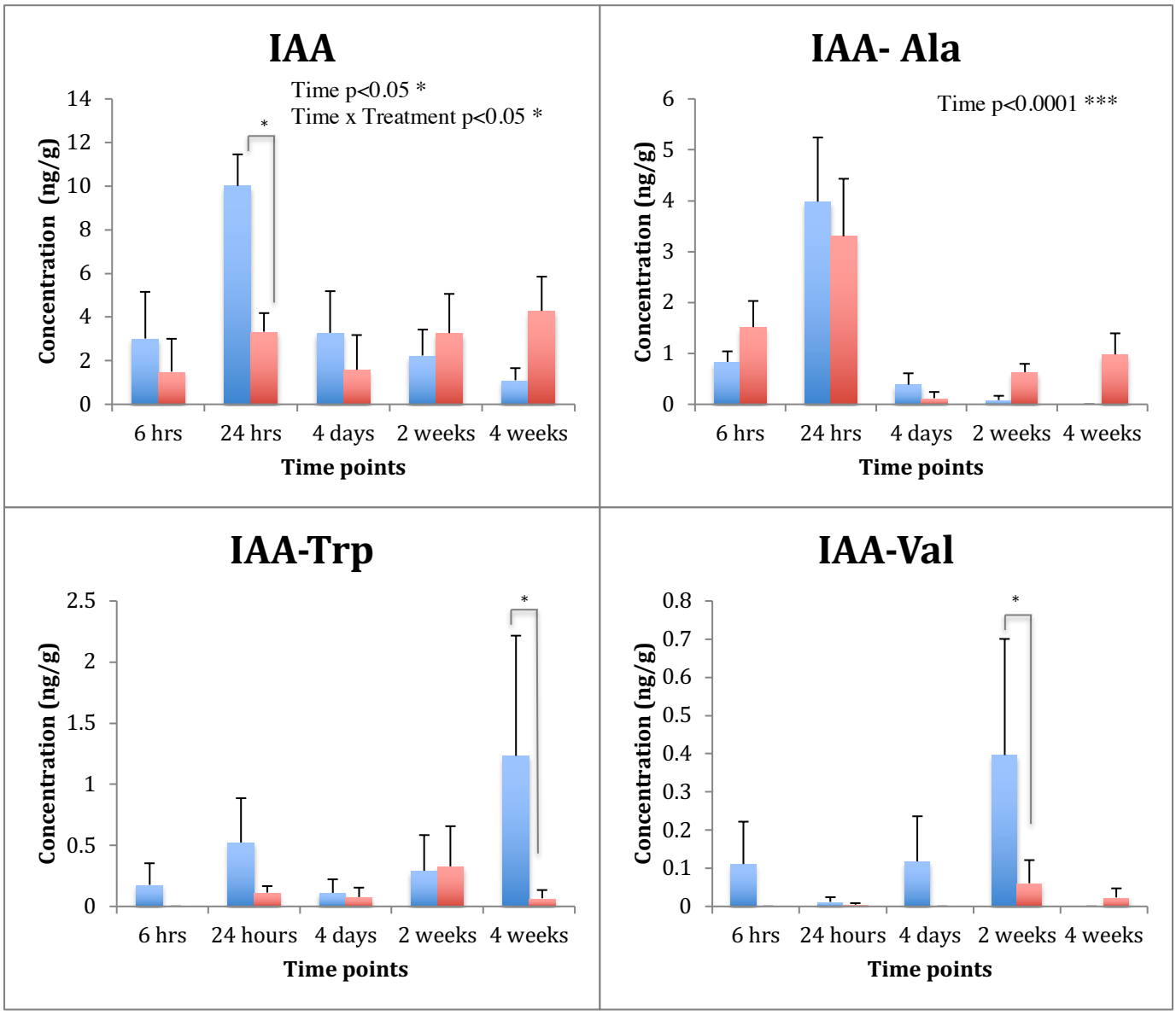

Figure 5.8: Auxin quantification of uninfected and *Meloidogyne javanica* infected *Medicago truncatula* cv. 2HA at 6 hours, 24 hours, 4 days, 2 weeks and 4 weeks post inoculation. Blue bars represent uninfected roots, whereas red bars represent infected roots. Statistical analysis was based on linear mixed model for the treatment, time and interaction between time and treatment factors. Asterisks indicate statistically significant differences ($p<0.05$). Error bars represent standard errors. N=3.

5.3.3. Auxin responses in roots and galls of *M. truncatula GH3::GUS* transgenic plants

At 6 hours post inoculation, *GH3::GUSa* staining was observed in the vascular bundles and the pericycle cells surrounding the vascular bundles in both control and nematode-infected roots (Figures 5.9 A-B and 5.10 A-B). Nevertheless, infected roots showed very weak *GH3::GUSa* expression at the elongation zone (Figure 5.9 B), as opposed to no *GH3::GUSa* expression in the control roots (Figure 5.9 A). In the following time point, 24 hours, the elongation zone of infected roots showed very weak *GH3::GUSa* expression, whereas this was not observed in control roots (Figure 5.9 C-D). Cross-sections of control and infected roots at 24 hours did not reveal prominent differences in *GH3::GUSa* expressions (Figure 5.10 C-D). Young galls, which had started to emerge by 4 days post inoculation, showed strong *GH3::GUSa* expression in the galls (Figure 5.9 F). Upon closer inspection, these young galls showed distinct anatomical changes, such as enlarged cortical cells and the presence of giant cells in the vascular bundles, as well as *GH3:: GUSa* expressions in the pericycle and cortex (Figure 5.10 F). Control roots at 4 days also showed *GH3::GUSa* expressions in the pericycle and cortex at lateral root primordia but were mainly unstained at other parts of the root (Figures 5.9 E and 5.10 E). In the late infection stages such as 2 weeks and 4 weeks, *GH3:: GUSa* expression in the galls had mostly diminished (Figures 5.9 H and J). Weak *GH3:: GUSa* expression was observed for 2 week old galls in the cortex and pericycle, but by 4 weeks, this *GH3::GUSa* expression was absent, except in lateral roots and lateral root primordia (Figures 5.10 H and J). On the other hand, control roots at 2 weeks and 4 weeks showed patchy *GH3:: GUSa* expressions in the cortex, and were mainly unstained except at lateral root primordia (Figures 5.9 G and I, and 5.10 G and I).

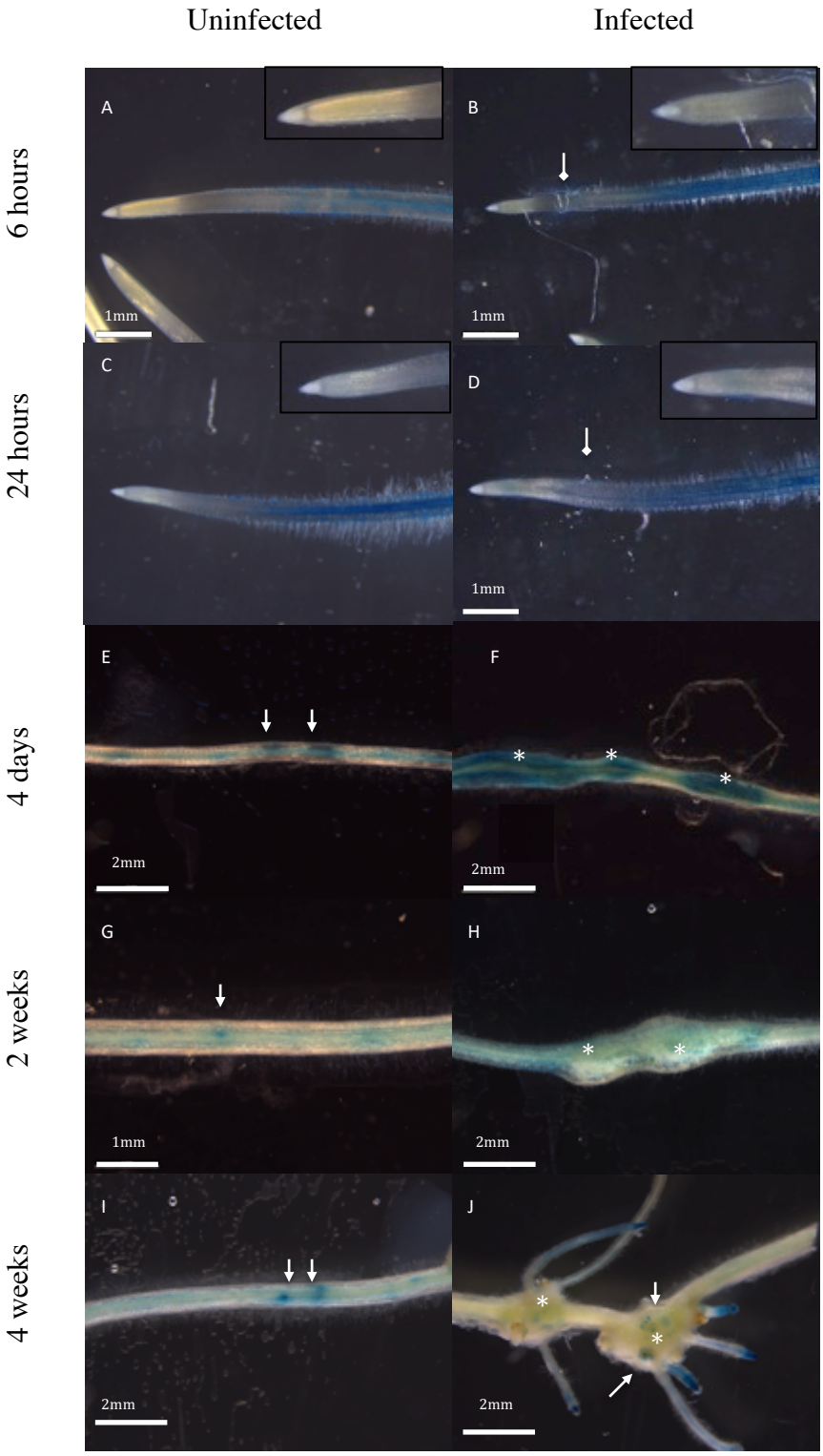

Figure 5.9: Root overview of *GH3: GUSa* expression in *M. truncatula GH3:GUSa* roots infected by *M. javanica* at 6 hours, 24 hours, 4 days, 2 weeks and 4 weeks post inoculation. Eight plants were sampled in each group. **(A)** A 6 hours uninoculated root showed weak *GH3: GUSa* expression in the vascular bundle and patchy expression in the cortex. Blown-up photo showed no *GH3: GUSa* expression in the root cap. **(B)** A 6 hours post-inoculated root showed *GH3: GUSa* expression in the vascular bundle and cortex. The diamond arrow indicates nematodes. Blown-up photo

showed no *GH3: GUSa* expression in the root cap. **(C)** A 24 hours uninoculated root showed *GH3: GUSa* expression in the vascular bundle and cortex. Blown-up photo showed no *GH3: GUSa* expression in the root cap. The diamond arrow indicates a nematode. **(D)** A 24 hours post inoculated root showed *GH3: GUSa* expression in the vascular bundle, cortex and root cap. Blown-up photo showed very faint *GH3: GUSa* expression in the root cap. **(E)** A 4 days uninoculated root showed localised *GH3: GUSa* expression in the cortex at sites of lateral root primordia (blue arrows). **(F)** A 4 days post inoculation root showed strong localised *GH3:GUSa* expression in galls (indicated by asterisks). **(G)** A 2 weeks uninoculated root showed localised *GH3: GUSa* expression in the cortex at sites of lateral root primordia (blue arrows). **(H)** A 2 weeks post inoculation root showed weak *GH3:GUSa* expression in galls (indicated by asterisks), with patchy expression in the cortex. **(I)** A 4 weeks uninoculated root showed localised *GH3: GUSa* expression in the cortex at sites of lateral root primordia (blue arrows). **(J)** A 4 weeks post inoculation root showed minimal *GH3: GUSa* expression in the galls, with some localised expression at emerging lateral root primordia (blue arrows). Lateral roots that had emerged from the galls showed strong *GH3: GUSa* expression in the vascular bundle and root tip.

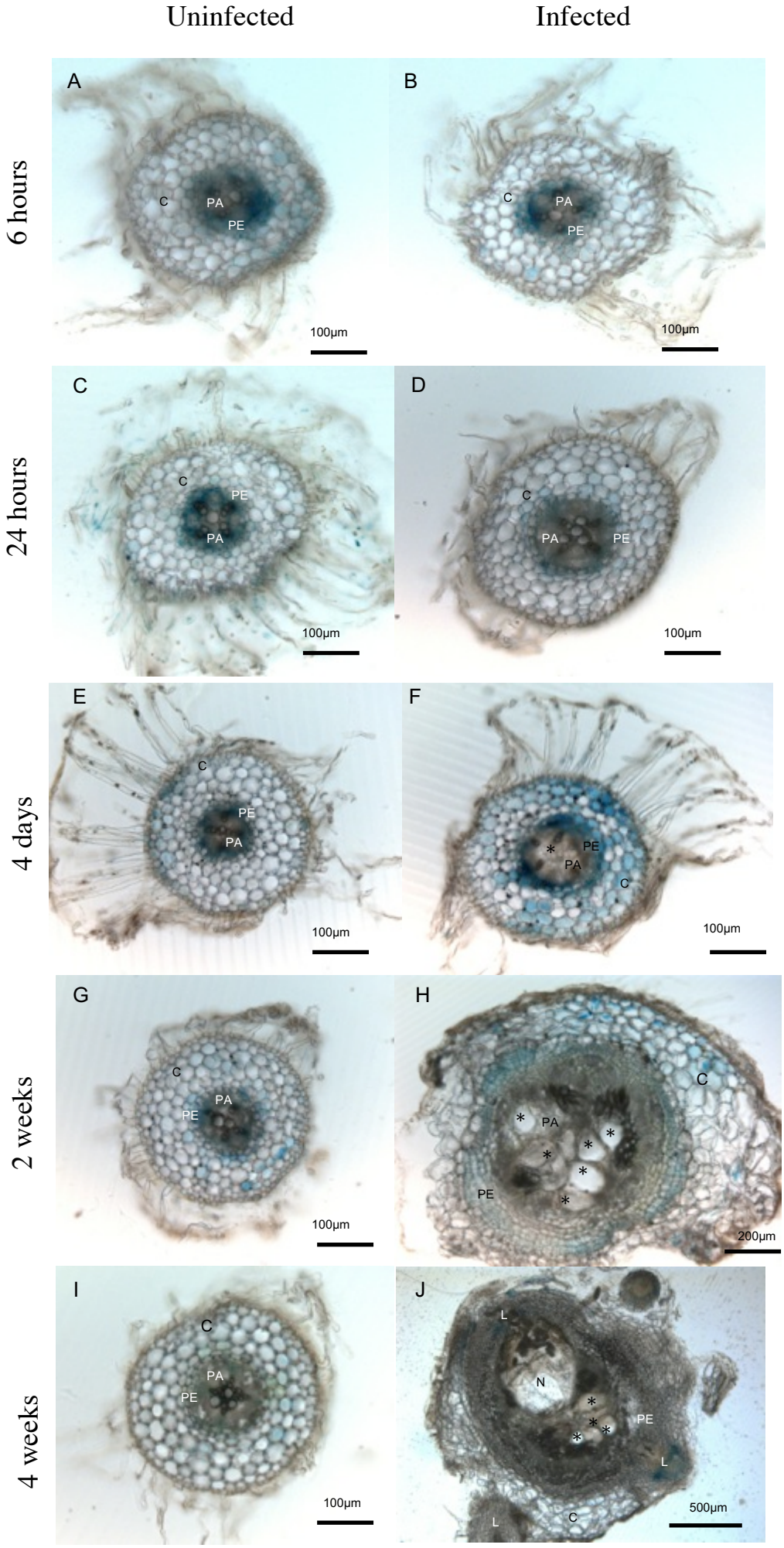
Uninfected
Infected
6 hours
24 hours
4 days
2 weeks
4 weeks
A
B
C
D
E
F
G
H
I
J
C
PA
PE
L
N
100µm
200µm
500µm

Figure 5.10: Cross sections of *GH3: GUSa* expression in *M. truncatula GH3:GUSa* roots infected by *M. javanica* at 4 days, 2 weeks and 4 weeks post inoculation. C= cortex, PA= parenchyma, PE= pericycle, *= giant cell(s), N= nematode crevice. Eight plants were sampled from each group **(A)** A 6 hours uninoculated root showed strong *GH3: GUSa* expression in the vascular bundle and pericycle and weak expression in the cortex. **(B)** A 6 hours post-inoculated root showed strong *GH3: GUSa* expression in the vascular bundle and pericycle and weak expression in the cortex. **(C)** A 24 hours uninoculated root showed strong *GH3: GUSa* expression in the vascular bundle and pericycle and weak expression in the cortex. **(D)** A 24 hours post inoculated root showed strong *GH3: GUSa* expression in the vascular bundle and pericycle and weak expression in the cortex. **(E)** A 4 days old uninoculated root showed *GH3: GUSa* expression in the vascular bundle but weak expression in the cortex. **(F)** A 4 days old inoculated root showed *GH3: GUSa* expression in the cortex and pericycle. The parenchymal cells enlarged to form giant cells. Cortical cell divisions have resulted in enlargement of the cortex. **(G)** A 2 weeks old uninoculated root showed *GH3: GUSa* expression in the cortex and pericycle. **(H)** A 2 weeks old inoculated root showed *GH3: GUSa* expression in the cortex and pericycle. Mature giant cells were formed from parenchymal cells, resulting in distorted vascular bundle. There were cell divisions in the pericycle. **(I)** A 4 weeks old uninoculated root showed weak *GH3: GUSa* expression in the cortex. **(J)** 4 weeks old inoculated roots showed weak *GH3: GUSa* expression in the pericycle, with sparse *GH3: GUSa* expression in the cortex. Most *Gh3: GUSa* expression in the roots was localised in lateral roots.

5.4 Discussion

5.4.1 Local transient auxin response was accompanied by acropetal auxin transport inhibition without increase in auxin concentrations in *M. truncatula* 2HA galls

The auxin inducible promoter, *GH3,* was activated in the vascular bundle and pericycle in young roots, regardless of their infection status at 24 hours (Figure 5.10). The lack of change in auxin transport capacities between infected and uninfected roots reflects the occurrence of long distance polar auxin transport from the shoot to the root in the vascular bundle (Figure 5.4, Table 5.4) (Petrášek and Friml, 2009). In contrast, IAA concentration was significantly reduced at this time point (Figure 5.8, Table 5.4). This may be the result of auxins leaching out of the root due to tissue damages or the dilution of auxins during root segment sampling.

At 4 days, a strong and local *GH3:GUSa* activation was observed in the gall, within the pericycle and cortex (Figures 5.9 and 5.10). Cabrera et al. (2014), Hutangura et al. (1999) and Karczmarek et al. (2004) also reported increased auxin responsive promoter induction, such as *GH3* and *DR5* promoters in young galls around 3 days post inoculation. The increase in auxin response was corroborated by the activation of auxin transcription factors and auxin signaling genes in young galls (3-6 days) such as *WRKY* (eg. *WRKY62, WRKY70*), *auxin responsive factor* (eg. *ARF5, ARF11), auxin responsive protein* (eg. *IAA8*) and auxin induced protein (Barcala et al., 2010, Kyndt et al., 2012, Oliveira et al., 2014). The increase in auxin response is induced by the increase in auxin concentration to activate auxin signaling (Hagen, 2015). Several studies have shown evidence of different auxin species and conjugates in J2 secretions, which suggested that auxins may be directly injected into plant cells, possibly to initiate auxin response (De Meutter et al., 2005, Yu and Viglierchio, 1964, Viglierchio and Yu, 1968). The auxin biosynthesis gene, *OsYUCCA1* transcript was strongly upregulated in galls at 3 days post infection (Kydnt et al., 2012). Interestingly, this is juxtaposed by auxin quantification results, which did not reflect increases in auxin concentrations (Figure 5.8, Table 5.4). Whilst application of exogenous IAA, and synthetic auxins alpha-naphthaleneacetic acid and

2,4,5-trichlororophenoxyacetic acid at concentrations 10^{-8} to 10^{-3} induced *GH3:: GUSa* expression (Hagen and Guilfoyle, 1985, Hagen et al., 1991), other types of auxin including IBA (indole butyric acid) and other conjugated forms of IAA have yet to be tested. Hence, it is plausible that *GH3:: GUSa* expression was induced by other types of auxins since IBA and conjugated auxins were untested in this system. In addition, the *GH3::GUSa* system is limited to auxin response localisation, but neither the magnitude of auxin response nor auxin concentrations (particularly decrease in auxin concentrations), as *GH3::GUSa* staining is only an indication of the absence or presence auxin responses.

Alternatively, giant cells with higher metabolism and growth (de Almeida Engler et al., 1999) may had rapidly utilized auxin or may have conjugated auxins into different forms which were not targeted in our auxin quantification. A study by Doyle and Lambert (2003) proposed that *M. javanica* J2s secreted chorismate mutase protein about 3 days after infection into the cytoplasms of giant cell progenitors (procambium) to suppress auxin formation and plant cell vascularization. This in turn, resulted in the competition of nematode-derived chorismate mutase with plant chorismate mutase, which is thought to redirect the shikimate pathway into other phenolic production, such as the salicylic acid and flavonoid pathways (Doyle and Lambert, 2003). The differential local auxin concentrations in giant cells compared to neighboring cells is perhaps the key to the specific differentiation of selected procambium cells into giant cells. This theory is consistent with observations of auxin responsive promoters at early time points in the procambium prior to 3 days, followed by the loss of auxin response in giant cells at later dates (Hutangura et al., 1999, Karczmarek et al., 2004).

Nonetheless, the inhibition of auxin transport in infected roots, especially in segments basal of young galls (Figure 5.3) revealed that the redirection of auxin transport was a definite strategy to initiate a local auxin maximum in the root. Promoter-reporter and protein localization analyses of auxin influx transporters *AUX1* and *LAX3,* and auxin efflux transporters *PIN1, PIN2, PIN3, PIN4* and *PIN7* by Kyndt et al. (2016) demonstrated increased expression and localizations of these genes and transporters in young galls (3 and 7 days) to redirect auxin flow into the giant cells and/or the neighboring cells. In addition, the manipulation of auxin transport may be common in endoparasitic PPNs, as *Heterodera schachtii* regulated the expression and

localization of *PIN1* and *PIN3* at its feeding site (Grunewald et al., 2009) and secreted an effector protein, 19CO7 that interacted with LAX3 to enhance auxin influx.

Auxin responses in galls were transient, as evident by the loss of *GH3:GUSa* expressions in older galls aged 2 week old onwards, except at sites of lateral root primordia (Figures 5.9 and 5.10). The losses of auxin responsive promoter expressions were also observed in older galls (10 days onwards) in studies by Hutangura et al. (1999), Karczmarek et al. (2004), but were not observed by Cabrera et al (2014) in 13 and 21 days old galls. This highlights the limitations in comparative studies of auxin responsive promoters sampled in different plants infected with different *Meloidogyne* spp., and at different time points. Although auxin response had susbsided, auxin transport inhibition at the gall and tissues basal to the gall were still maintained at 4 weeks post inoculation (Figure 5.3). Additionally, auxin transport inhibition in basal root tissue at 4 weeks (80%) was stronger than auxin transport inhibition at 4 days (68%) (Table 5.2).

Even though auxin transport in infected roots was significantly higher than uninfected roots at 4 weeks post inoculation, (Table 5.1) auxin transport inhibition in root tissues basal to the gall showed high reduction (80%) in auxin transport (Table 5.2 and Figure 5.3). This suggests that the nematode continuously maintains and modulates auxin transport at the gall throughout its life cycle. In the study by Kyndt et al. (2016), the promoter activation of the aforementioned *PIN* genes was maintained from 7 days post inoculation to 14 days post inoculation. Although no studies have been done on mature galls, it seems likely the nematode had extensively modulated auxin transporters by 7 days post inoculation. Moreover, auxin quantification in mature galls at 4 weeks showed that IAA and IAA-Ala concentrations increased (although not significant) in infected roots when compared with uninfected roots, whereas a significant decrease in IAA-Trp concentration was observed (Figure 5.8). Lateral root initiation is preceded by the increase of auxin and auxin response, as well as auxin transport inhibition (De Smet et al., 2006), which may have been reflected as the increases in IAA and IAA-Ala (Figure 5.8). IAA-Trp is thought to inhibit IAA by interfering with IAA responses such as root gravitrophism, root growth inhibition caused by IAA and IAA induced lateral root growth (Staswick, 2009). Hence, lateral root initiation at the gall is likely IAA induced, as a result of auxin accumulation, accompanied by the reduction of IAA-Trp that possibly inhibited IAA action in lateral

roots of 4 week old galls. Furthermore, *GH3::GUSa* response in the lateral root primordium of galls and auxin transport inhibition in the tissue basal to the gall were observed, which were consistent with the initiation of lateral roots (Table 5.4). Nevertheless, this trend was not upheld at the prior time points at 24 hours and 4 days, with IAA and IAA-Trp trends sharing similar trends, which did not coincide with lateral root induction (Figure 5.8). Moreover, as IAA and IAA-Trp did not exhibit a clear inverse relationship, this suggests that nematodes were able to control auxin conjugation for specific functions, although this mechanism has never been studied. Auxin conjugates such as IAA-Ala and IAA-Val were synthesized upon high IAA exogenous treatment in pea and *Arabidopsis,* and were postulated to act as slow release storage forms of IAA (Barratt et al., 1999, Hangarter and Good, 1981, Venis, 1972). These auxin conjugates were possibly synthesized due to high auxin accumulation in the gall to be timely hydrolyzed back into IAA.

Auxin studies / Timeline	Auxin responsive promoter expression	Auxin content	Auxin transport
24 hours	Expression in vascular bundle and pericycle, similar to control roots. Very weak expression in root tip.	Significant decrease in IAA.	No change
4 days	Strong expression in the gall. Within the gall, strong expression in the pericycle and patchy expression in the cortex.	Slight decrease (not significant) in IAA and IAA-Val.	Extremely significant reduction in auxin transport, particularly in segment below inoculation site.
4 weeks	Very weak expression in the gall, except for sites where lateral roots emerged.	Increases in IAA and IAA-Ala. Significant decrease in IAA-Trp.	Significant increase in auxin transport, particularly in inoculated segment and the above segment. However, segment below inoculated segment showed extremely significant decrease in auxin transport.

Table 5.4: A summary of three auxin assays on nematode-infected roots of *M. truncatula* 2HA at 24 hours, 4 days and 4 weeks.

5.4.2. Polar auxin transport during gall formation is affected by isoflavonoid pathway modification

In spite of the significant variations in auxin transport in the wild-type 2HA and IFS transgenics at all time points (Figure 5.2 and Table 5.1), all four genotypes were able to produce galls (Figure 4.9, previously discussed in chapter 4). All genotypes demonstrated auxin transport inhibition in the basal tissues of galls at 4 days and 4 weeks , with the exception of IFSOE 10-3 plants demonstrating auxin transport inhibition only at 4 weeks post inoculation (Table 5.2), likely as a conserved mechanism to achieve local auxin maxima in the galls to promote cell division in the gall.

Overall, nematode-infected IFSi 42-7 and IFSi 101-2 roots showed similar auxin transport counts at 24 hours, 4 days and 4 weeks (Figure 5.2). Additionally, both IFSi lines produced comparable proportions of terminal and non-terminal galls (Table 5.3), and shared similar auxin transport capacity, thus resulting in nearly identical acropetal auxin transport patterns in galls (Figure 5.7). Nevertheless, IFSi 42-7 and IFSi 101-2 lines differed in relative change in auxin transport between uninfected and infected groups, with the former increasing its auxin transport when infected at 4 weeks, whereas the latter decreased its auxin transport when infected at the same time (Table 5.1). This indicates that the formation of non-terminal and terminal galls is possibly dependent on auxin transport changes at earlier time, sometime at 4 days, when both genotypes showed -86% and -80% inhibition, respectively, at segments basal to the gall (Table 5.2). This in turn, resulted in the blockage of auxin efflux in terminal galls, thereby resulting in the loss auxin transport gradients (Figure 5.7). Such extreme auxin transport inhibition at 4 days and the lack of auxin gradients may have contributed to the determinate growth of terminal galls, possibly by preventing stem cell niche reestablishment and the reformation of stem cells in quiescent centers (Sabatini et al., 1999). Future experiments incorporating exogenous applications of auxin transport inhibitors such as 1-N-naphthylphthalamic acid and 2,3,5-triiodobenzoic acid will be required to verify this. Therefore, the silencing of isoflavone pathway has appeared to result in stronger auxin transport inhibition around the gall segment, possibly from the utilization of alternate

flavonoids possibly, flavonols as auxin transport inhibitors (Brown et al., 2001, Jacobs and Rubery, 1988, Peer and Murphy, 2007, Yin et al., 2014). In contrast, 2HA and IFSOE 10-3 roots, with exclusively non-terminal galls exhibited strong auxin inhibitions in segments basal to the gall at -80% and -85% respectively at a later time, 4 weeks (Table 5.2). Although flavonols have been proposed as endogenous auxin transport inhibitors, the link between flavonol accumulation and changes in auxin transport capacities at 24 hours post inoculation is unclear. Previous flavonoid quantification in 2HA and IFS transgenics at 24 hours (and 6 weeks post nematode inoculation) (Chapter 4) showed that IFS transgenics produced higher amounts of k-3-rutinoside (Supplementary Figure 5.1), k-gluc (Supplementary Figure 5.2), and k-glyc-like (Supplementary Figure 5.4) compared with 2HA plants. However, auxin transport capacities at 24 hours in infected roots in all genotypes were unchanged despite the changes in flavonol concentrations (Figures 5.3-5.6). Nevertheless, these flavonols may have accumulated in IFSi transgenics at 4 days post inoculation and in IFSOE 10-3 plants at 4 weeks post inoculation respectively to increase auxin transport inhibition. Therefore, a detailed and systematic flavonoid and auxin transport quantification in infected roots, involving more time points will be required to further ascertain this.

On the other hand, the over-expression of isoflavonoids in IFSOE 10-3 roots resulted in delayed auxin transport inhibition, as noticeable changes in acropetal auxin transport occurred late at 4 weeks (Figure 5.6). This suggests that isoflavonoids either don't function or were the less preferred auxin transport inhibitors during gall formation, although indirect changes to other flavonoids cannot be excluded. Currently, there have been few studies on isoflavonoids as auxin transport inhibitors. An *in vitro* study by Mathesius (2001) showed that the isoflavonoid formononetin enhanced auxin turnover by peroxidase. Moreover, it is plausible that flavonoids in general play minor roles as auxin transport inhibitors during the gall initiation, as gall numbers and giant cell size in flavonoid deficient roots were unaffected by the lack of the complete flavonoid pathway (Wasson et al., 2009). Alternatively, PIN proteins, which are likely targets of flavonoids, may not be central in regulation of auxin efflux in galls as loss of function *pin* mutants, *pin 4* and *pin7* formed the same number of galls as control (Kydnt et al., 2016).

5.5 Conclusion

Young galls in *M. truncatula* 2HA exhibited local and transient increase in auxin response, which was accompanied by the inhibition of acropetal polar auxin transport at the site of gall formation. However, this pattern changed when galls matured, at which time a minimal auxin response was observed in the galls in spite of strong inhibition of auxin transport below the gall. Changes in auxin response did not correlate with measurements of auxin concentrations, suggesting differences in auxin signalling response and biosynthesis. Despite the modification of the isoflavonoid pathway either by silencing or over-expression in transgenic plants, these plants were still able to form galls. Silencing of the isoflavonoid pathway resulted in extreme auxin transport inhibition at 4 days, which likely resulted in the formation of some terminal galls. In contrast, the over-expression of isoflavonoid pathway resulted in delayed auxin transport inhibition at 4 weeks, and these plants never formed terminal galls. Whether the gall phenotype ws related to changes in auxin transport would need to be tested in future studies. These results suggested that modification of the isoflavonoid pathway affected auxin transport to some extent, but this did not prevent gall formation.

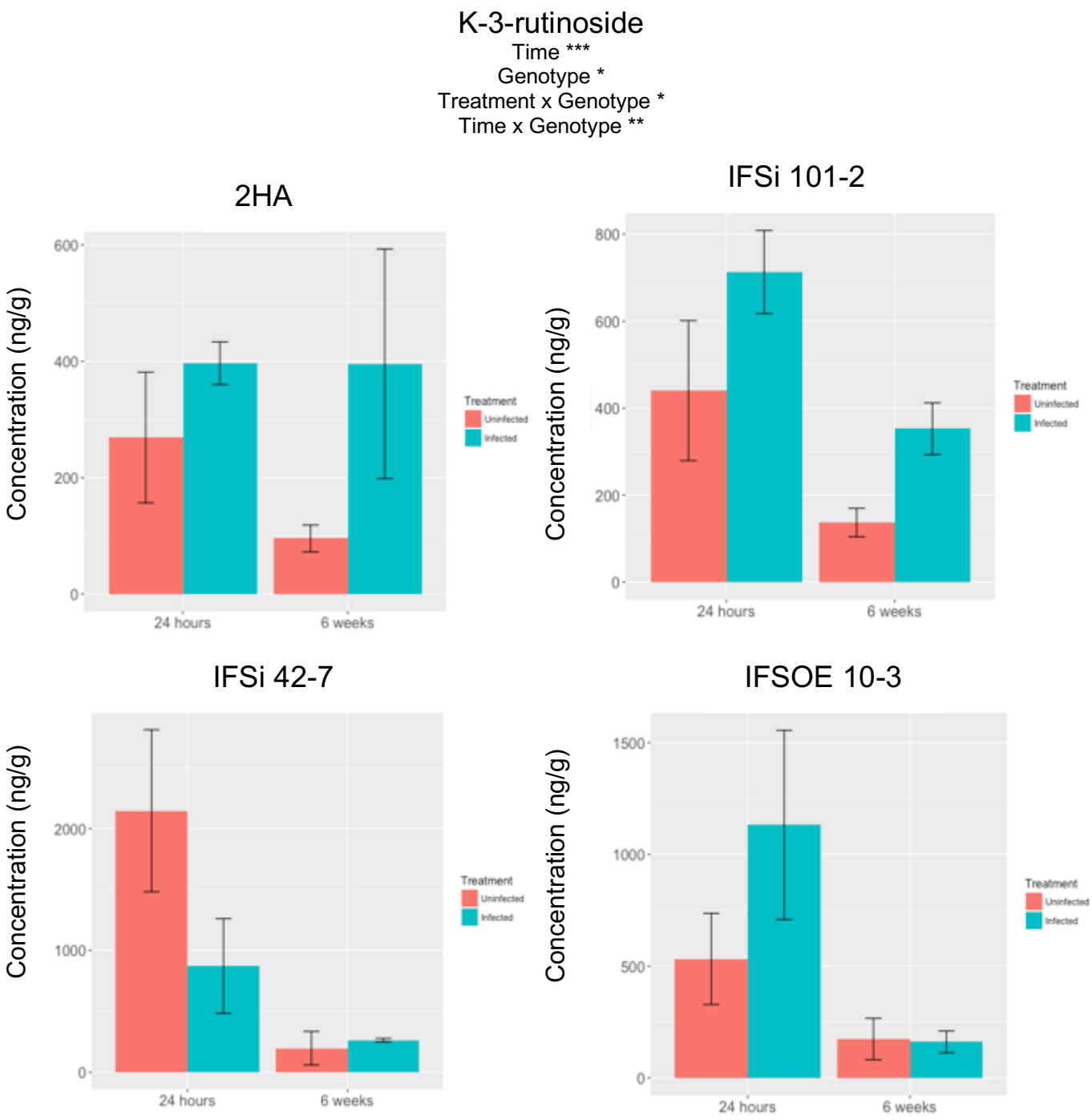

Supplementary Figure 5.1: K-3-rutinoside concentrations based on fresh weight in root segments of uninfected and *Meloidogyne javanica* infected roots (galls) of *Medicago truncatula* wild type cv. 2HA and isoflavone synthase transgenics, silenced lines, IFSi 101-2 and IFSi 42-7 and over-expression line, IFSOE 10-3. Statistical analyses were based on linear mixed analysis to test the effects of genotype, time, treatment factors and the interactions between these factors. Columns represent means. Error bars represent standard errors. (N=3)

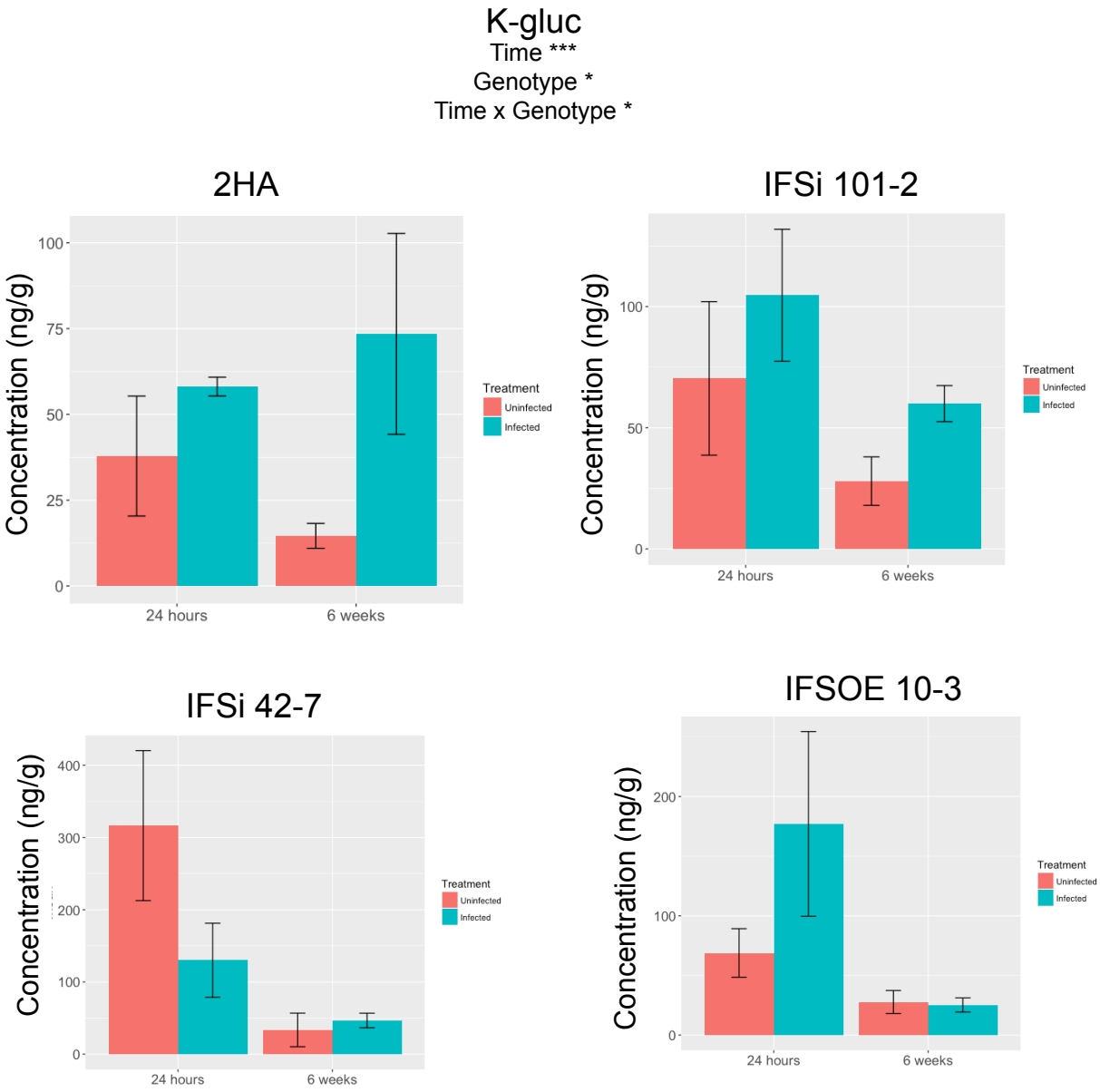

Supplementary Figure 5.2: K-gluc concentrations based on fresh weight in root segments of uninfected and *Meloidogyne javanica* infected roots (galls) of *Medicago truncatula* wild type cv. 2HA and isoflavone synthase transgenics, silenced lines, IFSi 101-2 and IFSi 42-7 and over-expression line, IFSOE 10-3. Statistical analyses were based on linear mixed analysis to test the effects of genotype, time, treatment factors and the interactions between these factors. Columns represent means. Error bars represent standard errors. (N=3)

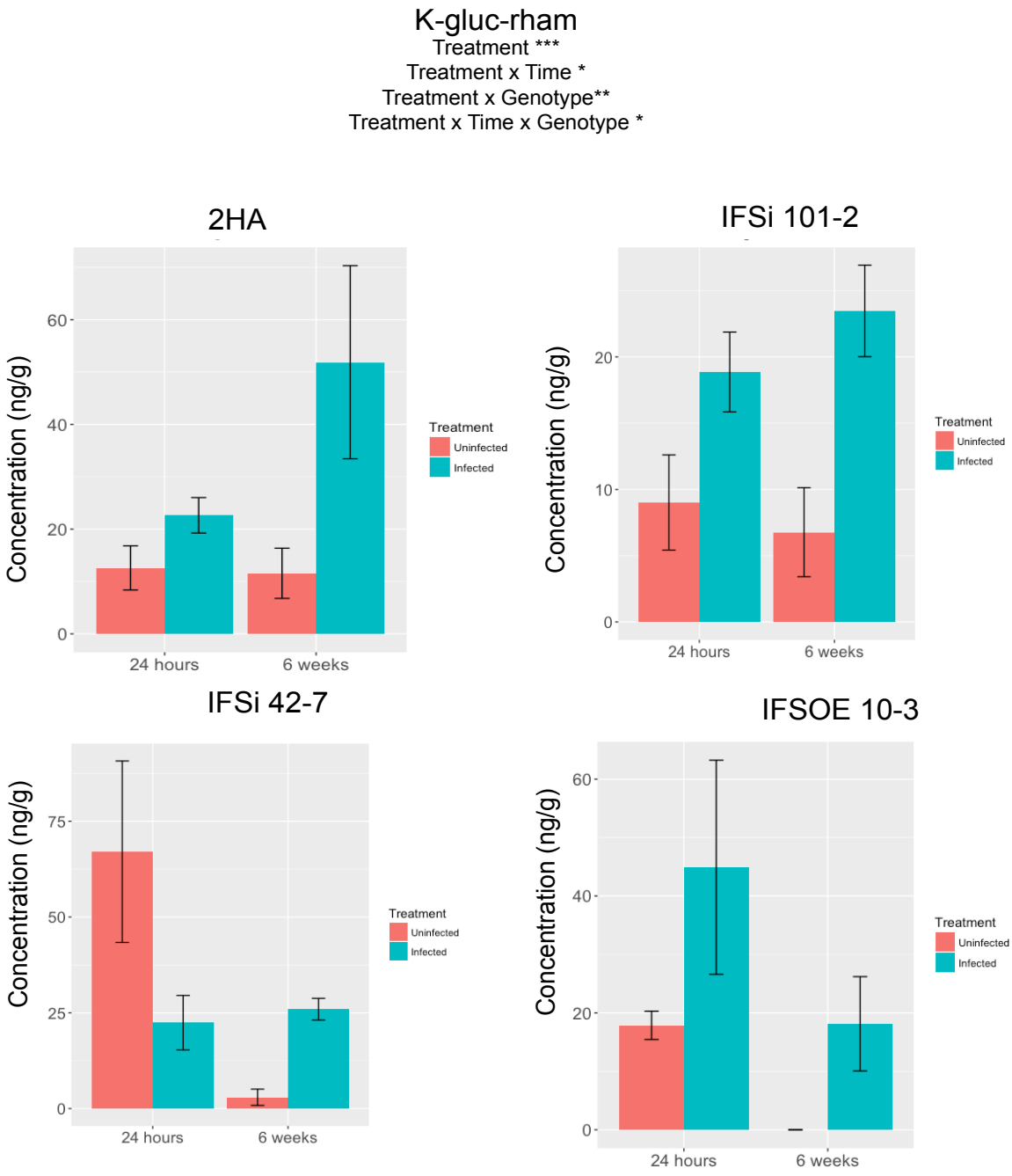

Supplementary Figure 5.3: K-gluc-rham concentrations based on fresh weight in root segments of uninfected and *Meloidogyne javanica* infected roots (galls) of *Medicago truncatula* wild type cv. 2HA and isoflavone synthase transgenics, silenced lines, IFSi 101-2 and IFSi 42-7 and over-expression line, IFSOE 10-3. Statistical analyses were based on linear mixed analysis to test the effects of genotype, time, treatment factors and the interactions between these factors. Columns represent means. Error bars represent standard errors. (N=3)

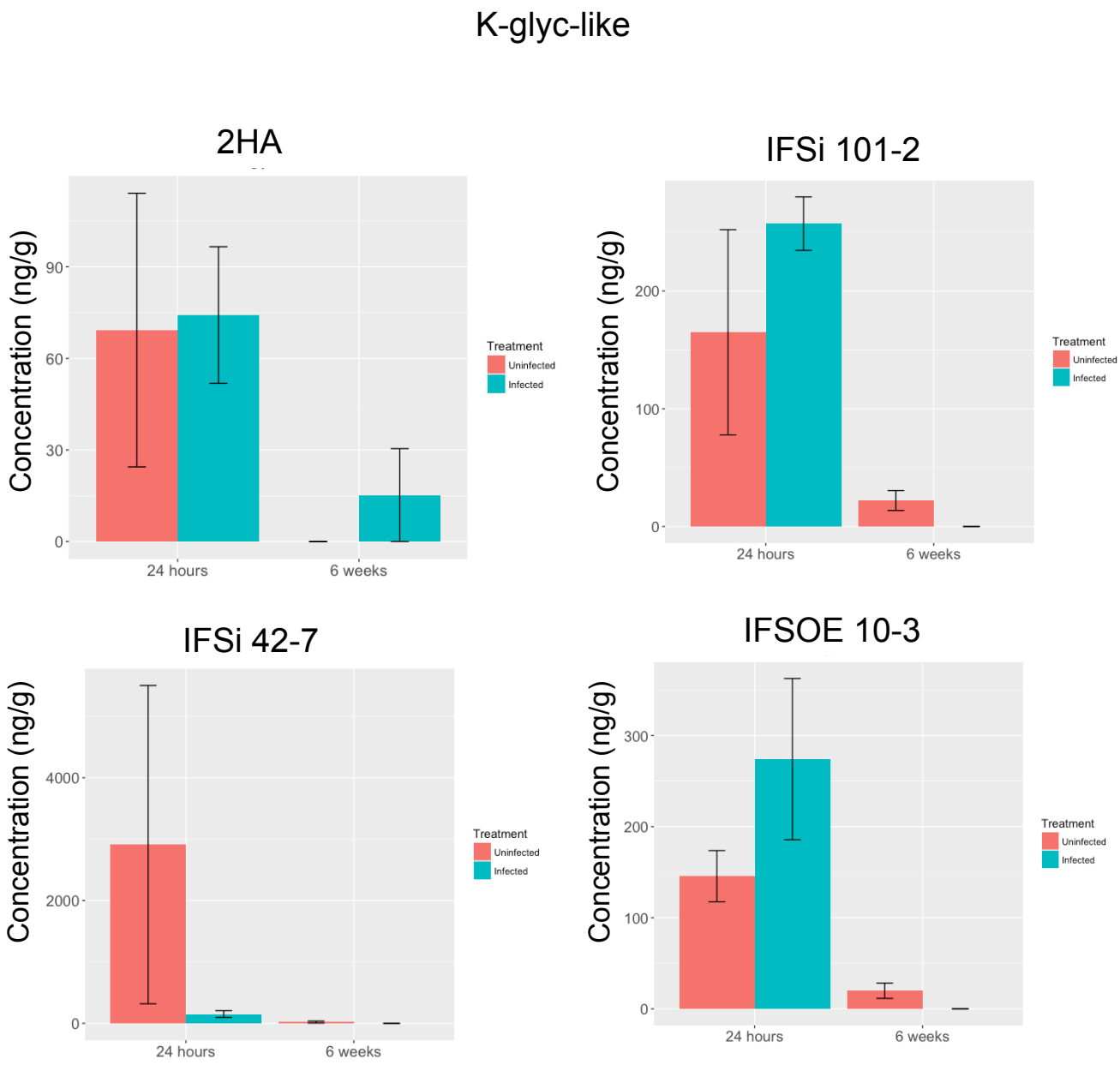

Supplementary Figure 5.4: K-glyc-like concentrations based on fresh weight in root segments of uninfected and *Meloidogyne javanica* infected roots (galls) of *Medicago truncatula* wild type cv. 2HA and isoflavone synthase transgenics, silenced lines, IFSi 101-2 and IFSi 42-7 and over-expression line, IFSOE 10-3. Statistical analyses were based on linear mixed analysis to test the effects of genotype, time, treatment factors and the interactions between these factors. Columns represent means. Error bars represent standard errors. (N=3)

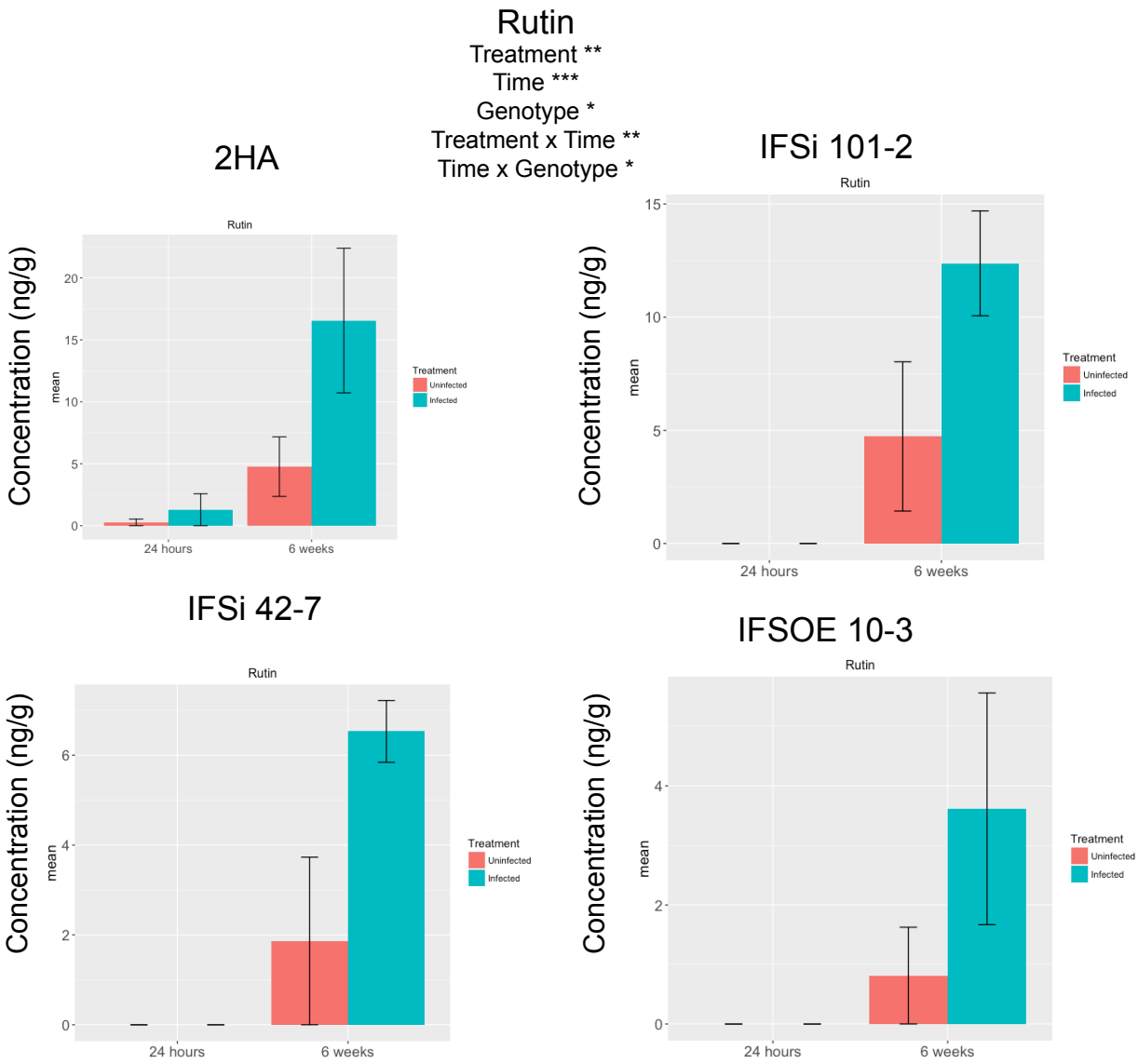

Supplementary Figure 5.5: Rutin concentrations based on fresh weight in root segments of uninfected and *Meloidogyne javanica* infected roots (galls) of *Medicago truncatula* wild type cv. 2HA and isoflavone synthase transgenics, silenced lines, IFSi 101-2 and IFSi 42-7 and over-expression line, IFSOE 10-3. Statistical analyses were based on linear mixed analysis to test the effects of genotype, time, treatment factors and the interactions between these factors. Columns represent means. Error bars represent standard errors. (N=3)

Chapter 6: General discussion

6.1. Isoflavonoids protect the host against root-knot nematode infection

6.2. Flavonoids play minor roles in auxin homeostasis in nematode galls

6.3. Overview of the role of flavonoids in plant-nematode interactions

6.4 Future directions

6.1. Isoflavonoids protect the host against root-knot nematode infection

Isoflavonoids, particularly medicarpin and afromosin showed bioactivities against *Meloidogyne javanica* J2s, by inhibiting motility and repelling them (Figures 4.20 and 4.26). Early induction of medicarpin and afromosin in IFSOE 10-3 transgenics at 24 hours post inoculation (Figure 4.14 and Supplementary Figures 4.17 and 4.20) likely resulted in better host outcome, with reduced nematode egg production, smaller galls, less galls and minimal biomass loss from nematode infection (Figures 4.8, 4.9 and 4.10). On the other hand, accession F83005, which accumulated the highest amount of medicarpin at 6 weeks (Supplementary Figure 4.20) showed reduced nematode egg production (Figure 4.2). Although these transgenics, accessions and cultivars showed variations in flavonoid regulation and production, both of these isoflavonoids were consistently upregulated during infection (Figures 4.4 and 4.13). Furthermore, isoflavonoids also accumulated in the event of other PPN and pathogenic infections such as root-lesion and stem nematodes (Baldridge et al., 1998, Cook et al., 1995, Edwards et al., 1995) and fungal infections *eg*. of *Rhizoctonia solani, Phoma medicaginis* and *Verticillium albo-altrum* (Blount et al., 1992, Guenoune et al., 2001, Jasiński et al., 2009, Latunde-Dada and Lucas, 1985).

Despite evidence of the roles of isoflavonoids in defence, the underlying mechanism of their broad-spectrum antimicrobial activity remains elusive. Medicarpin was demonstrated to inhibit oxygen respiration in *C. elegans,* the mouse lymphotic leukemia cell line L 1210 and filamentous fungi, but not bacteria (Stadler et al., 1994), indicating that medicarpin specifically interferes with cellular metabolism in eukaryotes. Medicarpin and afromosin also likely modulate reactive oxygen species (ROS) (Agati et al., 2012, Brunetti et al., 2013), although it has never been established if they catalyse or quench ROS production or chelate metals. The increase in ROS production to result in hypersensitive response to *M. javanica* would be advantageous for such obligate biotrophic interaction to prevent the nematode from establishing a feeding site, whereas the activity of chelating metals may affect enzymatic functions in the nematode. Interestingly, although the different genotypes of *M. truncatula* in our experiments accumulated very high levels of medicarpin and

afromosin, up to 300 ng/g plant fresh weight (Supplementary Figures 4.17, 4.18, 4.19 and 4.20), the nematodes persisted and were able to lay eggs. This suggests that root-knot nematodes likely acquired detoxifying enzymes to reduce isoflavonoid toxicity, particularly as sedentary parasitic nematodes cannot evade the presence of isoflavonoids. The modification of flavonoids by pathogens has been reported in fungi, *Pyricularia oryzae* and *R. solani,* which metabolised sakuranetin produced by rice (Katsumata et al., 2018), and *Nectria haematococca* demethylated the pea flavonoid pisatin (Tegtmeier and VanEtten, 1981). Flavonoid metabolism in nematodes has also been observed by some studies. The nematode model, *Caenorhabiditis elegans* can conjugate genistein into 11 metabolites (Soukup et al., 2012). Likewise, *Globodera rostochiensis* and *G. pallida* can convert quercetin and kaempferol into a non-plant phenolic, quercentagetin (Vlachopoulos and Smith, 1993). As opposed to sedentary parasitic stages, the pre-parasitic J2s can actively detect and evade isoflavonoids present in the soil, as shown by the results of our chemotaxis assays. This behavioural change must be preceded by chemoperception of compounds in the soil using sensory organs, the amphids in the head, and possibly through the phasmid in the tail (Perry, 1996). Although not much is known about chemoperception in *Meloidogyne*, our experiments indicated that J2s can detect and respond to very low concentrations of flavonoids, as low as 10^{-11} M (Figure 4.26), possibly by klinotaxis, the successive comparisons of concentrations in time by side-to-side displacement of receptors (Curtis et al., 2009). Flavonoids, which are exuded in the soil (most studies detected 10^{-9} M to 10^{-6} M concentrations in hydroponics) (Cesco et al., 2010) can therefore reduce new nematode infections by making the roots repellent to J2s. However based on the results of J2 chemotaxis assay to IFSOE 10-3 root exudate (Figure 4.28), J2s likely also integrate signals from other metabolites, sugar, amino acids and etc to determine host suitability. This could be further studied by nematode penetration assays using acid fuschin stain to determine the number of J2s that have decided to invade the root, post-chemoperception. In addition, J2s may overcome initial flavonoid avoidance after becoming habituated to the avoidance response, as observed in *C. elegans* (Rose and Rankin, 2001).

The accumulation of isoflavonoids, particularly medicarpin, also was also associated with reduced nematode fertility, whereby early or higher accumulation in IFSOE 10-3 and F83005 respectively resulted in reduced egg production. It is unclear

if such flavonoids impacted the quality of feeding sites, therefore reduced nutrient availability to feeding nematodes and/or skewed the male to female ratio, as nutrionial deficiency increases male population (Grundler et al., 1991) and/or delayed nematode devlopment. Alternatively, very high amounts of isoflavonoids can continue to accumulate past 4 weeks, as measured in our experiments to create lethal concentrations that could not be readily detoxified by the sedentary nematodes. *In vitro* submersion of *C. elegans* in flavonoids demonstrated that flavonoids such as quercetin and quercetin-3-*O*-glucoside extended *C. elegans* lifespan at lower concentrations, 100- 200μM and 10-25 μM respectively, but decreased lifespan at higher concentrations above 250μM and 50-200 μM respectively(Dueñas et al., 2013, Pietsch et al., 2011). Additionally, long-term and trans-generational effect of isoflavonoids on *Meloidogyne* health and fitness has never been studied and should be tested by examining J2 recovery after flavonoid treatment for a specified duration and infection capacities in offspring of adult female nematodes treated with high levels of pterocarpans.

Defensive flavonoids are not limited to medicarpin and afromosin, but other flavonoids classes can also play similar roles, albeit with less efficacy, such as the flavonols quercetin and kaempferol (repelled nematodes but did not inhibit motility), isoflavonoids genistein, daidzein and formononetin (variable activities in repellence and motility) and the flavone, 7,4'-DHF (weak motility inhibitor) (Figures 4.20 and 4.26). As the isoflavonoid pathway has been reported in four classes of the plant kingdom, Bryopsida, Pinopsida, Liliopsida and Magnoliopsida (Lapčík, 2007, Mackova et al., 2006, Reynaud et al., 2005), the use of defensive isoflavonoids against *Meloidogyne* spp. may be widespread. This presents the opportunity to bio-engineer crops with high producing isoflavonoids to reduce root-knot nematode infection.

On the other hand, reduced flavonoid levels may adversely affect nematode infection. IFSi 101-2 roots produced significantly less upstream flavonoids (Figure 4.7) and downregulated most flavonoids during infection (Figure 4.14) had the lowest nematode egg production (Figure 4.10) and smaller galls (Figure 4.9). Specific flavonoids may possibly be utilised by the nematode to enhance its egg production and/or increase the quality of giant cells for higher nutritional content. Nonetheless, this hypothesis requires more systematic studies into gall size and egg production. For

example, Wuyts et al. (2006a) reported that *Arabidopsis tt3, tt4, tt5* and *tt7* mutants did not show changes in *M. incognita* reproduction, while this study did not examine gall phenotypes; on the other hand, Wasson et al. (2009), who observed reduced pericycle cell expansion in *M. javanica* galls, did not count egg production. Interestingly, reduced reproduction of root knot nematodes in tomato was associated with expression of a cell wall peroxidase (Portillo et al., 2013). As some flavonoids can inhibit or activate peroxidases (Mathesius, 2001), it would be interesting to test in the future whether the reduced numbers of eggs in the IFSi 101-2 transgenic plants were associated with changes in peroxidase expression.

In future, a more systematic study of nematode infection phenotypes in flavonoid mutants will be necessary. This includes a more systematic evaluation of off-target effects of modifying the flavonoid pathway by mutation or gene silencing, eg. Indirect effects could includes changes to cell wall composition and flavonoids and lignings share common precursors (Besseau et al., 2007). In addition, it would be interesting to inhibit specific end products of the flavonoid pathway, for example the synthesis of medicarpin or afromosin specifically.

6.2. Flavonoids play minor roles in auxin homeostasis homeostasis in nematode gall

Gall organogenesis at 4 days post inoculation was preceded by the induction of an auxin response (Figure 5.9) and the inhibition of acropetal polar auxin transport (Figure 5.3), which may be regulated by flavonoids. Hutangura et al. (1999) first suggested that flavonoids were involved in auxin modulation in the gall as increased flavonoid reporter expression coincided with auxin response reporter expression.

Linear regression analyses found correlations between auxin and flavonoid concentrations in nematode infected wild-type *M. truncatula* 2HA (Table 6.1). IAA-Ala was positively correlated with nar-7-gluc, gen-7-gluc, DHF glyc-like, but negatively correlated with form-7-gluc and compound 448 (Figure 6.1). IAA-Trp showed a positive linear relationship with gen-7-gluc (Figure 6.2), whereas IAA-Val showed an extreme negative linear relationship with 7,4'-DHF (Figure 6.3). Flavonoids that are positively correlated to auxin levels, such as nar-7-gluc, gen-7-gluc and DHF glyc-like may behave as auxin transport inhibitors or prevent auxin breakdown. *Vice versa*, flavonoids that showed inverse relationships with auxins, such as form-7-gluc, compound 448 and 7,4'-DHF may accelerate auxin breakdown. A flavonoid may have a broad action of several flavonoids or play multiple roles as shown by the positive correlations between gen-7-gluc to IAA-Ala and IAA-Trp. Alternatively, multiple flavonoids may work in tandem to exert additive or regressive effects.

While the correlations found here might point to interesting flavonoid candidates involved in auxin homeostasis, future experiments could establish a mre direct relationship by tersgeting more specific flavonoid products through genetic modification, and then testing galls formed on these transgenic plants for altered auxin content, auxin response and/or auxin transport.

Although naringenin, genistein and naringin were reported to stimulate IAA breakdown by oxidase, the former two also increased acropetal auxin transport, whereas the latter inhibited acropetal auxin transport (Stenlid, 1963, Stenlid, 1968, Stenlid, 1976). 7,4'-DHF and its derivative had been shown *in vitro* to reduce IAA breakdown by peroxidase to accumulate auxin during nodulation (Mathesius, 2001),

whereas another study by Schwalm et al. (2003) proposed that during Agrobacterium-induced tumor formation., 7,4'-DHF acted as an auxin transport inhibitor, which reduced auxin transport and therefore reduced auxin response in white clover plants transformed with the *GH3::GUSa* auxin reporter. Mathesius (2001) also reported that formononetin adversely affected auxin accumulation by accelerating its breakdown by peroxidase. These studies highlight the complexities and limitations in extrapolating the relationship between an auxin transport inhibitor and its role with IAA oxidase using *in vitro* experiments, as well as the different roles between aglycones and their glycosides. Moreover, as all studies on the effect of flavonoids on auxin transport had only utilised radioactive IAA, resultantly not much is known on how flavonoids affect other forms of auxins. Future experiments to verify the role of these flavonoids as auxin transport inhibitors should include exogenous applications of these flavonoids, either by flooding or spot inoculation, followed by auxin transport measurements using radioactive auxins, including conjugates (Rashotte et al., 2003). Likewise, the study of the effects of flavonoids on auxin breakdown by fluorometric quantification of auxin breakdown by horseradish peroxidase when co-incubated with flavonoids should also expand to include auxin conjugates.

In spite of kaempferol, quercetin, apigenin and bestatin being prime candidates as auxin transport inhibitors, based on their ability to reduce IAA transport and in displacing synthethic auxin transport inhibitor, NPA (Jacobs and Rubery, 1988, Murphy et al., 2000b), our experiments failed to detect high levels of kaempferol, quercetin and apigenin, whilst bestatin was not targeted (Figure 3.3). Instead, kaempferol glycosides and an apigenin glycoside, apigenin-7-*O*-neohesperidoside were detected, although their concentrations did not correlate with neither the timing of auxin transport inhibition at 4 days (Figure 5.9) nor changes in auxin transport (Figure 5.3). However, some kaempferol glycosides may be involved in maintaining auxin transport inhibition in mature galls (more than 4 weeks old). The kaempferol glycoside, k-gluc-rham was consistently upregulated in seven different *M. truncatula* genotypes (F83005, DZA045, A17, 2HA, IFSi 101-2, IFSi 42-7 and IFSOE 10-3) late in infection, at 6 weeks (Figures 4.4 and 4.13) and was strongly influenced by nematode infection (Figure 4.31). Strong auxin transport inhibition during late infection in IFSOE 10-3 galls (Figure 5.6 and Table 5.1) may be the result of the upregulation of flavonols glycosides such as k-gluc, k-3-rutinoside, k-glyc-like, k-

gluc-rham and rutin (Figure 4.14). Flavonol aglycones, which were applied exogenously on the plant, could be glycosylated into glycosides *in planta* to act as auxin transport inhibitors. Kaempferol-3-*O*-7-*O*-rhamnoside was implicated as an auxin transport regulator as the accumulation of this flavonol led to developmental changes associated with reduced auxin transport, such as dwarfed growth and slow gravitropic response (Yin et al., 2014).

The modification of *IFS* genes suggests that isoflavonoids are unlikely to be involved as auxin transport inhibitors for gall organogenesis, as higher levels of isoflavonoids in IFSOE 10-3 roots showed delayed auxin transport inhibition during nematode infection, and *vice versa* for IFSi 42-7 and IFSi 101-2 roots which showed extreme auxin transport inhibition in young galls (Figures 5.4, 5.5 and 5.6).

Generally, flavonoids are not necessary for auxin transport modulation during gall formation because flavonoid deficient roots were able to form galls (Wasson et al., 2009, Wuyts et al., 2006a). This may be due to the use of different strategies by the plant to regulate PIN proteins such as the use of different interacting proteins eg. aminopeptidases (Murphy et al., 2000b) or inhibitors, e.g. cis-cinnamic acid (Steenackers et al., 2017), by the disruption of PIN recycling via GNOM, by the disruption of PIN localisation through PINOID protein kinases or the regulation of PIN abundance using MODULATOR OF PIN (MOP) proteins (Titapiwatanakun and Murphy, 2009). Moreover, as flavonoids are non-essential endogenous modulators of polar auxin transport (Brown et al., 2001, Buer and Muday, 2004, Peer and Murphy, 2007), the nematodes likely target essential endogenous regulators to achieve precise auxin transport manipulation. In addition, nematodes may bypass the use of PIN transporters to regulate auxin efflux from the gall, hence do not require flavonoids to modulate PIN transporters. Mutations in *pin1, pin2, pin3, pin4* and *pin7 Arabidopsis* single mutants did not abolish gall formation, and *pin4* and *pin7* mutants formed the same number of galls as wild-type *Arabidopsis* (Kyndt et al., 2016). Lastly, flavonoid accumulation may coincide with auxin accumulation in the gall (Hutangura et al., 1999) as a consequent of increased auxin levels, instead of the scenario in which auxin accumulated due to flavonoid inhibition of PIN proteins. For example, exogenous application of 1μM IAA on *Arabidopsis* root tips resulted in an increase of certain flavonoids (Buer and Muday, 2004).

Auxins / Flavonoids	IAA-Ala	IAA-Trp	IAA-Val
Nar-7-gluc	0.0312*	0.14	0.322
Gen-7-gluc	0.0135*	0.045*	0.211
Form-7-gluc	0.0354*	0.958	0.667
7,4'-DHF	0.877	0.298	<0.0001***
DHF glyc-like	0.0257*	0.414	0.866
448	0.007**	0.667	0.536

Table 6.1: P-values of simple linear regressions of the relationship between flavonoid and auxin concentrations (log 10) in *Medicago truncatula* cv. 2HA in uninfected and infected roots at 6 hours, 24 hours, 4 days, 2 weeks and 4 weeks post inoculation with *Meloidogyne javanica*. Asterisk indicates statistically significant ($p<0.05$).

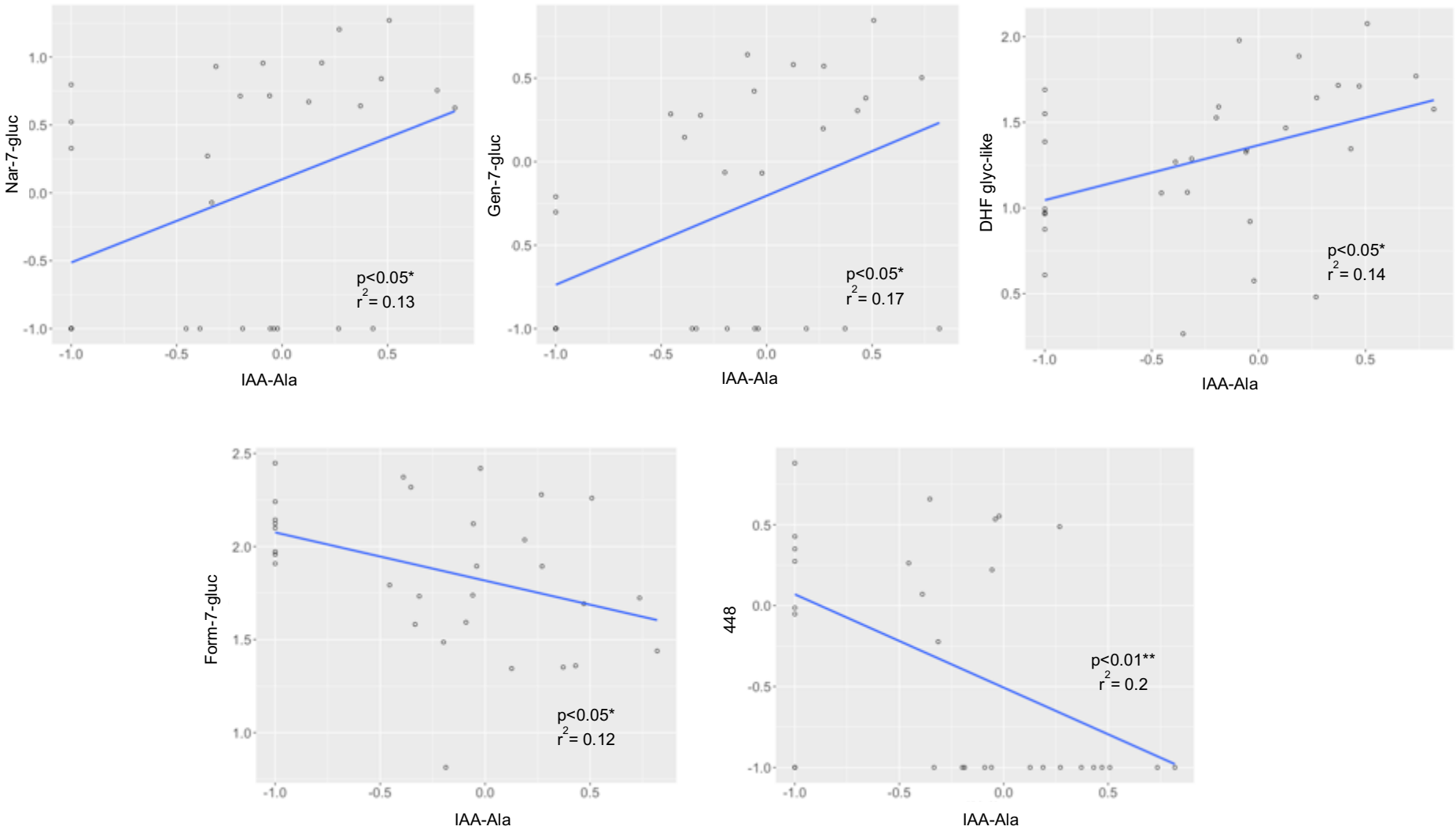

Figure 6.1: Scatter plots of flavonoids with statistically significant linear relationships with IAA-Ala in uninfected and nematode infected *Medicago truncatula* cv. 2HA roots at 6 hours, 24 hours, 4 days, 2 weeks and 4 weeks.

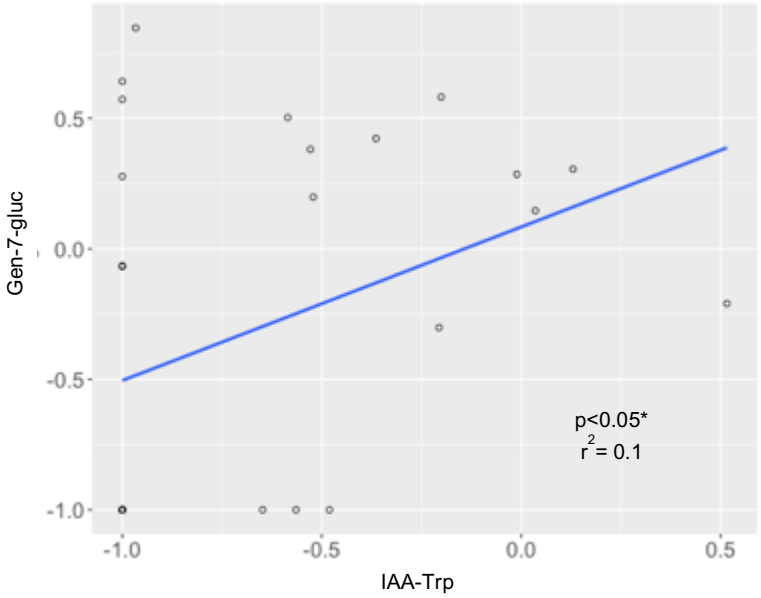

Figure 6.2: Scatter plot of the positive linear relationship between gen-7-gluc and IAA-Trp in uninfected and nematode infected *Medicago truncatula* cv. 2HA roots at 6 hours, 24 hours, 4 days, 2 weeks and 4 weeks.

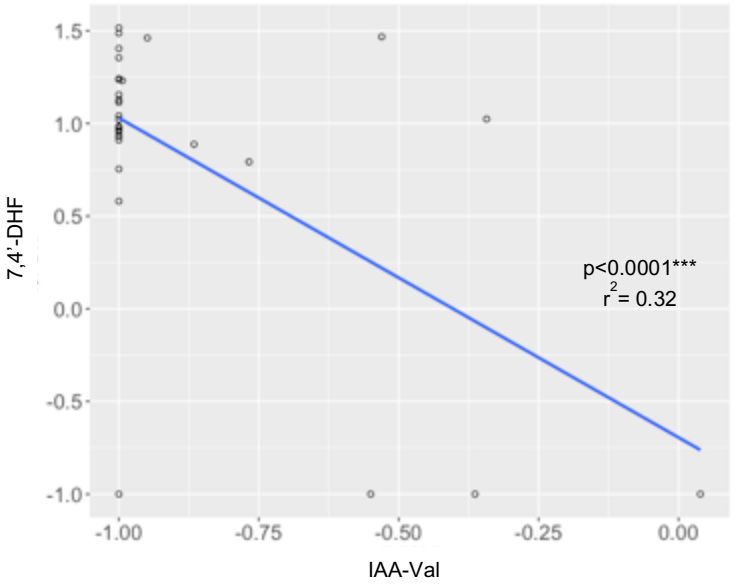

Figure 6.3: Scatter plot of the negative linear relationship between 7,4'-DHF and IAA-Val in uninfected and nematode infected *Medicago truncatula* cv. 2HA roots at 6 hours, 24 hours, 4 days, 2 weeks and 4 weeks.

6.3. Overview of flavonoids in plant-nematode interactions

Flavonoids are metabolites that play multiples roles in the plant, from important functions such as regulating plant development, cell cycle, pollen fertility, nodulation, stress and defence response to aesthetic roles as pigments (Winkel-Shirley, 2001). This versatility presents a unique opportunity for root-knot nematodes to manipulate multiple plant functions by targeting a single pathway that is ubiquitous throughout the plant kingdom and may enable root-knot nematodes to infect a broad range of plants. In our experimental context, we present a model on how flavonoids mediate the plant-nematode interactions (Figure 6.4). Defense-related flavonoids, particularly the isoflavonoids medicarpin and afromosin reduced nematode motility and reduced nematode chemotaxis (Chapter 4). *M. truncatula* roots that exude high concentrations of isoflavonids, such as IFSOE 10-3 plants, are therefore likely to be less attractive hosts, although this would have to be tested in soil environments in the future. *In planta,* continuous accumulation of isoflavonoids around the gall in which the nematode resides may negatively alter nematode fitness. Furthermore, plants that accumulate isoflavonoids either early during infection or extremely high concentrations of isoflavonoids showed reduced nematode egg production. The isoflavonoids possibly affected nematode reproduction directly by being toxic to the adult female nematode or indirectly by altering the female to male sex ratios (males do not contribute to reproduction as females reproduce asexually by mitotic parthenogenesis (Truong, 2015 #659)). Flavonoids may be recruited during gall maturation to reduce auxin efflux from the gall. Flavonol glycosides such as k-gluc-rham and rutin were upregulated at this stage, possibly to act as auxin transport inhibitors, to likely contribute to the accumulation of auxin and associated expansion of pericycle and cortical cells to accommodate the increase in size of adult females.

Whilst regulating the flavonoid pathway is akin to "killing two birds with one stone", there are limitations to this paradigm. Firstly, although flavonoids are common in all land plants, they are not equal- different plants have evolved additional pathways such as phlobaphenes in sorghum, maize and gloxinia, and stilbenes in grape, peanut and pine (Winkel-Shirley, 2001). Besides that, the same flavonoids may be utilised differently in another plant species. Secondly, root-knot nematodes do not

require the presence of flavonoids to infect the plant. This is evident in flavonoid deficient *M. truncatula* and *Arabidopsis* which formed galls and supported nematode reproduction (Wasson et al., 2009, Wuyts et al., 2006a).

In conclusion, our study reveals that flavonoids mediate the host defence responses against invading root-knot nematodes. Isoflavonoids and pterocarpans are likely the major classes of defensive flavonoids and the increased production of these flavonoids is associated with improved host outcomes. However, these flavonoids are unlikely utilised as auxin transport modulators as the silencing and over-expression of *IFS* gene(s) showed phenotypes inconsistent with auxin transport inhibition.

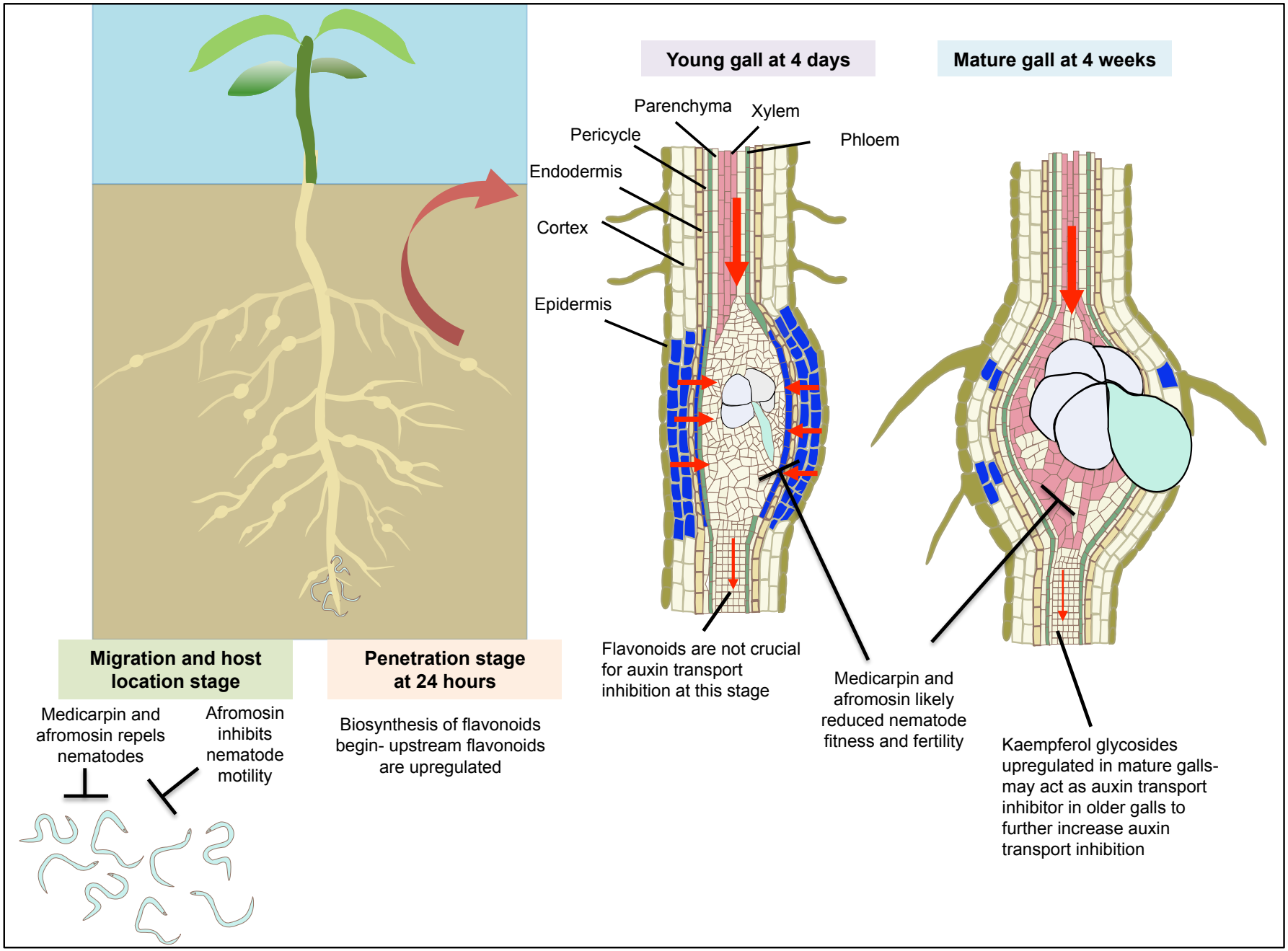
Young gall at 4 days
Mature gall at 4 weeks
Parenchyma
Xylem
Pericycle
Phloem
Endodermis
Cortex
Epidermis
Migration and host location stage
Penetration stage at 24 hours
Medicarpin and afromosin repels nematodes
Afromosin inhibits nematode motility
Biosynthesis of flavonoids begin- upstream flavonoids are upregulated
Flavonoids are not crucial for auxin transport inhibition at this stage
Medicarpin and afromosin likely reduced nematode fitness and fertility
Kaempferol glycosides upregulated in mature galls- may act as auxin transport inhibitor in older galls to further increase auxin transport inhibition

Figure 6.4: A schematic diagram illustrating how flavonoids mediate the interaction between *Medicago truncatula* and *Meloidogyne javanica*. Flavonoids can act as the first line of defence by repelling and inhibiting the motility of pre-parasitic J2s present in the rhizosphere. Flavonoid biosynthesis is activated upon J2 penetration and migration inside the root. Isoflavonoids such as medicarpin and afromosin accumulate in the root and likely continually act against sedentary nematodes. Auxin response is induced (indicated as dark blue) at 4 days old young galls and auxin transport (indicated as red arrow; width is proportional to auxin transport capacity) was redirected to the gall. Isoflavonoids are unlikely involved as auxin transport inhibition at this stage. During gall maturation at 4 weeks, flavonoids such as kaempferol glycosides may be additionally recruited to maintain auxin transport inhibition.

6.4. Future directions

Whilst the genetic modifications made to the isoflavonoid pathway in this thesis did not result in complete repression or overexpression of the pathway, it has led to the suggestion of several candidate flavonoids correlated with changes in gall formation. These flavonoids likely play roles in defense or gall development, as well as nematode reproduction. To test the specific role of these candidate flavonoids, it will be necessary to specifically alter parts of the flavonoid pathway to make more targeted changes in flavonoid composition. For example, it would be interesting to silence or overexpress the gene encoding vestitone reductase, the enzyme catalysing the formation of medicarpin. It would be expected that plants overexpressing vestitone reductase are more resistant to nematode infection.

Another test that should be done is whether alteration of flavonoid exudation in host plants actually leads to altered attraction of nematodes to the root. While chemotaxis assays suggested that certain flavonoids have repellent activity against nematodes, this has not been tested under soil conditions, where nematodes would have to navigate complex gradients of flavonoids in the soil.

In addition, it would be insightful to characterise the action of flavonoids on nematodes more directly. The motility assays suggested that certain flavonoids inhibited nematode motility. Although motility assay could indicate effects of flavonoids on nematode locomotion directly, it is also possible that altered motility indicates direct toxicity to nematodes. Transcriptomic analysis of nematodes treated with specific flavonoids might reveal specific target genes in the nematode. For example, while flavonoids might inhibit movement of nematodes towards the root, a toxicity effect could explain reduced motility as well as effects on nematode reproduction observed here.

Bibliography

ABAD, P. & WILLIAMSON, V. M. 2010. Plant nematode interaction: a sophisticated dialogue. *Advances in Botanical Research,* Volume 53**,** 147-192.

ABAWI, G. S., VAN ETTEN, H. D. & MAI, W. F. 1971. Phaseollin production induced by *Pratylenchus penetrans* in *Phaseolus vulgaris Journal of Nematology,* 3**,** 301.

ABSMANNER, B., STADLER, R. & HAMMES, U. Z. 2013. Phloem development in nematode-induced feeding sites: The implications of auxin and cytokinin. *Frontiers in Plant Science,* 4.

AGATI, G., AZZARELLO, E., POLLASTRI, S. & TATTINI, M. 2012. Flavonoids as antioxidants in plants: Location and functional significance. *Plant Science,* 196**,** 67-76.

BADRI, D. V., LOYOLA-VARGAS, V. M., BROECKLING, C. D., DE-LA-PEÑA, C., JASINSKI, M., SANTELIA, D., MARTINOIA, E., SUMNER, L. W., BANTA, L. M., STERMITZ, F. & VIVANCO, J. M. 2008. Altered profile of secondary metabolites in the root exudates of *Arabidopsis* ATP-binding cassette transporter mutants. *Plant Physiology,* 146**,** 762-771.

BALASUBRAMANIAN, M. & RANGASWAMI, G. 1962. Presence of indole compound in nematode galls. *Nature,* 194**,** 774-775.

BALDRIDGE, G., D., O'NEILL, N. R. & SAMAC, D. A. 1998. Alfalfa (*Medicago sativa* L.) resistance to the root-lesion nematode, *Pratylenchus penetrans*: defense-response gene mRNA and isoflavonoid phytoalexin levels in roots. *Plant Molecular Biology,* 38**,** 999-1010.

BARCALA, M., GARCÍA, A., CABRERA, J., CASSON, S., LINDSEY, K., FAVERY, B., GARCÍA-CASADO, G., SOLANO, R., FENOLL, C. & ESCOBAR, C. 2010. Early transcriptomic events in microdissected Arabidopsis nematode-induced giant cells. *The Plant Journal,* 61**,** 698-712.

BARRATT, N. M., DONG, W., GAGE, D. A., MAGNUS, V. & TOWN, C. D. 1999. Metabolism of exogenous auxin by *Arabidopsis thaliana*: Identification of the conjugate *Nα-* (indol-3-ylacetyl)-glutamine and initiation of a mutant screen. *Physiologia Plantarum,* 105**,** 207-217.

BEKAL, S., NIBLACK, T. L. & LAMBERT, K. N. 2003. A chorismate mutase from the soybean cyst nematode *Heterodera glycines* shows polymorphisms that correlate with virulence. *Molecular Plant- Microbe Interactions,* 16**,** 439-449.

BESSEAU, S., HOFFMANN, L., GEOFFROY, P., LAPIERRE, C., POLLET, B. & LEGRAND, M. 2007. Flavonoid accumulation in Arabidopsis repressed in lignin synthesis affects auxin transport and plant growth. *The Plant Cell,* 19**,** 148-162.

BIRD, A. F. 1959a. The attractiveness of roots to the plant parasitic nematodes *Meloidogyne javanica* and *M. hapla*. *Nematologica***,** 322-335.

BIRD, A. F. 1959b. Development of the root-knot nematodes *Meloidogyne javanica* (Treub) and *Meloidogyne hapla* Chitwood in tomato. *Nematologica***,** 31-42.

BIRD, A. F. 1961. The ultrastructure and histochemistry of a nematode-induced giant cell. *Journal of Biophysical and Biochemical Cytology,* 11**,** 701-715.

BIRD, A. F. 1962. The inducement of giant cells by *Meloidogyne javanica*. *Nematologica,* 8**,** 1-10.

BIRD, A. F. 1974. Plant response to root-knot nematode. *Annual Review of Phytopathology***,** 69-85.

BIRD, A. F. 1987. Moulting of parasitic nematodes. *International Journal for Parasitology,* 17**,** 233-239.
BIRD, D. M. 2004. Signaling between nematodes and plants. *Current Opinion in Plant Biology,* 7**,** 372-376.
BIRD, D. M. & KALOSHIAN, I. 2003. Are roots special? Nematodes have their say. *Physiological and Molecular Plant Pathology,* 62**,** 115-123.
BLASCO, H., BŁASZCZYŃSKI, J., BILLAUT, J. C., NADAL-DESBARATS, L., PRADAT, P. F., DEVOS, D., MOREAU, C., ANDRES, C. R., EMOND, P., CORCIA, P. & SŁOWIŃSKI, R. 2015. Comparative analysis of targeted metabolomics: Dominance-based rough set approach versus orthogonal partial least square-discriminant analysis. *Journal of Biomedical Informatics,* 53**,** 291-299.
BLILOU, I., XU, J., WILDWATER, M., WILLEMSEN, V., PAPONOV, I., FRIML, J., HEIDSTRA, R., AIDA, M., PALME, K. & SCHERES, B. 2005. The PIN auxin efflux facilitator network controls growth and patterning in Arabidopsis roots. *Nature,* 433**,** 39.
BLOUNT, J. W., DIXON, R. A. & PAIVA, N. L. 1992. Stress responses in alfalfa (*Medicago sativa* L.) XVI. Antifungal activity of medicarpin and its biosynthetic precursors; implications for the genetic manipulation of stress metabolites. *Physiological and Molecular Plant Pathology,* 42**,** 333-349.
BÖHL, M., TIETZE, S., SOKOLL, A., MADATHIL, S., PFENNIG, F., APOSTOLAKIS, J., FAHMY, K. & GUTZEIT, H. O. 2007. Flavonoids affect actin functions in cytoplasm and nucleus. *Biophysical Journal,* 93**,** 2767-2780.
BROWN, D. E., RASHOTTE, A. M., MURPHY, A. S., NORMANLY, J., TAGUE, B. W., PEER, W. A., TAIZ, L. & MUDAY, G. K. 2001. Flavonoids act as negative regulators of auxin transport i*n vivo* in Arabidopsis. *Plant Physiology,* 126**,** 524-535.
BRUESKE, C. H. 1980. Phenylalanine ammonia lyase activity in tomato roots infected and resistant to the root-knot nematode, *Meloidogyne incognita*. *Physiological Plant Pathology,* 16**,** 409-414.
BRUNETTI, C., DI FERDINANDO, M., FINI, A., POLLASTRI, S. & TATTINI, M. 2013. Flavonoids as antioxidants and developmental regulators: Relative significance in plants and humans. *International Journal of Molecular Sciences,* 14**,** 3540-3555.
BUER, C. S., KORDBACHEH, F., TRUONG, T. T., HOCART, C. H. & DJORDJEVIC, M. A. 2013. Alteration of flavonoid accumulation patterns in transparent testa mutants disturbs auxin transport, gravity responses, and imparts long-term effects on root and shoot architecture. *Planta,* 238**,** 171-189.
BUER, C. S. & MUDAY, G. K. 2004. The *transparent testa4* mutation prevents flavonoid synthesis and alters auxin transport and the response of *Arabidopsis* roots to gravity and light. *The Plant Cell,* 16**,** 1191-1205.
CABRERA, J., DÍAZ-MANZANO, F. E., BARCALA, M., ARGANDA-CARRERAS, I., DE ALMEIDA-ENGLER, J., ENGLER, G., FENOLL, C. & ESCOBAR, C. 2015a. Phenotyping nematode feeding sites: three-dimensional reconstruction and volumetric measurements of giant cells induced by root-knot nematodes in Arabidopsis. *New Phytologist***,** n/a-n/a.
CABRERA, J., DÍAZ-MANZANO, F. E., FENOLL, C. & ESCOBAR, C. 2015b. Chapter Seven - Developmental pathways mediated by hormones in nematode feeding sites. *In:* ESCOBAR, C. & FENOLL, C. (eds.) *Advances in Botanical Research*. Academic Press.
CABRERA, J., DÍAZ-MANZANO, F. E., SANCHEZ, M., ROSSO, M.-N., MELILLO, T., GOH, T., FUKAKI, H., CABELLO, S., HOFMANN, J., FENOLL, C. &

ESCOBAR, C. 2014. A role for *LATERAL ORGAN BOUNDARIES-DOMAIN 16* during the interaction *Arabidopsis–Meloidogyne* spp. provides a molecular link between lateral root and root-knot nematode feeding site development. *New Phytologist,* 203**,** 632-645.

CAILLAUD, M., DUBREUIL, G., QUENTIN, M., PERFUS-BARBEOCH, L., LECOMTE, P., DE ALMEIDA ENGLER, J., ABAD, P., ROSSO, M. & FAVERY, B. 2008. Root-knot nematodes manipulate plant cell functions during a compatible interaction. *Journal of Plant Physiology,* 165**,** 104-113.

CASIMIRO, I., BEECKMAN, T., GRAHAM, N., BHALERAO, R., ZHANG, H., CASERO, P., SANDBERG, G. & BENNETT, M. J. 2003. Dissecting *Arabidopsis* lateral root development. *Trends in Plant Science,* 8**,** 165-171.

CASIMIRO, I., MARCHANT, A., BHALERAO, R. P., BEECKMAN, T., DHOOGE, S., SWARUP, R., GRAHAM, N., INZÉ, D., SANDBERG, G., CASERO, P. J. & BENNETT, M. 2001. Auxin transport promotes *Arabidopsis* lateral root initiation. *The Plant Cell,* 13**,** 843-852.

ČEPULYTĖ, R., DANQUAH, W. B., BRUENING, G. & WILLIAMSON, V. M. 2018. Potent attractant for root-knot nematodes in exudates from seedling root tips of two host species. *Scientific Reports,* 8**,** 10847.

CESCO, S., NEUMANN, G., TOMASI, N., PINTON, R. & WEISSKOPF, L. 2010. Release of plant-borne flavonoids into the rhizosphere and their role in plant nutrition. *Plant Soil,* 329**,** 1-25.

CHABAUD, M., RATET, P., DE SOUSA ARAÚJO, S., LOPES, A. S. R., DUQUE, A., HARRISON, M. & BARKER, D. G. 2007. *Agrobacterium tumafaciens-mediated transformation and in vitro plant regeneration of M. truncatula* [Online]. Noble Research Institute. [Accessed 2014].

CHEBIL, L., HUMEAU, C., ANTHONI, J., DEHEZ, F., ENGASSER, J.-M. & GHOUL, M. 2007. Solubility of flavonoids in organic solvents. *Journal of Chemical & Engineering Data,* 52**,** 1552-1556.

CHITWOOD, D. J. 2003. Research on plant-parasitic nematode biology conducted by the United States Department of Agriculture–Agricultural Research Service. *Pest Management Science,* 59**,** 748-753.

CHU, S., WANG, J., CHENG, H., YANG, Q. & YU, D. 2014. Evolutionary study of the isoflavonoid pathway based on multiple copies analysis in soybean. *BMC Genetics,* 15**,** 76-76.

COLLINGBORN, F. M. B., GOWEN, S. R. & MUELLER-HARVEY, I. 2000. Investigations into the biochemical basis for nematode resistance in roots of three *Musa* cultivars in response to *Radopholus similis* infection. *Journal of Agricultural and Food Chemistry,* 48**,** 5297-5301.

COOK, R., TILLER, S. A., MIZEN, K. A. & EDWARDS, R. 1995. Isoflavonoid metabolism in resistant and susceptible cultivars of white clover infected with the stem nematode *Ditylenchus dipsaci*. *Journal of Plant Physiology,* 146**,** 348-354.

CURTIS, R. H. C. 2008. Plant-nematode interactions: environmental signals detected by the nematode's chemosensory organs control changes in the surface cuticle and behaviour. *Parasite***,** 310-316.

CURTIS, R. H. C., ROBINSON, A. F. & PERRY, R. N. 2009. Hatch and host location. *In:* PERRY, R. N., MOENS, M. & STARR, J. L. (eds.) *Root-knot Nematodes*. UK: CAB International.

CUYCKENS, F. & CLAEYS, M. 2004. Mass spectrometry in the structural analysis of flavonoids. *Journal of Mass Spectrometry,* 39**,** 1-15.

DAKORA, F. D. & PHILLIPS, D. A. 1996. Diverse functions of isoflavonoids in legumes transcend anti-microbial definitions of phytoalexins. *Physiological and Molecular Plant Pathology,* 49**,** 1-20.

DALZELL, J., KERR, R., CORBETT, M., FLEMING, C. & MAULE, A. 2011. Novel bioassays to examine the host-finding ability of plant-parasitic nematodes. *Nematology,* 13**,** 211-220.

DAVIES, K. G. & SPIEGEL, Y. 2011. Biological control of plant-parasitic nematodes: Towards understanding field variation through molecular mechanisms. *In:* JONES, J. T., GHEYSEN, G. & FENOLL, C. (eds.) *Genomics and Molecular Genetics of Plant-Nematode Interactions*. Springer.

DAVIES, L. J., LILLEY, C. J., KNOX, P. & URWIN, P. E. 2012. Syncytia formed by adult female *Heterodera schachtii* in *Arabidopsis thaliana* roots have a distinct cell wall molecular architecture. *New Phytologist,* 196**,** 238-246.

DAVIES, P. J. 1995. Plant hormones: Physiology, biochemistry and molecular biology. *Davies, Peter J.*: Springer Science+ Business Media Dordrecht.

DE ALMEIDA ENGLER, J., DE VLEESSCHAUWER, V., BURSSENS, S., CELENZA, J. L., INZÉ, D., VAN MONTAGU, M., ENGLER, G. & GHEYSEN, G. 1999. Molecular markers and cell cycle inhibitors show the importance of cell cycle progression in nematode-induced galls and syncytia. *The Plant Cell,* 11**,** 793-807.

DE ALMEIDA ENGLER, J. & GHEYSEN, G. 2012. Nematode-induced endoreduplication in plant host cells: Why and how? *Molecular Plant-Microbe Interactions,* 26**,** 17-24.

DE ALMEIDA ENGLER, J., KYNDT, T., VIEIRA, P., VAN CAPPELLE, E., BOUDOLF, V., SANCHEZ, V., ESCOBAR, C., DE VEYLDER, L., ENGLER, G., ABAD, P. & GHEYSEN, G. 2012. CCS52 and DEL1 genes are key components of the endocycle in nematode‐induced feeding sites. *The Plant Journal,* 72**,** 185-198.

DE ALMEIDA ENGLER, J., RODIUC, N., SMERTENKO, A. & ABAD, P. 2010. Plant actin cytoskeleton re-modeling by plant parasitic nematodes. *Plant Signaling & Behavior,* 5**,** 213-217.

DE ALMEIDA ENGLER, J., VAN POUCKE, K., KARIMI, M., DE GROODT, R., GHEYSEN, G., ENGLER, G. & GHEYSEN, G. 2004. Dynamic cytoskeleton rearrangements in giant cells and syncytia of nematode‐infected roots. *The Plant Journal,* 38**,** 12-26.

DE ALMEIDA ENGLER, J., VIEIRA, P., RODIUC, N., GROSSI DE SA, M. F. & ENGLER, G. 2015. Chapter four - The plant cell cycle machinery: Usurped and modulated by plant-parasitic nematodes. *In:* ESCOBAR, C. & FENOLL, C. (eds.) *Advances in Botanical Research*. Academic Press.

DE MEUTTER, J., TYTGAT, T., PRINSEN, E., GHEYSEN, G., VAN ONCKELEN, H. & GHEYSEN, G. 2005. Production of auxin and related compounds by the plant parasitic nematodes *Heterodera schachtii* and *Meloidogyne incognita*. *Communications in Agricultural and Applied Biological Sciences,* 70**,** 51-60.

DE RIJKE, E., OUT, P., NIESSEN, W. M. A., ARIESE, F., GOOIJER, C. & BRINKMAN, U. A. T. 2006. Analytical separation and detection methods for flavonoids. *Journal of Chromatography A,* 1112**,** 31-63.

DE SMET, I., VANNESTE, S., INZÉ, D. & BEECKMAN, T. 2006. Lateral root initiation or the birth of a new meristem. *Plant Molecular Biology,* 60**,** 871-887.

DEAVOURS, B. E., LIU, C.-J., NAOUMKINA, M. A., TANG, Y., FARAG, M. A., SUMNER, L. W., NOEL, J. P. & DIXON, R. A. 2006. Functional analysis of members of the isoflavone and isoflavanone O-methyltransferase enzyme

families from the model legume Medicago truncatula. *Plant molecular biology,* 62**,** 715-733.
DECRAEMER, W. & HUNT, D. J. 2006. Structure and classification. *In:* PERRY, R. N. & MOENS, M. (eds.) *Plant Nematology*. Wallingford, Oxfordshire: CAB International.
DEWICK, P. M. 1998. The biosynthesis of shikimate metabolites. *Natural Product Reports,* 15**,** 17-58.
DHANDAYDHAM, M., CHARLES, L., ZHU, H., STARR, J. L., HUGUET, T., COOK, D. R., PROSPERI, J.-M. & OPPERMAN, C. H. 2008. Characterization of root-knot nematode resistance in *Medicago truncatula*. *Journal of Nematology,* 40**,** 46-54.
DIEZ, J. A. & DUSENBERY, D. B. 1989. Repellent of root-knot nematodes from exudate of host roots. *Journal of Chemical Ecology,* 15**,** 2445-2455.
DIXON, R. A. 2001. Natural products and plant disease resistance. *Nature,* 411**,** 843-847.
DIXON, R. A. & STEELE, C. L. 1999. Flavonoids and isoflavonoids – a gold mine for metabolic engineering. *Trends in Plant Science,* 4**,** 394-400.
DOU, J., LEE, V. S. Y., TZEN, J. T. C. & LEE, M.-R. 2007. Rapid identification of acylated flavonol tetraglycosides in oolong teas using HPLC-MSn. *Phytochemical Analysis,* 19**,** 251-257.
DOYLE, E. A. & LAMBERT, K. N. 2003. *Meloidogyne javanica* chorismate mutase 1 alters plant cell development. *Molecular Plant-Microbe Interactions,* 16**,** 123-131.
DUEÑAS, M., SURCO-LAOS, F., GONZÁLEZ-MANZANO, S., GONZÁLEZ-PARAMÁS, A. M., GÓMEZ-ORTE, E., CABELLO, J. & SANTOS-BUELGA, C. 2013. Deglycosylation is a key step in biotransformation and lifespan effects of quercetin-3-O-glucoside in *Caenorhabditis elegans*. *Pharmacological Research,* 76**,** 41-48.
EDENS, R. M., ANAND, S. C. & BOLLA, R. I. 1995. Enzymes of the phenylpropanoid pathway in soybean infected with *Meloidogyne incognita* or *Heterodera glycines*. *Journal of Nematology,* 27**,** 292-303.
EDWARDS, R., MIZEN, T. & COOK, R. 1995. Isoflavonoid conjugate accumulation in the roots of lucerne (*Medicago sativa*) seedlings following infection by the stem nematode (*Ditylenchus dipsaci*). *Nematologica***,** 51-66.
EVANS, A. A. F. & PERRY, R. N. 2009. Survival mechanisms. *In:* PERRY, R. N., MOENS, M. & STARR, J. L. (eds.) *Root-knot Nematodes*. CAB International.
FAIZI, S., FAYYAZ, S., BANO, S., YAWAR IQBAL, E., LUBNA, SIDDIQI, H. & NAZ, A. 2011. Isolation of nematicidal compounds from *Tagetes patula* L. yellow flowers: Structure–activity relationship studies against cyst nematode *Heterodera zeae* infective stage larvae. *Journal of Agricultural and Food Chemistry,* 59**,** 9080-9093.
FALCONE FERREYRA, M. L., RIUS, S. P. & CASATI, P. 2012. Flavonoids: biosynthesis, biological functions and biotechnological applications. *Frontiers in Plant Science,* 3.
FARAG, M. A., HUHMAN, D. V., DIXON, R. A. & SUMNER, L. W. 2008. Metabolomics reveals novel pathways and differential mechanistic and elicitor-specific responses in phenylpropanoid and isoflavonoid biosynthesis in *Medicago truncatula* cell cultures. *Plant Physiology,* 146**,** 387-402.
FARAG, M. A., HUHMAN, D. V., LEI, Z. & SUMNER, L. W. 2007. Metabolic profiling and systematic identification of flavonoids and isoflavonoids in roots and cell suspension cultures of Medicago truncatula using HPLC–UV–ESI–MS and GC–MS. *Phytochemistry,* 68**,** 342-354.

FUDALI, S. L., WANG, C. & WILLIAMSON, V. M. 2012. Ethylene signaling pathway modulates attractiveness of host roots to the root-knot nematode *Meloidogyne hapla*. *Molecular Plant-Microbe Interactions,* 26**,** 75-86.
FULLER, V. L., LILLEY, C. J. & URWIN, P. E. 2008. Nematode Resistance. *New Phytologist,* 180**,** 27-44.
GANG, S. S. & HALLEM, E. A. 2016. Mechanisms of host seeking by parasitic nematodes. *Molecular and Biochemical Parasitology,* 208**,** 23-32.
GHEYSEN, G. & FENOLL, C. 2002. Gene expression in nematode feeding sites. *Annual Review of Phytopathology,* 40**,** 191-219.
GLAZER, I., EPSTEIN, E., ORION, D. & APELBAUM, A. 1986. Interactions between auxin and ethylene in root-knot nematode (*Meloidogyne javanica*) infected tomato roots. *Physiological and Molecular Plant Pathology,* 28**,** 171-179.
GONZÁLEZ, J. A. & ESTÉVEZ-BRAUN, A. 1998. Effect of (*E*)-Chalcone on Potato-Cyst Nematodes (*Globodera pallida* and *G. rostochiensis*). *Journal of Agricultural and Food Chemistry,* 46**,** 1163-1165.
GOVERSE, A. & SMANT, G. 2014. The activation and suppression of plant innate immunity by parasitic nematodes. *Annual Review of Phytopathology,* 52**,** 243-265.
GRANDISON, G. S. 1977. Relationships of plant-parasitic nematodes and their hosts. *The New Zealand Entomologist,* 6**,** 262-266.
GRUNDLER, F., BETKA, M. & WYSS, U. 1991. Influence of changes in the nurse cell system (syncytium) on sex determination and development of the cyst nematode *Heterodera schachtii*: total amounts of proteins and amino acids. *Physiology and Biochemistry,* 81**,** 70-74.
GRUNEWALD, W., CANNOOT, B., FRIML, J. & GHEYSEN, G. 2009. Parasitic nematodes modulate PIN-mediated auxin transport to facilitate infection. *PLoS Pathog,* 5**,** e1000266.
GRÜNZ, G., HAAS, K., SOUKUP, S., KLINGENSPOR, M., KULLING, S. E., DANIEL, H. & SPANIER, B. 2012. Structural features and bioavailability of four flavonoids and their implications for lifespan-extending and antioxidant actions in C. elegans. *Mechanisms of Ageing and Development,* 133**,** 1-10.
GUENOUNE, D., GALILI, S., PHILLIPS, D. A., VOLPIN, H., CHET, I., OKON, Y. & KAPULNIK, Y. 2001. The defense response elicited by the pathogen *Rhizoctonia solani* is suppressed by colonization of the AM-fungus *Glomus intraradices*. *Plant Science,* 160**,** 925-932.
HAGEN, G. 2015. Auxin signal transduction. *Essays in biochemistry,* 58**,** 1-12.
HAGEN, G. & GUILFOYLE, T. J. 1985. Rapid induction of selective transcription by auxins. *Molecular and Cellular Biology,* 5**,** 1197-1203.
HAGEN, G., MARTIN, G., LI, Y. & GUILFOYLE, T. J. 1991. Auxin-induced expression of the soybean GH3 promoter in transgenic tobacco plants. *Plant Molecular Biology,* 17**,** 567-579.
HANGARTER, R. P. & GOOD, N. E. 1981. Evidence that IAA conjugates are slow release source of free IAA in plant tissues. *Plant Physiol,* 68**,** 1424-1427.
HASSAN, S. & MATHESIUS, U. 2012. The role of flavonoids in root-rhizosphere signalling: opportunities and challenges for improving plant-microbe interactions. *Journal of Experimental Botany,* 63**,** 3429-3444.
HAWES, M. C., BRIGHAM, L. A., WEN, F., WOO, H. H. & ZHU, Y. 2008. Function of root border cells in plant health: Pioneers in the rhizosphere. *Annual Review of Phytopathology,* 36**,** 311-327.
HE, X.-Z. & DIXON, R. A. 2000. Genetic manipulation of isoflavone 7-*O*-methyltransferase enhances biosynthesis of 4′ -*O*-methylated isoflavonoid phytoalexins and disease resistance in alfalfa. *The Plant Cell,* 12**,** 1689-1702.

HIDA, H., NISHIYAMA, H., SAWA, S., HIGASHIYAMA, T. & ARATA, H. 2015. Chemotaxis assay of plant-parasitic nematodes on a gel-filled microchannel device. *Sensors and Actuators B: Chemical*.
HOLBEIN, J., GRUNDLER, F. M. W. & SIDDIQUE, S. 2016. Plant basal resistance to nematodes: an update. *Journal of Experimental Botany,* 67**,** 2049-2061.
HUANG, G., DONG, R., ALLEN, R., DAVIS, E. L., BAUM, T. J. & HUSSEY, R. S. 2004. Two chorismate mutase genes from the root-knot nematode *Meloidogyne incognita*. *Molecular Plant Pathology,* 6**,** 23-30.
HUANG, J.-S. & BARKER, K. R. 1991. Glyceollin I in soybean-cyst nematode interactions: Spatial and temporal distribution in roots of resistant and susceptible soybeans. *Plant Physiology,* 96**,** 1302-1307.
HUTANGURA, P., MATHESIUS, U., JONES, M. G. K. & ROLFE, B. G. 1999. Auxin induction is a trigger for root gall formation caused by root-knot nematodes in white clover and is associated with the activation of the flavonoid pathway. *Functional Plant Biology,* 26**,** 221-231.
INGHAM, J. L. 1976. Fungal modification of pterocarpan phytoalexins from *Melilotus alba* and *Trifolium pratense*. *Phytochemistry,* 15**,** 1489-1495.
ISABELLE, D., FABIEN, B.-C., JULIE, H., EMILIE, A., SANDRINE, B., PHILIPPE, L., ALAIN, P., PIERRE, A., BRUNO, F. & DIDIER, H. 2012. Plant genes involved in harbouring symbiotic rhizobia or pathogenic nematodes. *New Phytologist,* 194**,** 511-522.
ITHAL, N., RECKNOR, J., NETTLETON, D., HEARNE, L., MAIER, T., BAUM, T. J. & MITCHUM, M. G. 2007. Parallel genome-wide expression profiling of host and pathogen during soybean cyst nematode infection of soybean. *Molecular Plant-Microbe Interactions,* 20**,** 293-305.
JACOBS, M. & RUBERY, P. H. 1988. Naturally occurring auxin transport regulators. *Science,* 241**,** 346.
JASIŃSKI, M., KACHLICKI, P., RODZIEWICZ, P., FIGLEROWICZ, M. & STOBIECKI, M. 2009. Changes in the profile of flavonoid accumulation in *Medicago truncatula* leaves during infection with fungal pathogen Phoma medicaginis. *Plant Physiology and Biochemistry,* 47**,** 847-853.
JAUBERT, S., MILAC, A. L., PETRESCU, A. J., DE ALMEIDA-ENGLER, J., ABAD, P. & ROSSO, M.-N. 2005. In planta secretion of a calreticulin by migratory and sedentary stages of root-knot nematode. *Molecular Plant-Microbe Interactions,* 18**,** 1277-1284.
JEFFERSON, R. A. 1987. Assaying chimeric genes in plants: The GUS gene fusion system. *Plant Molecular Biology Reporter,* 5**,** 387-405.
JONES, J., FURLANETTO, C. & PHILLIPS, M. 2007. The role of flavonoids produced in response to cyst nematode infection of *Arabidopsis thaliana*. 9**,** 671-677.
JONES, J. T., FURLANETTO, C., BAKKER, E., BANKS, B., BLOK, V., CHEN, Q., PHILLIPS, M. & PRIOR, A. 2002. Characterization of a chorismate mutase from the potato cyst nematode *Globedera pallida*. *Molecular Plant Pathology,* 4**,** 43-50.
JONES, J. T., HAEGEMAN, A., DANCHIN, E. G. J., GAUR, H. S., HELDER, J., JONES, M. G. K., KIKUCHI, T., MANZANILLA-LÓPEZ, R., PALOMARES-RIUS, J. E., WESEMAEL, W. M. L. & PERRY, R. N. 2013. Top 10 plant-parasitic nematodes in molecular plant pathology. *Molecular Plant Pathology,* 14**,** 946-961.
KAKAR, K., WANDREY, M., CZECHOWSKI, T., GAERTNER, T., SCHEIBLE, W.-R., STITT, M., TORRES-JEREZ, I., XIAO, Y., REDMAN, J. C., WU, H. C., CHEUNG, F., TOWN, C. D. & UDVARDI, M. K. 2008. A community resource

for high-throughput quantitative RT-PCR analysis of transcription factor gene expression in *Medicago truncatula*. *Plant Methods,* 4**,** 1-12.
KAMPKÖTTER, A., GOMBITANG NKWONKAM, C., ZURAWSKI, R. F., TIMPEL, C., CHOVOLOU, Y., WÄTJEN, W. & KAHL, R. 2007. Effects of the flavonoids kaempferol and fisetin on thermotolerance, oxidative stress and FoxO transcription factor DAF-16 in the model organism *Caenorhabditis elegans*. *Archives of Toxicology,* 81**,** 849-858.
KAMPKÖTTER, A., TIMPEL, C., ZURAWSKI, R. F., RUHL, S., CHOVOLOU, Y., PROKSCH, P. & WÄTJEN, W. 2008. Increase of stress resistance and lifespan of *Caenorhabditis elegans* by quercetin. *Comparative Biochemistry and Physiology Part B: Biochemistry and Molecular Biology,* 149**,** 314-323.
KAPLAN, D. T., KEEN, N. T. & THOMASON, I. J. 1980a. Association of glyceollin with the incompatible response of soybean roots to *Meloidogyne incognita*. *Physiological Plant Pathology,* 16**,** 309-318.
KAPLAN, D. T., KEEN, N. T. & THOMASON, I. J. 1980b. Studies on the mode of action of glyceollin in soybean incompatibility to the root knot nematode, *Meloidogyne incognita*. *Physiological Plant Pathology,* 16**,** 319-325.
KARCZMAREK, A., OVERMARS, H., HELDER, J. & GOVERSE, A. 2004. Feeding cell development by cyst and root-knot nematodes involves a similar early, local and transient activation of a specific auxin-inducible promoter element. *Molecular Plant Pathology,* 5**,** 343-346.
KARIMI, M., INZÉ, D. & DEPICKER, A. 2002. GATEWAY™ vectors for *Agrobacterium*-mediated plant transformation. *Trends in Plant Science,* 7**,** 193-195.
KATSUMATA, S., TOSHIMA, H. & HASEGAWA, M. 2018. Xylosylated detoxification of the rice flavonoid phytoalexin sakuranetin by the rice sheath blight fungus *Rhizoctonia solani*. *Molecules,* 23**,** 276.
KELEBEK, H. 2016. LC-DAD–ESI-MS/MS characterization of phenolic constituents in Turkish black tea: Effect of infusion time and temperature. *Food Chemistry,* 204**,** 227-238.
KENNEDY, M. J., NIBLACK, T. L. & KRISHNAN, H. B. 1999. Infection by *Heterodera glycines* elevates isoflavonoid production and influenes soybean nodulation. *Journal of Nematology,* 31**,** 341-347.
KIKUCHI, T., EVES-VAN DEN AKKER, S. & JONES, J. T. 2017. Genome evolution of plant-parasitic nematodes. *Annual Review of Phytopathology,* 55**,** 333-354.
KIM, N., SHIN, Y. J., PARK, S., YOO, G., KIM, Y., YOO, H. H. & KIM, S. H. 2017. Simultaneous determination of six compounds in *Hedera helix* L. using UPLC-ESI–MS/MS. *Chromatographia,* 80**,** 1025-1033.
KLINK, V. P., HOSSEINI, P., MATSYE, P. D., ALKHAROUF, N. W. & MATTHEWS, B. F. 2010. Syncytium gene expression in *Glycine max*[PI 88788] roots undergoing a resistant reaction to the parasitic nematode *Heterodera glycines*. *Plant Physiology and Biochemistry,* 48**,** 176-193.
KOCHBA, J. & SAMISH, R. M. 1971. Effect of kinetin and 1-napthylacetic acid on root-knot nematodes in resistant and susceptible peach root-stocks. *Journal of American Society of Horticultural Science* 97**,** 458-461.
KOES, R., VERWEIJ, W. & QUATTROCCHIO, F. 2005. Flavonoids: a colorful model for the regulation and evolution of biochemical pathways. *Trends in Plant Science,* 10**,** 236-242.
KOWALSKA, I., STOCHMAL, A., KAPUSTA, I., JANDA, B., PIZZA, C., PIACENTE, S. & OLESZEK, W. 2007. Flavonoids from barrel medic (*Medicago truncatula*) aerial parts. *Journal of Agricultural and Food Chemistry,* 55**,** 2645-2652.

KUHN, B. M., ERRAFI, S., BUCHER, R., DOBREV, P., GEISLER, M., BIGLER, L., ZAŽÍMALOVÁ, E. & RINGLI, C. 2016. 7-Rhamnosylated Flavonols Modulate Homeostasis of the Plant Hormone Auxin and Affect Plant Development. *Journal of Biological Chemistry,* 291**,** 5385-5395.
KYNDT, T., DENIL, S., HAEGEMAN, A., TROOSKENS, G., BAUTERS, L., VAN CRIEKINGE, W., DE MEYER, T. & GHEYSEN, G. 2012. Transcriptional reprogramming by root knot and migratory nematode infection in rice. *New Phytologist,* 196**,** 887-900.
KYNDT, T., GOVERSE, A., HAEGEMAN, A., WARMERDAM, S., WANJAU, C., JAHANI, M., ENGLER, G., DE ALMEIDA ENGLER, J. & GHEYSEN, G. 2016. Redirection of auxin flow in Arabidopsis thaliana roots after infection by root-knot nematodes. *Journal of Experimental Botany*.
KYNDT, T., VIEIRA, P., GHEYSEN, G. & DE ALMEIDA-ENGLER, J. 2013. Nematode feeding sites: unique organs in plant roots. *Planta,* 238**,** 807-818.
LAMBERT, K. N., ALLEN, K. D. & SUSSEX, I. M. 1999. Cloning and characterization of an esophageal-gland specific chorismate mutase from the phytoparasitic nematode *Meloidogyne javanica*. *Molecular Plant- Microbe Interactions,* 12**,** 328-336.
LAMBERT, K. N. & BEKAL, S. 2002. Introduction to plant parasitic nematodes. *The Plant Health Instructor*.
LAMBERT, K. N., BEKAL, S., DOMIER, L. L., NIBLACK, T. L., NOEL, G. R. & SMYTH, C. A. 2005. Selection of *Heterodera glycines chorismate mutase-1* alleles on nematode-resistant soybean. *Molecular Plant- Microbe Interactions,* 18**,** 595-601.
LAPČÍK, O. 2007. Isoflavonoids in non-leguminous taxa: A rarity or a rule? *Phytochemistry,* 68**,** 2909-2916.
LATUNDE-DADA, A. O. & LUCAS, J. A. 1985. Involvement of the phytoalexin medicarpin in the differential response of callus lines of lucerne *(Medicago sativa)* to infection by *Verticillium albo-atrum*. *Physiol Plant Pathol,* 16**,** 31-42.
LEE, S. B. & CHUNG, D.-W. 2014. Synthesis and purification of kaempferol by enzymatic hydrolysis of tea seed extract. *Biotechnology and Bioprocess Engineering,* 19**,** 298-303.
LI, Y., DUAN, S., JIA, H., BAI, C., ZHANG, L. & WANG, Z. 2014. Flavonoids from tartary buckwheat induce G2/M cell cycle arrest and apoptosis in human hepatoma HepG2 cells. *Acta Biochimica et Biophysica Sinica,* 46**,** 460-470.
LIU, C.-W. & MURRAY, J. D. 2016. The role of flavonoids in nodulation host-range specificity: An update. *Plants,* 5**,** 33.
MACKOVA, Z., KOBLOVSKA, R. & LAPCIK, O. 2006. Distribution of isoflavonoids in non-leguminous taxa- An update. *Phytochemistry,* 67**,** 846-855.
MANOSALVA, P., MANOHAR, M., VON REUSS, S. H., CHEN, S., KOCH, A., KAPLAN, F., CHOE, A., MICIKAS, R. J., WANG, X., KOGEL, K.-H., STERNBERG, P. W., WILLIAMSON, V. M., SCHROEDER, F. C. & KLESSIG, D. F. 2014. Conserved nematode signalling molecules elicit plant defenses and pathogen resistance. *Nature Communications,* 7795.
MARCELLINO, C., GUT, J., LIM, K. C., SINGH, R., MCKERROW, J. & SAKANARI, J. 2012. WormAssay: A novel computer application for whole-plate motion-based screening of macroscopic parasites. *PLOS Neglected Tropical Diseases,* 6**,** e1494.
MATHESIUS, U. 2001. Flavonoids induced in cells undergoing nodule organogenesis in white clover are regulators of auxin breakdown by peroxidase. *Journal of Experimental Botany,* 52**,** 419-426.

MATSUDA, F., YONEKURA-SAKAKIBARA, K., NIIDA, R., KUROMORI, T., SHINOZAKI, K. & SAITO, K. 2009. MS/MS spectral tag-based annotation of non-targeted profile of plant secondary metabolites. *The Plant Journal,* 57**,** 555-577.

MIERZNAK, J., KOSTYN, K. & KULMA, A. 2014. Flavonoids as important molecules of plant interactions with the environment. *Molecules,* 19**,** 16240-16265.

MOENS, M., PERRY, R. N. & STARR, J. L. 2009. *Meloidogyne* species- a diverse group of novel and important plant parasites. *In:* PERRY, R. N., MOENS, M. & STARR, J. L. (eds.) *Root-knot Nematodes*. CAB International.

MUKHTAR, E., ADHAMI, V. M., SECHI, M. & MUKHTAR, H. 2015. Dietary flavonoid fisetin binds to β-tubulin and disrupts microtubule dynamics in prostate cancer cells. *Cancer Letters,* 367**,** 173-183.

MURPHY, A., PEER, W. A. & TAIZ, L. 2000a. Regulation of auxin transport by aminopeptidases and endogenous flavonoids. *Planta,* 211**,** 315-324.

MURPHY, A. S., PEER, W. A. & TAIZ, L. 2000b. Regulation of auxin transport by aminopeptidases and endogenous flavonoids. *Planta,* 211**,** 315-324.

NAOUMKINA, M., FARAG, M. A., SUMNER, L. W., TANG, Y., LIU, C.-J. & DIXON, R. A. 2007. Different mechanisms for phytoalexin induction by pathogen and wound signals in *Medicago truncatula*. *Proceedings of the National Academy of Sciences,* 104**,** 17909-17915.

NG, J., PERRINE-WALKER, F., WASSON, A. & MATHESIUS, U. 2015a. The control of auxin transport in parasitic and symbiotic root–microbe interactions. *Plants,* 4**,** 606.

NG, J. L. P., HASSAN, S., TRUONG, T. T., HOCART, C. H., LAFFONT, C., FRUGIER, F. & MATHESIUS, U. 2015b. Flavonoids and auxin transport inhibitors rescue symbiotic nodulation in the *Medicago truncatula* cytokinin perception mutant *cre1*. *The Plant Cell,* 27**,** 2210-2226.

NG, J. L. P. & MATHESIUS, U. 2016. Measuring auxin transport capacity in seedling roots of Medicago truncatula. *Bio-protocol,* 6**,** e1842.

NICOL, J. M., TURNER, S. J., COYNE, D. L., NIJS, L. D., HOCKLAND, S. & MAAFI, Z. T. 2011. Current nematode threats to world agriculture. *Genomics and Molecular Genetics of Plant-Nematode Interactions*. Springer.

OLIVEIRA, J., ARAUJO-FILHO, J., GRANGEIRO, T., GONDIM, D., SEGALIN, J., PINTO, P., CARLINI, C., SILVA, F., LOBO, M., COSTA, J. & VASCONCELOS, I. 2014. Enhanced synthesis of antioxidant enzymes, defense proteins and leghemoglobin in rhizobium-free cowpea roots after challenging with *Meloidogyne incognita*. *Proteomes,* 2**,** 527.

ONKOKESUNG, N., REICHELT, M., VAN DOORN, A., SCHUURINK, R. C., VAN LOON, J. J. A. & DICKE, M. 2014. Modulation of flavonoid metabolites in *Arabidopsis thaliana* through overexpression of the *MYB75* transcription factor: role of kaempferol-3,7-dirhamnoside in resistance to the specialist insect herbivore *Pieris brassicae*. *Journal of Experimental Botany,* 65**,** 2203-2217.

PALOMARES-RIUS, J. E., ESCOBAR, C., VOVLAS, A. & CASTILLO, P. 2017. Anatomical alterations in plant tissues induced by plant-parasitic nematodes. *Frontiers in Plant Science,* 8.

PARDEDE, A., ADFA, M., JULIARI KUSNANDA, A., NINOMIYA, M. & KOKETSU, M. 2017. Flavonoid rutinosides from *Cinnamomum parthenoxylon* leaves and their hepatoprotective and antioxidant activity. *Medicinal Chemistry Research,* 26**,** 2074-2079.

PEER, W. A., BANDYOPADHYAY, A., BLAKESLEE, J. J., MAKAM, S. N., CHEN, R. J., MASSON, P. H. & MURPHY, A. S. 2004. Variation in expression and

protein localization of the PIN family of auxin efflux facilitator proteins in flavonoid mutants with altered auxin transport in *Arabidopsis thaliana*. *The Plant Cell,* 16**,** 1898-1911.
PEER, W. A. & MURPHY, A. S. 2007. Flavonoids and auxin transport: modulators or regulators? *Trends in Plant Science,* 12**,** 556-563.
PERRIN, D. R. & BOTTOMLEY, W. 1961. Pisatin: an antifungal substance from *Pisum sativum* L. *Nature,* 191**,** 76.
PERRY, R. N. 1996. Chemoreception in plant parasitic nematodes. *Annual Review of Phytopathology,* 34**,** 181-199.
PERRY, R. N. & MOENS, M. 2011. Introduction to plant-parasitic nematodes; Modes of parasitism. *In:* JONES, J., GHEYSEN, G. & FENOLL, C. (eds.) *Genomics and Molecular Genetics of Plant-Nematode Interactions*. Springer.
PETRÁŠEK, J. & FRIML, J. 2009. Auxin transport routes in plant development. *Development,* 136**,** 2675-2688.
PETRUSSA, E., BRAIDOT, E., ZANCANI, M., PERESSON, C., BERTOLINI, A., PATUI, S. & VIANELLO, A. 2013. Plant flavonoids- biosynthesis, transport and involvement in stress responses. *International Journal of Molecular Sciences,* 14**,** 14950-14973.
PIETSCH, K., SAUL, N., CHAKRABARTI, S., STÜRZENBAUM, S. R., MENZEL, R. & STEINBERG, C. E. W. 2011. Hormetins, antioxidants and prooxidants: defining quercetin-, caffeic acid- and rosmarinic acid-mediated life extension in C. elegans. *Biogerontology,* 12**,** 329-347.
PLAZA, M., POZZO, T., LIU, J., GULSHAN ARA, K. Z., TURNER, C. & NORDBERG KARLSSON, E. 2014. Substituent effects on *in vitro* antioxidizing properties, stability, and solubility in flavonoids. *Journal of Agricultural and Food Chemistry,* 62**,** 3321-3333.
PLINE, M. & DUSENBERY, D. B. 1986. Responses of plant-parasitic nematode *Meloidogyne incognita* to carbon dioxide determined by video camera-computer tracking. *Journal of Chemical Ecology,* 13**,** 873-888.
PLOWRIGHT, R. A., GRAYER, R. J., GILL, J. R., RAHMAN, M. L. & HARBORNEZ, J. B. 1996. The induction of phenolic compounds in rice after infection by the stem nematode *Ditylenchus angustus*. *Nematologica,* 42**,** 564-578.
PROT, J.-C. 1980. Migration of plant parasitic nematodes towards plant roots. *Revue Nematol.,* 3**,** 305-318.
QUITST, C. W., SMANT, G. & HELDER, J. 2015. Evolution of plant parasitism in the phylum Nematoda. *Annual Review of Phytopathology,* 53**,** 289-310.
RASHOTTE, A. M., POUPART, J., WADDELL, C. S. & MUDAY, G. K. 2003. Transport of the two natural auxins, indole-3-butyric acid and indole-3-acetic acid, in *Arabidopsis*. *Plant Physiol,* 133**,** 761-772.
RASMANN, S., ALI, J. G., HELDER, J. & VAN DER PUTTEN, W. H. 2012. Ecology and evolution of soil nematode chemotaxis. *Journal of Chemical Ecology,* 38**,** 615-628.
RENGARAJAN, S. & HALLEM, E. A. 2016. Olfactory circuits and behaviors of nematodes. *Current Opinion in Neurobiology,* 41**,** 136-148.
REYNAUD, J., GUILET, D., TERREUX, R., LUSSIGNOL, M. & WALCHSHOFER, N. 2005. Isoflavonoids in non-leguminous families: an update. *Natural Product Reports,* 22**,** 504-515.
REYNOLDS, A. M., DUTTA, T. K., CURTIS, R. H. C., POWERS, S. J., GAUR, H. S. & KERRY, B. R. 2011. Chemotaxis can take plant-parasitic nematodes to the source of a chemo-attractant via the shortest possible routes. *Journal of The Royal Society Interface,* 8**,** 568-577.

RICH, J. R., KEEN, N. T. & THOMASON, I. J. 1977. Association of coumestans with the hypersensitivity of Lima bean roots to *Pratylenchus scribneri*. *Physiological Plant Pathology,* 10**,** 105-116.
RICHARDSON, L. & PRICE, N. S. 1984. Observations on the biology of *Meloidogyne incognita* and the diageotropica tomato mutant. *Revue Nematol.,* 7**,** 000-999.
ROBARDS, K. 2003. Strategies for the determination of bioactive phenols in plants, fruit and vegetables. *Journal of Chromatography A,* 1000**,** 657-691.
ROSE, J. K. & RANKIN, C. H. 2001. Analyses of habituation in *Caenorhabditis elegans*. *Learning and Memory,* 8**,** 63-69.
ROSE, R. J. 2008. Medicago truncatula as a model for understanding plant interactions with other organisms, plant development and stress biology: past, present and future. *Functional Plant Biology,* 35**,** 253-264.
ROSE, R. J., NOLAN, K. E. & BICEGO, L. 1999. The development of the highly regenerable seed line Jemalong 2HA for transformation of *Medicago truncatula* — Implications for regenerability via somatic embryogenesis. *Journal of Plant Physiology,* 155**,** 788-791.
ROSSO, M.-N., VIEIRA, P., DE ALMEIDA-ENGLER, J. & CASTAGNONE-SERENO, P. 2011. Proteins secreted by root-knot nematodes accumulate in the extracellular compartment during root infection. *Plant Signaling & Behavior,* 6**,** 1232-1234.
RUAN, Q., QIAO, Y., ZHAO, Y., XU, Y., WANG, M., DUAN, J. & WANG, D. 2016. Beneficial effects of *Glycyrrhizae radix* extract in preventing oxidative damage and extending the lifespan of *Caenorhabditis elegans*. *Journal of Ethnopharmacology,* 177**,** 101-110.
RUIJTER, J. M., RAMAKERS, C., HOOGAARS, W. M. H., KARLEN, Y., BAKKER, O., VAN DEN HOFF, M. J. B. & MOORMAN, A. F. M. 2009. Amplification efficiency: linking baseline and bias in the analysis of quantitative PCR data. *Nucleic Acids Research,* 37**,** e45-e45.
SABATINI, S., BEIS, D., WOLKENFELT, H., MURFETT, J., GUILFOYLE, T., MALAMY, J., BENFEY, P., LEYSER, O., BECHTOLD, N., WEISBEEK, P. & SCHERES, B. 1999. An auxin-dependent distal organizer of pattern and polarity in the *Arabidopsis* root. *Cell,* 99**,** 463-472.
SASSER, J. N. & FRECKMAN, D. W. 1987. A world perspective on nematology: The role in society. *In:* VEECH, J. A. & DICKSON, D. W. (eds.) *Vistas on nematology: A commemoration of the twenty-fifth anniversary of the Society of Nematologists*. Hyattsville, MD: Society of Nematologists, Inc.
SCHWALM, K., ALONI, R., LANGHANS, M., HELLER, W., STICH, S. & ULLRICH, C. I. 2003. Flavonoid-related regulation of auxin accumulation in *Agrobacterium tumefaciens*-induced plant tumors. *Planta,* 218**,** 163-178.
SHAUKAT, S. S., SIDDIQUI, I. A., ALI, N. A., ALI, S. A. & KHAN, G. H. 2003. Nematicidal and allelopathic responses of *Lantana camara* root extract. *Phytopathologica Mediterranea,* 42**,** 71-78.
SIDDIQUE, S. & GRUNDLER, F. M. W. 2015. Chapter five - Metabolism in nematode feeding sites. *In:* ESCOBAR, C. & FENOLL, C. (eds.) *Advances in Botanical Research*. Academic Press.
SIJMONS, P. C., ATKINSON, H. J. & WYSS, U. 1994. Parasitic strategies of root nematodes and associated host cell responses. *Annual Review of Phytopathology,* 32**,** 235-259.
SMANT, G., HELDER, J. & GOVERSE, A. 2018. Parallel adaptations and common host cell responses enabling feeding of obligate and facultative plant parasitic nematodes. *The Plant Journal,* 93**,** 686-702.

SOMMERVILLE, R. I. & DAVEY, K. G. 2002. Diapause in parasitic nematodes: a review. *Canadian Journal of Zoology,* 80**,** 1817-1840.
SORIANO, I. R., ASENSTORFER, R. E., SCHMIDT, O. & RILEY, I. T. 2004. Inducible flavone in oats (*Avena sativa*) is a novel defense against plant-parasitic nematodes. *Phytopathology,* 94**,** 1207-1214.
SOUKUP, S. T., SPANIER, B., GRÜNZ, G., BUNZEL, D., DANIEL, H. & KULLING, S. E. 2012. Formation of phosphoglycosides in *Caenorhabditis elegans*: a novel biotransformation pathway. *PLOS ONE,* 7**,** e46914.
STADLER, M., DAGNE, E. & ANKE, H. 1994. Nematicidal activities of two phytoalexins from *Taverniera abyssinica*. *Planta Med,* 60**,** 550-552.
STASWICK, P. E. 2009. The tryptophan conjugates of jasmonic and indole-3-acetic acids are endogenous auxin inhibitors. *Plant Physiology,* 150**,** 1310-1321.
STASZKÓW, A., SWARCEWICZ, B., BANASIAK, J., MUTH, D., JASIŃSKI, M. & STOBIECKI, M. 2011. LC/MS profiling of flavonoid glycoconjugates isolated from hairy roots, suspension root cell cultures and seedling roots of *Medicago truncatula*. *Metabolomics,* 7**,** 604-613.
STEENACKERS, W., KLÍMA, P., QUARESHY, M., CESARINO, I., KUMPF, R. P., CORNEILLIE, S., ARAÚJO, P., VIAENE, T., GOEMINNE, G., NOWACK, M. K., LJUNG, K., FRIML, J., BLAKESLEE, J. J., NOVÁK, O., ZAŽÍMALOVÁ, E., NAPIER, R., BOERJAN, W. & VANHOLME, B. 2017. Cis-cinnamic acid is a novel, natural auxin efflux inhibitor that promotes lateral root formation. *Plant Physiology,* 173**,** 552-565.
STENLID, G. 1963. The effects of flavonoid compounds on oxidative phosphorylation and on the enzymatic destruction of indoleacetic acid. *Physiologia Plantarum,* 16**,** 110-120.
STENLID, G. 1968. On the physiological effects of phloridzin, phloretin and some related substances upon higher plants. *Physiologia Plantarum,* 21**,** 882-894.
STENLID, G. 1976. Effects of flavonoids on the polar transport of auxins. *Physiologia Plantarum,* 38**,** 262-266.
STEVENSON, P. C., TURNER, H. C. & HAWARE, M. P. 1997. Phytoalexin accumulation in the roots of chickpea (*Cicer arietinum* L.) seedlings associated with resistance to fusarium wilt (*Fusarium oxysporum* f.sp. *ciceri*). *Physiological and Molecular Plant Pathology,* 50**,** 167-178.
STIRLING, G. R. & PATTISON, B. 2008. Beyond chemical dependency for managing plant-parasitic nematodes: examples from the banana, pineapple and vegetable industries of tropical and subtropical Australia. *Australasian Plant Pathology,* 37**,** 254-267.
STIRLING, G. R. & STANTON, J. 1997. Nematode diseases and their control. *In:* BROWN, J. F. & OGLE, H. F. (eds.) *Plant Pathogens and Plant Diseases*. Australian Plant Pathology Society.
STIRLING, G. R., STANTON, J. & MARSHALL, J. W. 1992. The importance of plant-parasitic nematodes to Australian and New Zealand agriculture. *Australasian Plant Pathology,* 21**,** 104-115.
SUGIYAMA, A., SHITAN, N. & YAZAKI, K. 2007. Involvement of a soybean ATP-binding cassette-type transporter in the secretion of genistein, a signal flavonoid in legume-*rhizobium* symbiosis. *Plant Physiology,* 144**,** 2000-2008.
TAYLOR, A. L., SASSER, J. N. & NELSON, L. A. 1982. Relationship of climate and soil characteristics to geographical distribution of *Meloidogyne* species in agricultural soils. *International Meloidogyne Project***,** 1-65.
TAYLOR, L. P. & GROTEWOLD, E. 2005. Flavonoids as developmental regulators. *Current Opinion in Plant Biology,* 8**,** 317-323.

TEFFT, P. M. & BONE, L. W. 1985. Plant-induced hatching of eggs of the soybean cyst nematode, *Heterodera glycines*. *Journal of Nematology,* 17**,** 275-279.
TEGTMEIER, K. J. & VANETTEN, H. D. 1981. The role of pisatin tolerance and degradation in the virulence of *Nectria haematococca* on peas: a genetic analysis. *Physiology and Biochemistry,* 72**,** 608-612.
TITAPIWATANAKUN, B. & MURPHY, A. S. 2009. Post-transcriptional regulation of auxin transport proteins: cellular trafficking, protein phosphorylation, protein maturation, ubiquitination, and membrane composition. *Journal of Experimental Botany,* 60**,** 1093-1107.
TREUTTER, D. 2005. Significance of flavonoids in plant resistance and enhancement of their biosynthesis. *Plant Biology,* 7**,** 581-591.
TYTGAT, T., DE MEUTTER, J., GHEYSEN, G. & COOMANS, A. 2000. Sedentary endoparasitic nematodes as a model for other plant parasitic nematodes. *Nematology,* 2**,** 113-121.
URBANCZYK-WOCHNIAK, E. & SUMNER, L. W. 2007. MedicCyc: a biochemical pathway database for *Medicago truncatula*. *Bioinformatics,* 23**,** 1418-1423.
VANHOLME, B., KAST, P., HAEGEMAN, A., JACOB, J., GRUNEWALD, W. & GHEYSEN, G. 2009. Structural and functional investigation of a secreted chorismate mutase from the plant-parasitic nematode *Heterodera schachtii* in the context of related enzymes from diverse origins. *Molecular Plant Pathology,* 10**,** 189-200.
VENIS, M. A. 1972. Auxin-induced conjugation systems in peas. *Plant Physiology,* 49**,** 24-27.
VIGLIERCHIO, D. R. & YU, P. K. 1968. Plant growth substances and plant parasitic nematodes. *Experimental Parasitology,* 23**,** 88-95.
VILLETH, G. R. C., CARMO, L. S. T., SILVA, L. P., FONTES, W., GRYNBERG, P., SARAIVA, M., BRASILEIRO, A. C. M., CARNEIRO, R. M. D., OLIVEIRA, J. T. A., GROSSI-DE-SÁ, M. F. & MEHTA, A. 2015. Cowpea–*Meloidogyne incognita* interaction: Root proteomic analysis during early stages of nematode infection. *Proteomics,* 15**,** 1746-1759.
VLACHOPOULOS, E. G. & SMITH, L. 1993. Flavonoids in potato cyst nematodes. *Fundamental and Applied Nematology,* 16**,** 103-106.
WALKER, G. E. & STIRLING, G. R. 2008. Plant-parasitic nematodes in Australian viticulture: key pests, current management practices and opportunities for future improvements. *Australasian Plant Pathology,* 37**,** 268-278.
WANG, C., BRUENING, G. & WILLIAMSON, V. M. 2009a. Determination of preferred pH for root-knot nematode aggregration using Pluronic F-127 gel. *Journal of Chemical Ecology,* 35**,** 1242-1251.
WANG, C., LOWER, S. & WILLIAMSON, V. M. 2009b. Application of Pluronic gel to the study of root-knot nematode behaviour. *Nematology,* 11**,** 453-464.
WASSON, A. P., RAMSAY, K., JONES, M. G. K. & MATHESIUS, U. 2009. Differing requirements for flavonoids during the formation of lateral roots, nodules and root knot nematode galls in *Medicago truncatula*. *New Phytologist,* 183**,** 167-179.
WESTON, L. A. & MATHESIUS, U. 2013. Flavonoids: their structure, biosynthesis and role in the rhizosphere, including allelopathy. *Journal of Chemical Ecology,* 39**,** 283-297.
WILLIAMSON, V. M. & GLEASON, C. A. 2003. Plant-nematode interactions. *Current Opinion in Plant Biology,* 6**,** 1-7.
WINKEL-SHIRLEY, B. 2001. Flavonoid biosynthesis: A colourful model for genetics, biochemistry, cell biology and biotechnology. *Plant Physiology,* 126**,** 485-493.

WINKEL-SHIRLEY, B. 2002. Biosynthesis of flavonoids and effects of stress. *Current Opinion in Plant Biology,* 5**,** 218-223.
WOODWARD, A. W. & BARTEL, B. 2005. Auxin: Regulation, action, and interaction. *Annals of Botany,* 95**,** 707-735.
WORLEY, B. & POWERS, R. 2013. Multivariate analysis in metabolomics. *Current Metabolomics,* 1**,** 92-107.
WUYTS, N., LOGNAY, G., SWENNEN, R. & DE WAELE, D. 2006a. Nematode infection and reproduction in transgenic and mutant *Arabidopsis* and tobacco with an altered phenylpropanoid metabolism. *Journal of Experimental Botany,* 57**,** 2825-2835.
WUYTS, N., SWENNEN, R. & DE WAELE, D. 2006b. Effects of plant phenylpropanoid pathway products and selected terpenoids and alkaloids on the behaviour of the plant-parasitic nematodes *Radopholus similis* , *Pratylenchs penetrans* and *Meloidogyne incognita*. *Nematology,* 8**,** 89-101.
WYSS, U. & GRUNDLER, F. M. W. 1992. Feeding behavior of sedentary plant parasitic nematodes. *European Journal of Plant Pathology,* 98**,** 165-173.
WYSS, U., GRUNDLER, F. M. W. & MÜNCH, A. 1992. The parasitic behaviour of second-stage juveniles of *Meloidogyne incognita* in roots of *Arabidopsis thaliana*. *Nematologica,* 38**,** 98-111.
YIN, R., HAN, K., HELLER, W., ALBERT, A., DOBREV, P. I., ZAŽÍMALOVÁ, E. & SCHÄFFNER, A. R. 2014. Kaempferol 3-O-rhamnoside-7-O-rhamnoside is an endogenous flavonol inhibitor of polar auxin transport in *Arabidopsis* shoots. *New Phytologist,* 201**,** 466-475.
YIN, R., MESSNER, B., FAUS-KESSLER, T., HOFFMANN, T., SCHWAB, W., HAJIREZAEI, M.-R., VON SAINT PAUL, V., HELLER, W. & SCHÄFFNER, A. R. 2012. Feedback inhibition of the general phenylpropanoid and flavonol biosynthetic pathways upon a compromised flavonol-3-O-glycosylation. *Journal of Experimental Botany*.
YOUNG, N. D., DEBELLÉ, F., OLDROYD, G. E. D., GEURTS, R., CANNON, S. B., UDVARDI, M. K., BENEDITO, V. A., MAYER, K. F. X., GOUZY, J., SCHOOF, H., VAN DE PEER, Y., PROOST, S., COOK, D. R., MEYERS, B. C., SPANNAGL, M., CHEUNG, F., DE MITA, S., KRISHNAKUMAR, V., GUNDLACH, H., ZHOU, S., MUDGE, J., BHARTI, A. K., MURRAY, J. D., NAOUMKINA, M. A., ROSEN, B., SILVERSTEIN, K. A. T., TANG, H., ROMBAUTS, S., ZHAO, P. X., ZHOU, P., BARBE, V., BARDOU, P., BECHNER, M., BELLEC, A., BERGER, A., BERGÈS, H., BIDWELL, S., BISSELING, T., CHOISNE, N., COULOUX, A., DENNY, R., DESHPANDE, S., DAI, X., DOYLE, J. J., DUDEZ, A.-M., FARMER, A. D., FOUTEAU, S., FRANKEN, C., GIBELIN, C., GISH, J., GOLDSTEIN, S., GONZÁLEZ, A. J., GREEN, P. J., HALLAB, A., HARTOG, M., HUA, A., HUMPHRAY, S. J., JEONG, D.-H., JING, Y., JÖCKER, A., KENTON, S. M., KIM, D.-J., KLEE, K., LAI, H., LANG, C., LIN, S., MACMIL, S. L., MAGDELENAT, G., MATTHEWS, L., MCCORRISON, J., MONAGHAN, E. L., MUN, J.-H., NAJAR, F. Z., NICHOLSON, C., NOIROT, C., O'BLENESS, M., PAULE, C. R., POULAIN, J., PRION, F., QIN, B., QU, C., RETZEL, E. F., RIDDLE, C., SALLET, E., SAMAIN, S., SAMSON, N., SANDERS, I., SAURAT, O., SCARPELLI, C., SCHIEX, T., SEGURENS, B., SEVERIN, A. J., SHERRIER, D. J., SHI, R., SIMS, S., SINGER, S. R., SINHAROY, S., STERCK, L., VIOLLET, A., WANG, B.-B., et al. 2011. The *Medicago* genome provides insight into the evolution of rhizobial symbioses. *Nature,* 480**,** 520-524.

YU, P. K. & VIGLIERCHIO, D. R. 1964. Plant growth substances and parasitic nematodes. I. Root knot nematodes and tomato. *Experimental Parasitology,* 15**,** 242-248.

ZHAO, J. & DIXON, R. A. 2009. The 'ins' and 'outs' of flavonoid transport. *Trends in Plant Science,* 15**,** 72-80.

ZIJLSTRA, C., DONKERS-VENNE, D. T. H. M. & FARGETTE, M. 2000. Identification of *Meloidogyne incognita*, *M. javanica* and *M. arenaria* using sequence characterised amplified region (SCAR) based PCR assays. *Nematology,* 2**,** 847-853.